

CRANFIELD UNIVERSITY

INSTITUTE OF BIOSCIENCE AND TECHNOLOGY

Academic years 1999-2002

MANUELA LOTIERZO

BIOLOGICAL AND ARTIFICIAL RECEPTORS IN AFFINITY SENSOR FOR WATER TOXINS DETECTION

Supervisor: Dr I.E. Tothill

Ph.D. Thesis

January 2003

This thesis is submitted for the degree of Doctor of Philosophy

ProQuest Number: 10832146

All rights reserved

INFORMATION TO ALL USERS

The quality of this reproduction is dependent upon the quality of the copy submitted.

In the unlikely event that the author did not send a complete manuscript and there are missing pages, these will be noted. Also, if material had to be removed, a note will indicate the deletion.



ProQuest 10832146

Published by ProQuest LLC (2019). Copyright of the Dissertation is held by Cranfield University.

All rights reserved.

This work is protected against unauthorized copying under Title 17, United States Code
Microform Edition © ProQuest LLC.

ProQuest LLC.
789 East Eisenhower Parkway
P.O. Box 1346
Ann Arbor, MI 48106 – 1346

ACKNOWLEDGEMENTS

Thank you to Dr Ibtsam Tothill for supervising this project.

Thank you to Dr Sergey Piletsky for its support and precious advises on MIP technology.

Thank you to Dr Jane Rixon and Dr Steve White for great suggestions in Science and English.

Thank you to all the people supporting me in the lab, especially Dr Elena Piletska,

Dr Kal Karim, Dr Judith Taylor and Dr John Bolbot.

Thank you to Iva for her optimistic presence inside and outside the lab.

Thank you to all the smiling people I met during my time in England

who made everything look brighter despite the weather.

Thank you to my parents who let me go and do it!

ABSTRACT

Molecular recognition is the basis for many of the chemical and biochemical phenomena occurring in living organisms. For example, antibodies, which are one of the different classes of natural receptor molecules, are capable of selectively recognising a specific target molecule or structure. They are therefore routinely utilised as analytical reagents in clinical and research laboratories. The design and synthesis of biomimetic recognition systems, capable of binding target molecules with affinities and specificities comparable to natural receptors, is regarded as one of the greatest challenges in bioorganic chemistry. Molecularly imprinted polymers (MIPs) have been shown to mimic the binding sites of antibodies and are, therefore, constantly gaining in interest for applications based on specific molecular recognition.

This project aimed to develop affinity sensors for the detection of algal and cyanobacterial toxins such as microcystin-LR and domoic acid in water samples. Following the investigation, a heterogeneous direct competitive enzyme-linked immunosorbent assay (ELISA) format for microcystin detection was developed. The system was then transferred to an affinity membrane sorbent based ELISA. This was an amenable format for immunoassay incorporation into a disposable amperometric immunosensor device.

A three-electrode system immunosensor was fabricated using thick film screen-printing technology. Amperometric HRP transduction of hydrogen peroxide catalysis, at low reducing potentials, versus Ag/AgCl reference and carbon counter electrode, was facilitated by hydroquinone mediated electron transfer. A detection limit of $0.5 \mu\text{g l}^{-1}$ for microcystin-LR was achieved.

The work undertaken also describes the design and synthesis of biomimetic recognition systems based on MIP, capable of binding target molecules with affinities and specificities on a par with natural receptors. A MIP synthetic receptor selective for microcystin-LR was studied using an enzyme-linked competitive assay and found to be comparable to polyclonal antibodies, whilst the MIP had superior stability over natural

receptors. Methacrylic acid based MIP had a detection limit of $1 \mu\text{g l}^{-1}$, approximately twenty times higher than that of anti microcystin-LR polyclonal antibody.

A molecularly imprinted polymer was also directly synthesised by grafting on the gold chip of a surface plasmon resonance (SPR) based bioanalytical instrument system: the BIAcore 3000TM. Such a chip based platform allowed a simple test of the specific MIP receptor for the marine toxin domoic acid. A full characterisation of the grafting procedure was initially carried out on a bare gold surface, and each step of the polymerisation was investigated by contact angle measurements and AFM imaging. The surface photo-initiated MIP film was obtained and its thickness and homogeneity evaluated.

Domoic acid is a molecule that is too small for direct analysis, hence a competition reaction was performed in presence of the conjugate DA-HRP and a detection limit of $2 \mu\text{g l}^{-1}$ could be achieved with the BIAcore 3000TM system.

LIST OF CONTENTS

ACKNOWLEDGEMENTS	I
ABSTRACT.....	II
LIST OF CONTENTS.....	IV
LIST OF ABBREVIATIONS	X
LIST OF FIGURES.....	XIII
LISTS OF TABLES.....	XVII
LISTS OF PLATES.....	XVIII
CHAPTER 1:.....	1
LITERATURE REVIEW	1
1.1 BACKGROUND	2
1.2 CYANOTOXINS	5
1.2.1 <i>Hepatotoxins Cyclic Peptides-Microcystins</i>	6
1.2.2 <i>Microcystin-LR as Liver Tumour Promoters</i>	10
1.3 AMNESIC SHELLFISH POISONS: DOMOIC ACID	11
1.4 LEGISLATION AND ENVIRONMENTAL MONITORING.....	12
1.5 DETECTION OF WATER TOXINS	14
1.5.1 <i>Microcystins</i>	14
1.5.2 <i>Domoic Acid</i>	15
1.6 IMMUNOASSAY	16
1.6.1 <i>Antibody as Immunochemical Reagent</i>	16
1.6.2 <i>Antibody Structure and Function</i>	17
1.6.3 <i>Polyclonal Antibodies</i>	19
1.6.4 <i>Monoclonal Antibodies</i>	20
1.6.5 <i>Antibody-Antigen Interaction</i>	20
1.6.6 <i>Enzyme-Linked Immuno-Sorbent Assay</i>	22

1.6.6 Enzyme-Linked Immuno-Sorbent Assay.....	22
1.7 BIOSENSORS	25
1.7.1 Electrochemical Analysis.....	26
1.7.2 Affinity Sensor: Immunosensors	27
1.8 MOLECULAR IMPRINTED POLYMER	31
1.8.1 Covalent Approach	33
1.8.2 Non-Covalent Approach.....	34
1.8.3 Physical Forms and Preparation Methods of MIP.....	35
1.8.4 MIP Application.....	36
1.8.5 MIP in Assay and Sensor Technology	38
1.8.6 MIPs based on Computational Approach.....	41
1.9 AIMS AND OBJECTIVES	43
1.10 THESIS FLOWCHART.....	45
CHAPTER 2:.....	47
MATERIALS & METHODS	47
2.1 MATERIALS.....	48
2.1.1 Chemicals.....	48
2.1.2 Antibodies	49
2.1.3 Toxins and Conjugates.....	50
2.1.4 Electrode Fabrication.....	51
2.1.5 Electrode Configuration	52
2.2 METHODS: IMMUNOREAGENTS CHARACTERISATION.....	53
2.2.1 SPR-based Biacore System	53
2.2.2 BIAcore Analysis of Anti-Microcystin-LR Antibody: Coupling Reaction	55
2.2.3 Sample Preparation and Analysis for BIAcore.....	56
2.3 METHODS: IMMUNOASSAY DEVELOPMENT	57
2.3.1 Assessment of Anti-Microcystin-LR Polyclonal Antibody.....	57
2.3.2 Gelatin Coating Conjugate Optimisation.....	58
2.3.3 Competitive ELISA Optimisations	58
2.3.4 ELISA Data Analysis	59

2.4.1 MELISA based on Antigen Coating.....	62
2.4.2 MELISA based on Antibody Coating.....	63
2.5 METHODS: ELECTROCHEMICAL TECHNIQUES.....	63
2.5.1 Cyclic Voltammetry.....	64
2.5.2 Chrono-Amperometry.....	65
2.5.3 Electrochemical Substrate Detection.....	65
2.5.4 Electrochemical FIA MELISA.....	67
2.6 MIP-BASED RECEPTOR FOR MICROCYSTIN-LR.....	69
2.6.1 Synthesis of Bulk-Imprinted Polymer for Microcystin-LR.....	69
2.6.2 Characterisation of MIP by Enzyme-Linked Competitive Assay.....	69
2.6.3 Physical Characteristics of the Polymers.....	70
2.6.4 Optimisation of Enzyme-Linked MIP Assay.....	71
2.6.5 Comparison Study with Anti-Microcystin-LR Antibody.....	71
2.7 MIP-BASED RECEPTOR FOR DOMOIC ACID.....	73
2.7.1 Computationally Designed MIP for Domoic Acid.....	73
2.7.2 Synthesis of Imprinted Polymer for Domoic Acid.....	76
2.7.3 Enzyme-Linked Competitive MIP Assay for Domoic Acid.....	76
2.7.4 Fluorescence Study of OPA-Modified Polymer.....	77
2.7.5 Grafting Photo-Polymerisation.....	77
2.7.6 Characterisation of Photo-Grafted MIP by Atomic Force Microscopy.....	79
2.7.7 MIP Characterisation by BIAcore Analysis.....	79
2.7.8 Biacore Analysis of Anti-Domoic Acid Antibody.....	80
CHAPTER 3: RESULTS.....	82
IMMUNOREAGENTS CHARACTERISATION AND IMMUNOASSAY	
DEVELOPMENT.....	82
3.1 INTRODUCTION.....	83
3.2 IMMUNOREAGENT CHARACTERISATION.....	83
3.2.1 Evaluation of Rabbit anti-Microcystin-LR Antibody.....	83
3.3 ASSESSMENT OF ANTI-MICROCYSTIN-LR POLYCLONAL ANTIBODY.....	91

3.3.1 <i>Anti-Microcystin-LR IgG Reagent Sensitivity and Affinity</i>	92
3.3.2 <i>Gelatin Coating Conjugate</i>	94
3.4 MICROCYSTIN-LR DETECTION BY COMPETITIVE ELISA	95
3.4.1 <i>Optimisation of Competitive Reaction Incubation Conditions</i>	96
3.4.2 <i>Immunosorbent Coating and Blocking Incubation Duration</i>	97
3.4.3 <i>Microcystin-LR IgG Cross-Reactivity Analysis</i>	99
3.4.4 <i>Matrix Effects</i>	100
3.7 CONCLUSION	102
CHAPTER 4: RESULTS	104
IMMUNOSENSOR DEVELOPMENT	104
4.1 INTRODUCTION	105
4.2 ELISA OPTIMISATION FOR THE DETECTION OF MICROCYSTIN-LR	105
4.3 MEMBRANE SORBENT SELECTION	106
4.3.1 <i>Microcystin-LR–Gelatin Coating Titration</i>	106
4.3.2 <i>Comparing Membrane Blocker Efficiency</i>	108
4.4 ANTIBODY-BASED FORMAT FOR MELISA.....	111
4.4.1 <i>Antibody Titration on Membrane</i>	111
4.5 IMMUNOSENSOR DEVELOPMENT.....	114
4.5.1 <i>Hydroquinone Electro-Activity</i>	114
4.5.2 <i>Potential Determination</i>	115
4.5.3 <i>Optimising the Hydroquinone and Peroxidase Concentrations</i>	117
4.6 COMPETITIVE MICROCYSTIN-LR IMMUNOSENSOR.....	118
4.6.1 <i>Mediated HRP Amperometric Detection</i>	118
4.7 ELECTROCHEMICAL ABTS DETECTION.....	121
4.7.1 <i>ABTS Electro-Activity</i>	122
4.8 FLOW INJECTION ASSAY FOR MELISA COLORIMETRIC ASSAY	125
4.8.1 <i>Flow Rate Optimisation</i>	125
4.8.2 <i>Competitive FIA with Amperometric ABTS Detection</i>	128
4.9 CONCLUSION	129

CHAPTER 5: RESULTS	131
AFFINITY RECEPTORS BASED ON MIP FOR MICROCYSTIN-LR.....	131
5.1 INTRODUCTION	132
5.2 BULK IMPRINTING SYNTHESIS OF A MIP FOR MICROCYSTIN-LR.....	132
5.3 COMPETITIVE ENZYME-LINKED ASSAY FOR IMPRINTED POLYMER.....	135
5.3.1 <i>Optimisation of Microcystin-HRP Conjugate.....</i>	<i>137</i>
5.3.2 <i>Optimisation of Polymer Suspension Concentration.....</i>	<i>138</i>
5.3.3 <i>Comparing Specificity of Imprinted and Non-Imprinted Polymers.....</i>	<i>139</i>
5.3.4 <i>Comparing Sensitivity and Affinity for Microcystin-LR Receptors</i>	<i>140</i>
5.3.5 <i>Comparing Cross-Reactivity for Microcystin-LR Receptors.....</i>	<i>142</i>
5.3.6 <i>Comparing Stability of Microcystin-LR Receptors.....</i>	<i>143</i>
5.4 CONCLUSIONS.....	148
CHAPTER 6: RESULTS	150
AFFINITY RECEPTORS BASED ON MIP FOR DOMOIC ACID	150
6.1 INTRODUCTION	151
6.2 COMPUTATIONAL-BASED MIP FOR DOMOIC ACID	151
6.3 MIP FLUORESCENCE ASSAY FOR DOMOIC ACID DETECTION	157
6.4 GRAFTING TECHNIQUE FOR DOMOIC ACID POLYMER.....	160
6.4.1 <i>Characterisation of Grafting Process by Atomic Force Microscope Imaging</i>	<i>161</i>
6.4.2 <i>Characterisation of MIP Grafting by Surface Plasmon Resonance.....</i>	<i>164</i>
6.5 MIP SENSOR FOR DOMOIC ACID BASED ON THE SPR SYSTEM	167
6.6 IMMUNOSENSOR FOR DOMOIC ACID BASED ON SPR SYSTEM.....	169
6.6.1 <i>Antibody Immobilisation by the BIAcore 3000TM</i>	<i>170</i>
6.6.2 <i>Optimisation of Conjugate HRP-DA Bound Format.....</i>	<i>171</i>
6.6.3 <i>Cross-Reactivity for MIP and anti-Domoic Acid Antibody.....</i>	<i>173</i>
6.7 CONCLUSIONS.....	175

CHAPTER 7:	177
DISCUSSION	177
7.1 INTRODUCTION	178
7.2 EVALUATION OF ANTI-MICROCYSTIN-LR ANTIBODY.....	179
7.3 COMPETITIVE ELISA ASSAY FOR MICROCYSTIN-LR DETECTION.....	180
7.4 AFFINITY MEMBRANE MELISA.....	185
7.5 OPTIMISATION OF MEMBRANE COMPETITIVE ASSAY	187
7.6 ANTIBODY IMMOBILISED FORMAT FOR THE MELISA ASSAY	189
7.7 IMMUNOSENSOR DEVELOPMENT.....	191
7.8 ELECTROCHEMICAL SUBSTRATE DETECTION.....	196
7.9 MOLECULAR IMPRINTING FOR MICROCYSTIN-LR	200
7.10 MOLECULAR IMPRINTING FOR DOMOIC ACID	205
7.11 GRAFTED IMPRINTED POLYMER FOR DOMOIC ACID	208
CHAPTER 8:	215
CONCLUSIONS AND FURTHER WORK	215
PUBLICATIONS	222
REFERENCES	224
APPENDIX	239

LIST OF ABBREVIATIONS

ABTS	2,2'-Azino-bis(3-Ethylbenz-Thiazoline-6-Sulfonic Acid)
Adda	(2 <i>S</i> ,3 <i>S</i> ,8 <i>S</i> ,9 <i>S</i>)-3-Amino-9-Methoxy-2,6,8-Trimethyl-10-Phenyldeca-4,6-Dienoic Acid
AFM	Atomic Force Microscopy
Ala	Alanine
AMPSA	2-Acrylamido-2-Methyl-1-Propane Sulfonic Acid
APBA	3-Aminophenylboronic Acid
Arg	Arginine
ASP	Amnesic Shellfish Poisoning
BET	Brunauer-Emmett-Teller Theory
BSA	Bovine Serum Albumin
CA	Chrono-Amperometry
CLIA	Chemiluminescence Immunoassay
CM-MIP	Computationally-designed Molecularly Imprinted Polymer
CV	Cyclic Voltammetry
2,4 D	2,4-dichlorophenoxy Acetic Acid
DA	Domoic Acid
Dha	Dehydro-alanine
DMF	N,N-Dimethyl Formamide
DMSO	Dimethyl Sulphoxide
DSP	Diarrheic Shellfish Poisoning
EDC	N-Ethyl-N'-(3-Dimethylaminopropyl)Carbodimide Hydrochloride
EGDMA	Ethylene Glycol Dimethyl Acrylate
EIAs	Enzyme Immunoassays
ELISA	Enzyme Linked Immuno-Sorbent Assay
Fs	Femtoseconds
FIA	Flow Injection Analysis system
FLIA	Fluorescence immunoassay

HPLC	High-Performance Liquid Chromatography
IA	Itaconic Acid
Ig	Immunoglobulin
IUPAC	International Union of Pure and Applied Chemistry
kD	kDalton
KLH	Keyhole Limpet Hemocyanin
LC	Liquid Chromatographic
LC-MS	Liquid Chromatographic-Mass Spectrometry
LD ₅₀	Lethal dose to 50 % of the population of the animals tested
Leu	Leucine
MAA	Methacrylic Acid
MAA-MIP	Methacrylic Acid-based Molecularly Imprinted Polymer
MBA	<i>N,N</i> -Methylenebis (acrylamide)
MC-LR	Microcystin-LR
Mdha	<i>N</i> -Methyldehydroalanine
MELISA	Membrane Enzyme Linked Immuno-Sorbent Assay
MHz	Megahertz
MIAs	Molecularly Imprinted Sorbent Assays
MIPs	Molecularly Imprinted Polymer
MW	Molecular Weight
NHS	<i>N</i> -Hydroxysuccinimide
NIP	Non-Imprinted Polymer
OA	Okadaic Acid
OPA	O-phthalaldehyde
OVA	Ovalbumin
Phe	Phenylalanine
PL-a	Phosphorylase-a
PP1	Protein Phosphatases 1
ppb	part per billion
ppt	part per trillion
RA IgG	Antisera IgG raised in rabbit

RIA	Radio-Immunoassay
rpm	Revolutions per minute
RT	Room Temperature
RU	Response Unit
SD	Standard Deviation
SDS	Sodium Dodecyl Sulphate
SH anti-MC-LR IgG	Anti-microcystin-LR Antibody raised in sheep
SPE	Screen-Printed Electrodes
SPR	Surface Plasmon Resonance
SPS	Screen-Printed Sensor
TBA	3-Thiopheneboronic Acid
TMB	3,3',5,5'-Tetramethyl Benzidine Hydrochloride
TR-FIA	Time-Resolved Fluorometry Immunoassay
Trp	Tryptophane
Tyr	Tyrosine
UA	Urocanic Acid
UAEE	Urocanic Acid Ethyl Ester
UV	Ultraviolet Light
WHO	World Health Organisation

LIST OF FIGURES

	Page
FIGURE 1.1: STRUCTURE OF MICROCYSTINS MOLECULE.	7
FIGURE 1.2: STRUCTURE OF NODULARIN.	8
FIGURE 1.3: PROTEIN SERINE-THREONINE PHOSPHATASE 1 ISOFORM TYPE COMPLEX (RIBBONS).	10
FIGURE 1.4: STRUCTURE OF DOMOIC ACID AND ANALOGUES.	12
FIGURE 1.5: BASIC IMMUNOGLOBULIN STRUCTURE.	18
FIGURE 1.6: SCHEMATIC REPRESENTATION OF DIFFERENT IMMUNOASSAY FORMATS.	23
FIGURE 1.7: AN OVERVIEW OF TRANSDUCER PRINCIPLES IN BIOSENSOR CONSTRUCTION (KRÖGER, 1998).	26
FIGURE 1.8: SCHEME OF THE GENERAL IMMUNOSENSOR DESIGN DEPICTING THE INTIMATE INTEGRATION OF IMMUNOLOGICAL RECOGNITION AT THE SOLID-STATE SURFACE AND THE SIGNAL TRANSDUCTION.	29
FIGURE 1.9: SCHEMATIC REPRESENTATION OF SELF-ASSEMBLY APPROACH FOR MOLECULAR IMPRINTING.	35
FIGURE 2.1: SCHEME OF SPR SYSTEM.	54
FIGURE 2.2: AMINE COUPLING CHEMISTRY (HTTP://WWW.BIACORE.COM).	55
FIGURE 2.3: SCHEME OF IMMUNOSENSOR.	66
FIGURE 2.4: SYBYL WINDOWS FOR ENERGY MINIMISATION.	74
FIGURE 2.5: MOST COMMON MONOMERS INCLUDED IN THE VIRTUAL LIBRARY.	75
FIGURE 2.6: SCHEME OF THE GRAFTING PROCEDURE.	78
FIGURE 3.1: TYPICAL IMMOBILISATION SEQUENCE OBSERVED USING THE BIACORE 3000™.	84
FIGURE 3.2: OPTIMISATION OF THE IMMOBILISATION FOR MC-LR-OVA ON THE CHIP. .	85
FIGURE 3.3: BINDING OF THE ANTI-MC-LR IGG CONCENTRATIONS (0-50 MG L ⁻¹) TO THE IMMOBILISED MC-LR-OVA CONJUGATE. THE INJECTION VOLUME WAS 40 µL AT A FLOW RATE OF 15 µL MIN ⁻¹	86
FIGURE 3.4: DISPLACEMENT ASSAY FOR MICROCYSTIN-LR.	89

FIGURE 3.5: DISPLACEMENT ASSAY FOR MICROCYSTIN-LR-OVA.....	89
FIGURE 3.6: DISPLACEMENT ASSAY SENSORGRAM AFTER (A)- INJECTION OF CONJUGATE MC-LR-OVA (3 mg L^{-1}) AND (B)- FREE MC-LR (100 mg L^{-1}).....	90
FIGURE 3.7: CHECKERBOARD TITRATION FOR SH ANTI-MICROCYSTIN-LR POLYCLONAL ANTIBODY.....	91
FIGURE 3.8: THE TITRATION CURVE (A)- AND HUGHES –KLOTZ PLOT (B)- FOR SH IGG.	93
FIGURE 3.9: GELATIN CONJUGATE COATING TITRATION.	95
FIGURE 3.10: COMPARING INCUBATION REACTION CONDITIONS ON ASSAY SENSITIVITY.	96
FIGURE 3.11: INVESTIGATION OF COATING AND BLOCKING INCUBATION DURATION.	97
FIGURE 3.12: COMPETITIVE ELISA ASSAY FOR MICROCYSTIN-LR.	98
FIGURE 3.13: CROSS REACTIVITY CURVES FOR MICROCYSTIN-LR AND ITS ANALOGUES.	99
FIGURE 3.14: MATRIX EFFECT FOR ANALYTE MICROCYSTIN-LR.	101
FIGURE 3.15: MATRIX EFFECTS FOR PRIMARY ANTIBODY ANTI MICROCYSTIN-LR.....	102
FIGURE 4.1: COATING ANTIGEN-CONJUGATE TITRATION.	107
FIGURE 4.2: RESULTS FROM THE BLOCKING AGENTS INVESTIGATION.	109
FIGURE 4.3: OPTIMISATION OF ANTIBODY CONCENTRATIONS FOR THE COMPETITIVE MELISA ASSAY.	110
FIGURE 4.4: TITRATION OF ANTI-MICROCYSTIN-LR ANTIBODY.....	112
FIGURE 4.5: COMPETITIVE ASSAY WITH IGG IMMOBILISATION ON MEMBRANE.	113
FIGURE 4.6: CYCLIC VOLTAMMOGRAM OF HYDROQUINONE.	115
FIGURE 4.7: HYDROQUINONE HRP MEDIATED CHRONOAMPEROMETRY AT DIFFERENT POTENTIALS.	116
FIGURE 4.8: MEDIATED HRP RESPONSE TO DIFFERENT HYDROQUINONE CONCENTRATIONS.....	117
FIGURE 4.9: MEDIATED HRP RESPONSE TO DIFFERENT PEROXIDE CONCENTRATIONS..	118
FIGURE 4.10: A CHRONO-AMPEROMETRY CURRENT/TIME TRACE OF MICROCYSTIN-LR.	120
FIGURE 4.11: COMPETITIVE MC-LR IMMUNOSENSOR RESPONSE.	121
FIGURE 4.12: CYCLIC VOLTAMMOGRAM OF ABTS.....	122
FIGURE 4.13: CHRONO-AMPEROMETRY FOR COMPETITIVE MELISA USING ABTS DETECTION.....	123

FIGURE 4.14: COMPETITIVE MC-LR IMMUNOSENSOR RESPONSE.	124
FIGURE 4.15: FLOW RATE OPTIMISATION OF THE MC-LR COMPETITIVE ASSAY.	126
FIGURE 4.16: ON-LINE COMPETITIVE MELISA ASSAY FOR MC-LR.....	127
FIGURE 4.17: ON-LINE DETECTION OF THE COMPETITIVE MELISA ASSAY FOR MC-LR.	128
FIGURE 5.1: INTERACTION BETWEEN MICROCYSTIN-LR (CENTRE OF THE PICTURE) AND (A)-10 MAA MOLECULES (YELLOW), (B)- DIFFERENT MONOMERS SELECTED (IN BALLS AND STICKS).....	134
FIGURE 5.2: SCHEME OF THE COMPETITIVE ENZYME ASSAY.	136
FIGURE 5.3: OPTIMISATION OF MICROCYSTIN-HRP CONJUGATE CONCENTRATION.....	137
FIGURE 5.4: ENZYME-LINKED COMPETITIVE ASSAY CURVES OBTAINED USING FOUR DIFFERENT CONCENTRATIONS OF THE POLYMER SUSPENSIONS (5 g L^{-1} , 0.5 g L^{-1} , 0.1 g L^{-1} , 0.05 g L^{-1}).....	138
FIGURE 5.5: MIP-BASED ASSAY FOR THE MAA-POLYMER.	139
FIGURE 5.6: STABILITY TEST WITH ANTI-MICROCYSTIN-LR POLYCLONAL ANTIBODY. .	144
FIGURE 5.7: STABILITY TEST WITH ANTI-MICROCYSTIN-LR MONOCLONAL ANTIBODY. .	145
FIGURE 5.8: STABILITY TEST WITH MAA-MIP FOR MICROCYSTIN-LR.....	146
FIGURE 5.9: STABILITY TEST WITH MAA-MIP FOR MICROCYSTIN-LR.....	147
FIGURE 6.1: TEMPLATE DOMOIC ACID AND THREE MONOMERS INTERACTION AS RESULT AFTER SIMULATED ANNEALING STUDY.	152
FIGURE 6.2: ENZYME-LINKED MIP ASSAY WITH DIFFERENT CONCENTRATIONS OF DA- HRP.....	154
FIGURE 6.3: ENZYME-LINKED MIP ASSAY USING DIFFERENT CONCENTRATIONS OF POLYMER.	155
FIGURE 6.4: CALIBRATION CURVE FOR DOMOIC ACID.	156
FIGURE 6.5: REACTION OF OPA REAGENT WITH THE AMINO GROUP OF ALLYLAMINE. .	157
FIGURE 6.6: DEVELOPMENT OF FLUORESCENCE EMISSION FROM THE OPA-MODIFIED POLYMER.	158
FIGURE 6.7: (A)- PLANAR TOPOGRAPHIC IMAGE. (B)- 3D TOPOGRAPHIC IMAGE OF GOLD CHIP WITH GRAFTED MIP.....	161

FIGURE 6.8: 6 $\mu\text{m} \times 6 \mu\text{m}$ AFM IMAGE OF A 2 $\mu\text{m} \times 2 \mu\text{m}$ SCRAPPED AREA ON THE LEFT AND A PLOT OF PIXEL HEIGHT VS. FREQUENCY PLOT OF THE GRAFTED MIP ON THE RIGHT.....	162
FIGURE 6.9: CROSS SECTION ANALYSIS OF FIGURE 6.8.	163
FIGURE 6.10: TWO CONSECUTIVE REGENERATION PHASES ALTERNATED BY ONE INJECTION OF THE ANALYTE.....	165
FIGURE 6.11: SPECIFIC BINDING OF DA-HRP CONJUGATE TO GRAFTED MIP COMPARED TO NON-SPECIFIC BINDING OF NATIVE HRP.	166
FIGURE 6.12: SENSORGRAM OF A COMPETITIVE MIP REACTION.....	167
FIGURE 6.13: COMPETITIVE CALIBRATION CURVE FOR THE DOMOIC ACID MIP SENSOR.	168
FIGURE 6.14: CROSS-REACTIVITY OF DA ANALOGUES OBTAINED WITH THE MIP SENSOR.	169
FIGURE 6.15: SENSORGRAM FOR THE MONOCLONAL ANTIBODY IMMOBILISATION.....	170
FIGURE 6.16: SENSORGRAM OF THE ANTIBODY-BASED SENSOR AFTER THE COMPETITIVE REACTION.	172
FIGURE 6.17: CALIBRATION CURVE FOR ANTI-DA MONOCLONAL ANTIBODY.....	173
FIGURE 6.18: SENSORGRAM FOR CROSS-REACTIVITY OF DOMOIC ACID ANALOGUES. ...	174
FIGURE 7.1: MEDIATED FAST ELECTRON TRANSFER FOR THE ENZYME HORSERADISHPEROXIDASE.....	192
FIGURE 7.2: REDOX REACTION OF HYDROQUINONE.	196
FIGURE 7.3: REDOX REACTION FOR ABTS.	198
FIGURE 7.4: POSSIBLE CHANGES IN THE MIP NETWORK STRUCTURE.....	207
FIGURE I.1: MALDI MASS SPECTROMETRY SPECTRA FOR MC-LR-HRP CONJUGATE.	240
FIGURE I.2: MALDI MASS SPECTROMETRY SPECTRA FOR HRP ENZYME.....	241
FIGURE II.1: SYBYL WINDOWS FOR LEAPFROG ALGORITHM.	242
FIGURE II.2: SYBYL WINDOWS FOR LEAPFROG ALGORITHM.	243
FIGURE II.3: SYBYL WINDOWS FOR ENERGY MINIMISATION OF THE SOLVATED BOX..	244

LISTS OF TABLES

	Page
TABLE 1.1: HEPATOTOXINS AND NEUROTOXINS FROM CYANOBACTERIA.....	3
TABLE 1.2: MARINE ALGAL TOXINS AND THEIR MODE OF ACTION (CLARK <i>ET AL.</i> , 1999)..	4
TABLE 1.3: TOXICITY OF MICROCYSTIN-LR AND SOME ANALOGUES (RINEHART <i>ET AL.</i> , 1994).....	8
TABLE 2.1: OPTIMISED PARAMETERS FOR PRINTING THREE-ELECTRODE SYSTEMS (KRÖGER, 1998).....	51
TABLE 3.1: SUMMARY OF RESULTS OF THE SPR ANALYSIS WITH BIACORE 3000™ BEFORE AND AFTER A PRE-INCUBATION STEP WITH OVA (1 MG ML ⁻¹).....	88
TABLE 3.2: CROSS-REACTIVITY VALUES SHOWED BY ANTI-MC-LR ANTISERA.	100
TABLE 5.1: COMPOSITION OF MONOMER MIXTURE USED FOR MIP PREPARATION AND THE PHYSICAL PROPERTIES OF THE SYNTHESIZED POLYMERS.....	135
TABLE 5.2: VALUES OF AFFINITY AND RANGE OF SENSITIVITY FOR MICROCYSTIN-LR RECEPTORS.	141
TABLE 5.3: CROSS-REACTIVITY FOR MIP AND ANTIBODIES WITH MICROCYSTIN-LR ANALOGUES.	142
TABLE 5.4: RECEPTOR ACTIVITY MEASUREMENTS CARRIED OUT AFTER DIFFERENT TREATMENTS (N= 3, ± SD).	148
TABLE 6.1: COMPOSITION OF POLYMERISATION MIXTURE FOR DOMOIC ACID MIP BASED ON COMPUTATIONAL DESIGN.	153
TABLE 6.2: IMPRINTING FACTORS FOR THE POLYMER CALCULATED IN THE PRESENCE AND ABSENCE OF DOMOIC ACID.....	159
TABLE 6.3: THICKNESS OF FILMS GENERATED DURING THE GRAFTING PROCEDURE.	164
TABLE 6.4: COMPARISON BETWEEN MIP AND MONOCLONAL ANTIBODY SPECIFIC FOR DOMOIC ACID.	175
TABLE 7.1: DEVELOPED OF SOME RECEPTORS FOR MICROCYSTIN-LR.....	184
TABLE 7.2: SUMMARY OF THE PRINCIPAL RECEPTORS SYSTEMS SPECIFIC FOR DOMOIC ACID.....	214

LISTS OF PLATES

	Page
PLATE 1.1: ANABAENOPSIS SP. BLOOM IN BEDETTI LAKE, SANTA FE, ARGENTINA.	5
PLATE 2.1: THE SCREEN-PRINTING PROCESS IN SENSOR FABRICATION (BASKEYFIELD, 2001).	52
PLATE 2.2: SCREEN-PRINTED ELECTRODE CONFIGURATION (A)-MEMBRANE COMPATIBLE SPE DESIGN; (B) FIA SPE DESIGN.	53
PLATE 2.3: FIA SPE AND MEMBRANE DISC FLOW CELLS.	68

CHAPTER 1:
LITERATURE REVIEW

1.1 BACKGROUND

The contamination of water resources and drinking water supplies poses a major human health concern. While recent advances in science have led to the generation of many analytical systems for the early detection of water pollutants, human progress during this last century has contributed to the appearance of new and unknown risks, threatening the health of humans and animals. Toxic substances, such as metals and synthetic organic compounds, have emerged only in the latter half of the twentieth century and eutrophication has become a growing concern since the 1950s.

As a possible consequence of eutrophication, toxins from algae and other water microorganisms have become widely recognised as a contributory factor to human health problems. In domestic water supplies, as well as in freshwater and marine water, several large families of microorganisms producing toxins have been clearly defined in the last twenty years. One of these families is cyanobacteria, a frequent component of many freshwater and marine ecosystems. Species that live dispersed in the water are part of the phytoplankton, whilst those that grow on sediments form part of the phytobenthos. Because they are aquatic and photosynthetic, cyanobacteria are often called "blue-green algae." Although this name is convenient for describing organisms that live in water and synthesise their own food, it does not reflect any relationship between the cyanobacteria and other organisms called algae.

Under certain conditions, especially where waters are rich in nutrients and exposed to sunlight, cyanobacteria may multiply to high densities and create water blooms. The primary sources for nutrients (e.g. phosphates and nitrates) are raw sewage spills, industrial effluents, and run-off from agricultural and urban regions. Warm summer conditions such as high temperatures and light intensities coupled with calm, stable waters (low turbidity, no wind) also contribute to bloom formation. In several countries, the association of cyanobacterial blooms with animal poisoning episodes and human health problems has raised the possibility of toxin production by the common bloom-

forming cyanobacteria (Codd *et al.*, 1989). A list of the most important toxins from cyanobacteria is given in Table 1.1.

Table 1.1: Hepatotoxins and neurotoxins from cyanobacteria.

TOXIN		MOLECULAR STRUCTURE	NUMBER OF VARIANTS	SOURCES	MODE(S) OF TOXICITY
H E P A T O T O X I N S	NODULARIN	Cyclic pentapeptide	6	<i>Nodularia</i>	Hepatotoxic Tumor promoters, PPase inhibitors
	MICROCYSTINS	Cyclic heptapeptide	>60	<i>Microcystis</i> <i>Anabaena</i> <i>Nostoc</i> <i>Oscillatoria</i>	Hepatotoxic Tumor promoters, PPase inhibitors
	CYLINDROSPERMOPSIN	Cyclic guanidine alkaloid	1	<i>Cylindrospermopsis</i> <i>Umezakia</i>	-
N E U R O T O X I N S	ANATOXIN-A	Secondary amine alkaloid	1	<i>Anabaena</i> , <i>Microcystis</i> , <i>Oscillatoria</i> , <i>Phormidium</i> , <i>Aphanizomenon</i>	Neurotoxic, depolarizing neuro- muscular blocker
	HOMOANTOTOXIN-A	As above	1	<i>Phormidium</i>	-
	PSP TOXINS (SAXITOXIN, NEO-SAXITOXIN, GTX AND CTX TOXINS)	Alkaloids	At least 8	<i>Anabaena</i> , <i>Aphanizomenon</i>	Neurotoxic, sodium channel blockers
	ANATOXIN-A (S)	Guanidinium phosphate ester	1	<i>Anabaena</i>	Neurotoxic, cholinesterase inhibitor

Similarly, the proliferation of dinoflagellates and small marine organisms has been responsible for “red tides” or “blooms” in oceans and along coastlines around the world.

Epidemics of shellfish toxicity have often been linked to the presence of these blooms. Marine algal toxins are summarised in Table 1.2, where the attention has been focused on the mode of action of specific algal toxins.

Table 1.2: Marine algal toxins and their mode of action (Clark *et al.*, 1999).

TOXIN	BIOCHEMICAL SITE OF ACTION	PHYSIOLOGICAL EFFECT
PARALYTIC SHELLFISH POISONS	Site 1 on voltage dependent sodium channel	Inhibition of ion conductance
DIARRHOEIC SHELLFISH POISONS	Catalytic subunit of phosphorylase phosphatases	Inhibition of phosphorylase phosphatases 1 and 2a
NEUROTOXIC SHELLFISH POISONS	Site 5 on voltage dependent sodium channel	Repetitive firing, shift of voltage dependence of activation
CIGUATERA POISONS: CIGUATOXIN	Site 5 on voltage dependent sodium channel	Repetitive firing, shift of voltage dependence of activation
MAITOTOXIN	Calcium channels	Calcium ion influx
AMNESIC SHELLFISH POISONS: DOMOIC ACID	Kainate receptor in central nervous system	Receptor-induced depolarisation and excitation

Falconer (1999) reported the occurrence of toxic blooms and scum in phytoplankton and recorded it as a worldwide phenomenon. Blooms have been found in over 30 countries in fresh, brackish, or marine waters throughout Europe, North and South America, Australia, Africa, and Asia.

1.2 CYANOTOXINS

Cyanobacteria are Gram-negative bacteria; they are aquatic photosynthetic bacteria, usually unicellular, though they often grow in suspended colonies (e.g. *Microcystis aeruginosa*), or filaments (e.g. *Anabaena*), large enough to be seen (Plate 1.1).



Plate 1.1: *Anabaenopsis* sp. Bloom in Bedetti Lake, Santa Fe, Argentina. (<http://www-cyanosite.bio.purdue.edu/images/images.html>, 25/03/02).

Cyanobacteria produce a wide variety of chemically unique secondary metabolites. Secondary metabolites refer to those compounds that are not used by the organism for its primary metabolism (Carmichael, 1992). Toxins are secondary compounds that have a harmful effect on other tissues, cells, or organisms. While it is still unclear why cyanobacteria produce toxins, one hypothesis is that they may function as protective compounds e.g. defence or deterrence against grazing (Codd *et al.*, 1984).

Toxins from cyanobacteria constitute a major source of natural toxins, ‘biotoxins’, that are often found in surface supplies of freshwater. The biotoxins include the neurotoxins,

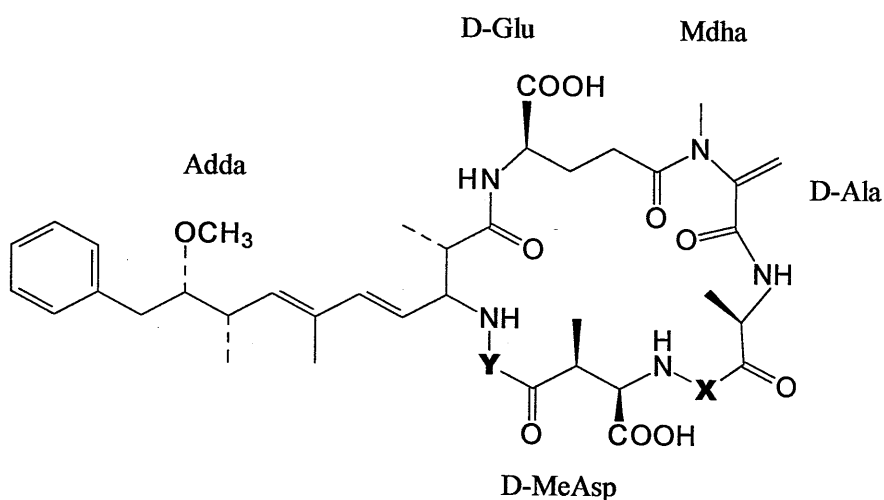
anatoxin-a, anatoxin-a (s) and saxitoxins plus the hepatotoxins: microcystins, nodularin and cylindrospermopsin. Neurotoxins affect the nervous system and are fast-acting, small molecules. Hepatotoxins affect the liver and are cyclic peptide molecules acting more slowly than neurotoxins.

1.2.1 Hepatotoxic Cyclic Peptides-Microcystins

Acute hepatotoxicosis, involving the hepatotoxins (liver toxins), is the most commonly encountered toxicosis involving cyanobacteria. Hepatotoxins are produced by strains of species within the genera *Microcystis*, *Anabaena*, *Hapalosiphon*, *Nodularia*, *Nostoc* and *Oscillatoria* (Carmichael, 1992).

The microcystins are a group of cyclic heptapeptide hepatotoxins produced by a number of cyanobacterial genera; the most notable being the wide spread *Microcystis*, from which the toxins take their name. Over 60 microcystins have been isolated so far. They consist of a seven-amino acid peptide ring, which is made up of five non-protein amino acids and two protein amino acids.

A remarkable characteristic of microcystins is the presence of the C₂₀ amino acid, 3-amino-9-methoxy-2, 6, 8-trimethyl-10-phenyl-4, 6-decadienoic acid (abbreviated Adda), with its β-amino group, multiple methyl substitution, and diene unit. Microcystins also contain a dehydroamino acid; N-methyldehydroalanine, two D-amino acids, D-glutamic and D-erythro-β-methylaspartic acid, and two protein amino acids distinguish microcystins from one another (Rinehart *et al.*, 1994). Using amino acid single letter code nomenclature, each microcystin is designated by a name depending on the variable amino acids, which complete their structure. The most common and potently toxic microcystin-LR contains the amino acids leucine (L) and arginine (R), in these variable positions (Figure 1.1).



MICROCYSTIN	<u>LR</u>	<u>RR</u>	<u>YR</u>	<u>LW</u>	<u>LF</u>	<u>LY</u>	<u>LA</u>
Y	Leu	Arg	Tyr	Leu	Leu	Leu	Leu
X	Arg	Arg	Arg	Trp	Phe	Tyr	Ala

Figure 1.1: Structure of microcystins molecule.

X and Y are variable L-amino acids. D-MeAsp is *D-erythro*- β -methylaspartic acid, Adda is (2*S*,3*S*,8*S*,9*S*)-3-amino-9-methoxy-2,6,8-trimethyl-10-phenyldeca-4,6-dienoic acid and Mdha is N-methyldehydroalanine (Dha = dehydroalanine).

Microcystin-LR (MW= 994 Daltons) is one of the major hepatotoxins produced by certain freshwater cyanobacteria including: *Anabaena flos-aquae*, *Microcystis aeruginosa* and *Oscillatoria agardhii*. Nodularin, (Figure 1.2) isolated from the toxic brackish water cyanobacterium *Nodularia spumigen*, is a hepatotoxic and cyclic pentapeptide and is structurally similar to the cyclic heptapeptide microcystin-LR (Ohta *et al.*, 1994).

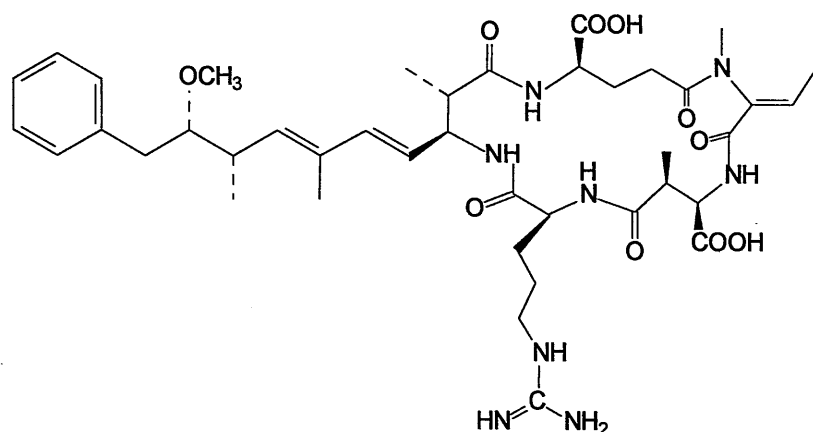


Figure 1.2: Structure of nodularin.

Table 1.3 shows the LD_{50} values for microcystin-LR and its analogues including nodularin, which was present in the concentration of test material and is lethal to 50 % of the population of the animals tested (LD_{50}).

Table 1.3: Toxicity of microcystin-LR and some analogues (Rinehart *et al.*, 1994).

TOXIN	LD_{50} ($\mu\text{g kg}^{-1}$)
NODULARIN	50
MICROCYSTIN-LR	50
MICROCYSTIN-LA	50
MICROCYSTIN-LY	90
MICROCYSTIN-YR	70
MICROCYSTIN-YM	56

The primary effect on health is toxicity to liver cells, because of the selective transport mechanisms, which concentrate the peptide toxins from the blood into the liver. As with all toxic material consumed in food or drinking water, the toxins need to traverse the gut lining in order to enter the bloodstream. The underlying biochemical effect is a powerful inhibition of specific phosphatase enzymes, resulting in the hyperphosphorylation of proteins. This leads to the breakdown of intermediate filaments of the cell cytoskeleton and a retraction of actin microfilaments. The cell distortion is such that the organisational structure of the liver itself falls apart, and the animal bleeds into its own liver causing death. Hence, the mechanism of action for these hepatotoxins at the cellular and molecular level shows that they have a preferred affinity for the liver, followed by a specific binding to serine/threonine protein phosphatases 1 (PP1) and 2A (Runnegar *et al.*, 1988; Nishiwakimatsushima *et al.*, 1992).

Phosphatases that act on phosphorylated serine and threonine residues are present in all eukaryotic cell types and participate in the control of a wide range of cellular processes; including cell-cycle progression, cell proliferation, protein synthesis, transcriptional regulation and neurotransmission (Goldberg *et al.*, 1995). Microcystin toxins bind to PP1 in such a way as to interact with three distinct regions of the surface: the metal binding site, the hydrophobic groove and the edge of the C-terminal groove near the active site. The long hydrophobic Adda side chain packs into the hydrophobic groove, forming a bound structure (Figure 1.3).

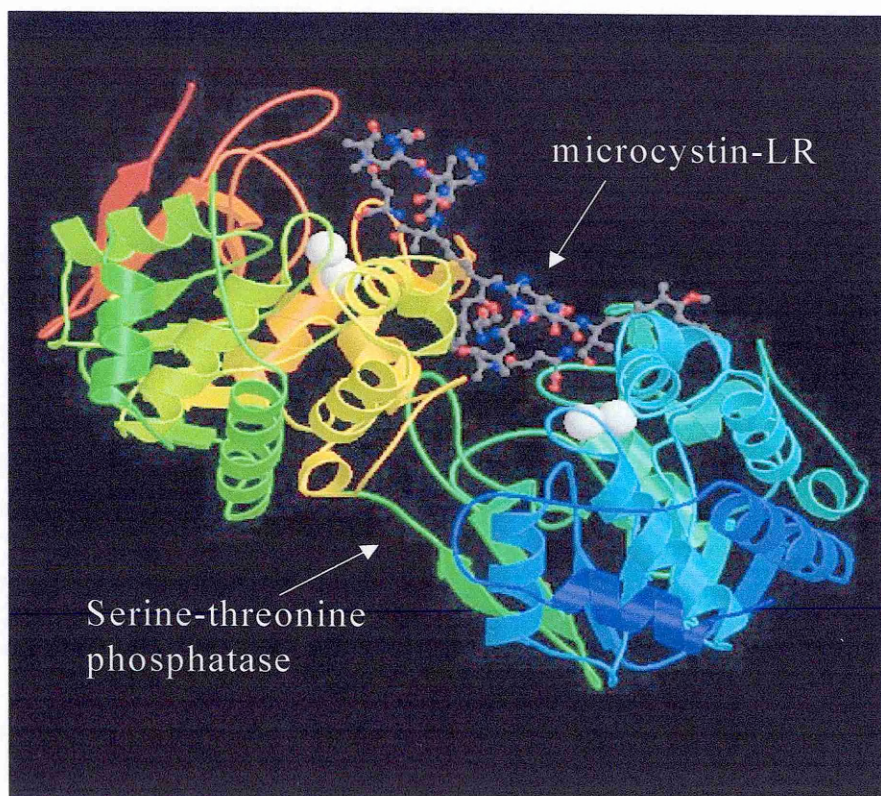


Figure 1.3: Protein serine-threonine phosphatase 1 isoform type complex (ribbons). Microcystin-LR toxin is in the center of the picture (bold and sticks) (<http://www.rcsb.org/pdb>).

1.2.2 Microcystin-LR as Liver Tumour Promoters

The importance of the risk from cyanotoxin became apparent with the realisation that, as inhibitors of protein phosphatases, microcystins, and nodularin could also be tumour promoters. The evidence was obtained from the high incidences of primary liver cancer in China, which is closely associated with drinking water contaminated with cyanobacteria, the microcystins have been presumed to be one of the possible environmental tumour promoters for humans (Carmichael, 1997). To date, no data has been available on the mechanism by which those toxins are responsible for promoting tumours.

1.3 AMNESIC SHELLFISH POISONS: DOMOIC ACID

Domoic acid (DA) is a water-soluble, natural excitatory and neurotoxic amino acid, previously isolated from two red algae: *Chondria armata* and *Alsidium coralliu*. This toxin can also originate from marine diatoms (such as *Nitzchia pungens*), mussels (such as *Mytilus edulis*) or crabs and anchovies. The marine alga *Nitzchia pungens* tends to grow, or bloom, in cold waters, particularly during the autumn and spring seasons. It is a single-celled diatom that floats on the surface and at midwater levels.

Whilst the alga *Nitzchia pungens* itself is never consumed by humans; it can pass through the food chain to finfish, molluscs, and crustaceans. Domoic acid is heat-resistant and cannot be removed from seafood products by cooking. On ingestion by humans, DA contaminated shellfish may cause an intoxication syndrome known as amnesic shellfish poisoning (ASP). The ASP syndrome is characterised by gastrointestinal symptoms such as vomiting, cramps, and diarrhoea and by neurological symptoms including severe headache, seizures, and either temporary or permanent memory loss.

Domoic acid (Figure 1.4) is similar in structure to the excitatory dicarboxylic amino acid, kainic acid. In comparison with kainic acid, domoic acid probably has an agonistic effect at the glutamatergic kainate receptors in the dorsal hippocampus of the brain, competing with glutamic acid as a neurotransmitter. Domoic acid has been shown to have three times greater affinity than kainic acid for the kainic acid receptor (Osada *et al.*, 1995). Due to the worldwide distribution of toxigenic alga species, there is considerable interest in rapid detection methods for domoic acid, especially in public health agencies and seafood industries.

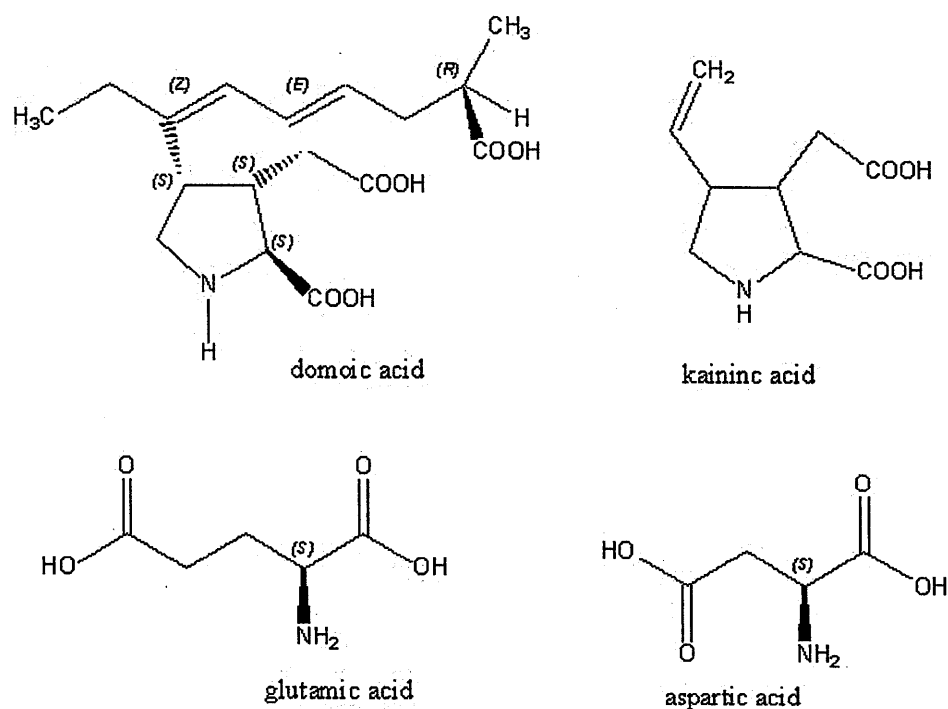


Figure 1.4: Structure of domoic acid and analogues.

1.4 LEGISLATION AND ENVIRONMENTAL MONITORING

The implication of microcystins as the major contributing factor in liver failure and death of at least 52 humans, in 1996, at a haemodialysis center in Caruaru (Brazil) highlights the role of cyanotoxins as a health hazard in drinking water. Since most of the world's reservoirs and lakes-based water supplies are subject to increasing nutrients levels, it is probable that episodes of cyanotoxin poisoning will continue unless measures are taken to improve our understanding of their role in water-based disease (Codd *et al.*, 1999).

Considering the current knowledge of microcystins toxicity, the World Health Organisation (WHO) has proposed a provisional guideline value of $1 \mu\text{g l}^{-1}$ microcystin-LR in drinking water (free and cell-bound toxin), since microcystin-LR is the most known and abundant toxin amongst the microcystin family.

Recently, Ueno (Ueno *et al.*, 1999) published results from a long-term study that investigated the chronic oral toxicity of microcystin-LR on female mice. The report recommended a value of $0.01 \mu\text{g l}^{-1}$ as a maximum acceptable level for microcystins in drinking water. In order to measure these low concentrations of microcystins in drinking and surface water, a highly sensitive analytical method is required. Both the low concentration and the large number of more than 60 known analogues of microcystins represent a considerable challenge for the analysis of microcystins.

With regard to the presence of marine toxins, several poisoning episodes have been reported in the last 20 years. During the winter of 1987, 153 people suffered from acute intoxication after consuming cultured blue mussels (*Mytilus edulis*), originating from Prince Edward Island in Charlottetown (Canada) (Clark *et al.*, 1999). The cause of the intoxication was ascertained to be domoic acid, a natural product of some marine phytoplankton. This was the first recorded human poisoning with phytoplankton responsible identified as the pinnate diatom, *Nitzschia pungens*. The scallops grazing on this phytoplankton concentrated the toxin in their mid-gut gland (hepato-pancreas). Since this initial occurrence, several other incidents have occurred at various sites throughout Canada, the USA, and Europe.

In Monterey Bay (CA, USA), domoic acid was identified in anchovies and pelicans; the source of domoic acid on this occasion was found to be *Pseudonitzschia australis*. In Washington and Oregon states (USA), domoic acid was found in razor clams and crabs harvested in November 1999. In Canada, control mechanisms have been put in place to prevent harvesting if domoic acid levels reach a concentration of greater than or equal to $20 \mu\text{g DA g}^{-1}$ in edible tissues; this limit has now been adopted in Europe. This regulatory level allows a maximum 5,000-fold dilution of the samples containing this DA level. Since the incidences of domoic acid are so widespread, the need for rapid identification and screening of this toxin is emphasised (Hallegraeff, 1993).

1.5 DETECTION OF WATER TOXINS

The most common methods used for the detection of marine and freshwater toxins are:

- Bioassay
- Chromatography techniques
- Chemical assay
- Immunoassay techniques

Recently, new approaches based on artificial receptors, have attracted great interest (Carmichael, 1992) and offer scope for rapid, inexpensive and accurate detection systems.

1.5.1 Microcystins

The mouse bioassay is a rapid, low technology test, which requires licensed, specially trained operators. It is the longest established technique, and in the past was the most extensively used method for the determination of toxins, especially as an initial screen for detecting the presence of toxins in cyanobacterial blooms or cultures. Quantification of toxicity is still determined as: the concentration of test material, which is lethal to 50 % of the population of the animals dosed (LD_{50}). In the case of cyanotoxins, from the signs of poisoning it is possible to distinguish hepatotoxins from neurotoxins and even the different types of neurotoxins (Carmichael, 1997). The disadvantages of the mouse bioassay include its inability to detect low levels of toxins, especially in drinking water supplies, and the failure to distinguish between homologues of different toxins. The mouse bioassay is fast being replaced by other bioassay, chemical and immunological methods. For a number of years, the routine analysis of microcystins has been carried out by high-performance liquid chromatography (HPLC), which is often hindered by the sample processing steps required prior to analysis (Meriluoto, 1997).

In the case of microcystins and nodularin, their toxic effects (through a potent and specific inhibition of serine/threonine protein phosphatases, especially PP1 and PP2),

have made the use of a protein phosphatase inhibition assay, for their detection and screening, particularly attractive (Ash *et al.*, 1995; Ward *et al.*, 1997; Rivasseau *et al.*, 1999).

Recently, enzyme linked immuno-sorbent assay (ELISA), using either polyclonal or monoclonal antibodies have been developed for the detection of microcystins. These assays do not require sample pre-processing and are capable of monitoring microcystins within the guideline levels for drinking water recently set by the WHO.

An immunoassay based on time-resolved fluorometry (TR-FIA) was recently developed for the detection of microcystin in water (Mehto *et al.*, 2001). The assay was performed in a competitive mode and utilised a monoclonal antibody raised against microcystin-LR. In an attempt to avoid problems of steric hindrance in the antibody-antigen reaction, a relatively small marker molecule (europium), was coupled to microcystin. The sensitivity of the assay was $0.1 \mu\text{g l}^{-1}$. Nevertheless, this method does not seem to be appropriate for *in situ* experiments, mainly because of the laborious protocol.

1.5.2 Domoic Acid

Several analytical methods have been developed for the quantitative determination of domoic acid in shellfish and marine phytoplankton. The original method used for the detection of this toxin was the mouse bioassay, involving intra-peritoneal injection of mice with an acidic extract of whole mussels. A positive effect produces a characteristic syndrome in mice, that is distinct from other marine toxins (Iverson *et al.*, 1989). This method has been replaced by liquid chromatographic methods, which have greater sensitivity and do not require animal facilities and immunochemical methods (Mos, 2001).

Since domoic acid possesses a conjugate diene moiety, regulatory agencies have employed a liquid chromatographic method with photodiode-array ultraviolet detection (LC-UV), which showed a detection limit of $0.5 \mu\text{g DA g}^{-1}$ (100 times better than mouse

bioassays) (Lawrence, 1989). More recently, a new rapid, sensitive liquid chromatographic (LC) method was developed for the determination of DA in various marine samples. The DA in marine biological materials was derivatised with 4-fluoro-7-nitro-2,1,3-benzoxadiazole and analysed using isocratic reversed-phase LC with fluorimetric detection. This fluorescent derivatisation method is very sensitive and has a detection limit of $1 \mu\text{g l}^{-1}$ (James *et al.*, 2000).

A sensitive liquid chromatographic-mass spectrometry (LC-MS) method has also been developed for the determination of DA in various marine biological samples. The characteristic fragmentation pathways for DA were established using multiple stage MS on selected daughter ions, which were sequentially trapped and fragmented. This method was applied to determine the concentration of DA in scallop tissues, which subsequently led to the closure of several shellfish harvesting sites on the west coast of Ireland (Furey *et al.*, 2001).

An assay for domoic acid, which utilises a cloned rat (GLUR6) glutamate receptor, expressed in cell membranes, has been developed by Van Dolah (Van Dolah *et al.*, 1997). Applications of the assay to analyse domoic acid in seawater and shellfish has been also reported (Quilliam, 1999). Moreover, the detection of domoic acid by an enzyme immunosorbent assay has gained significant interest leading to enhance anti-domoic acid antibodies production during the last decade.

1.6 IMMUNOASSAY

1.6.1 Antibody as Immunochemical Reagent

Antibodies (=Immunoglobulins, e.g. Ig) are multifunctional binding proteins. They are produced by the immune system of vertebrates and form an essential part of the defence system. Antibodies are responsible for specific recognition of pathogens, toxins, and xenobiotics.

Any foreign substance, which induces specific antibody synthesis after its injection into the body, is an antigen (antibody generator). Antigens are principally macromolecules, e.g. proteins, polysaccharides, or nucleic acids. The part of an antigen, which binds an antibody, is called an antigenic determinant or epitope. An antigen usually displays several different epitopes. The protective function of antibodies is related to their ability to form specific antigen-antibody complexes, which subsequently activate defined effector mechanisms of the immuno-system; followed by neutralisation, destruction, and elimination of the antigen. The manner in which antibodies are produced gives rise to the specificity that they possess and, ultimately, the discriminating power that is harnessed as the basis for all immunochemical techniques for targeted detection and analysis. Low molecular weight antigen molecules (haptens), such as toxins less than 1kD in size, do not elicit an immune response. Immunogenicity can be realised, however, if the hapten is conjugated to a larger globular carrier protein that is naturally immunogenic (Hock, 1997).

1.6.2 Antibody Structure and Function

Antibodies can be found in varying proportions in serum as five distinct immunoglobulin (Ig) classes referred to as: IgA, IgD, IgE, IgM and IgG. These all differ from one another in function, valency (number of binding sites), molecular mass, amino acid composition, and carbohydrate content. IgG can be divided into four subclasses and is the most abundant, at 80 %, of total immunoglobulins in serum (Roitt, 1994).

IgG is a monomeric protein consisting of four tightly folded polypeptide chains, in a 'Y' shape conformation, with an average molecular mass between 146-160 kDaltons (kD). These chains consist of two large or 'heavy' chains and two smaller or 'light' chains. The light (L) chains have a molecular mass of about 25 kD and are common to all classes of immunoglobulins. Whereas the heavy (H) chains, 55-77 kD, differ structurally depending upon the class. Each chain is divided into a constant region (C_L and C_H) and a variable region (V_L and V_H). The 'Y' conformation is linked by disulphide bonds and can hinge to enable the binding of both N-terminal antigen-binding

sites. Thus, IgG has a binding valency of two. The binding arms are known as Fab and $F(ab')_2$, whereas the constant region which binds to the lymphocyte is termed Fc (the crystallisable fragment). The variable regions arise from hypervariable regions of the coding genes, resulting in a great variation of amino acid sequence and diverse specificity (Harlow *et al.*, 1988). A basic immunoglobulin structure is presented in Figure 1.5.

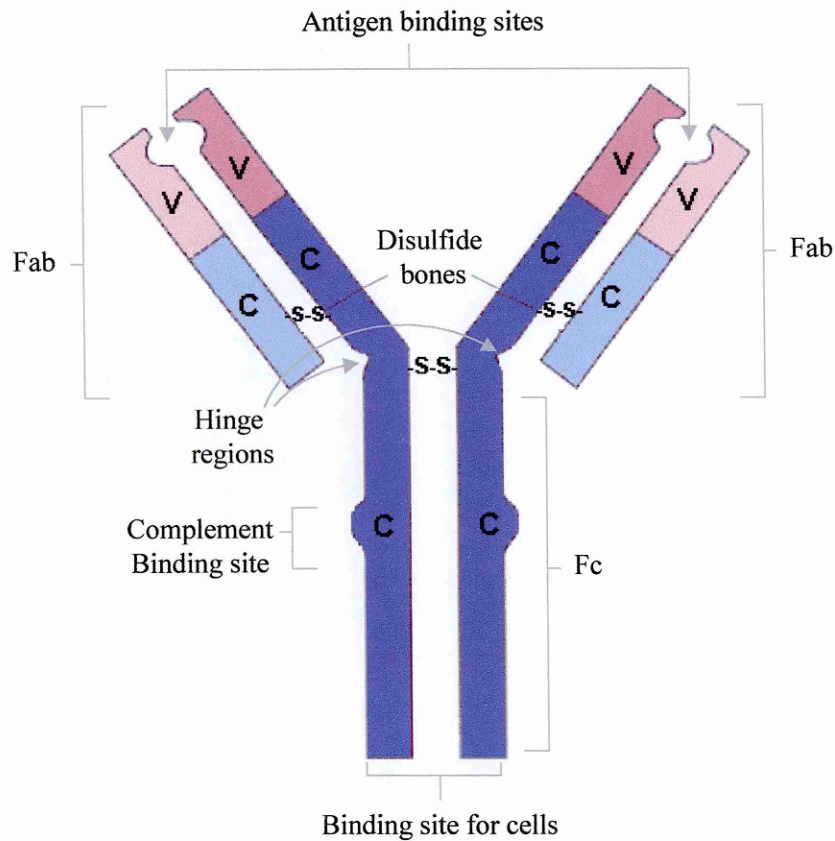


Figure 1.5: Basic immunoglobulin structure.

Two very different forms of antibody preparation are available, each with differing specific binding properties: polyclonal antibodies and monoclonal antibodies. Both

forms of antibody are produced in entirely different ways, and are suitable for different applications, depending upon their binding specificity and the assay requirements.

1.6.3 Polyclonal Antibodies

Since antibodies are produced in response to foreign molecules, by challenging an animal's immune system with an antigen (to which antibodies are desired), antisera can be collected. An antiserum is the product of many responding clones of lymphocytes (polyclonal), and is as a result heterogeneous at many levels: in the classes and subclasses (isotypes) of the antibody produced, in their specificity, titre, and affinity. Within the antisera, there may be antibodies to several separate antigens (polyspecific), to a few antigens (oligospecific) or to a single antigen (unispecific). However, even a unispecific reagent is not homogeneous as single immunogens are still multi-determinant structures, which stimulate a polyclonal, multi-determinant-specific response often displaying several isotypes.

The major advantage of polyclonal antisera is their ability to form large insoluble immune complexes with antigen, and aggregate cells easily, such that the reactions can be determined spectro-photometrically. This broad binding nature of polyclonal antisera is a useful property, and is utilised for many enzyme immunoassays (EIAs) especially as an antigen-capture antibody preparation.

Due to its multispecificity, conventional antisera cannot be prepared either easily or routinely to the degree of specificity often required. Although purification is beneficial, an antibody preparation demonstrating complete homogeneity is often preferred. Monoclonal antibody preparations, however, provide this characteristic.

1.6.4 Monoclonal Antibodies

Antibody preparations of monoclonal origin are homogeneous, in specificity, affinity, and epitopes. Unlike polyclonal antisera, monoclonal antibodies are produced *in vitro* and secreted from a single cloned hybrid cell, called a hybridoma. This difference allows the homogeneity of monoclonal antibodies preparation; where each monoclonal product is monospecific to a single epitope, due to the identical amino acid and tertiary structure of its variable region. The hybridoma is produced by the fusion of a lymphocyte from the spleen of an immunised animal with a type of B-cell tumour known as a myeloma cell. Successfully fused hybridomas possess the antibody-secreting characteristic of the original lymphocyte, whilst also gaining the immortal tumour properties of the myeloma (Köhler *et al.*, 1975).

In contrast to antisera, monoclonal antibodies can solve many of the problems concerning sensitivity and specificity that accompany the use of polyclonal reagents in assays for soluble antigens. This renders many assays that were previously complex more routine and much simpler to perform, as well as extending the range of molecules available for investigation. With regard to production, another advantage is that each monoclonal antibody's specificity can be prepared and maintained almost indefinitely *in vitro*, in unlimited quantities, resulting in the availability of standardised reagents.

The major disadvantages of monoclonal antibody included the cost of production and lack or poor antigen-precipitation properties as single reagents. This drawback is reduced if mixtures of monoclonal antibodies are used. However, polyclonal antisera can fulfil this role.

1.6.5 Antibody-Antigen Interaction

Immunoassays can be defined as analytical methods that are based on the detection and measurement of the antibody-antigen reaction. Two essential elements of an immunoassay system are the reagents and the format. Reagents include antibodies,

antigens, and other chemicals used to visualise the primary binding reaction. The format refers to the device or system into which the reagents are placed to perform the assay.

One of the first immuno-analytical techniques developed was the radio-immunoassay (RIA), based on the isotopic labelling of the antigen or the antibody. It constituted a great advance in the field of quantitative immunoassay, taking advantage of the high sensitivity inherent in the radioactivity-based measurements. The next important advance in immunoassay was the development of the enzyme immunoassay (EIA) (Puchades *et al.*, 1992). The principles and procedures of EIAs are similar to those of RIA techniques, except that instead of using a radiolabel, an enzyme-label is used, activity being measured by enzyme action upon a specific substrate. One of the most widely used EIA methods is the enzyme-linked immuno-sorbent assay (ELISA). Other important immunochemical techniques include fluorescence immunoassay (FLIA) and chemiluminescence immunoassay (CLIA).

Immunoassays techniques can be classified as either heterogeneous or homogeneous. Heterogeneous immunoassays are characterised by the requirement for separating the free from the solid phase bound fraction. Either the bound fraction is used for signal generation (as is the case for solid phase enzyme immunoassays) or the unbound fraction, as similar to the radio-immunoassays (RIAs).

In contrast, homogeneous immunoassays do not require any phase separation, i.e. the physical separation of free and antigen-bound components. Antibody-ligand binding as well as detection (by means of a tracer) takes place in a homogeneous solution. The detection principle is based on the fact that the antibody not only binds the tracer but also influences the subsequent reaction of the tracer. The omission of a separation step simplifies the assay compared to the heterogeneous approach. However, interferences by matrix effects play a significant role, whereas phase separation in heterogeneous assays removes a significant proportion of the interfering substances. Therefore heterogeneous immunoassays are much more common than homogeneous assays; they are used in practically all commercial immunoassays as well as immunosensors.

1.6.6 Enzyme-Linked Immuno-Sorbent Assay

The enzyme-linked immuno-sorbent assay (ELISA) is among the most widely used analytical techniques and has been applied successfully to an extensive range of substances, from single molecules to whole cells. The ELISA technique can be performed using a competitive, non-competitive or displacement format. With the competitive ELISA, either the antigen or antibody is conjugated with a label and competes with the unlabelled antigen (in the sample) for binding sites. Two different set-ups are possible: either the antigens are immobilised on the solid support and the binding of labelled antibodies is divided proportionally between free and immobilised antigen, or the antibodies are immobilised and labelled antigens compete with free antigens (analyte) for binding sites. Non-competitive assays involve an immobilised antibody capturing the antigen and a second, labelled antibody in solution that binds to a different epitope of the antigen, forming a “sandwich” and generating the signal. This format requires relatively large antigens, as they have to possess two distinct epitopes for antibody binding; this approach is not applicable for low molecular weight molecules. With the third format, the displacement assay, the binding between antibody and labelled antigen occurs prior to contact with the sample. The free antigen from the sample, subsequently, displaces a proportion of labelled antigen, resulting in a signal reduction. To ensure preferential binding of the free antigen, the labelled compound is often an antigen-derivative, for which the immobilised antibodies possess a lower affinity. While direct measurement techniques measure the binding event between antigen and antibody, indirect techniques rely on the use of a label to generate a signal. Figure 1.6 shows the different assay formats for immunoassays.

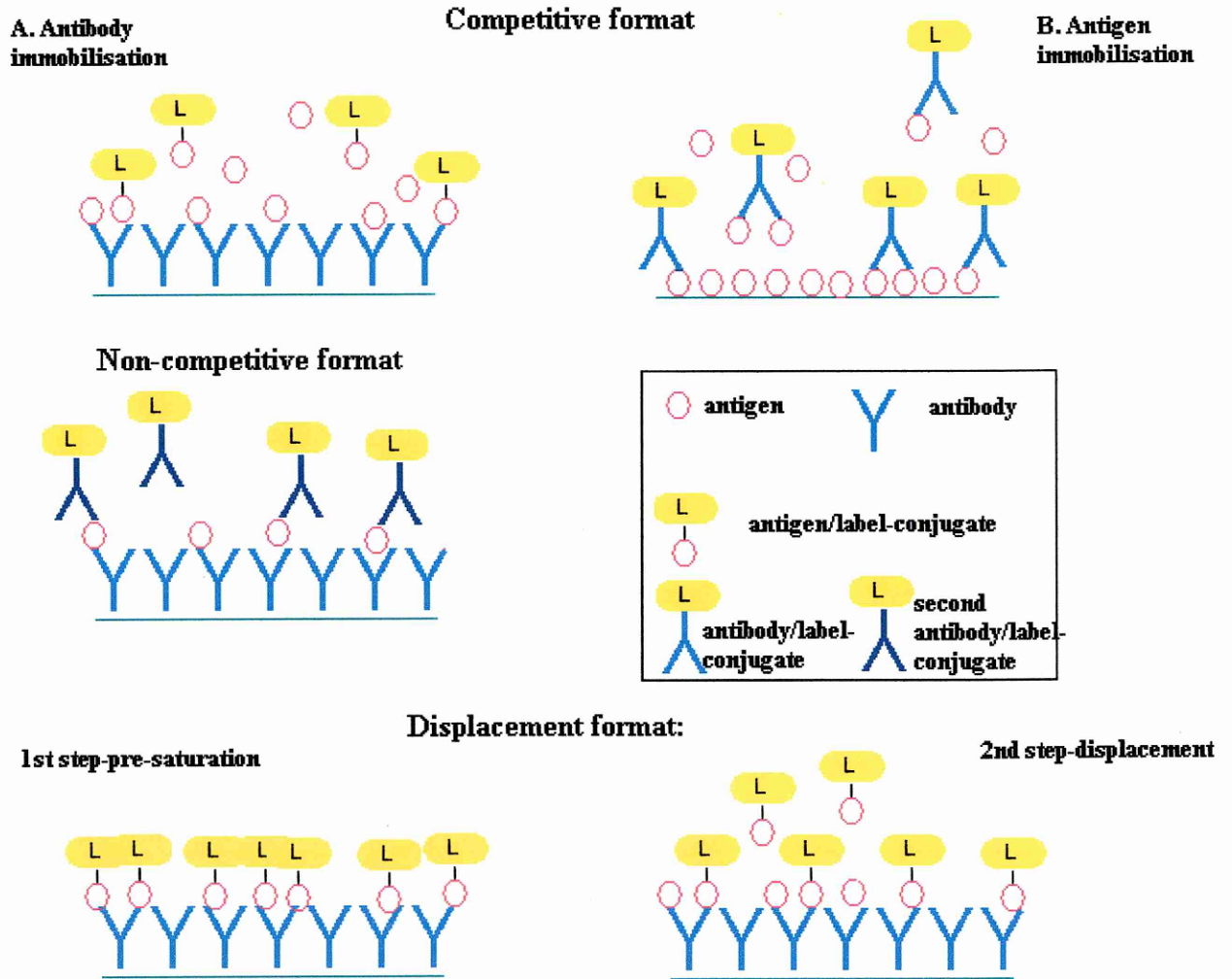


Figure 1.6: Schematic representation of different immunoassay formats.

Assay specificity describes the ability of an antibody to produce a measurable response only for the analyte of interest. Cross-reactivity is a measurement of antibody response to substances other than the analyte. A binding site is the unique specificity of the antibody that renders them so useful in analytical techniques, it is not surprising that the analysis of specificity and cross-reactivity should form an important part of the evaluation for any immuno-analytical technique.

Many different polyclonal and monoclonal antibodies for algal toxins have been raised in the last 15 years (Baier *et al.*, 2000). The first ELISA, reported by Chu (Chu *et al.*, 1990), was based on a direct competitive ELISA format and involved coating anti-microcystin-LR antibodies on a microtiter plate and using microcystin-LR-peroxidase as the enzyme marker. This latter competed with free microcystin-LR in the samples, for binding to the antibody sites. This ELISA assay showed a working range of 0.5 to 10 $\mu\text{g l}^{-1}$, with a minimum detection level of 0.2 $\mu\text{g l}^{-1}$ in water, largely below the WHO requirement. Likewise, An (An *et al.*, 1994) used anti-microcystin-LR polyclonal antibodies and developed an ELISA kit with a working range of 0.5-50 $\mu\text{g L}^{-1}$.

More recently, monoclonal antibodies against microcystin-LR have been developed by two Japanese research groups (Saito *et al.*, 1994; Nagata *et al.*, 1995b; Nagata *et al.*, 1997). Sensitivity in the range of $\mu\text{g l}^{-1}$ (ppb) was reported and the assay was used to detect microcystins in environmental samples.

An ELISA developed with anti-domoic acid serum raised in rabbits was effective in determining domoic acid concentrations in rat urine, with a reported lower quantification limit of 40 $\mu\text{g l}^{-1}$ (Osada *et al.*, 1995). The successful production of a domoic acid immunogen and the development of a competitive ELISA led to the accurate determination of domoic acid concentrations in human plasma, urine and milk (Smith *et al.*, 1994).

With regard to monoclonal antibodies for domoic acid, the only report of their use in an immunoassay was from Kawatsu (Kawatsu *et al.*, 1999). The antibodies, obtained from mice were highly specific for domoic acid and showed minor cross-reactivity with the isomers of domoic acid. An indirect competitive enzyme immunoassay was developed for the measurement of domoic acid. The working range for the quantitative measurement of domoic acid and the quantification limit for the toxin in shellfish were estimated to be 0.15-10 $\mu\text{g l}^{-1}$ and less than 0.04 $\mu\text{g g}^{-1}$, respectively.

As an alternative to conventional immunoassay procedures, considerable attention is now being given to the development of biosensors that can provide continuous, *in situ*, and rapid measurement of biochemical concentrations in environmental monitoring.

1.7 BIOSENSORS

In general, a biosensor can be defined as an analytical device incorporating a biological or biologically derived sensing element, which is either intimately associated with or integrated within a transducer (Turner, 1987). More recently the IUPAC definition of an electrochemical biosensor has been given as: a self-contained integrated device, which is capable of providing specific quantitative or semi-quantitative analytical information using a biological recognition element (biochemical receptor) which is retained in direct spatial contact with an electrochemical transducer (Thévenot *et al.*, 2001). The biological sensing elements that have been applied to biosensors are wide ranging including enzymes, antibodies, receptors, membranes, tissue, cells and organelles (Tothill *et al.*, 1996).

The transducer detects the interaction of the biospecific-sensing element with the analyte. The signal generated by the transducer requires amplification and processing, hence a signal processor is employed to convert this signal into a processable form. An overview of different transducer principles used in biosensor construction is shown in Figure 1.7.

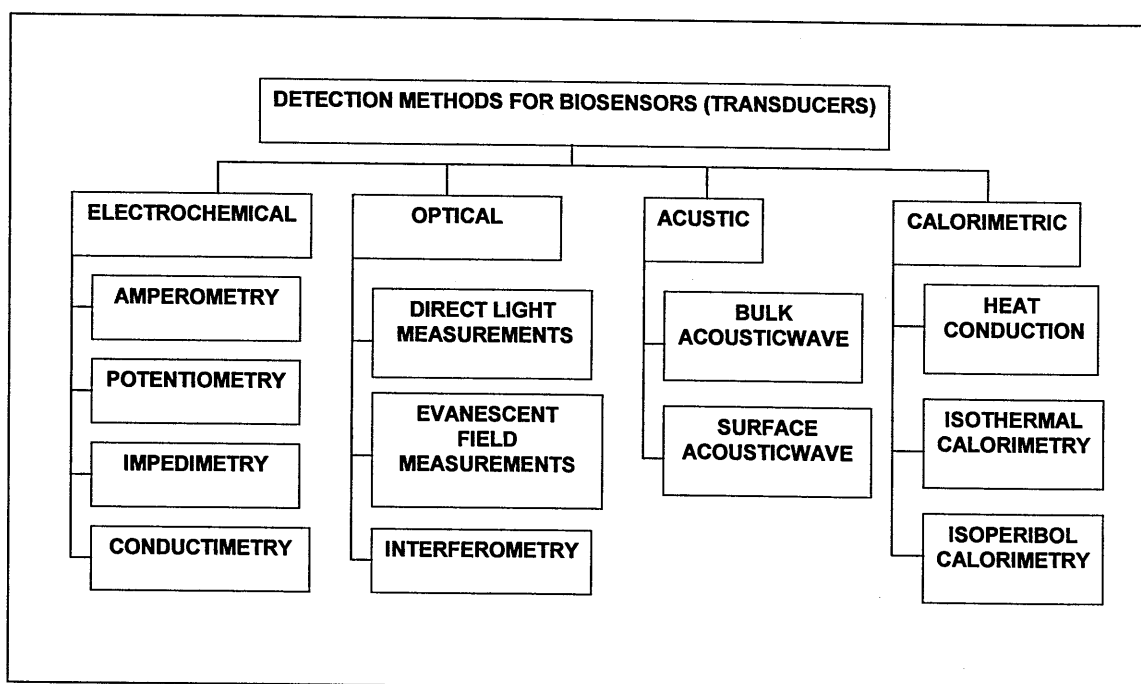


Figure 1.7: An overview of transducer principles in biosensor construction (Kröger, 1998).

Since the first “enzyme electrode” reported by Clark (Clark *et al.*, 1962), many electrochemical biosensors have been developed with broad applications in medicine, the food industry (Issert *et al.*, 1997) and more recently for environmental monitoring (Marco *et al.*, 1996). The ideal enzymes for biosensors can be characterised as possessing high stability, activity, purity, and abundance that allows a low cost. The enzymes glucose oxidase and horseradish peroxidase have found a particular niche in biosensors and have been reviewed by Wilson (Wilson *et al.*, 1992) and Ryan (Ryan *et al.*, 1994). Very recently, a few papers have been published describing biosensors based on magnetic transduction (Tothill *et al.*, 2003).

1.7.1 Electrochemical Analysis

The predominant electrochemical analysis system for biosensors involves hydrogen peroxide (H₂O₂) detection. Hydrogen peroxide can be detected by both oxidation and

reduction and is particularly important for environmental analysis due to its extensive use in industry as a sterilant and in wastewater treatment (Thomas, 1995). Many enzyme catalytic transformations utilize H_2O_2 , which makes it ubiquitous in biological reactions. The oxidation reaction of glucose by glucose-oxidase produces gluconolactone/gluconic acid and H_2O_2 . Horseradish peroxidase utilises H_2O_2 as its substrate and is a widely used enzyme marker for immunological detection, enabling the reaction to be monitored electrochemically in addition to spectrophotometrically with the aid of redox substrates. H_2O_2 can, therefore, be used to monitor reactions as either a consumed reactant or an increasing product. However, direct electrochemical H_2O_2 detection, requires large potentials. This can lead to problems arising from interference due to other electroactive species present in a sample such as ascorbic or humic acids. Solutions to reduce interferences have included the application of selectively permeable membranes (Christie *et al.*, 1992), noble metals acting as catalysts for electron transfer (Gorton *et al.*, 1991) and the use of mediators.

Electrochemical biosensors (amperometric, potentiometric, conductometric and impedimetric) are an attractive proposition allowing cost effective, large volume testing which could be conducted outside the laboratory. The biosensors can be produced by thick-film printing technologies such as ink-jet printing, cavro-printing, and especially screen-printing (Nagata *et al.*, 1995a; Newman *et al.*, 1995). This allows the cheap mass production (Alvarez-Icaza *et al.*, 1993) of small, plastic, and disposable electrodes, as demonstrated by the success of the ExacTech glucose biosensor pen electrodes (Thornton *et al.*, 1991).

1.7.2 Affinity Sensor: Immunosensors

By utilising the affinity and immunorecognition properties of antibodies through 'immunosensors', the specific binding events with antigens can be monitored without relying upon any inhibition mechanism (Hock, 1997). Immunosensors have been reviewed by Marco *et al.* (1995) and more recently by Ghindilis *et al.* (1998) and Mallat *et al.* (2001a). Ghindilis *et al.* stated that the possible advantages of

of immunosensors over conventional immunoanalysis methods are: an increase in sensitivity and a decrease in detection limit, a decrease of analysis time, simplification of the analysis procedure (fewer stages), miniaturisation of equipment and automation. The same principles for EIAs can be transferred and modified for immunosensors, which are often competitive because of the small size of the analytes (Tothill, 2001).

Immunosensors can be divided into direct and indirect measurement devices, with direct devices detecting the recognition event between immuno-reagent and analyte and indirect devices relying on a label, such as an enzyme, to create the signal. The direct approach appears simpler and therefore more desirable, but is not often employed. One example of a direct optical immunosensor is the BIAcore, which employs surface plasmon resonance (SPR). While direct immunosensors might offer great potential for the future, to date, the majority of immunosensors developed for small molecules analysis have been based on indirect measurements using enzyme labels.

A schematic representation of an immunosensor is presented in Figure 1.8.

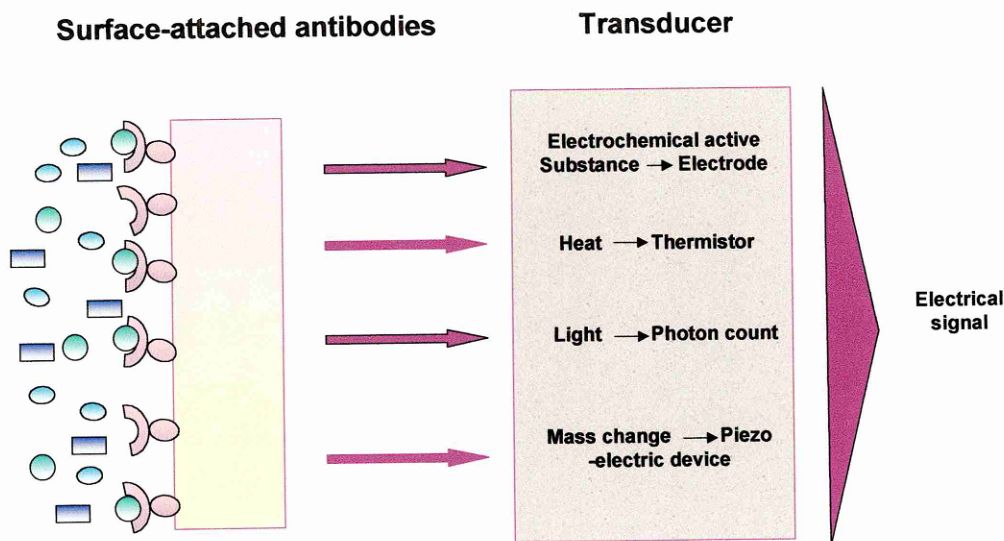


Figure 1.8: Scheme of the general immunosensor design depicting the intimate integration of immunological recognition at the solid-state surface and the signal transduction.

Electrochemical immuno-sensing has also been applied to quasi-continuous ‘flow-through’ monitoring, analogous to immuno-affinity chromatography where the antibodies are bound to a matrix column, containing a dispersed carbon material that also functioned as a working electrode (Ghindilis *et al.*, 1997).

The performance and applications of the prototype FIA River ANALyser or RIANA system has been described recently by Mallat (Mallat *et al.*, 2001b). The RIANA system incorporates immunoanalysis of multiple analytes based upon total internal reflection fluorescence within 15 minutes for each analysis. Antibodies labelled with a fluorescent dye compete with the free analyte. The transducer consists of a quartz slide with spatially resolved surface modifications for antigen derivative immobilisation, along which a coupled laser beam propagates by total internal reflection. The surface bound antigen corresponds to the reflection spots of the propagated laser, which excites bound

fluorophore labels present in the evanescent field. The fluorescence corresponding to each analyte is detected in parallel via individually coupled fibre optics.

A recent development has been the application of membrane-integrated receptor systems for analyte recognition and signal transduction in biosensors (Scheller *et al.*, 2001b). The proper functioning of biosensors depends essentially on the immobilisation of the ligand on the sensor surface, their correct orientation and homogeneity. It is obvious that recombinant approaches for the synthesis of bio-molecules for the recognition part of the biosensor can meet the demand for homogeneous preparations in virtually unlimited amounts. In addition, they are also used intensively for the modification of available structures, e.g. for the attachment of anchor groups, change of binding properties or improvement of stability.

With respect to toxins detection, there is great interest in the use of biosensors, mainly because they would represent an important step forward in environmental detection. There are few reports regarding the use of sensor technology for toxin detection. A chemiluminescent immunosensor, integrated in a flow injection analysis system, was developed for the detection of a 'diarrheic shellfish poisoning' (DSP) toxin okadaic acid (OA). Anti-OA monoclonal antibodies were labelled with horseradish peroxidase for their use in a competitive assay, in which the free antigen of the sample competes with immobilised OA. Based on commercially available polyethersulfone membranes, this bioanalytical system exhibits low non-specific binding of antibodies in the presence of mussel homogenate. The immunosensor was used in a semi-automated analysis procedure in which the free OA containing sample was injected in the flow system concomitantly with the labelled antibodies. With an overall measurement time of 20 min, the immunosensor has a detection limit of 0.2 μg OA/100g mussel homogenate (Marquette *et al.*, 1999).

Yang (Yang *et al.*, 1999) used a biosensor based on surface plasmon resonance (SPR) to examine the effects of three microcystins, -LR,-RR,-YR, on the binding between PP-2A and its substrate phosphorylase-a (PL-a) during the first step of the interaction. The SPR

biosensor provides real-time information on the association and dissociation kinetics of PL-a with immobilised PP-2A in the absence and presence of microcystins. It was found that the affinity of PL-a to microcystin-bound PP-2A was five times smaller compared to unbound PP-2A, due to a 50 % decrease in the association rates and a two-fold increase in the dissociation rates of PL-a binding to PP-2A. The test of sensitivity to any compound likely to inhibit PP-2A activity, through a specific binding to the enzyme, is significant since it gives a measure of the whole toxinogenic potential of the sample. However, in samples responding positively, the accurate toxin determination and identification requires the complementary use of an analytical technique such as LC-UV or LC-MS.

1.8 MOLECULAR IMPRINTED POLYMER

Although immunosensors have the potential for diverse analyte detection, they are often limited by the availability, stability and the price of the antibody required. Researchers have attempted to replace antibodies and biological receptors with smaller, more stable counterparts, and have been searching for alternative ways to obtain antibody-like receptors. This has led, for example, to the development of 'minibodies' and 'diabodies', which are bio-engineered antibody fragments. These are smaller than antibodies but retain the ability to bind an antigen (Cortese *et al.*, 1996).

An alternative approach involves the use of artificial receptors. The design and synthesis of bio-mimetic receptor systems (Lehn, 1995), capable of binding target molecules with affinities and specificities on a par with natural receptors, is regarded as one of the greatest challenges in bioorganic chemistry. One technique that is being increasingly adopted for the generation of artificial macromolecular receptors is molecular imprinting.

Molecularly imprinted polymer (MIP) can serve as artificial binding mimics of natural receptors and can be used as a recognition element for immunoassay-type analyses. The

molecularly imprinted sorbent assays (MIAs) described by Vlatakis (Vlatakis *et al.*, 1993) were based on competitive radioligand binding protocols and not only showed a very good correlation with antibody-based enzyme immunoassays, but also displayed a cross-reactivity profile very similar to those reported for natural receptors. The applicability of the artificial antibodies was exemplified by their use in a new ligand-binding assay for the accurate determination of drug levels in human serum. Under favourable binding conditions, the artificial antibodies exhibited K_d values as low as 10^{-8} M. The recognition sites obtained by molecular imprinting, typically, possess binding affinities approaching those demonstrated by antibody-antigen systems and have been called “plastic antibodies” (Ramstrom *et al.*, 1998).

There are several reasons why the use of such synthetic recognition materials as substitutes for biomolecules are attractive:

- Superior stability in harsh conditions such as high temperature, pressure, (e.g., sterilisation conditions), extreme pH values, and organic solvents
- Ease of preparation
- Relatively low cost of production
- Easy integration in standard micro- and nano-fabrication processes

These are all relevant advantages of MIP versus biomolecules as antibodies (Sellergren, 1997b; Haupt *et al.*, 1998b). Moreover, this approach obviates the need for animals, which are used to produce antibodies.

It is of particular relevance that polymers can be imprinted with compounds against which natural antibodies are difficult to obtain, such as immunosuppressive drugs and small non-immunogenic molecules. Small compounds have to be coupled to a carrier molecule in order to raise antibodies against them. Antibodies raised against these small molecules have sometimes very low affinity and high cross-reactivity with many other similar compounds, because antigenic properties may often change considerably as a result of the coupling step.

Molecular imprinting of synthetic polymers (most often polyacrylates or polyvinyl polymers) involves a radical polymerisation of monomers and cross-linker in the presence of a target molecule acting as a template. Removal of the template leaves polymer-binding sites that can specifically recognise the target molecule. Thus, the use of appropriate functional monomers for polymerisation allows for the generation of sites with a geometrical shape and functionalities complementary to the template molecule.

Currently, two basic approaches to molecular imprinting may be distinguished:

- The covalent approach, where the complexes in solution prior to polymerisation are maintained by (reversible) covalent bonds;
- The self-assembly approach, where the pre-arrangement between the imprinted antigen and the functional monomers is formed by non-covalent or metal coordination interactions.

The current upsurge in interest in the technique can be attributed to the development of the conceptually and practically simple non-covalent approach. This 'self assembly' approach is similar to natural processes, since most biomolecular interactions are non-covalent in nature (Sellergren, 1997a; Ramstrom *et al.*, 1998).

1.8.1 Covalent Approach

With the covalent approach, the template molecules are co-polymerised with a cross-linking monomer. In order for the MIP to be useful for chromatographic applications, these interactions must be reversible. Reversible covalent bonds that have been used in MIPs include boronic acid ester linkages and Schiff base formation (Wulff, 1995).

For covalent imprinting, a polymerisable derivative of the imprint molecule has to be synthesised and after synthesis of the polymer, the imprint molecule has to be removed by chemical cleavage. Due to the greater stability of the bonds, covalent imprinting protocols should yield a more heterogeneous population of binding sites (Haupt *et al.*,

2001). The covalent approach leads to restrictions in the choice of monomers; thus covalent MIPs are less popular for many applications.

1.8.2 Non-Covalent Approach

In biological systems, molecular complexes are often formed by a plethora of non-covalent interactions such as hydrogen bonding and ion pairing. Although these interactions, when considered individually, are weak in comparison with covalent bonds, the concerted action of these bonds often leads to complexes with a very high stability. The high degree of specificity that can be achieved, in combination with the dynamic properties of the interactions, makes these bond types a prerequisite for many biological processes.

On this basis, Mosbach and co-workers (Mosbach, 1994; Mosbach *et al.*, 1996) developed a non-covalent MIP approach. The method relied on the formation of a pre-polymerisation complex between monomers carrying suitable functional groups and the template through non-covalent bonds, such as ionic interactions or hydrogen bonding. Using this approach, the functional groups are held in position by the polymeric network. Following polymerisation, the template can be removed simply by solvent extraction. The principal means of re-binding the target molecule to these polymers is achieved again through non-covalent interactions.

Modern polymerisation chemistry offers a broad variety of functional monomers, which can be used for imprinted polymers. Typical interaction types that have been exploited are ionic interactions, hydrogen bonds, P-P-interactions, and hydrophobic interactions. A schematic representation of the non-covalent approach is shown in Figure 1.9.

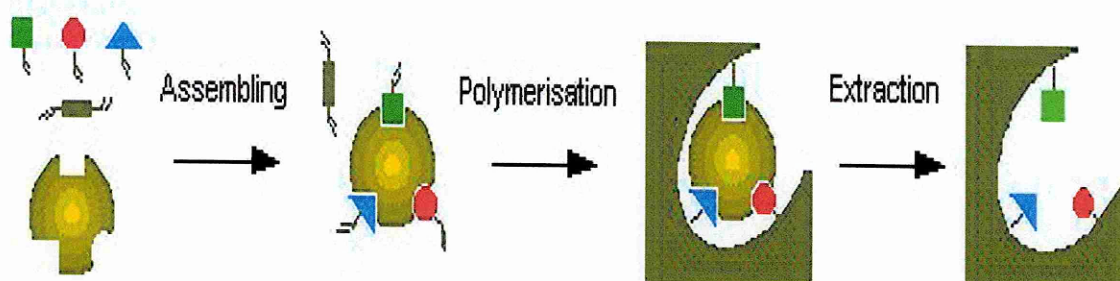


Figure 1.9: Schematic representation of self-assembly approach for molecular imprinting.

The functional monomers are arranged around the imprint antigen as a result of the interactions between complementary chemical functionalities. After polymerisation, the imprint is removed by extraction, exposing recognition sites possessing a “memory” for the shape and chemical functionality of the imprint antigen (Ramstrom *et al.*, 1998).

The non-covalent imprinting approach is more flexible, allowing a greater choice of functional monomers, target templates and imprinting materials. However, the pre-polymerisation complex is an equilibrium system, the stability of which depends on the affinity between the imprint molecule and the functional monomers. Therefore, non-covalently imprinted polymers contain a heterogeneous population of binding sites with a range of different affinities; they are comparable to polyclonal antibodies (Mosbach *et al.*, 1996).

1.8.3 Physical Forms and Preparation Methods of MIP

Traditionally, MIPs have been prepared as bulk polymer monoliths mechanically ground to obtain small micrometer-sized particles. Whereas the material obtained through this somewhat inelegant method still seems to be useful for many applications such as chromatography, other applications require MIPs in defined physical forms, for which specially adapted synthesis methods are needed.

During the past few years, three aspects of MIP preparation have been addressed:

- The synthesis of small spherical particles of below micrometer size
- The synthesis of thin layers
- The creation of surface imprints

MIP nano-beads can be synthesised by different methods such as precipitation polymerisation and emulsion polymerization. MIP microspheres have been readily synthesised using a precipitation, polymerisation method. More precisely, uniform MIP microspheres can be obtained from a dilute monomer solution by controlling the phase separation point during the cross-linking polymerisation. MIP microspheres display binding characteristics similar to the traditional particles obtained by the grinding and sieving method, but with improved binding kinetics. The regular form and narrow size distribution of the microspheres make them easy to handle for various applications, such as MIP-based sensors and ELISA-type assays. Since MIP microspheres display binding characteristics similar to that of an affinity adsorbent with immobilised polyclonal antibodies, they may be used as substitute natural antibodies for various affinity separations, sensors and assays (Ye *et al.*, 2001).

With regard to the emulsion polymerisation approach, Perez (Perez *et al.*, 2000) described molecularly imprinted nanoparticles prepared by core-shell emulsion polymerisation. Particles of this type, prepared with a cholesterol- imprinted ethyleneglycol dimethacrylate shell and in the absence of porogen, were found to be 76 nm in diameter with a surface area of 82 m² g⁻¹. Cholesterol uptake from a 1 mM solution in isohexane was measured at both 10 and 30 mg ml⁻¹, with the imprinted polymer showing considerable binding (up to 57 %).

1.8.4 MIP Application

A large number of substances have been imprinted, for various practical applications. Molecularly imprinted polymers have been used in separation and isolation processes, as antibody and receptor binding site mimics in assay systems and as recognition

elements in biosensors. Molecular imprinting chromatography has been the most extensively studied application area. Of special interest are chiral separations, which have exhibited high separation factors and resolution. Imprinting is highly suitable for separation allowing the preparation of tailor-made supports with pre-determined selectivity. Depending on which enantiomeric form was used as print molecule, the elution order of enantiomers can be controlled (Andersson *et al.*, 1999).

Imprinted polymer based assays are readily carried out using radiolabels, because the labelled analyte has the same structure as the original template. However, this involves the handling of radioactive materials and produces radioactive waste. Other alternative assay formats can use an enzymatic reaction or fluorescence for the detection process. Fluorescence assays are probably among the best adapted for use with imprinted polymers, because they are usually highly sensitive and can be performed in both aqueous and organic solvents (Piletsky *et al.*, 1999).

Silica particles containing surface-bound free radical initiators have been used as a support for the grafting of thin MIP films. This technique offers a means of fine-tuning the layer thickness, for improved kinetic properties or enhanced capacity in chromatographic or sensor application. Thus, polymers grafted as thin films (ca. 0.8 nm average film thickness) on silica with 10 nm average pore diameter showed the highest column efficiency for enantiomer separation (Sulitzky *et al.*, 2002).

The uses of thin imprinted polymer films have been reported on several occasions and seem to be useful for many applications involving MIP. A novel preparation protocol for MIP film coatings for capillary columns has been reported (Schweitz, 2002). The MIP coatings were synthesised *in situ* under conditions that allowed a wide variability of the MIP composition. By immobilizing a photolabile radical initiator to the capillary surface prior to the introduction of the pre-polymerisation mixture, the polymerisation reaction was confined to the vicinity of the capillary surface, resulting in a covalently attached MIP coating. The use of different solvents (porogens) during the polymerisation reaction facilitates control of the MIP coating in term of morphology

and appearance. The MIP coatings synthesised using solvents such as toluene, dichloromethane, and acetonitrile, all provide enantiomer separation of the amino alcohol propranolol, when the S enantiomer was used as a template for the MIP.

A new method in which the polymer is synthesised *in situ* in the wells of a microtiter plate has recently been reported (Piletsky *et al.*, 2000b). Oxidative polymerisation was performed in the presence of template, monomers: 3-aminophenylboronic acid (APBA), 3-thiopheneboronic acid (TBA) and aniline. Polymerisation was carried out in water and the polymers grafted onto the polystyrene surface of the microplate. It was found that this process resulted in the creation of synthetic materials with antibody-like binding properties.

Piletsky (Piletsky *et al.*, 2000a) developed a general method for molecular imprinting the surface of a stable synthetic polymer, which could also be used for the functionalisation of optimised porous membranes with MIPs. Microfiltration membranes made of polypropylene were used as the matrix. Surface photo-graft copolymerisation in the presence of the template desmetryn introduces specific binding sites into the porous membrane without damaging its pore structure and thus preserving its transport properties. Using a benzophenone coating as photoinitiator, 2-acrylamido-2-methylpropanesulfonic acid (AMPSA) as the functional monomer, and *N,N*-methylenebis(acrylamide) (MBA) as cross-linker a suitable MIP membrane was synthesised.

1.8.5 MIP in Assay and Sensor Technology

Early attempts to utilise the recognition properties of MIPs for chemical sensing included development of a conductometric sensor for atrazine (Sergeyeva *et al.*, 1999). A competitive amperometric morphine sensor based on an agarose immobilised molecularly imprinted polymer has also been described (Kriz *et al.*, 1995). The method of morphine detection involves two steps. In the first step, morphine binds selectively to the molecularly imprinted polymer in the sensor. Secondly, an electroinactive

competitor (codeine) is added in excess, hence some of the bound morphine is released. The released morphine is detected by an amperometric method and the morphine could be measured in a concentration range of 0.1-10 mg l⁻¹.

A high-performance MIP based assay using a chemiluminescence-imaging format has been recently reported (Surugiu *et al.*, 2001a). Microtiter plates were coated with MIP microspheres, using poly(vinyl)alcohol as a glue. The microspheres are obtained by precipitation polymerisation and appeared to have a higher number of accessible surface binding sites, compared to a bulk polymer synthesised using the same monomers. The analyte 2,4-dichlorophenoxy acetic acid (2,4 D) was then added, together with a small amount of enzyme-labelled analyte, and incubated until equilibrium was reached. The amount of polymer-bound 2,4-D-peroxidase conjugate was detected using luminol as the chemiluminescent substrate. A flow injection competitive assay, analogous to enzyme immunoassays, has been developed by the same group (Surugiu *et al.*, 2001b). In this paper, they described the development of a flow injection assay using a glass capillary with the inner wall coated with imprinted polymer as a reaction chamber. For covalent coating, the capillary was silanised with (3-methacryloxypropyl) trimethoxysilane. The chamber was then filled with the polymerization solution, and during polymerization a polymer layer formed at the capillary wall; consisting of precipitated MIP microparticles.

In another report, films of TiO₂ were imprinted with chloroaromatic acids (such as 2,4-D) and used as recognition layers for sensors based on ion-sensitive field-effect transistors (Lahav *et al.*, 2001). Selective detection of the sodium salts of the imprinted molecules was possible with detection limits in the micromolar range and an equilibration time of approximately 5 minutes.

One application described the use of a voltammetric sensor for the herbicide 2,4-D. The electroactive compound 2,5-dihydroxyphenylacetic acid was used as a probe instead of the labelled analyte. MIP particles were coated as a thin layer on a disposable screen-printed carbon electrode. The electrode was then incubated with the sample to which the

probe was added. In the presence of the analyte, some of the probe was competitively displaced, and the remaining probe was directly quantified by differential pulse voltammetric measurements (Kröger *et al.*, 1999).

A highly sensitive sensor for the hydrolysis product of the chemical warfare nerve agent soman and sarin has been described (Jenkins *et al.*, 1999); based on a polymer-coated fiber optic probe and a luminescent europium complex used for detection. The complex of europium ligated by divinylmethyl benzoate and by the analyte pinacoyl methylphosphonate was co-polymerised with styrene, after which the analyte molecule was removed by washing. Re-binding of the analyte was quantified from laser-excited luminescence spectra. Although it is not clear whether imprinting had contributed to the selectivity of the sensor, this detection principle appears attractive as very low detection limits can be obtained (7 ppt in this particular case). In following work, the direct imprinting of non-hydrolysed organophosphates (including pesticides and insecticides) has been described. The detection limits for these MIP sensors were less than 10 parts per trillion (ppt), with long, linear dynamic ranges (ppt to ppm) and response times of less than 15 minutes (Jenkins *et al.*, 2001).

A surface plasmon resonance (SPR) sensor using a molecularly imprinted polymer – coated sensor chip for the detection of sialic acid has been developed (Kugimiya *et al.*, 2001). The thinly coated polymer was prepared by co-polymerizing *N,N,N*-trimethylaminoethyl methacrylate, 2-hydroxyethyl methacrylate and ethyleneglycol dimethacrylate; in the presence of *p*-vinylbenzeneboronic acid ester with sialic acid. The sensor displayed a selective response to ganglioside, of which sialic acid is located at the non-reducing end, and gave a linear response from 0.1 to 1.0 mg of ganglioside. The molecularly imprinted polymer-coated SPR chips can be supplied less expensively than natural biomaterial-coated SPR chips. For example, the sialic acid imprinted polymer could be supplied at a cost approximately 200 times lower than that for the sialic acid selective lectin, E-selectin. The sensor reported in this work was capable of measurement over the concentration range of clinical levels and could be utilized for clinical diagnosis in the future.

An enantioselective chemical sensor has been designed and fabricated (Haupt *et al.*, 1999). The sensor was based on a molecularly imprinted polymer, serving as the recognition element, and a quartz crystal microbalance (QCM), used as the transducer. The polymer, imprinted with the chiral beta-blocking drug S- propranolol, was cast as a thin permeable film onto a gold electrode deposited on the quartz crystal vibrator. The mass increase of the polymer due to analyte binding was quantified by piezoelectric microgravimetry, using the QCM. The sensor was able to discriminate between the R- and S-propranolol enantiomers in acidified acetonitrile solutions, due to the enantioselectivity of the imprinted sites: the detection limit of S- propranolol was $50 \mu\text{mol dm}^{-3}$.

The development of a label-free direct piezoelectric immunosensor has also been reported (Horacek *et al.*, 1997). The piezoelectric crystals were modified with 2,4-dichlorophenoxyacetic acid (2,4-D); using coupling procedures based on self-assembled monolayers of suitable thio-compounds (aminothiophenol, cysteamine, cystine and dithiobis(succinimidyl)propionate) on the surface of the gold electrodes of the crystals. The piezoelectric biosensor was placed in a flow-through cell and the binding affinity of two monoclonal antibodies (against 2,4-D on the modified piezoelectric crystals) was studied in real time without additional labels. The system was used for the competitive determination of free 2,4-D in water and the limits of detection (10% decrease of relative binding of the antibody) for free 2,4-D were 0.27 and $0.24 \mu\text{g l}^{-1}$, respectively. The total time for one measurement was below 25 min.

To date there are few reports on application of MIPs as receptors for water toxin analysis.

1.8.6 MIPs based on Computational Approach

The development of a general procedure for MIP design is one of the most challenging problems for molecular imprinting. Thermodynamic calculations and combinatorial screening approaches have been successfully used to identify the best monomer

candidates for imprinting (Takeuchi *et al.*, 1999). This work became difficult with the increasing size of monomer libraries, which now include thousands of polymerisable compounds. One possible solution to this problem is the use of molecular modeling software and searching algorithms traditionally applied in drug design, which were recently adopted for the design of affinity polymers (Piletsky *et al.*, 2001).

The MIPs based on a computational approach are innovative and promising. With this method, the choice of monomers for the polymerisation process is made using the SYBYL molecular modeling software, which is commercially available and has been applied for the design of amino acids for many years (Böhm, 1992). A first attempt to develop MIPs based on a computer-aided rational design has been recently reported (Subrahmanyam *et al.*, 2001; Chianella *et al.*, 2002).

The process includes the design of a virtual library of functional monomers containing electrostatic, hydrophobic, van der Waals forces, dipole-dipole interactions, or reversible covalent bonds. A molecular model of the template molecule is also prepared; charges for each atom are calculated and the structure of the template and monomers refined using molecular mechanics methods. Each of the monomers in the virtual library is probed to investigate possible interactions with the template molecule using the Leapfrog program. The subsequent results show the list of monomers giving the highest binding score, this represents the best candidates for polymer preparation. Simulated annealing is then used to simulate pre-arrangement of the functional monomers with the template in the monomers mixture, prior to polymerisation. At the end of the program, the number and the position of the functional monomers are examined.

1.9 AIMS AND OBJECTIVES

The aim of this work is to develop affinity sensors for the detection of algal and cyanobacterial toxins in environmental samples. Due to the wide variety of toxins with different molecular structure and mechanisms of action, the study was focused on specific toxin targets. Two different categories of toxins were selected:

- The family of microcystins toxins (with particular regard to microcystin-LR) produced by cyanobacteria and mainly present in freshwater.
- The amnesic shellfish poisons, domoic acid being the main toxin, generated by diatoms and often accumulated in shellfish and marine phytoplankton.

One of the project objectives was also to select the most sensitive receptor for sensor development. This included investigating the use of natural receptors (antibodies) and artificial receptors (based on molecular imprinted polymer) as sensing elements in the fabrication of affinity sensors. Antibodies against microcystin-LR were used as the natural receptors in the development of a disposable electrochemical immunosensors. The sensors were fabricated using screen-printed electrodes capable of directly transducing the response from an affinity membrane bound competitive enzyme immunoassay. Relevant comparisons between the natural and molecularly imprinted polymers, as artificial receptors for microcystin-LR, were carried out. An evaluation in terms of sensitivity and affinity as well as stability and cross-reactivity for both receptors was performed.

Artificial receptors specific for domoic acid, based on molecularly imprinted polymer, were synthesised and characterised for further sensor applications. In particular, a MIP sensor based on surface plasmon resonance system was developed and compared with monoclonal antibody receptors against domoic acid, applied in the same format.

The required stages and objectives of the thesis progression were as follows:

Reagent Characterisation and ELISA Development:

- Selection and IgG purification of anti-microcystin-LR specific antibodies.
- Immuno-reagent characterisation.
- Reagent incorporation into a colorimetric ELISA and assay suitability determination.
- Investigation of antibody binding characteristics and the most effective conditions for assay parameters to yield maximum performance.
- Determine the assays competitive sensitivity limit for microcystin-LR detection.
- Investigation of assay cross-reactivity and matrix effect.

Membrane Bound ELISA Development and Optimisation for Microcystin-LR:

- Transfer of the suitable antibodies and assay system to the development and optimisation of a membrane bound ELISA.
- Development and optimisation of the competitive ELISA format.

Immunosensor Development Incorporating the Membrane ELISA:

- Fabrication of screen-printed electrodes and immunosensor device construction incorporating a fixed membrane layer.
- Investigate and optimise amperometric detection system for ELISA transduction, adjusting assay parameters accordingly.
- Investigation of FIA Electrochemical Immunoassay.

Molecular Imprinted Polymers for Microcystin-LR:

- Bulk imprinting synthesis of microcystin-LR.
- MIPs molecular modeling design for synthesis of molecularly imprinted polymer (MIP).
- Competitive enzyme assay for MIPs characterisation.
- Comparing sensitivity and affinity for microcystin-LR receptors.

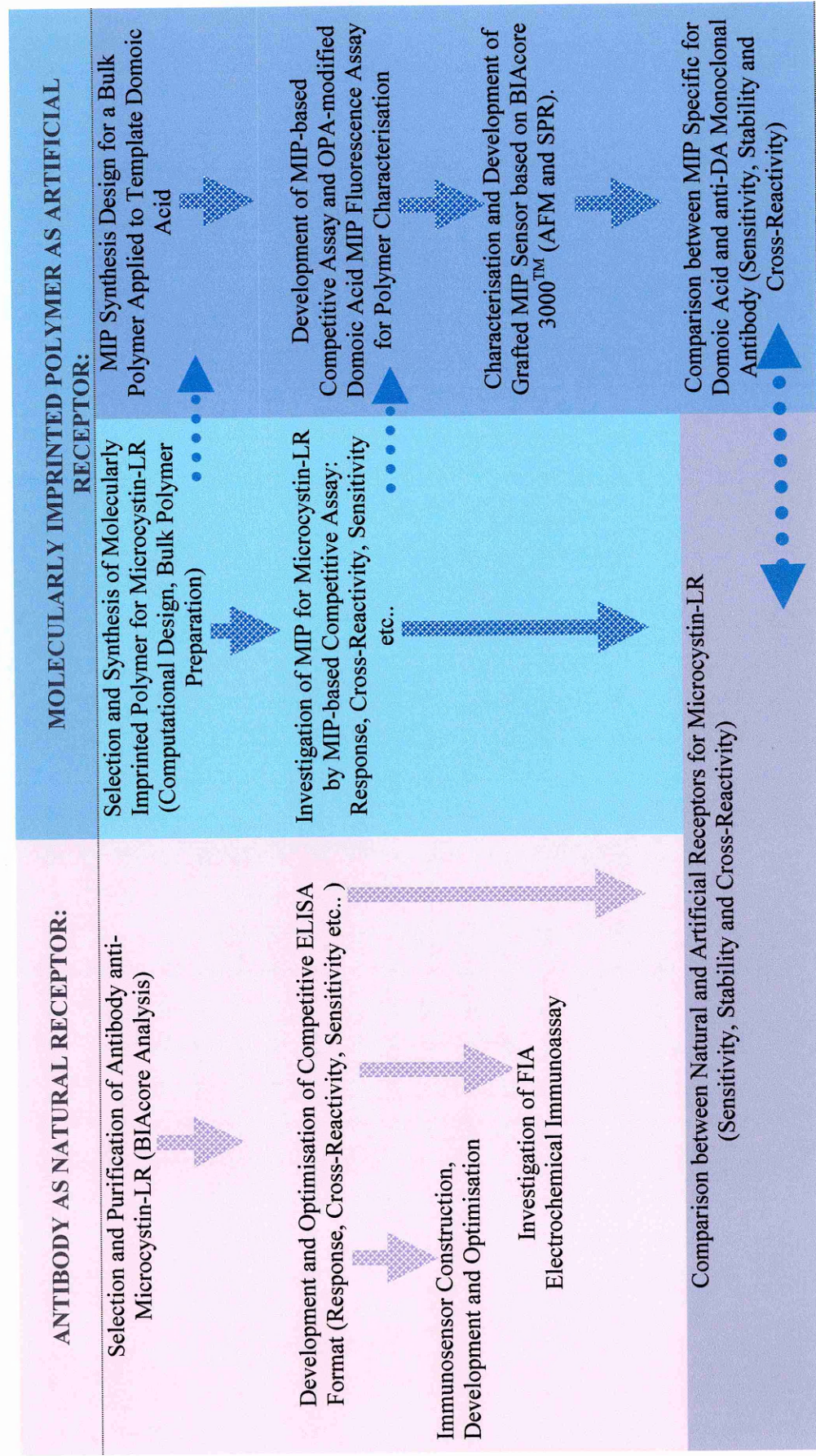
- Comparing cross reactivities for anti-microcystin-LR receptors.
- Comparing stability performances of anti-microcystin-LR receptors.

Molecular imprinted polymer for domoic acid:

- Computational designed synthesis of domoic acid imprinted polymer.
- Development of an OPA-modified DA MIP fluorescence assay.
- Grafting technique for domoic acid polymer.
- Characterisation of grafting by atomic force microscope imaging.
- Characterisation of grafting by surface plasmon resonance (SPR).
- Competitive assay based on BIAcore 3000™ for domoic acid-MIP.
- Evaluation of natural antibody for domoic acid by BIAcore analysis.
- Comparison between MIP specific for domoic acid and anti-DA monoclonal antibody.
- Performances in terms of sensitivity, stability and cross-reactivity.

1.10 THESIS FLOWCHART

- INTRODUCTION
- LITERATURE REVIEW
- MATERIALS AND METHODS
- RESULTS



CHAPTER 2:
MATERIALS & METHODS

2.1 MATERIALS

2.1.1 Chemicals

The following chemicals were all obtained from Sigma and Aldrich (Poole, U.K.): the monomers methacrylic acid (MAA) for 'traditional' microcystin-LR-MIP; allylamine, urocanic acid and acrilamide for domoic acid computational MIP synthesis as well as the cross-linker ethylene glycol dimethylacrylate (EGDMA) and initiator 1,1'-azobis (cyclohexane-carbonitrile). Methanol, ethanol, N,N-dimethylformamide (DMF), dimethylsulfoxide (DMSO) and acetone were used in several MIP experiment, as received from BDH (Gillingham, U.K.).

TMB liquid substrate used for the ELISA is a ready-to-use liquid substrate, provided by Sigma, containing the chromogen 3,3',5,5'-tetramethylbenzidine (TMB), prepared buffer and hydrogen peroxide. Other buffer constituents, PBS tablets (10 mM sodium phosphate, 0.0027 M potassium chloride, 0.137 M sodium chloride, Tween 20 0.05 %, pH 7.2), the chromogen 2,2'-azino-bis(3-ethylbenz-thiazoline-6-sulfonic acid) (ABTS), hydrogen peroxide 30 % as well as general laboratory chemicals and solvents were of analytical grade and supplied by BDH (Gillingham, U.K.), Aldrich (Gillingham, U.K.) or Sigma (Poole, U.K.). General laboratory water and that referred to, as 'distilled water' was Elga (High Wycombe, U.K.) Reverse Osmosis purified water.

Mercaptoethanol, o-phthaleic dialdehyde (OPA reagents) used in the fluorescence experiments, 2-mercapto-ethylamine for the self-assembled monolayer, photo-polymerisation initiator 4,4'-azo-bis (cyanovaleric acid), water soluble carbodiimide (EDC) for covalent binding and 1-hydroxybenzotriazole, added to enhance coupling reaction mediated by EDC were all supplied by Sigma. The monomer composition consisting of 2-(diethylamino) ethyl methacrylate, N,N'-methylenebisacrylamide (MBA) were also purchased from Sigma.

2.1.2 Antibodies

Two different anti-microcystin-LR polyclonal antibodies were supplied, already purified from serum by Dr. R. Abuknesha (King's College London, U.K.). The first batch was produced from rabbit using an immunogen containing ovalbumin protein, conjugated to microcystin-LR via a two-step N-hydroxy succinimidyl ester coupling method. Each antibody solution was tested using a BIAcore 3000™ (BIAcore AB Uppsala, Sweden) for real time evaluation of their specificity. The second batch of anti microcystin-LR polyclonal antibody was raised in sheep with immunogen bovine serum albumin (BSA) carrier-hapten, conjugated via the 'mixed anhydride' coupling method. This antibody solution was employed for the immunoassay study and for further immunosensor development.

Another pool of polyclonal antibody raised against microcystin-LR was supplied by Prof. Hennion (Department of Environmental and Analytical Chemistry, Paris, France). The purified IgG fraction was used for comparative studies between antibody receptors and molecularly imprinted polymers (MIPs)-based receptors for microcystin-LR (Chapter 5).

Anti-microcystin-LR monoclonal antibody from a microcystin-LR detection kit was purchased from Wako Pure Chemical Industries Ltd (Osaka, Japan). Similarly, anti-MC-LR polyclonal antibody was obtained (as a part of an EnviroGard® microcystin plate kit) from Adgen Limited (Scotland, U.K.) for use in comparison studies. Secondary antibody anti-sheep conjugated to horseradish peroxidase (HRP), used for a two-step indirect competitive ELISA (whole molecule, 1:10,000 titer) was supplied by Sigma (Poole, U.K.).

Anti-domoic acid monoclonal antibody, provided by Prof. B. Hock from University Technical University of Munich (Germany), was used in the BIAcore experiment as a comparison with the imprinted receptor for the same toxin. Three murine monoclonal antibody solutions were obtained from hybridoma clones, derived by fusion of mouse

myeloma cells with mouse immune spleen cells from animals immunised with domoic acid-keyhole limpet hemocyanin (KLH) conjugate, obtained via coupling N-ethyl-N'-(3-dimethylaminopropyl) carbodiimide hydrochloride (EDC) and N-hydroxysuccinimide (NHS).

2.1.3 Toxins and Conjugates

Microcystin-LR was purchased from the Alexis Corporation Ltd (Nottingham, U.K.). The analogues microcystin-RR, -YR, -LF, -LW, and nodularin, used in cross reactivity experiments, were also obtained from the same company.

The microcystin-LR-ovalbumin protein (albumin from chicken egg, OVA) conjugate used for the BIAcore experiments was supplied by Dr. R. Abuknesha as well as a gelatin conjugate used as a coating agent for the two steps competitive ELISA.

The microcystin-LR conjugated to HRP was part of a kit for microcystin-LR detection, purchased from Adgen Limited (Scotland, U.K.). This conjugate was used as a colorimetric label when the antibody-bound format on membrane was investigated. The same conjugate was also used in the enzyme-linked MIP competitive assay for microcystin-LR. The concentration of the conjugate was unknown, thus an evaluation of the amount of MC-LR-HRP conjugate present in the commercial solution was carried out.

Domoic acid toxin was supplied by Affiniti Research Products Ltd (Exeter, U.K.). The analogues kainic acid, glutamic acid and aspartic acid, used in cross-reactivity experiments, were from Sigma (Poole, U.K.). Both the domoic acid enzymes (HRP) and protein (OVA) conjugates were provided by Prof. B. Hock from Technical University of Munich (Germany).

2.1.4 Electrode Fabrication

The electrodes produced in the context of this work were manufactured using an automated screen-printing machine DEK 248 (DEK Printing Machines Ltd., Weymouth, England). Screens were produced to the required specifications by the DEK precision screen division (Newman *et al.*, 1995; Kröger *et al.*, 1997).

The sensors were printed onto 250 μm thick ‘Melinex’ polyester sheets (Cadillac Plastic, Swindon, U.K.) (229 mm x 305 mm), enabling each screen to print between 60-100 sensors per sheet depending on the design and dimensions. First, a layer of basal graphite tracks was printed with MCA I45R carbon ink, MCA service (Cambridge, U.K.), forming the basic working and counter electrodes. This was dried at room temperature and followed by a pad of reference electrode ink consisting of 15 % silver chloride in silver paste (Electrodag 477, Acheson Colloids, Plymouth, U.K.). The electrodes were then uniformly defined and the basal tracks insulated with a blue layer of 242-SB epoxy-resin based protective coating ink (Agmet ES, Reading, U.K.), cured by heat treatment at 125 °C for two hours. The print parameters applied after optimisation of the print process and the selected materials are summarised in Table 2.1.

Table 2.1: Optimised parameters for printing three-electrode systems (Kröger, 1998).

PRINT PARAMETERS	SETTING
Print mode	Print/Flood
Squeegee Pressure	4 Kg
Print gap	2.5 mm
Deposits	1
Forward Carrier Speed	50 mm/s
Reverse Carrier Speed	50 mm/s
Front Limit	40 mm
Rear Limit	400 mm
Separation Speed	70 %

Each screen-printed sensor (SPS) thus consisted of three individual screen-printed electrodes (SPE) in a single device. These electrodes were carbon (graphite) working and counter electrodes and a Silver/Silver Chloride (Ag/AgCl) reference electrode, illustrated in Plate 2.1.

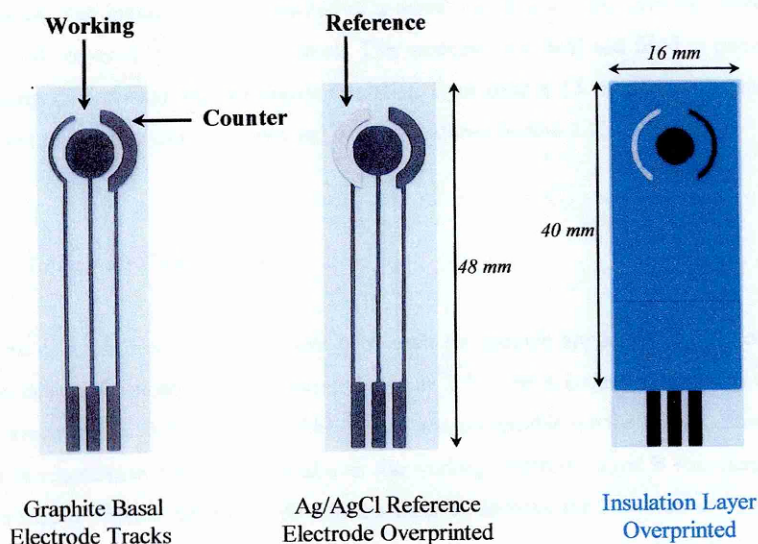


Plate 2.1: The screen-printing process in sensor fabrication (Baskeyfield, 2001).

2.1.5 Electrode Configuration

Two different designs of SPS were used for each specific application, reflected by their design. These designs are shown in Plate 2.2. Type A is the standard SPS used for electrochemical development with a 5 mm diameter-working electrode, giving a planar area of 19.6 mm². This design was compatible with the incorporation of a 6 mm membrane disc, located over the working electrode. The Type B design is narrower with a sequential electrode format designed for on-line analysis, as part of a Flow Injection Analysis (FIA) system. All the designs included identical terminal electrode connection dimensions.

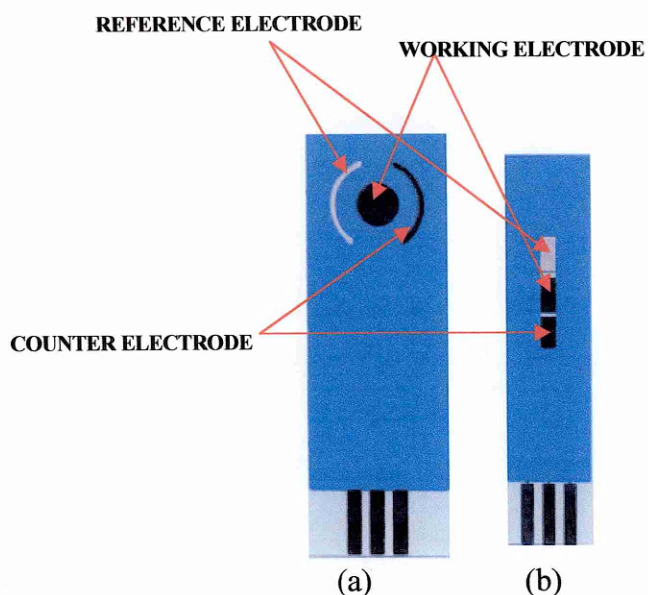


Plate 2.2: Screen-printed electrode configuration (a)-Membrane compatible SPE design; (b) FIA SPE design.

2.2 METHODS: IMMUNOREAGENTS CHARACTERISATION

2.2.1 SPR-based Biacore System

The BIAcore 3000™ instrument, BIAevaluation 3.0 software and reagents including research grade sensor chips CM5 and pioneer J1, HBS-EP buffer (10 mM HEPES, 150 mM NaCl, 3.4 mM EDTA and 0.005 % (v/v) surfactant P20 at pH 7.4), and the amine coupling kit containing N-ethyl-N'-(3-dimethylaminopropyl) carbodiimide hydrochloride (EDC), N-hydroxysuccinimide (NHS) and ethanolamine hydrochloride were purchased from Biacore AB (Uppsala, Sweden).

All experiments were performed on a BIAcore 3000™ instrument which is one of the most efficient instruments currently available for studying biomolecular binding events in real-time. The software used was the BIA Control 3.0 package. The BIAcore analytical system consists of a detection unit, an auto-sampler, and a liquid delivery system, controlled by a computer. The system combines a microfluidic unit in contact

with a sensor for surface plasmon resonance (SPR) detection. The sensor chip consists of a glass slide mounted in a plastic frame. On one side of the glass, a thin film, approximately 50 nm, of gold is deposited, and, in the case of CM5 chip, a dextran matrix is attached on top of this film. The sensor chip is inserted into the instrument with the dextran/gold side in contact with the flow cell. When the injected sample is passed through the flow cell, analyte binds to immobilize the ligand in the support. Light covering a span of angles of incidence falls on the glass side and is reflected into a 2D-array detector, where the intensity of the reflected light is measured. SPR occurs at a certain angle and is seen as a minimum in reflected light intensity (Figure 2.1).

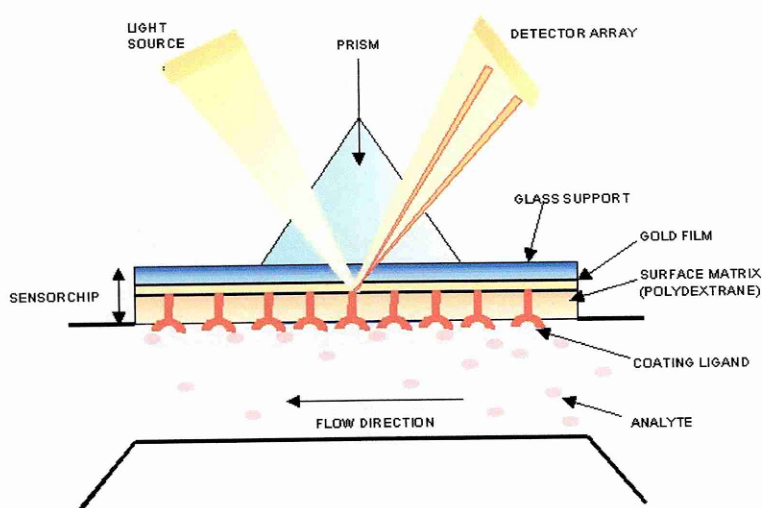


Figure 2.1: Scheme of SPR system.

When the refractive index close to the gold film is changed, for example, when immobilized antibody binds antigen, the angle at which SPR occurs is changed. This change is proportional to the amount of bound protein, and is expressed as refractive or response units (RU) on the Y-axis in function of the time (sensorgram).

Sample containing the analyte(s) is injected over the surface in a precisely controlled flow. Within the framework of real-time, the interactant immobilized on the sensor surface is referred to as the *ligand*, and the interactant in free solution as the *analyte*.

These terms refer to the experimental design of a real time BIA investigation, not to the biological role of the interactants. An antibody-antigen interaction, for example, may be monitored with either antibody or antigen as the ligand (Malmqvist, 1999).

2.2.2 BIAcore Analysis of Anti-Microcystin-LR Antibody: Coupling Reaction

Activation of the chip with a carboxymethylated dextran matrix (CM5 Research grade, BIAcore AB, Uppsala, Sweden) was carried out by mixing equal volumes of 0.2 M EDC and 0.05 M NHS (freshly prepared in ultrapure water and immediately stored at $-20\text{ }^{\circ}\text{C}$). The mixture was injected over the sensor chip surface for 7 min at flow rate of $5\text{ }\mu\text{l min}^{-1}$. The amine coupling introduces N-hydroxysuccinimide esters into the surface matrix by modification of the carboxymethyl groups. These esters then react spontaneously with amines and other nucleophilic groups on the ligand to form covalent links (Figure 2.2).

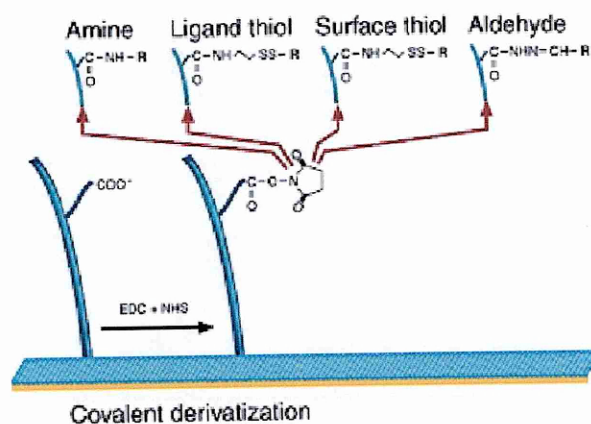


Figure 2.2: Amine coupling chemistry (<http://www.biacore.com>).

A continuous flow of HBS-EP buffer (10 mM HEPES, 150 mM NaCl, 3.4 mM EDTA and 0.005 % (v/v) surfactant P20 at pH 7.4) was maintained over the CM5 sensor chip surface at a flow rate of $5\text{ }\mu\text{l min}^{-1}$. The software controlling the BIAcore instrument permits work with either one or more channels of the chip. In this instance, three

channels were 'open', thus in contact with the solution injected for immobilisation, and one channel was left 'closed' for control. The purified microcystin-OVA, in a stock concentration of 10 g l^{-1} , was dissolved in acetate buffer at pH 4.3. The immobilisation onto the channels of the CM5-coated sensor was carried out at $25 \text{ }^\circ\text{C}$, with a flow rate of $5 \text{ } \mu\text{l min}^{-1}$ and total volume of $35 \text{ } \mu\text{l}$; by injecting three different concentrations ($100, 200, 300 \text{ mg l}^{-1}$). A second CM5 sensor chip was then inserted into the flow cell of the BIAcore instrument and, following EDC-NHS activation of the sensor chip surface, three other concentrations of the OVA-MC-LR conjugate were injected ($300, 500, 1000 \text{ mg l}^{-1}$) into the system. The immobilisation procedure was completed by a 7 min injection of 1 M ethanolamine hydrochloride ($35 \text{ } \mu\text{l}$) in order to block the remaining ester groups.

2.2.3 Sample Preparation and Analysis for BIAcore

The MC-LR-OVA conjugate (300 mg l^{-1} in acetate buffer, pH 4.3) was injected over a new sensor chip for a 7-minute immobilisation procedure at a flow rate of $5 \text{ } \mu\text{l min}^{-1}$. Anti-MC-LR IgG, ($40 \text{ } \mu\text{l}$), in a range of concentrations between 0 and 50 mg l^{-1} and at a flow rate of $15 \text{ } \mu\text{l min}^{-1}$, was injected over the MC-LR-OVA-coated surface. Each injection was carried out after regeneration of the sensor surface with $10 \text{ } \mu\text{l}$ of 0.2 % sodium dodecyl sulphate (SDS) in 10 mM HCl, at flow rate of $5 \text{ } \mu\text{l min}^{-1}$.

Anti-MC-LR IgG, at a concentration of 50 mg l^{-1} , was also injected over a chip where a channel was coated with OVA, acting as a control. One-hour pre-incubation of the anti-MC-LR antibody (1 ml , 50 mg l^{-1}) with OVA (1 ml , 1 mg ml^{-1}) at room temperature was carried out, in order to prevent cross-reactive binding of the OVA-specific antibody fraction to the MC-LR-OVA and OVA-coated surfaces.

A displacement experiment was carried out by injecting 50 mg l^{-1} of anti-MC-LR IgG (without pre-incubation with OVA) over the MC-LR-OVA coated surface. The control channel was maintained without a ligand coating. Different concentrations of MC-LR-

OVA, from 0 mg l⁻¹ to 3 mg l⁻¹, were injected onto the coated chip. Likewise, free MC-LR (with a range of concentrations from 0 to 500 mg l⁻¹) injections were performed over the sensor chip. The injections of analytes were carried out at a flow rate of 15 µl l⁻¹ and in a volume of 40 µl.

2.3 METHODS: IMMUNOASSAY DEVELOPMENT

2.3.1 Assessment of Anti-Microcystin-LR Polyclonal Antibody

Anti-microcystin-LR antisera, raised in sheep (SH Ig G anti-MC-LR), were analysed by an indirect solid phase enzyme-immunoassay. The method was based on using hapten-protein carrier conjugate as the solid phase antigen or on a plate coated with antigen (PCA), adsorbed to the wells of a 4HB 96-well microtitre plate with a high binding capacity (Dynex Technologies Ltd., Billingshurst, U.K.). Specific binding was measured using the double dilution checkerboard titration as the initial screening method. This was carried out in order to assess the presence of "specific" antibodies to the target toxin. Controls in the titration experiments included binding tests with unmodified and modified (by a different hapten) carrier protein and a negative test with the antibodies. Firstly, the antigen-gelatin conjugate (diluted in 100 mM carbonate-bicarbonate, pH 9.5) was used to coat the microtiter plate in a sequence of vertical dilutions from 1/200 to 1/6,400, overnight at 4 °C. The coated plate was then blocked for 1 hour with 0.5 % gelatin in PBS buffer (pH 7.2) at 37 °C. Once the plate was blocked and washed with PBS, by using an 8 channel manual washer (Nunc, Roskilde, Denmark), sheep anti MC-LR antisera were serially diluted in a horizontal direction on the assay plates; starting with a 1/200 working dilution up to a 1/376,800 dilution in antibody buffer (10 mM PBS pH 7.2, 0.5 % gelatin, 0.05 % Tween 20). Binding was allowed to proceed for 1 hour at 37 °C with gentle shaking (Incubator/Shake HT, LabSystems, Finland) to promote the interaction with the coated analyte. The plates were then washed again (as previously described), and the anti-sheep HRP-labelled secondary antibody (in a dilution of 1:20,000, as suggested from producer) was incubated for 1 hour at 37 °C. The HRP enzyme label activity was determined using

ABTS as a substrate (150 μ l, 0.5 g per litre of sodium acetate/citrate buffer, pH 4.1, to which 10 μ l of 30 % H_2O_2 was added). Colour development was allowed for 20 minutes in the dark at room temperature, and the optical density read at 450 nm using a spectrophotometer (MRX microplate reader, Dynex Technologies Inc., Billingshurst, U.K.).

2.3.2 Gelatin Coating Conjugate Optimisation

From the initial concentration of 1000 mg l^{-1} , sequential dilutions of gelatin-MC-LR conjugate were made and a volume of 150 μ l of each dilution was added to microtiter plate wells. The coating conjugate was left overnight at 4 °C. The following day the coating solution was discarded, the wells washed with PBS and then dried. The coated microtiter plate was blocked with 0.5 % gelatin blocker in PBS (150 μ l) for 1 hour at room temperature. The SH IgG anti-MC-LR (100 μ l) was added to each well in a dilution of 1/1500 and left to dry. The plate was washed again as previously described, and the anti sheep HRP-labelled secondary antibody (1:20,000) added and left to incubate for 1 hour at 37 °C. The HRP enzyme label activity was determined using ABTS as a substrate (150 μ l, 0.5 g per litre of sodium acetate/citrate buffer, pH 4.1 to which 10 μ l of 30% H_2O_2 was added). Colour development was allowed for 20 minutes in the dark at room temperature and the optical density read at 450 nm using a spectrophotometer.

2.3.3 Competitive ELISA Optimisations

Competitive ELISA inhibition tests consisted of mixing appropriately diluted antibody (1/1500) with analyte (microcystin-LR standards in range of 0-10 μ g l^{-1}) in buffer then incubating the solution in a water bath for approximately one hour at 37 °C. An aliquot of 150 μ l of the mixture was transferred to the toxin-gelatin conjugate (1/400) coated plates where an additional period of 30 minutes incubation at room temperature with gentle shaking was allowed. Following this procedure, plates were washed and

developed, as described above. The inhibition test was based on a solid phase competitive ELISA, where the absorbance, recorded at the end of the reaction is inversely proportional to the concentration of the free analyte (toxin). The washed plates were treated with secondary antibody-HRP conjugate and the assay completed, as described previously.

Incubation of the mixture anti-MC-LR IgG and microcystin-LR with conjugate gelatin coated plate was carried out at 37° C with 1150-rpm agitation in an incubated orbital shaker (30 minutes at room temperature). The polystyrene sorbent coating conditions and incubations were optimised for rapid and reproducible binding, yielding minimum background levels. High binding capacity microtiter plates (Immulon 4HB, Dynex Technologies Ltd., Billingshurst, U.K), were used with 0.1 M sodium carbonate-bicarbonate, pH 9.6 as the coating buffer and 0.5 % gelatin as blocking agent. The effects from different combinations of coating (60-15 minutes) and blocking (60-0 minutes) incubation times at room temperature (without shaking) were investigated.

The matrix effects were assessed by deriving calibration curves for MC-LR under varied conditions, where the standard analyte solutions were made up in ELISA buffer (50 mM sodium phosphate, pH 7.5, 100 mM sodium chloride, 0.1 % gelatin), in PBS, in tap water or filtered Thames water.

2.3.4 ELISA Data Analysis

Sensitivity may be defined as the limit of detection or quantification, or may be estimated from the slope of the dose-response curve or from a precision profile. A well-accepted definition for the lowest limit of detection (LLD) is: the smallest concentration of antigen giving a signal that can be distinguished from that obtained in the absence of antigen. For a competitive assay, this can be defined as:

$$LLD=B_0 - x Y SD_{B_0}$$

Where $Y = 3$, B_0 is the average of the signal obtained in the absence of free antigen and SD is the standard deviation of the signal B_0 (Gosling, 2000). Therefore, the LLD is estimated as the concentration corresponding to three standard deviations difference from the signal at zero concentration of free analyte (maximum signal). The lowest limit of detection (LLD) is often considered as LLD_{80} meaning that the lowest limit of detection set at 80 % of the maximum response. Throughout this work, the latter definition was used for the evaluation of all data.

All the experiments were replicated at least three times, unless otherwise stated. Error bars on the graph are standard deviations obtained with Microsoft Excel 2000 software. In addition, the coefficient of variation was calculated to check the precision of data. The errors are due to variance in signal measurement and reagent manipulations (pipetting, separation of bound and free antigen, washing steps) and can be evaluated in total by the estimation of the coefficient of variation (CV) of the average of signal, as measured in the assay:

$$CV (\%) = SD/\text{mean} \times 100$$

The 50% B_0 value is often considered to express the affinity between antigen and antibody in a competitive binding curve. Competitive binding experiments measure the binding of a single concentration of labelled ligand, in the presence of various concentrations of unlabelled ligand. The concentration of unlabelled analyte that binds to the 50 % of the sites available can be denoted as: IC_{50} = inhibitory concentration 50 % or EC_{50} = effective concentration 50 %. The lowest is the value of 50 % B_0 , the better the affinity between the analyte and its receptor (Gosling, 2000) (<http://www.curvefit.com>).

To define the detection limit alone is not sufficient. Confidence in the specificity of the detection antibody must be determined, usually by investigating its cross-reactivity behaviour to similar structurally related compounds e.g. analogues of the same family of toxins or different molecules. Cross-reactivity may be examined and expressed in

several ways. In competitive assays, the most common approach is to spike a pure sample of the cross-reacting substance into an analyte-free matrix to give a suitably wide range of concentrations. The cross-reactivity is often defined as the point where the reduction in signal corresponds to 50 % of the signal achieved in the absence of analyte (50% B/B₀) as a percentage of the analyte concentration, giving the same fall in signal.

$$\% \text{ CROSS-REACTIVITY} = \frac{\text{Concentration of analyte giving 50 \% B/B}_0}{\text{Concentration of cross-reactant giving 50 \% B/B}_0}$$

Where B₀ is the average of the signal obtained in the absence of free antigen and B is the average of the signal obtained in the presence of different dilutions of free antigen.

It is important to recognise, however, that the percentage cross-reactivity may vary across the assay range. This is particularly true when polyclonal antibodies are used. In such cases the observed cross-reactivity reflects the cross-reactivity of the particular antibody clone, having the most influence on the binding reaction at that analyte concentration (Wild, 2001).

2.4 METHODS: MEMBRANE ELISA OPTIMISATION

The assay format detailed in Section 2.3 was transferred and developed further to incorporate a membrane sorbent bound ELISA (MELISA) for the IgG assay. Initially all the parameters were kept the same as for the ELISA experiment, except for the coating and blocking procedure.

2.4.1 MELISA based on Antigen Coating

Gelatin-microcystin-LR conjugate was immobilised on UltraBind™ membranes, at different dilutions (12, 0.6, 0.12 g l⁻¹) in a coating buffer. A 5-10 µl aliquot of the conjugate was applied for 15 minutes to each side of a 15 mm diameter membrane disc. The membrane sorbent selected was UltraBind™ US-800 0.8 µm (Pall Gelman Science, Portsmouth, U.K.) covalent attachment membrane. Membrane discs of 6 mm diameter (28.3 mm² planar area) were cut and handled only with fine membrane forceps (BDH, Gillingham, U.K.).

This polyethersulfone pre-activated membrane contains active aldehyde groups, which covalently attach to the free amino groups of a coating analyte. The membrane was left to dry completely at room temperature before proceeding further. After the immobilisation procedure, the membrane discs were washed in phosphate buffered saline (PBS) containing 0.05 % Tween 20 (PBST). The remaining active sites on the membrane were blocked with 5 % gelatin in PBS buffer at pH 7.2 for 45 minutes (50 µl).

The primary antibody anti-microcystin-LR (50 µl of a 1/1500 dilution) was then added to the membrane and incubated for 1 hour at 37 °C with gentle shaking. After washing with buffer (3 times, 200 µl per each membrane), the secondary antibody, labelled with HRP (50 µl of 1/20,000 dilution), was added and incubated for 1 hour at 37 °C. The immobilised peroxidase activity was measured at 450 nm, after incubation with ABTS substrate (150 µl) solution for 20 minutes. A volume of 100 µl of the coloured solution was dispensed in empty wells and the optical density of the colorimetric reaction was measured at 405 nm.

Blocking procedures were investigated using several blocking agents at different concentrations. The membranes were coated with free gelatin or microcystin-LR-gelatin conjugate (0.6 g l⁻¹), then blocked with either 0.5 %, 2 %, 5 % gelatin, 2 % human

albumin, 1 % casein or 1 % ovalbumin. A control was prepared, whereby no blocking agent was used. Blocking was carried out for 30 minutes at 37 °C and the assay continued, as described previously.

2.4.2 MELISA based on Antibody Coating

Anti-microcystin-LR antibody dilutions (from 1/250 to 1/20,000) were applied to membrane discs for 15 minutes at room temperature. The membranes were blocked for 30 minutes with 1.0 % gelatin in PBS buffer. Following the washing step, the conjugate microcystin-LR-HRP (estimated as 1 mg l⁻¹) was added (50 µl) and incubated for 1 hour at 37 °C. The membranes were then washed twice and the activity of the enzyme conjugate determined by colourimetric detection, after addition of the ABTS substrate solution. The optical absorbance was read after 20 minutes at 405 nm.

A one-step competitive ELISA assay (incorporating antibody immobilisation on the membrane) was performed using an immunosensor format. The assay was performed as described above, after coating anti-microcystin-LR antibody at a dilution factor of 1/1000 (concentration 12.8 mg l⁻¹). The antibody-bound membrane was blocked as described above and a competitive reaction carried involving the conjugate and standard concentrations of the toxin analyte: microcystin-LR.

2.5 METHODS: ELECTROCHEMICAL TECHNIQUES

Electrochemical measurements were carried out in 20 mM sodium phosphate, 0.1 M KCl, pH 7.0 electrolytic buffer using a 5 ml cell volume (bulk solution) with mini standard electrodes. Volumes from 50 to 100 µl was applied to the SPE's, with either an electrolyte wicking filter paper (Whatman No.1) or llain voile 100 % polyester 250 µm² mesh material from John Lewis Plc. Irrespective of the electrode type, a carbon working and counter electrodes and a Ag/AgCl reference electrode system was employed.

Mini Ag/AgCl electrodes and glassy carbon electrodes, with an AlO₃ polishing kit were supplied by BAS Technicol (Utah, USA). The electrochemical procedures described were carried out using a computer controlled four channel 'Autolab Electrochemical Analyser' PGSTAT10 multipotentiostat (Ecochemie, Utrecht, The Netherlands) enabling simultaneous analysis, each as an individual three electrode cell. The data acquisition was through the supplied Ecochemie General-Purpose Electrochemical Software version 4. (GPES 4.7).

In order to connect the SPS's to the potentiostat, a flexible and robust connection system compatible with the electrode terminals was used. Connection leads were constructed in house in order to connect an array of at least four SPS's with consistently reliable electrical integrity. These were constructed from ribbon cable with IDC sockets, detachable PCB edge connectors, and terminating 4 mm cable sockets (Baskeyfield, 2001).

2.5.1 Cyclic Voltammetry

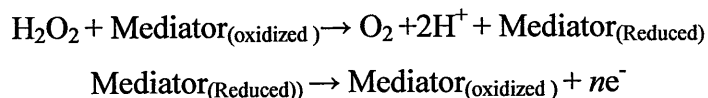
Cyclic voltammetry consists of linearly scanning the potential of a stationary working electrode, using a triangular potential waveform. It offers a rapid method for the location of redox potentials for the electroactive species, and a convenient evaluation of the effect of the media upon redox processes. During the potential sweep, the potentiostat measures the current resulting from the applied potential. The resulting plot of current versus potential is termed a cyclic voltammogram. To obtain the potential required for reducing the oxidized mediator, the cyclic voltammetry (CV) technique was carried in a magnetically stirred bulk solution. The experimental parameters included an initial 30 seconds equilibration time before at least 5-10 scans from a -1 Volt start potential to a first and second vertex potential of 1 V to -1 V respectively. These scans were set at a 200 mV sec⁻¹ scan rate with a 2.44 mV step potential. Cyclic voltammetry was also performed with ABTS substrate solution, using 0.1 M KCl as the basic electrolytic buffer.

2.5.2 Chrono-Amperometry

Chrono-amperometry (CA) measurements were obtained using a single fixed potential with a current monitoring interval of one second. The sensitivity range was set from nAmps to 10 μ Amps. A 10 seconds equilibration time was employed before the current data was measured with a horizontal SPS.

2.5.3 Electrochemical Substrate Detection

Horseradish peroxidase utilises H_2O_2 , enabling the reaction to be monitored electrochemically and/or spectrophotometrically, with the aid of redox substrates. However, direct electrochemical H_2O_2 detection, although simple, requires a large overpotential. This can lead to problems arising from interference due to other electroactive species present in a sample, such as ascorbic or humic acids. One solution for reducing interferences is by the use of mediators. Mediators are generally low molecular weight species that act as intermediate electron acceptors at low potentials; shuttling electrons from H_2O_2 to the electrode surface by the following mechanism:



The electrons are transferred from H_2O_2 and reduce the mediator, which is subsequently re-oxidised (electrochemically) producing a current at the electrode. Initially, hydroquinone was the mediator chosen for the electrochemical reaction with hydrogen peroxide substrate. A range of concentrations was studied and the most suitable combination of mediator and substrate concentrations selected.

In a second series of experiments, the intensity of the coloured product obtained after adding ABTS as a substrate (150 μ l, 0.5 g per litre of sodium acetate/citrate buffer, pH 4.1 and 10 μ l of 30% H_2O_2) for the HRP enzyme label activity was investigated electrochemically. By including an electrolyte of 0.1 M KCl with the ABTS substrate

solution, the reaction product could be measured amperometrically without dilution. A volume of 40 μl was applied directly to a standard (Type A) SPS (poised at + 150 mV potential versus Ag/AgCl reference electrode) and the current determined after 500 seconds.

The immunosensor development culminated in the combination of the optimised MELISA and amperometric detection systems. This brought the membrane immunosorbent into intimate contact with the SPE such that the assay response could be directly transduced amperometrically (Figure 2.3).

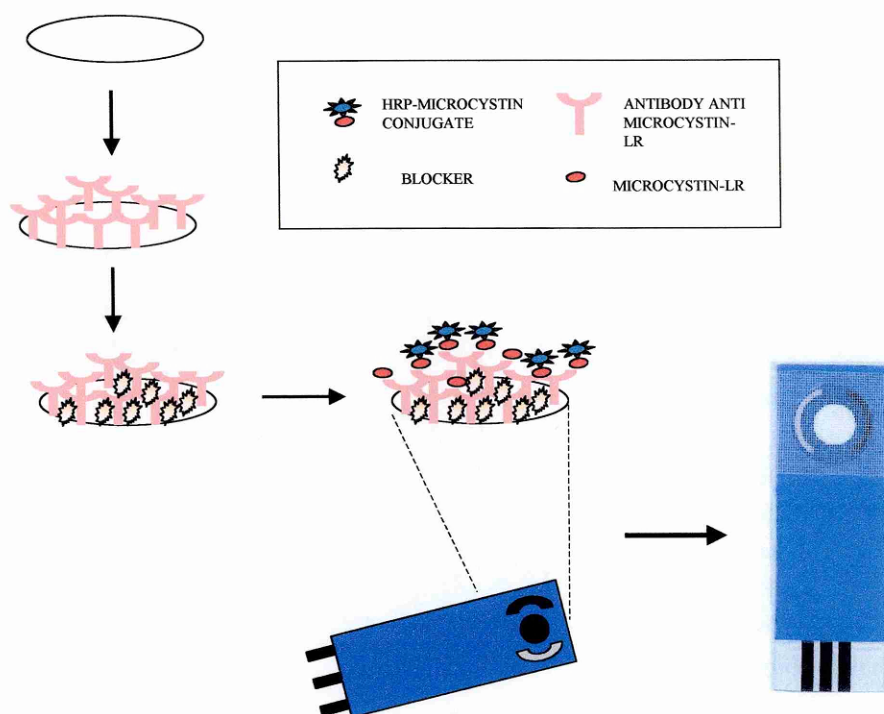


Figure 2.3: Scheme of immunosensor.

The immunosensor construction is illustrated in Figure 2.3. The membrane disc was placed over the working electrode and then covered by a 15 mm² piece of polyester 250 μm^2 mesh. This assembly was then held in place with 30 μl of electrolytic buffer, which

allowed the mesh to adhere to the electrode, thus trapping the membrane. The subsequent electrochemistry applied for the enzyme reaction measurement utilised amperometric analysis. The sensor system was assembled together with 50 μl of electrolytic buffer containing 1 mM hydroquinone mediator. After poisoning the electrodes at a - 300 mV reducing potential, the system sensor was allowed to equilibrate at room temperature for between 60-100 seconds. Then 10 μl of 0.5 mM hydrogen peroxide substrate in electrolytic buffer was added. The final current readings were taken between 300-400 seconds, when a steady state condition had been obtained. The difference in current was then measured between the two steady state equilibration's, indicating the substrate concentration.

Parameters investigated for optimisation in addition to antibody concentration included buffer stringency/ composition, sample volume, and the sample incubation conditions such as temperature and duration. When the ABTS substrate solution was used, the sensor was held in position with 30 μl of electrolytic buffer and ABTS substrate solution added after 50 seconds.

2.5.4 Electrochemical FIA MELISA

The competitive microcystin-LR enzyme immunoassay (EIA) was implemented as a flow injection assay with ABTS substrate, electrochemical detection. A disc size of the membrane UltraBind™ was inserted into a flow cell designed by Dr J. Bolbot from Cranfield University (Silsoe, U.K.) and constructed by Model Products Ltd (Wootton, U.K.) from Perspex and connected to white-black coded 0.57 mm Tygon tubing (Bennet Scientific Limited, Somerset, U.K.) linked to a peristaltic pump. The tube had an internal diameter of 0.57 mm, giving a standard 0.66 $\mu\text{l min}^{-1}$ flow rate at a 20-rev min^{-1} pump speed. A 2 revs min^{-1} pump speed was used to propel electrolytic buffer at a flow rate of 10 $\mu\text{l min}^{-1}$ through the flow cell. Anti-microcystin-LR antibody was immobilised by passing 250 μl of a 1/1000 dilution (in PBST buffer) through at a speed of 10 $\mu\text{l min}^{-1}$. After one minute washing by buffer, an equal volume of free toxin (200

μl , range $0.01\text{-}2\text{ ng ml}^{-1}$) and the microcystin-LR-HRP conjugate (1 mg l^{-1}) was propelled through the on-line system, at $10\text{ }\mu\text{l min}^{-1}$. To enhance the immuno-reactions the introduced volume could be stopped in the membrane flow-cell. A membrane without immobilised antibody was used as a control.

The substrate ABTS solution ($200\text{ }\mu\text{l}$) was passed through the flowcell at a flow rate of $10\text{ }\mu\text{l min}^{-1}$. Later, the coloured solution was collected and read colourmetrically at 405 nm . Alternatively, the oxidised product was determined electrochemically by either depositing the coloured solution on top of a SPS poised at potential of $+150\text{ mV}$ versus Ag/AgCl or by passing the solution over an electrode inserted in a flow cell connected both to the membrane and to the Autolab equipment. The flow was only permitted to pass through the SPE flow-cell for the substrate reaction determination. For the binding reaction part of the procedure, a valve directed the flow to waste before the SPE was reached. The FIA SPE and membrane disc flow cells are shown in Plate 2.3.

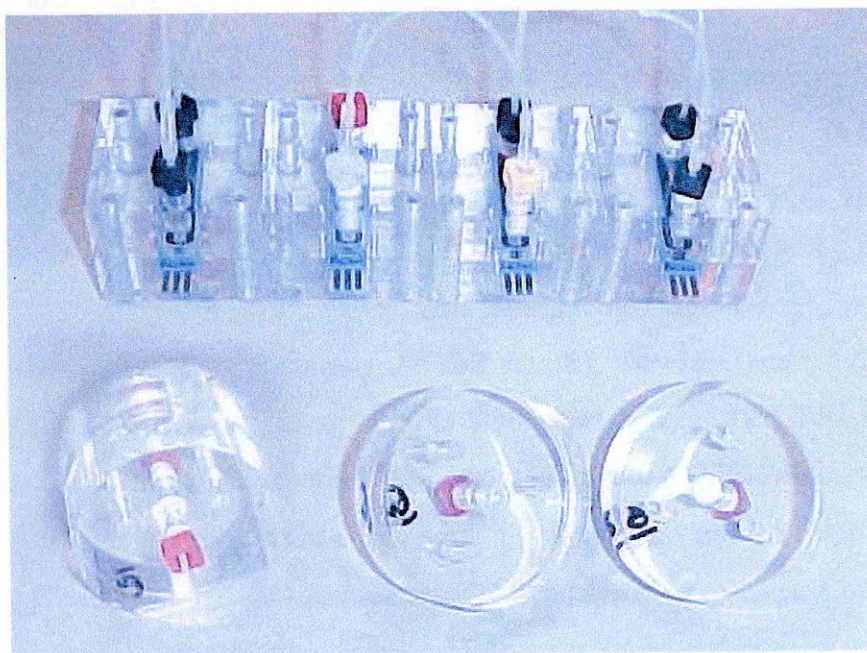


Plate 2.3: FIA SPE and membrane disc flow cells.

2.6 MIP-BASED RECEPTOR FOR MICROCYSTIN-LR

2.6.1 Synthesis of Bulk-Imprinted Polymer for Microcystin-LR

The template microcystin-LR (1×10^{-6} mol, 1 mg) was dissolved in 300 μ l of DMSO. The solution was then mixed in a glass bottle together with a polymerisation mixture, containing 1×10^{-5} mol (0.86 mg) of MAA as a monomer, EGDMA as a cross-linker (1.5×10^{-3} mol, 300 μ l) and 2.5×10^{-2} mol (6 mg) of 1,1'-azobis (cyclohexane-carbonitrile) as a radical initiator. The polymerisation was carried out at 80 °C for 24 hours in a silicon oil bath (Multiheat thermostatic circulator, LKB Bromma 2019).

After thermo-polymerisation, the bulk polymer was ground in a mechanical mortar and wet-sieved with acetone through 45 and 63 microns sieves (Endecotts Ltd., London, U.K.). The finest particles were removed by repeated sedimentation in acetone. Different particle sizes of the polymer were kept separated in order to have a working homogeneous polymer powder. The particles with dimensions between 45 and 63 microns were collected and extensively washed to extract the printed molecule. Initially, the polymer was washed with 500 ml of HCl 10 mM, using a glass filter holder and membranes with 35 mm filter diameter (Millipore, Watford, U.K.), connected to a vacuum pump. This was followed (sequentially) by 500 ml of distilled water, 500 ml of methanol and the same volume of distilled water again. Finally, the polymer particles were dried under vacuum and kept in a oven at 60 °C overnight. The polymer powder obtained was stored in a desiccator at room temperature.

2.6.2 Characterisation of MIP by Enzyme-Linked Competitive Assay

In order to ascertain whether the imprinted polymer had retained specificity for the target toxin, a suspension of the polymer (50 μ l, 0.5 g l⁻¹ in 50 mM sodium phosphate buffer, pH 7) was dispensed into a 96-well filtration microplate. To each well, 50 μ l of a solution of the conjugate MC-LR-HRP (dilution 1/10 from stock, approximately 0.1 mg

l^{-1}) and different dilutions of free toxin ($0.1-10 \mu\text{g } l^{-1}$ in 50 mM sodium phosphate buffer, pH 7.0) were added to each well. After 1 hour incubation at room temperature, the mixture was filtered using a MultiScreen System Resist Manifold (Millipore, Watford, U.K.), a vacuum manifold with broad chemical compatibility, resistant to all solvents and able to accommodate MultiScreen System 96-well plates for vacuum filtration. The filtrate was collected in a 96-well microtiter plate (Fisher Scientific UK, Loughborough, U.K.).

From each well, 10 μl of the filtrate solution containing the MC-LR- HRP conjugate was transferred to a microtiter plate and mixed with 90 μl of 3,3',5,5'-tetramethylbenzidine (TMB) liquid substrate, a ready-to-use liquid substrate containing the chromogen TMB, buffer and hydrogen peroxide. HRP activity was measured by optical density, using the following approach: After colour development for 20 minutes, a volume of 50 μl of HCl 1M was added to each of the microtiter plate wells to stop the reaction and the absorbance was read at 450 nm.

2.6.3 Physical Characteristics of the Polymers

The surface area and total pore volume of a computationally designed MIP (CM-MIP), a methacrylic acid-based MIP (MAA-MIP) and non-imprinted polymers (NIPs) were calculated using the BET (Brunauer-Emmett-Teller) theory and the BJH (Barrett-Joyner-Halenda) computational method. The experiments were performed by Micromeritics U.K. (Dunstable, U.K.), using the nitrogen adsorption/desorption method.

The BET theory states that most substance will adsorb a monomolecular layer of a gas, under certain conditions of partial pressure of gas and temperature. It is possible to estimate the number of molecules covering the adsorbent surface with a monolayer of adsorbed molecules; N_m . Multiplying N_m by the cross-sectional area of an adsorbate molecule yields the sample's surface area (Hiemenz *et al.*, 1997).

The BJH analysis is a computational method, which allows the computation of pore size from equilibrium gas pressures. The method is based on generating experimental curves or isotherms linking the adsorbed gas volumes, with relative saturation pressures at equilibrium and converts the results to cumulative (total) or differential pore size distributions.

2.6.4 Optimisation of Enzyme-Linked MIP Assay

A range of dilutions of the conjugate MC-LR-HRP was initially explored to ascertain the optimum concentration for the competitive enzyme-linked MIP assay. The assay test was performed as previously described and used three different dilutions of the labelled MC-LR conjugate (dilution 1/10, 1/20, 1/40). A polymer suspension (0.5 g l^{-1}) in 50 mM sodium phosphate buffer, pH 7.0 was used in this experiment, with increasing microcystin-LR concentrations ($0.1\text{-}150 \text{ } \mu\text{g l}^{-1}$).

Different concentrations of the polymer suspension (5 g l^{-1} , 0.5 g l^{-1} , 0.1 g l^{-1} , 0.05 g l^{-1}) were prepared in 50 mM sodium-phosphate buffer, pH 7.0 and tested. The competitive assay was carried out with 1/10 dilution of MC-HRP conjugate and increasing microcystin-LR concentrations ($0.1\text{-}100 \text{ } \mu\text{g l}^{-1}$).

2.6.5 Comparison Study with Anti-Microcystin-LR Antibody

A limited amount of anti-MC-LR polyclonal antibody was supplied by Prof. Hennion (Department of Environmental and Analytical Chemistry, Paris). The antibody was employed in a competitive ELISA assay, based on the commercial EnviroGard[®] kit protocol for microcystin-LR detection, as suggested by Prof. Hennion (Rivasseau *et al.*, 1996). The antibody was immobilised on a microtiter plate after diluting 1:1000 in PBS at pH 7.2 from the stock solution. The commercial conjugate MC-LR-HRP (estimated concentration of 1 mg l^{-1}) competed with free microcystin-LR in the standard samples for binding sites in the antibody coated well. The same procedure was adopted using polyclonal antibodies provided with the EnviroGard[®] microcystin-LR plate kit and

monoclonal antibodies obtained with another microcystin-LR ELISA kit from Wako (Osaka, Japan).

The cross-reactivity of the MAA and CM-MIP for microcystin-LR analogues such as microcystin-RR, microcystin-YR, and nodularin was evaluated using the enzyme-linked competitive assay. Different concentrations of each analogue (50 μl in 50 mM sodium-phosphate buffer, pH 7.0) were added to the 96-well filtration microplate with the polymer suspension.

Stability tests were performed by comparing the affinity of MIPs and antibodies to microcystin-LR before and after 2 hours of incubation, under predefined experimental conditions. Antibody solution (100 μl) and MIP suspension (0.5 g l^{-1} , 100 μl) were added to the same volume of each of the following solutions: 80 % dimethylformamide in sodium phosphate-buffered saline (10 mM PBS, pH 7.4), 10 mM HCl at pH 2.0, 50 mM NaOH at pH 11.0, and 10 mM CuSO_4 . In addition, 100 μl of antibody solution and polymer suspension were mixed with 100 μl of PBST buffer and the resultant mixture maintained at temperature of 80 $^{\circ}\text{C}$. After 2 hours of incubation under these conditions, the polymer and antibody solutions were reconditioned by adding 200 μl of 100 mM sodium phosphate buffer, pH 7.0. The remaining receptor affinity was evaluated using competitive assay as a percentage of the affinity under optimum conditions. Untreated polymer and antibody solution were used as positive controls.

$$\% \text{ Affinity} = \frac{\text{Affinity}_{\text{harsh conditions}}}{\text{Affinity}_{\text{max}}} \times 100$$

Where:

$\text{Affinity}_{\text{harsh conditions}}$ = maximum absorbance obtained with the receptor after treatment

$\text{Affinity}_{\text{max}}$ = maximum absorbance obtained with non-treated receptors.

The peroxidase activity was determined using TMB as a substrate solution; absorbance was determined at 450 nm after 20 minutes incubation at room temperature.

2.7 MIP-BASED RECEPTOR FOR DOMOIC ACID

2.7.1 Computationally Designed MIP for Domoic Acid

The polymer synthesis for the toxin domoic acid was based on a computer-aided rational design. The workstation used for this work was a Silicon Graphics Octane, running the IRIX 6.6 operating system; configured with two 195 MHz reduced instruction set processors, 712 MB memory and a 12 GB fixed drive. The system was used to execute the software packages SYBYL 6.7 Tripos Inc. (St.Louis, USA), able to simulate monomers-template interactions.

As a first step, the molecular model of the template and a virtual library (database) containing the most commonly used monomers (for the non-covalent approach) was created by using a Silicon Graphics Octane workstation. The domoic acid molecule and all the monomers were drawn, using the sketch molecule command and charged with the Gasteiger-Hückel method available in SYBYL software. A molecular mechanics method was applied for 2000 iterations, performing an energy minimisation process using the Powell option in MAXIMIN command. All the conditions applied for the energy minimisation are reported in Figure 2.4 (a) and (b).

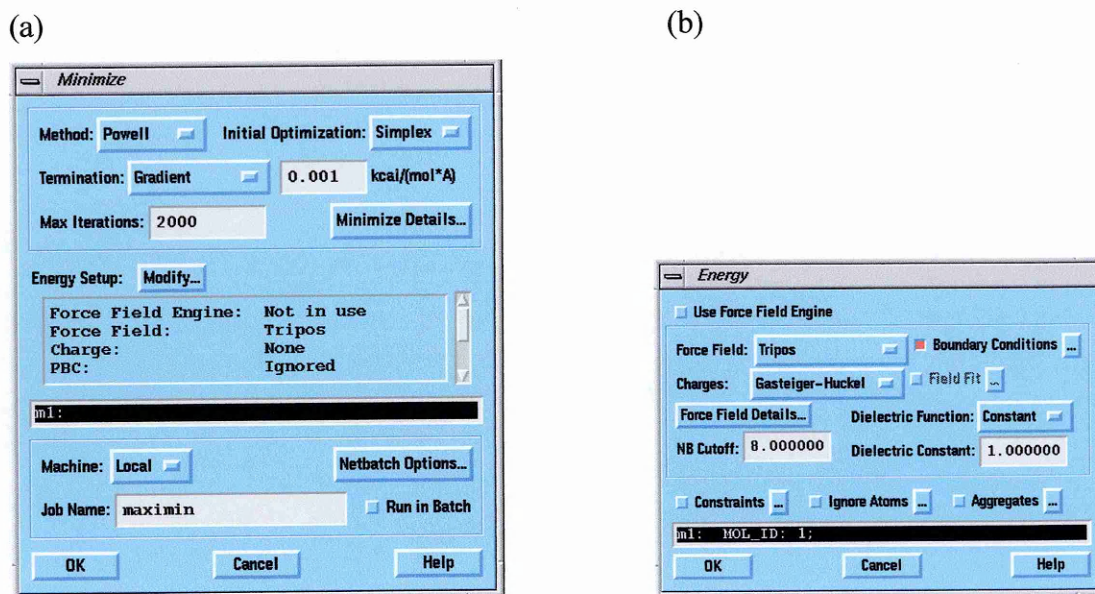


Figure 2.4: SYBYL windows for energy minimisation.

The main window (Minimize) showing the minimisation method, termination, iterations and convergence is reported in (a); the utilised charges and the dielectric function and constant are shown in (b).

A dielectric function and dielectric constant were used as the default parameters, which corresponded to a value of 1. The termination used was gradient and the convergence was reached after a maximum of 2000 interactions, when the difference in energy between one step and the other was less than 0.001 Kcal/mol. A table containing the structural information of each of the monomers contained in database was also created, inserting in the table all the drawn and minimised monomers.

The functional monomers in the database (Figure 2.5) possess residues that are capable of interacting with the template predominantly through electrostatic, van der Waals interactions and hydrogen bonds.

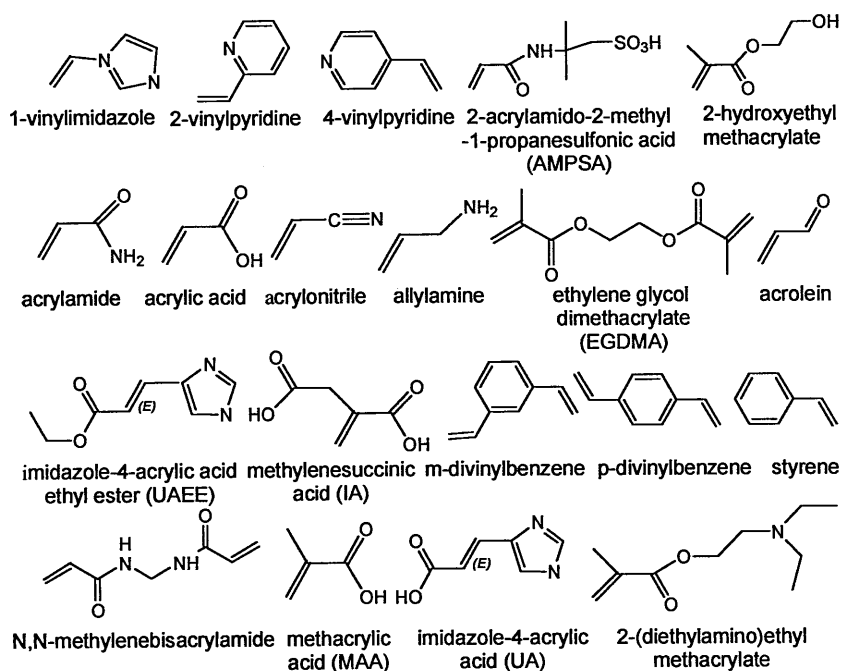


Figure 2.5: Most common monomers included in the virtual library.

Abbreviations: AMPSA, 2-acrylamido-2-methyl-1-propane sulfonic acid; EGDMA, ethylene glycol dimethacrylate; UAEE, imidazole-4-acrylic acid ethyl ester or urocanic acid ethyl ester; IA, methylenesuccinic acid or itaconic acid; UA imidazole-4-acrylic acid or urocanic acid.

In a second step, the Leapfrog program was used to screen the databases of functional monomers. Each of the monomers of the virtual library was probed for its possible interactions with domoic acid. Leapfrog is an algorithm that allows the evaluations of new ligand structures, mainly on the basis of their binding scores. This was calculated with electrostatic screening by repeatedly trying different ligands (one each time), in different positions of the template and by either keeping or discarding the results. During this work, Leapfrog screened electrostatically the monomers of the database. The synthesis of the polymer was then carried out using the monomer(s) composition predicted by computational modeling.

2.7.2 Synthesis of Imprinted Polymer for Domoic Acid

The template domoic acid (6.4×10^{-6} mol, 2 mg) was dissolved in 300 μ l DMF, under sonication. The solution was then mixed in a glass bottle together with a polymerisation mixture, containing the monomer composition predicted by the computational design: 6.4×10^{-6} mol (0.5 μ l) of allylamine, 6.4×10^{-6} mol (0.5 mg) of acrylamide and 6.4×10^{-6} mol (0.9 mg) of urocanic acid. The ratio template monomer was 1:1 for all the monomers selected. The cross-linker EGDMA (1.47×10^{-3} mol, 300 μ l) was added to the polymerisation mixture together with 1,1'-azobis (cyclohexane-carbonitrile) (2.4×10^{-2} mol, 6 mg), acting as a radical initiator for the reaction. The polymerisation was carried out at 80 °C for 24 hours in a silicon oil bath. The same procedure for the preparation of polymer particles and washings, already described for microcystin-LR, was followed for imprinting the polymer for domoic acid

2.7.3 Enzyme-Linked Competitive MIP Assay for Domoic Acid

A MIP-based assay was performed, as already described for microcystin-LR, in order to investigate whether the imprinted polymer had specificity for the target toxin. A suspension of the polymer (50 μ l of 0.5 g l⁻¹ in 50 mM sodium phosphate buffer, pH 7) was dispensed in a 96 well microplate, with solutions containing the conjugate DA-HRP (750 μ g l⁻¹) and different dilutions of free toxin (0.1-10 μ g l⁻¹). The analyte domoic acid was initially dissolved in water and then diluted in sodium phosphate buffer. After 1 hour incubation, the mixture was filtered using a microplate filter and the filtrate separated from the polymer and collected in a 96-well microtiter plate.

From each well, 10 μ l of the filtrate solution containing DA-HRP conjugate was transferred to fresh microtiter plate and 90 μ l of TMB liquid substrate, used for the HRP enzyme conjugate detection, was added. The absorbance was measured after 15-20 minutes at 450 nm after stopping the reaction with 50 μ l of HCl 1M.

2.7.4 Fluorescence Study of OPA-Modified Polymer

A suspension of the polymer (2.5 ml of 3 g l⁻¹ in 100 mM sodium-borate buffer, pH 10.0) was immersed into 4 ml cuvette cell and mixed with 30 µl of domoic acid solution (in the same buffer), containing 30 nmol of b-mercaptoethanol and 50 nmol o-phthaleic dialdehyde (OPA reagents). The same experiment was also repeated in the absence of the target analyte (50 µl of sodium borate buffer). The mixture was incubated and stirred for 15 minutes at room temperature. Fluorescence measurements were carried out using a Shimadzu RF-5001 PC spectrofluorophotometer, with a stirring system and thermostat incorporated. The excitation wavelength was 335 nm and the fluorescence was detected at 450 nm. A change of fluorescence was recorded as a function of time.

The imprinting factor was calculated using equation:

$$I = \Delta F(\text{MIP})/\Delta F(\text{Blank})$$

Where I- imprinting factor, ΔF (MIP)- response for imprinted polymer and ΔF (Blank)- response for blank polymer.

2.7.5 Grafting Photo-Polymerisation

The sensor chip consisted of a glass slide mounted in a plastic frame. On one side of the glass, a thin film, approximately 50 nm, of gold had been deposited. Before use, the BIAcore gold chips (Pioneer J1, BIAcore AB, Uppsala, Sweden), used for the grafting experiments, were cleaned by ultrasonication in ethanol for 30 minutes. The gold chip was then coated with a self-assembled monolayer of 1 mM 2-mercapto ethylamine in ethanol, by soaking for 24 hours at room temperature. Following a brief washing with water and ethanol, the gold surface was again ultrasonicated for 30 minutes in ethanol and left to dry.

The gold chip was coated for 18 hours (in the dark at room temperature) with 1 ml of a solution comprising: 20 mM 4,4'-azo-bis (cyanovaleric acid) photo-initiator, 100 mM water-soluble carbodiimide and 100 mM 1-hydroxybenzotriazole in ethanol. After another washing step with ethanol and ultrasonication for 30 minutes, 50 μ l of polymerisation solution in water (0.25 mmol of 2-(diethylamino) ethyl methacrylate, 0.5 mmol of N,N'-methylenebisacrylamide and 16 nmol of template DA) was deposited on top of the gold chip. The mixture on the chip was irradiated with ultraviolet light (UV-lamp model N° LX300F, Cermax collimated xenon arc lamp, ILC Technology, Inc., USA) for 30 minutes, which resulted in a MIP layer with a thickness of about 40 nm. After polymerisation, the grafted gold chip was incubated in methanol for two hours in order to remove some homopolymer, residual chemicals, and template. A schematic representation of the grafting procedure is presented in Figure 2.6.

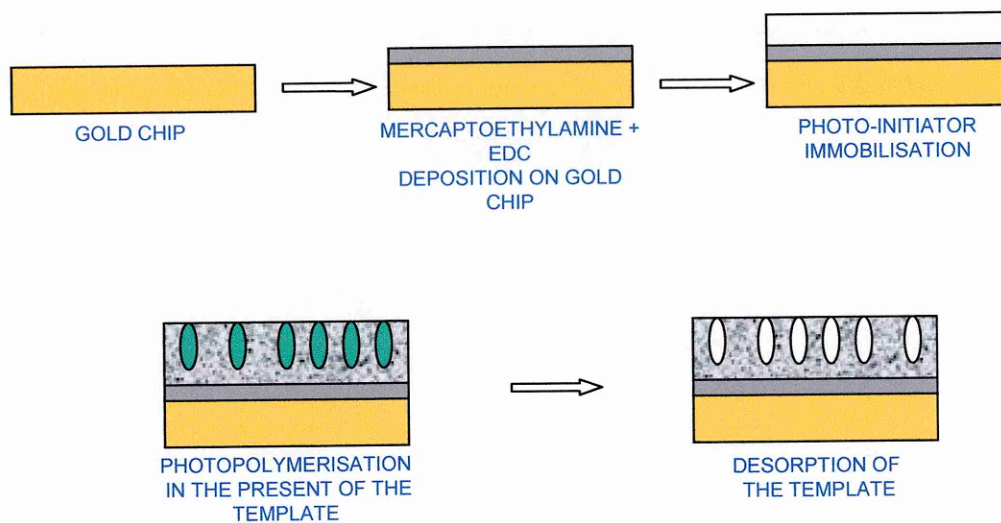


Figure 2.6: Scheme of the grafting procedure.

2.7.6 Characterisation of Photo-Grafted MIP by Atomic Force Microscopy

Photo grafting of the MIP thin films onto the treated gold surfaces (for SPR studies) was first investigated using atomic force microscopy (AFM). Atomic Force Microscopy images were obtained using the PicoScanTM model (Molecular Imaging Corporation, Suite, AZ)

The basic objective of the operation of the AFM is to measure the forces (at the atomic level) between a sharp probing tip (which is attached to a cantilever spring) and a sample surface. Images are taken by scanning the sample relative to the probing tip and measuring the deflection of the cantilever as a function of lateral position.

AFM can be used to investigate a range of forces. In the non-contact mode (with a distance greater than 10 Å between the tip and the sample surface), van der Waals, electrostatic, magnetic or capillary forces produce images of topography, whereas in the contact mode, ionic repulsion forces are the major factor. For this work, the samples were scanned using the contact mode. The “scrapping” experiment was performed with maximum additional force applied to the cantilever, so that the feed back loop would not be disturbed. The area studied was continuously scanned for one hour (approximately 50 scans). After the additional force was removed, the tip of the cantilever was slightly lifted and moved to scan a larger area (6µm by 6µm). The tip was re-engaged with the surface and the feed back loop re-set. From the topographical image it was possible to evaluate the MIP layer thickness, the software controlling the microscope allowed such calculation.

2.7.7 MIP Characterisation by BIAcore Analysis

The BIAcore 3000TM was used for grafted polymer testing and comparison with monoclonal antibody anti domoic acid. The instrument is described in Section 2.2.1. The grafted MIP sensor was inserted into the instrument with the gold side in contact with the flow cell. Running buffer was constantly passed through the chip at a flow rate

of $15 \mu\text{l min}^{-1}$ and the temperature was maintained at $25 \text{ }^\circ\text{C}$. A steady baseline in the sensorgram curves was achieved (average time 30 minutes-1 hour).

The interaction analysis with the BIAcore 3000TM biosensor was then carried out by injecting $80 \mu\text{l}$ of the conjugate DA-HRP, or native HRP, at concentrations ranging from 6 to 400 mg l^{-1} and at a flow rate of $5 \mu\text{l min}^{-1}$. Each injection was followed by a washing phase with HBS-EP buffer (two injections of $50 \mu\text{l}$ at flow rate of 30 ml min^{-1}) and one regeneration step comprising one injection of $10 \mu\text{l}$ 0.2% SDS in 10 mM HCl , $\text{pH } 2.5$ and at a flow rate of $5 \mu\text{l min}^{-1}$.

The competitive reaction was performed by injecting $150 \mu\text{l}$ of a solution containing an equal volume ($75 \mu\text{l}$) of the conjugate HRP-DA (200 mg l^{-1}) and free domoic acid at concentrations of $0.1\text{-}5 \times 10^6 \mu\text{g l}^{-1}$. The flow rate for each injection was of $30 \mu\text{l min}^{-1}$. Equal injections ($150 \mu\text{l}$) of HRP-DA conjugate and the target analytes (0 and $5 \mu\text{g l}^{-1}$) were made on the MIP sensor at flow rate of $30 \mu\text{l min}^{-1}$. Response units were calculated as the difference in response between two sequential data points in the sensorgram.

2.7.8 Biacore Analysis of Anti-Domoic Acid Antibody

The sensor activation was carried out as described in Section 2.2.2. The carboxylated dextran matrix of a gold chip CM5 was activated by mixing equal volumes of 0.2 M EDC and $0.05 \text{ M N-hydroxysuccinimide}$. The mixture was injected ($35 \mu\text{l}$) onto the sensor surface for 7 minutes at a flow rate of $5 \mu\text{l min}^{-1}$. The anti-domoic acid antibodies were immobilised on three different channels of the chip, at concentrations of $20, 50, 100 \text{ mg l}^{-1}$ in $10 \text{ mM acetate buffer pH } 5$. The immobilisation injection flow rate was $5 \mu\text{l min}^{-1}$, with a total volume of $35 \mu\text{l}$ for each sample at $25 \text{ }^\circ\text{C}$. The procedure was completed by a 7-min injection of $1 \text{ M ethanolamine hydrochloride}$ ($35 \mu\text{l}$), in order to block any remaining ester groups. One channel was used as a control with bound non-specific antibody.

Since the immobilised antibody lost a significant amount of their functionality when the regenerations steps were performed, a format with the conjugate immobilised was also investigated. Three different concentrations of the conjugate HRP-DA (150, 300, 500 mg l⁻¹) were immobilised by injecting a total volume of 35 µl of each sample at flow rate was of 5 µl min⁻¹ and temperature of 25 °C. The concentration of 150 mg l⁻¹ was chosen as optimal since increasing the amount of conjugate did not improve the immobilisation process. The conjugate surface was usually regenerated with a 1 min injection of regeneration buffer (SDS 0.2 %-HCl 10 mM, pH 2.5), every time the interaction with the ligand needed to be washed away.

Once the concentration of the conjugate was optimised, three channels were used to immobilise the same concentration of conjugate and one channel was used for immobilisation of HRP protein alone, acting as a control. The anti-DA antibody concentration was also optimised and a titration of antibody in the range of dilutions 1/5 up to 1/10000 was tested for interaction with the immobilised conjugate. The optimal concentration of antibody (75 µl, 6.6 µg ml⁻¹) was finally used for a competition reaction and injected together with different concentrations of the free analyte (75 µl, 0.5-5000 µg l⁻¹) in a total volume of 150 ml (flow rate 30 ml min⁻¹).

CHAPTER 3: RESULTS

IMMUNOREAGENTS CHARACTERISATION AND IMMUNOASSAY DEVELOPMENT

3.1 INTRODUCTION

The first step in this work was to select an appropriate antibody against the toxin microcystin-LR (MC-LR), required for the development of an immunoassay for the detection of MC-LR. The initial antibody preparation was antisera IgG from rabbit (RA IgG), already purified from the original serum. The antibody efficacy was evaluated by using the BIAcore instrument.

The second anti-MC-LR antibody preparation, obtained from Dr Abuknesha (King's College, London), had been purified specifically for MC-LR and was reported to have excellent sensitivity. Furthermore, the antibody was supplied with a gelatin coating conjugate, designed to compliment the antibody from the production stage. These reagents were sequentially incorporated into an enzyme immunoassay (EIA) format, allowing the reagents properties and interactions to be investigated. Firstly, a microtiter plate enzyme-linked immuno-sorbent assay (ELISA) was developed and optimised which then allowed the assay to be transferred to a membrane based ELISA with a view to an immunosensor application, described in Chapter 4.

3.2 IMMUNOREAGENT CHARACTERISATION

3.2.1 Evaluation of Rabbit anti-Microcystin-LR Antibody

BIAcore 3000TM equipment was chosen to assess the affinity and specificity of potential, specific anti-microcystin-LR antisera. The BIAcore instrument is based on surface plasmon resonance (SPR) system and has proven to be useful for the characterisation of antibodies (Reinartz *et al.*, 1996; Malmqvist *et al.*, 1997; Malmqvist, 1999).

The BIAcore system monitors continuously the change in mass at the sensor surface; dedicated software relays this information in response units as a function of time

(sensorgram). The steps involved in the antigen conjugate immobilisation are summarised in Figure 3.1.

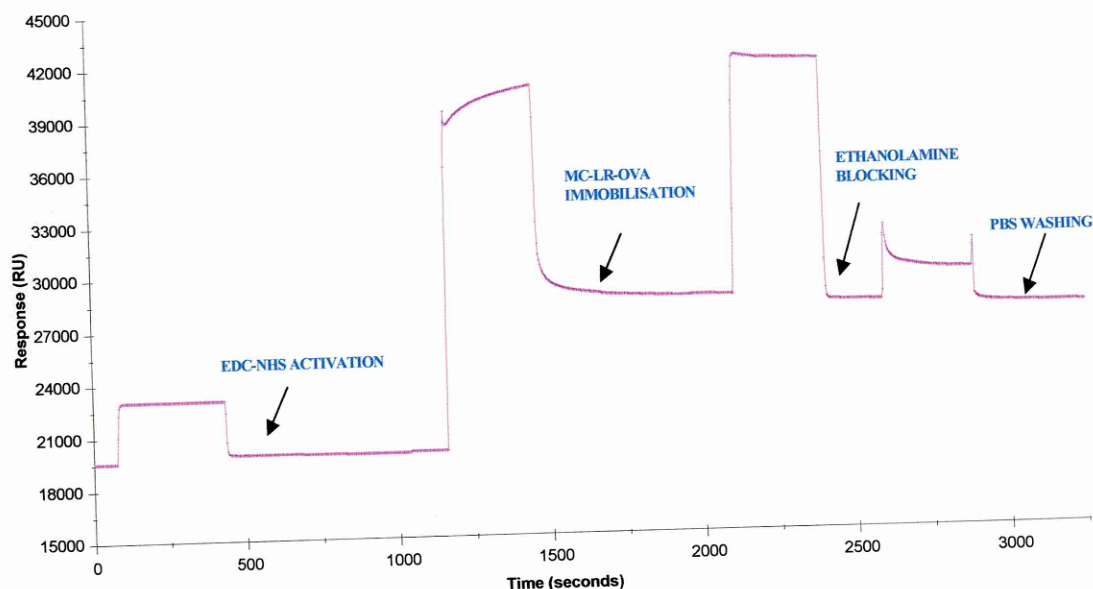


Figure 3.1: Typical immobilisation sequence observed using the BIAcore 3000TM. The immobilisation injection of MC-LR-OVA flow rate was $5 \mu\text{l min}^{-1}$ with $35 \mu\text{l}$ of volume. Data points were set at a steady baseline and the mass bound, expressed as response units (RU), was calculated as the difference in response between two subsequent data points.

To determine the most appropriate concentration of MC-LR-OVA for immobilisation, the sensor chip was initially activated by injecting a mixture of N-ethyl-N'-(3-dimethylaminopropyl) carbodiimide hydrochloride (EDC) and N-hydroxysuccinimide (NHS). These compounds reacted with carboxyl-methyl groups on the dextran matrix of the CM5 sensor chip initiating covalent binding to the ligand. The immobilisation of microcystin-LR-ovalbumin protein conjugate, provided by King's College in a stock concentration of 10 g l^{-1} , was evaluated at concentrations of 100, 200, 300 mg l^{-1} in acetate buffer (pH 4.3) on one chip (chip n° 1) and again 300, 500 and 1000 mg l^{-1} on another chip (chip n° 2). The chip had four separate channels and on each chip used, the fourth channel was kept as a control, with no immobilised ligand. A 7-minute injection of 1 M ethanolamine hydrochloride ($35 \mu\text{l}$) blocked the remaining ester groups; an

injection of PBS running buffer was finally used to re-establish the baseline. The results of the conjugate MC-LR-OVA immobilisation are shown in Figure 3.2.

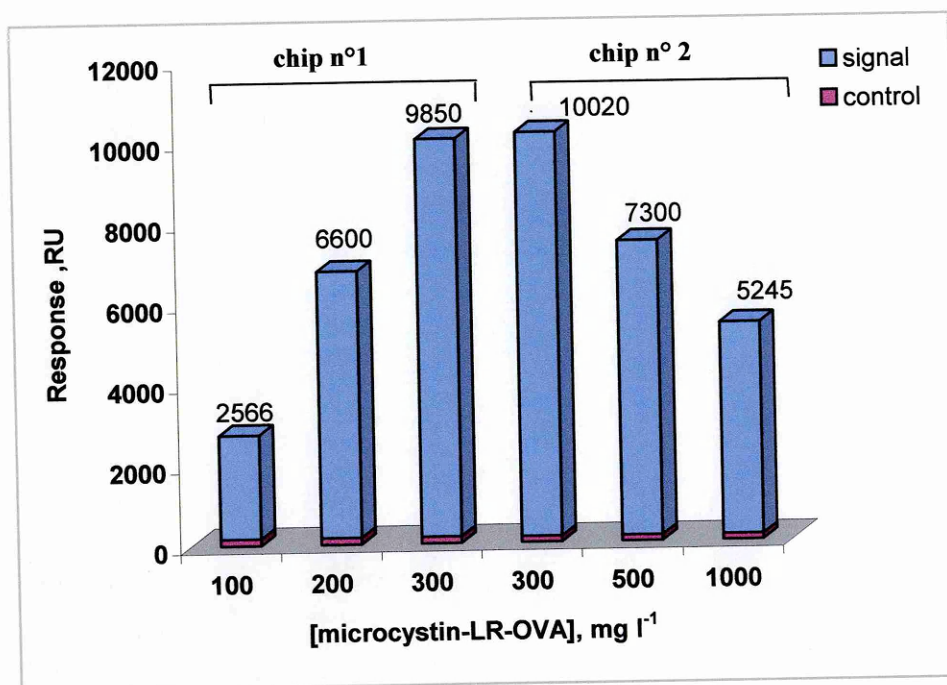


Figure 3.2: Optimisation of the immobilisation for MC-LR-OVA on the chip. MC-LR-OVA was immobilised onto the channels of the chip at 25 °C and concentrations: 100, 200, 300 mg l⁻¹ on one chip and 300, 500, 1000 mg l⁻¹ on a second chip. The flow rate was 5 µl min⁻¹ and the total volume was 35 µl.

The results, depicted in Figure 3.2, showed that on chip n° 1, the signal for 100 mg l⁻¹ of conjugate was approximately 2600 RU. This response was more than doubled for 200 mg l⁻¹ and increased to 9850 RU for 300 mg l⁻¹ of the microcystin-LR-OVA conjugate. In contrast, for chip n° 2, an increase in conjugate concentration did not correspond to a higher RU value. The injection at 300 mg l⁻¹ of microcystin-LR-OVA was repeated and a similar response in RU was observed (chip n° 1 = 9850 RU; chip n° 2 = 10020 RU). In the case of 500 and 1000 mg l⁻¹ of ligand, the signal was lower than 10000 RU. Therefore, saturation in MC-LR-OVA immobilisation was achieved with a concentration of approximately 300 mg l⁻¹, hence, this value was considered optimal for further analysis. Since 10,000 RU is equivalent to approximately 10 ng protein/mm²,

and the sensor chip surface is $1.2 \text{ mm}^2/\text{channel}$, a coupling level of $\sim 12 \text{ ng}$ in the working channel was obtained. Since the chips are very expensive and the immobilisation is not reversible, at this initial stage no further optimisation of the conjugate concentration was attempted.

The MC-LR-OVA conjugate (300 mg l^{-1} in acetate buffer, pH 4.3) was injected over a new sensor chip (chip n° 3) for a 7-minute immobilisation step, at a flow rate of $5 \mu\text{ l min}^{-1}$. The anti-MC-LR IgG, over a range of concentrations between 0 and 50 mg l^{-1} , was then injected over the MC-LR-OVA coated surfaces in order to evaluate the specificity of the antibody for the immobilised conjugate. Figure 3.3 shows the result achieved from this experiment.

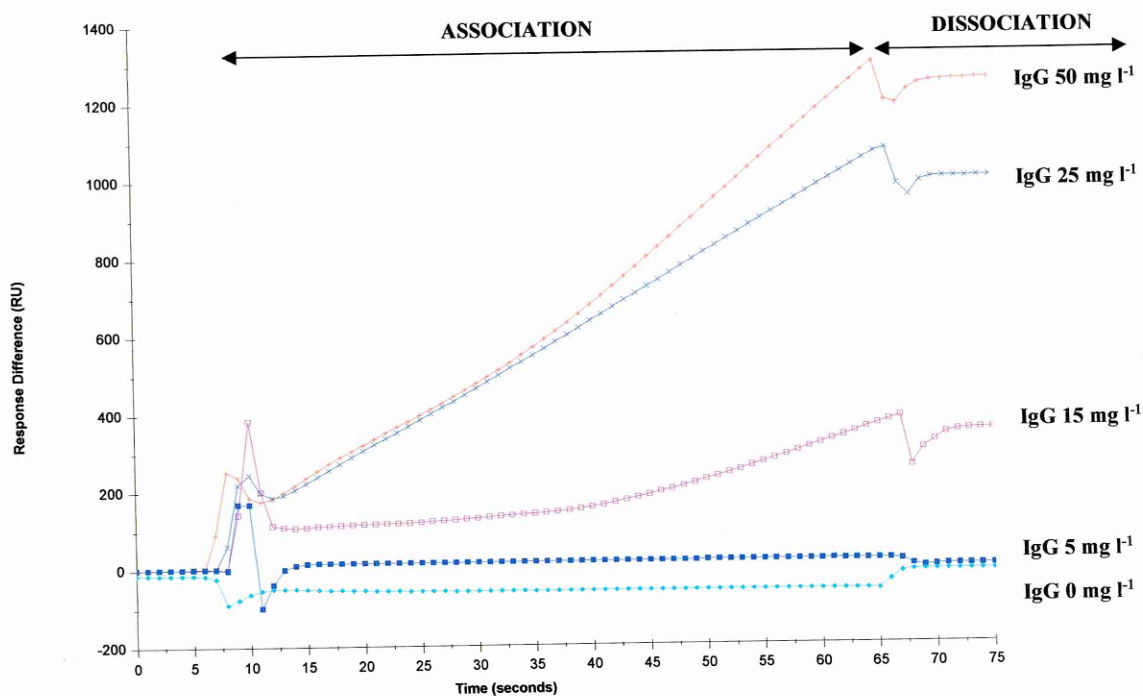


Figure 3.3: Binding of the anti-MC-LR IgG concentrations ($0\text{--}50 \text{ mg l}^{-1}$) to the immobilised MC-LR-OVA conjugate. The injection volume was $40 \mu\text{ l}$ at a flow rate of $15 \mu\text{ l min}^{-1}$.

The injections were carried out in sequence over one single sensorgram however, to simplify the analysis, the injections were aligned to the same starting point by using the software BIAevaluation 3.2 from the BIAcore package.

In the association phase of the experiment (from 10 to 67 seconds), the antibody solutions were introduced into the buffer flow above the sensor surface and the progress of complex formation at the sensor surface was monitored. An increasing RU value was more remarkable for 50 and 25 mg l⁻¹ than for the lower concentrations. This procedure was followed by the dissociation phase (from 68 to 75 seconds) in which the antibody was absent from the running buffer and the time-course of the complex dissociation was recorded. In order to remove the complex antigen-antibody, the sensor needed to be regenerated since the RU value did decrease very little during the time, meaning a strong interaction between antigen and antibody. One injection of 0.2 % SDS in 10 mM HCl (10 µl), at flow rate of 5 µl min⁻¹ was found to be sufficient to remove non-covalently attached material, while maintaining the biological activity of the immobilised ligand.

To determine the levels of non-specific binding and cross-reactivity, the RA anti-MC-LR IgG at a concentration of 50 mg l⁻¹ was injected over a chip where a channel was coated with OVA alone as a control. The antibody showed very high cross-reactivity binding to OVA with value of 300-800 RU. Pre-incubation of all the antibody dilutions with OVA (1 mg ml⁻¹) was then tried to prevent cross-reactive binding of the OVA-specific antibody fraction to the MC-LR-OVA and OVA-coated surfaces. In Table 3.1 the results of two experiments are summarised.

Table 3.1: Summary of results of the SPR analysis with BIAcore 3000™ before and after a pre-incubation step with OVA (1 mg ml⁻¹).

MASS BOUND [RU, mean ± SD (n= 3)]			
SAMPLES	Sequential run (MC-LR-OVA coated surface)	Control run (OVA coated surface)	Sequential run- Control run
RA IgG before pre-incubation	1640 ± 90	1332 ± 54	308
RA IgG after pre-incubation	837 ± 34	755 ± 68	82

Abbreviations: RU= response unit; RA IgG= antisera anti- microcystin-LR from rabbit; MC-LR-OVA= microcystin-LR- ovalbumin conjugate
SD= Standard deviation of the mean

The results in Table 3.1 illustrate that the pre-incubation step of the antibody dilutions with the protein ovalbumin did not improve the specific binding of antibody to the MC-LR-OVA. However, it did decrease the binding on both MC-LR-OVA and OVA-coated surfaces, suggesting that RA anti-MC-LR IgG had poor affinity for the antigen microcystin-LR, and exhibited a high cross-reactivity towards the carrier protein ovalbumin.

To confirm the above result, a displacement experiment was carried out. An injection of 50 mg l⁻¹ IgG (without pre-incubation with OVA) was performed over the MC-LR-OVA coated surface; the control channel was kept without a ligand coating. Different concentrations of MC-LR-OVA (from 0 mg l⁻¹ to 3 mg l⁻¹) were then injected into the coated chip sensor. Likewise free MC-LR (range of concentrations from 0 to 500 mg l⁻¹) injections were performed on the sensor chip (Figure 3.4 and Figure 3.5).

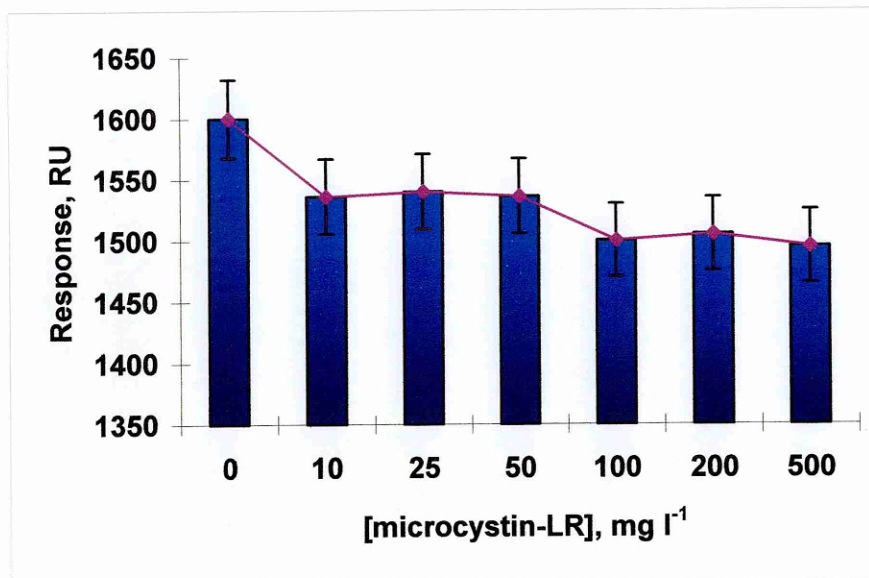


Figure 3.4: Displacement assay for microcystin-LR.

Concentrations of MC-LR from 0 to 500 mg l⁻¹ were injected onto the sensor chip, coated with the complex OVA (300 mg l⁻¹)-IgG (50 mg l⁻¹). The injection volume was 40 µl and the flow rate 15 µl min⁻¹. Error bars= ± SD, *n*= 2.

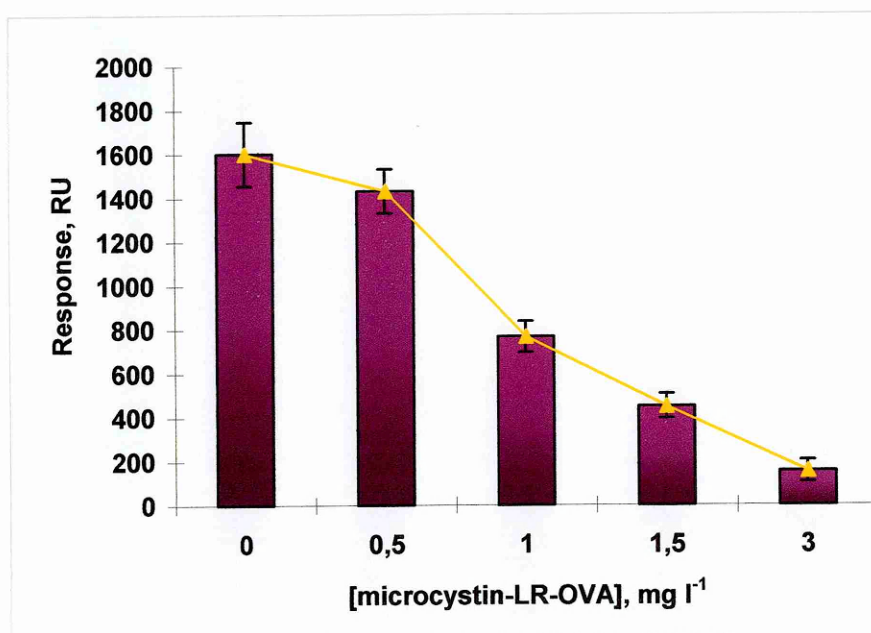


Figure 3.5: Displacement assay for microcystin-LR-OVA.

Concentrations of MC-LR-OVA from 0 mg l⁻¹ to 3 mg l⁻¹ were injected onto the sensor chip coated with the complex OVA (300 mg l⁻¹)-IgG (50 mg l⁻¹). The injection volume was 40 µl and the flow rate 15 µl min⁻¹. Error bars= ± SD, *n*= 2.

The results shown in Figure 3.4 and Figure 3.5 confirmed that the conjugate MC-LR-OVA was able to displace the anti-MC-LR antibody bound to the linked antigen-conjugate, this was not evident in the case of the free toxin. An example of the sensorgram showing this displacement is shown in Figure 3.6 (a) and (b).

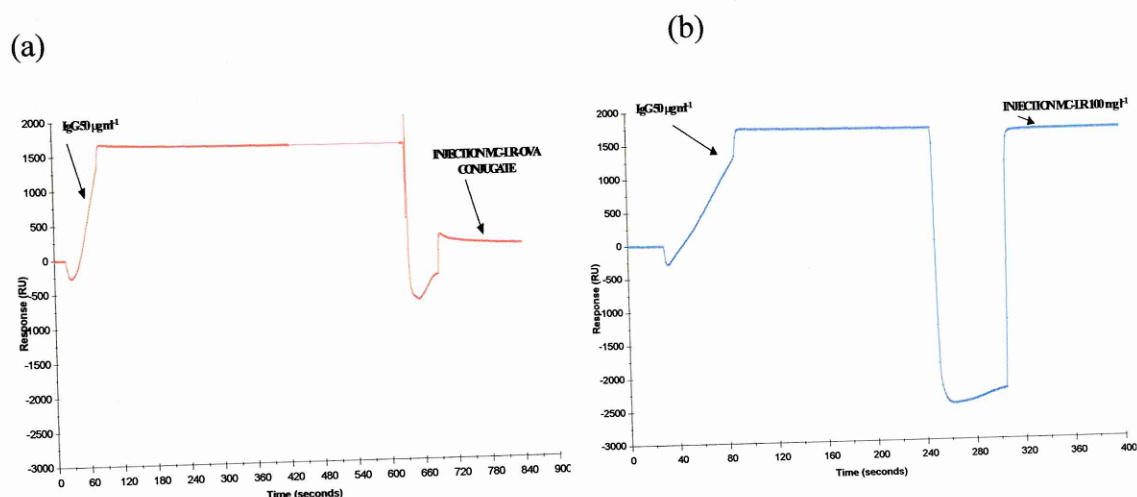


Figure 3.6: Displacement assay sensorgram after (a)- Injection of conjugate MC-LR-OVA (3 mg l⁻¹) and (b)- Free MC-LR (100 mg l⁻¹).

The sensorgram in Figure 3.6 (a) shows a rapid dissociation of antibody from immobilised conjugate following injection of the microcystin-LR-OVA conjugate (3 mg l⁻¹). The response after the IgG injection was approximately 1700 RU. The subsequent injection of conjugate provoked a decrease in the signal to approximately 150 RU. The sensorgram in Figure 3.6 (b) shows a low dissociation of antibody from the immobilised antigen conjugate after injection of free MC-LR in solution (100 mg l⁻¹). From 1700 RU, only approximately 100 RU were displaced by the injection of free MC-LR. The results confirmed that the earlier observed binding was substantially towards the carried albumin and not the toxin hapten.

3.3 ASSESSMENT OF ANTI-MICROCYSTIN-LR POLYCLONAL ANTIBODY

The second batch of anti-MC-LR antibody was raised in sheep (SH anti-MC-LR IgG) and affinity purified specifically for MC-LR detection. This antibody was provided with the appropriate antigen conjugate, designed in conjunction with the initial immunogen structure. The specific binding of SH anti-MC-LR IgG to the analyte conjugate (microcystin-LR-gelatin) was initially investigated using a double dilution checkerboard titration assay. With the checkerboard titration assay, both antisera and coated conjugate were serially diluted in one experiment. This analysis provides a demonstration for the presence of specific antibodies to target substances and shows the relationship between the concentrations of all reagents and their effect on an assay response in an experiment (Figure 3.7).

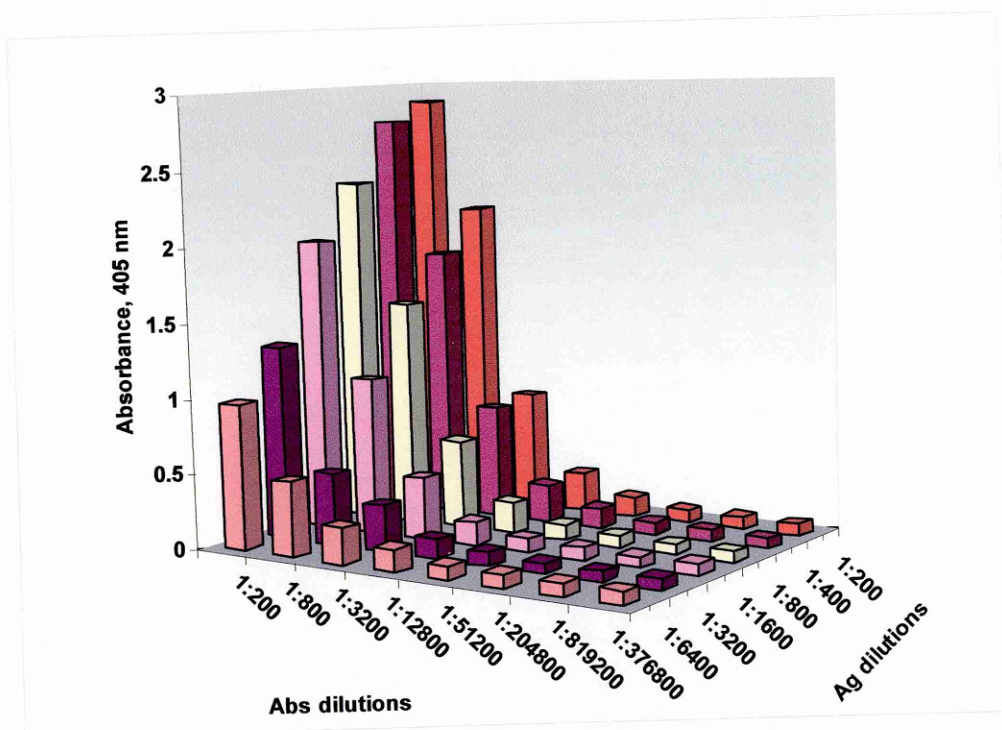


Figure 3.7: Checkerboard titration for SH anti-microcystin-LR polyclonal antibody. Abs= anti-MC-LR polyclonal antibody, Ag= microcystin-LR.

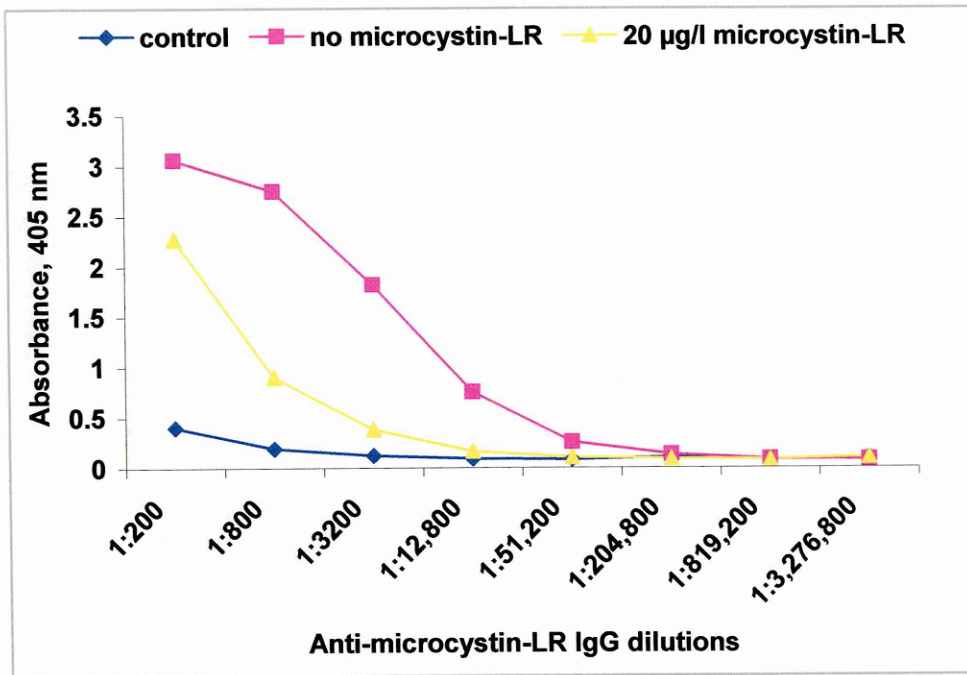
Checkerboard titration experiments were optimised in an indirect competitive ELISA format. After coating the Dynex Immulon 4HB plate with serially diluted gelatin-MC-LR conjugate for 1 hour, the washed plate was blocked for another hour with 0.5 % gelatin at room temperature. The anti-MC-LR primary antibody was incubated for 1 hour at 37 °C with gentle shaking to promote an interaction with the coated analyte. Following the washing, the anti sheep HRP-labelled secondary antibody (1:20,000) was incubated again for 1 hour at 37 °C. The immuno-reaction was revealed by adding ABTS substrate solution. After 20 minutes, the colorimetric reaction at 405 nm was recorded. It was shown that the antisera contained a specific binding activity to the adsorbed toxin-gelatin conjugate. This testing procedure provided information on antisera titres with varied concentrations of solid phase antigen and gave a guide to the best antibody dilution for further competitive ELISA development. The most appropriate dilution of antibody for the immunoassay development was approximately 1/1500 used in association with a 1/400 dilution of MC-LR-gelatin conjugate, since it was preferable to use the lowest possible concentration of antibody and conjugate which gave a value of 1-1.2 optical density.

3.3.1 Anti-Microcystin-LR IgG Reagent Sensitivity and Affinity

The sensitivity of SH anti-MC-LR IgG against gelatin-MC-LR antigen was further investigated and the dissociation constant K_d calculated, from the reciprocal Hughes-Klotz plot, as shown in Figure 3.8 (a) and (b).

The assay was performed in a similar manner to the checkerboard titration method, described earlier. The anti-MC-LR antibody dilutions were added to the coated plates over range of concentrations, from the stock solutions of $130 \mu\text{g l}^{-1}$, sequentially diluted to $0.25 \mu\text{g l}^{-1}$ and incubated for 1 hour at 37 °C. The secondary antibody anti-sheep, labelled to the enzyme HRP, was added and bound to the specific antibody (primary antibody) onto the plate at 37 °C; left to incubate for one hour. The colorimetric reaction was carried out as previously discussed.

(a)



(b)

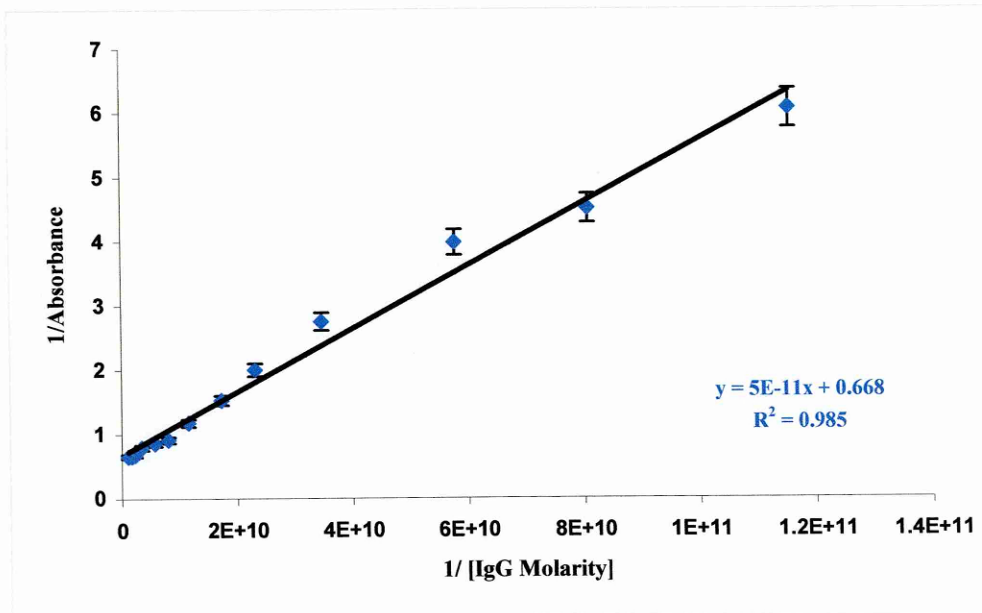


Figure 3.8: The titration curve (a)- and Hughes –Klotz plot (b)- for SH IgG. MC-LR-gelatin 1/400 and gelatin alone (control) coating. 0.5 % gelatin blocking, SH IgG titration from stock. 1/20,000 2° IgG-HRP incubation. Optical density read at 405 nm after 20 minutes of ABTS substrate solution incubation. Error bars = \pm SD, $n = 3$.

The graphs in Figure 3.8 (a) show a very low absorbance for non-specific binding to the modified gelatin (control). Binding to MC-LR-gelatin is shown in absence of any competing free microcystin-LR and in the presence of $20 \mu\text{g l}^{-1}$ of standard MC-LR. It is clear that the effect of added free MC-LR is to drastically reduce binding. This demonstrated the presence of specific antibodies to MC-LR and indicated the working conditions for a subsequent competitive ELISA. According to these data, the titre of this antibody was approximately 1/1200-1/2000. From the results in Figure 3.8 (b), the affinity constant was calculated (with Hughes-Klotz plot) as 5×10^{11} , meaning a strong affinity of the anti-MC-LR antibody for the antigen conjugate.

3.3.2 Gelatin Coating Conjugate

The gelatin-MC-LR conjugate was titrated to investigate its relative binding properties to the SH anti-MC-LR IgG; and to determine the concentrations required for sorbent coating on polyester microtiter plate and membranes, for the immunoassay development. Figure 3.9 shows the titration curve obtained for the conjugate diluted from stock of approximately $1200 \mu\text{g l}^{-1}$. The titration curve shows that the antibody had a high sensitivity to gelatin-MC-LR with a detection reaching extinction at approximately $0.2 \mu\text{g l}^{-1}$. This was to be expected as the SH IgG was affinity purified to specifically detect the microcystin-LR. A coating saturation was demonstrated at about $300 \mu\text{g l}^{-1}$, indicating an effective coating concentration. Such a concentration value corresponded approximately to a 1/400 dilution from the stock solution of gelatin conjugate.

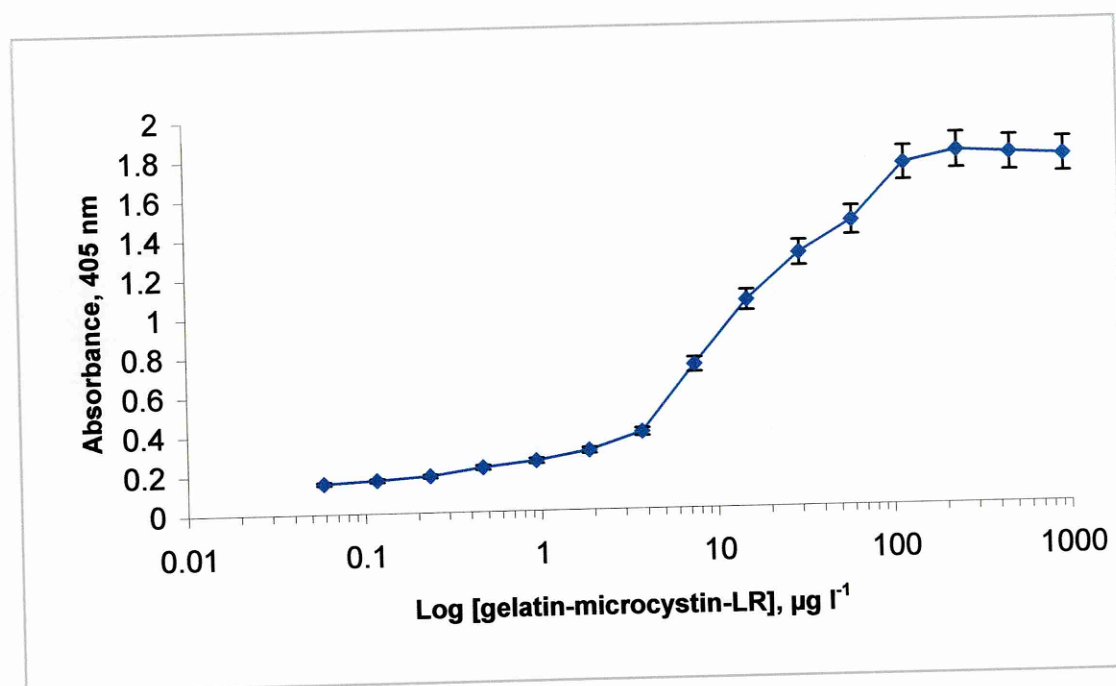


Figure 3.9: Gelatin conjugate coating titration.

The conjugate MC-LR-gelatin was titrated from stock (1000 mg l^{-1}). 0.5 % gelatin blocking, 1/1500 SH anti-MC-LR IgG, incubation for 1 hour at 37°C . 1/20,000 2° IgG-HRP incubation for 1 hour at 37°C . Optical density read at 405 nm after 20 minutes of ABTS substrate solution incubation. Error bars = \pm SD, $n = 3$.

3.4 MICROCYSTIN-LR DETECTION BY COMPETITIVE ELISA

The competitive ELISA procedure was carried out in a two steps fashion: suitably diluted antibody (1/1500) and analyte (microcystin-LR standards in range of $0\text{-}10 \mu\text{g l}^{-1}$) were incubated for approximately one hour at 37°C in a water bath. The reaction mixtures ($150 \mu\text{l}$) were transferred to the MC-LR gelatin coated plates, where an additional period of 30 minutes incubation at room temperature with gentle shaking was allowed. The washed plates were treated with secondary antibody-HRP conjugate and the assay continued, as described previously.

3.4.1 Optimisation of Competitive Reaction Incubation Conditions

The incubation of the mixture anti-MC-LR IgG and microcystin-LR with conjugate gelatin coated plate was carried out at 37 °C with 1150-rpm agitation in an incubated orbital shaker. The incubation duration was 30 minutes, although 15 minutes was determined to be sufficient at 37 °C. The coating and blocking steps, however, were carried out at room temperature (R.T.). It was therefore preferable for the competitive reaction to also be carried out at ambient temperature but with a gentle shaking. Competition curves of assays with these differing incubation parameters are shown in Figure 3.10.

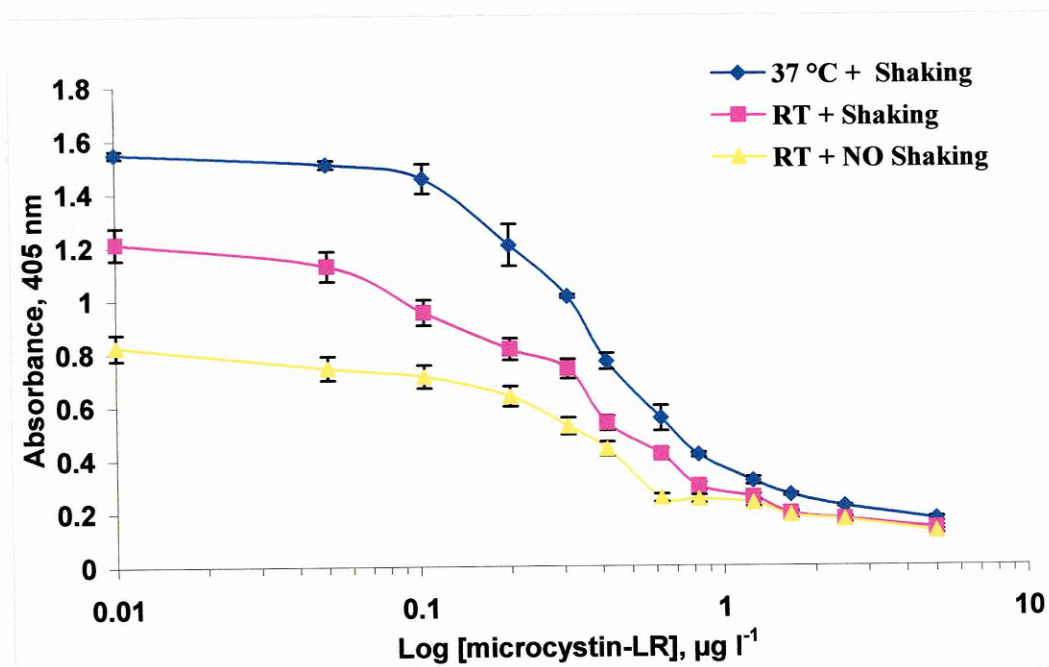


Figure 3.10: Comparing incubation reaction conditions on assay sensitivity. Gelatin-conjugate 1/400 coating. 0.5 % gelatin blocking. MC-LR standards pre-mixed with the IgG competed with either agitation at 37 °C or R.T. or without agitation at R.T. with a final dilution of SH IgG 1 /1500. 2° IgG-HRP 1/20,000 incubation for 1 hour at 37 °C. Optical density read at 405 nm after 20 minutes of ABTS substrate solution incubation. Error bars = \pm SD, $n = 4$.

3.4.2 Immunosorbent Coating and Blocking Incubation Duration

The polystyrene sorbent coating conditions and incubation periods were optimised for rapid and reproducible binding, yielding minimum background levels. High binding capacity microtiter plates were used as sorbent microtiter plates, using 0.1 M sodium carbonate-bicarbonate buffer, pH 9.6 as the coating buffer and 0.5 % gelatin as the blocking agent. The effect of different combinations of coating (15-60 minutes) and blocking (0-60 minutes) incubation times at room temperature, without shaking were investigated. The results are presented in Figure 3.11. The times reported correspond to the coating and the blocking incubation stages respectively.

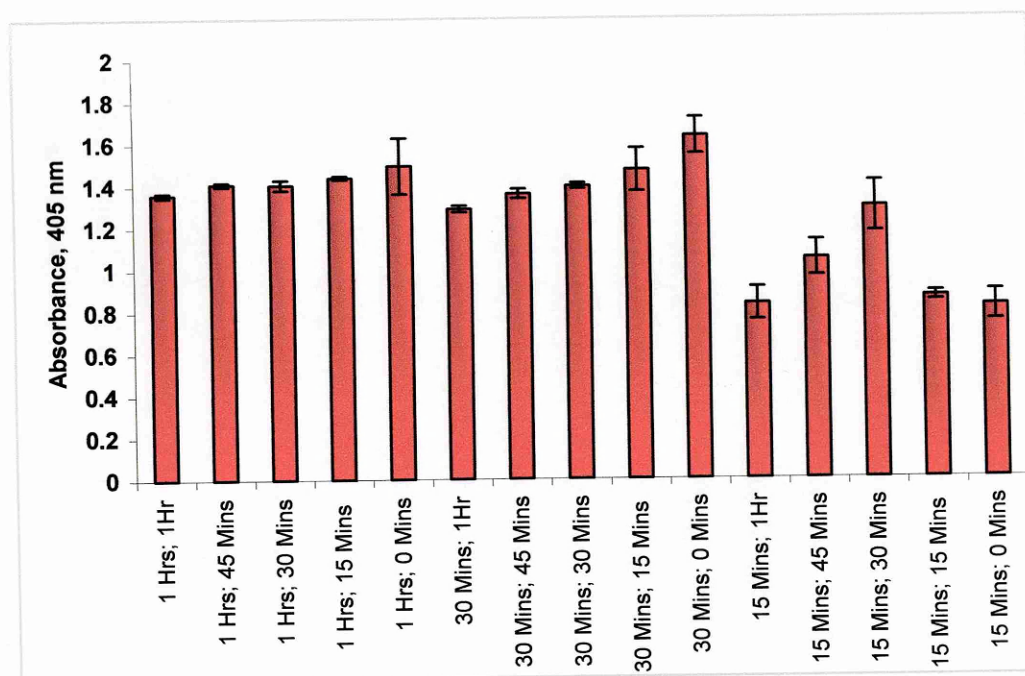


Figure 3.11: Investigation of coating and blocking incubation duration.

Coating with conjugate-gelatin 1/400 for between 15-120 mins and blocking with 0.5 % gelatin for between 0-60 mins. SH IgG 1 /1500 and 2° IgG-HRP 1/20,000 incubation for 1 hour at 37 °C. Optical density read at 405 nm after 20 minutes of ABTS substrate solution incubation. Mean assay % CV of 4.44. Error bars = \pm SD, $n = 3$.

The trend shows that the assay response decreased with a reduction in coating duration, decreasing by 30 % for a 15 minutes coating treatment. The data showed that the majority of effective blocking occurred within the first 15 minutes and that with an optimum gelatin-MC-LR coating and SH IgG concentration, no blocking could be used without detriment to the signal or background level. The preferable working conditions for this competitive ELISA assay development were 1 hour coating and 45 minutes blocking.

The calibration curve for the optimised competitive ELISA for microcystin-LR detection is presented in Figure 3.12.

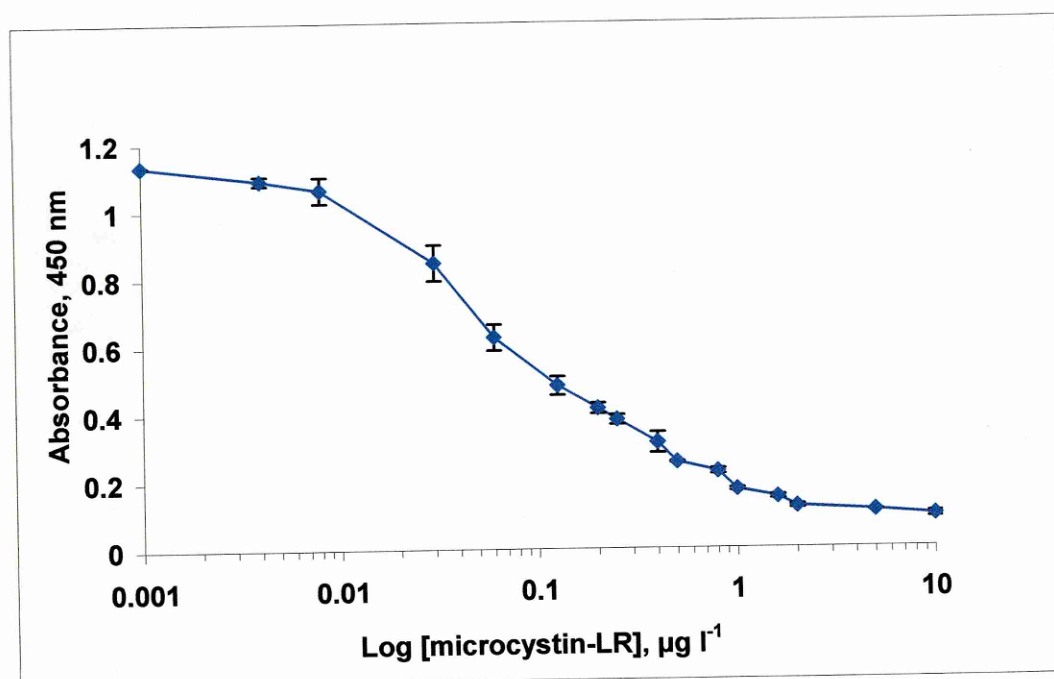


Figure 3.12: Competitive ELISA assay for microcystin-LR.

Assay was coated with gelatin-MC-LR and 0.5 % gelatin blocker. MC-LR standards and final dilution of 1/1500 MC-LR IgG followed by 1/20,000 2^o IgG-HRP. Optical density read at 405 nm after 20 minutes of ABTS substrate solution incubation. Error bars= \pm SD, $n=4$.

Under these experimental conditions, the values for the blank (A_0 , no toxin added) were generally about 1-1.2. The ELISA standard curve for microcystin-LR showed a typical sigmoidal response for microcystin-LR concentrations from zero to $10 \mu\text{g l}^{-1}$. The detection range considered was between 80 % and 20 % of the curve optical absorbance value of $0.022\text{-}0.8 \mu\text{g l}^{-1}$. The responses were highly reproducible, as indicated by the low standard deviations and the mean % CV for the assay. The ELISA's lowest limit of detection set at 80 % of the maximum response (in absence of free toxin), $0.022 \mu\text{g l}^{-1}$ of microcystin-LR.

3.4.3 Microcystin-LR IgG Cross-Reactivity Analysis

The competitive ELISA assay was performed as described in Section 3.4 and standards of different microcystins and nodularin toxin were used. The calibration curves obtained for all toxins are shown in Figure 3.13 and the data is summarised in Table 3.2.

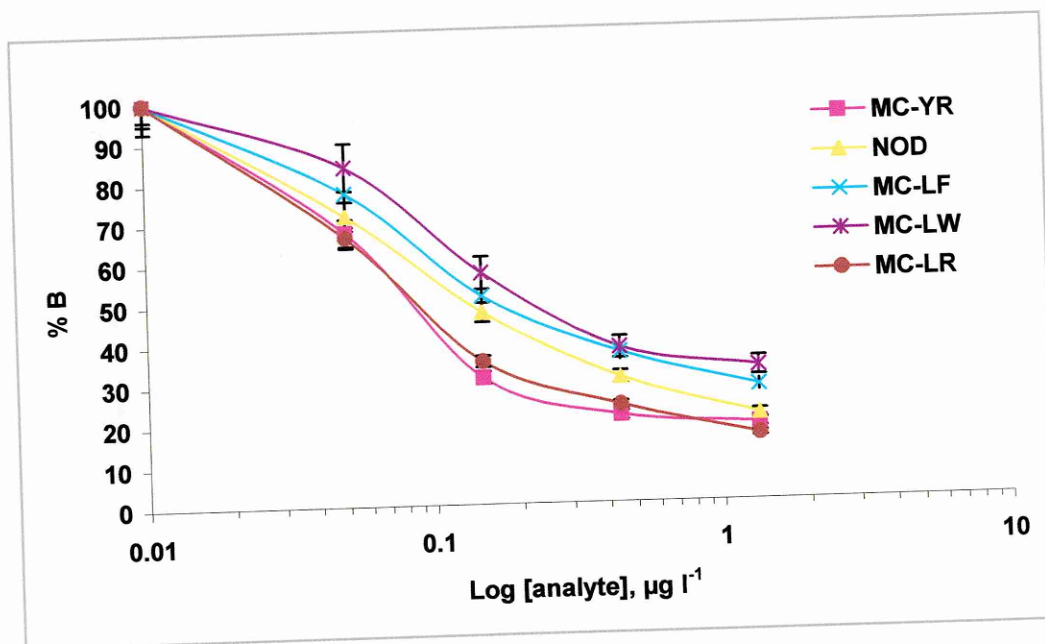


Figure 3.13: Cross reactivity curves for microcystin-LR and its analogues. Gelatin conjugate 1/400 coating. 0.5 % gelatin blocking. Toxin standards incubated with SH IgG 1 /1500 for 1 hour at 37°C . 2° IgG-HRP 1/20,000 incubation for 1 hour at 37°C . Optical density read at 405 nm after 20 minutes of ABTS substrate solution incubation. Error bars = \pm SD, $n = 3$. Abbreviations: MC=microcystin NOD=nodularin.

Table 3.2: Cross-reactivity values showed by anti-MC-LR antisera.

TOXINS	% Cross- Reactivity	EC₅₀ μg l⁻¹	Mean % CV	LLD₈₀ μg l⁻¹
MC-LR	100	0.08	3.5	0.022
MC-YR	96	0.09	4.7	0.035
NOD	78	0.12	1.2	0.054
MC-LF	61	0.19	3.3	0.041
MC-LW	46	0.27	4.1	0.061

The cross-reactivity of anti-microcystin-LR antibody was estimated using microcystin-LR as the reference analyte (cross-reactivity= 100 %). Cross reactivities were high with all cyclic peptides, with values ranging from over 100 % to 50 %. The results are in line with published data (Rivasseau *et al.*, 1999), which show that polyclonal antisera binds to substantially similar common structural moieties in the cyclic peptides. This means that such antisera may be used for rapid screening tests to indicate the presence (and levels) of these toxin families, without specific reference to a particular peptide.

3.4.4 Matrix Effects

Since the field samples will be mainly river and lake water (in addition to extracts of cells), it was necessary to assess the effects of tap water and filtered river water (from Thames river, U.K.) on the binding of anti-MC-LR antibodies. The matrix effects, due to the presence of salts or organic compounds (such as humic acid in water supplies) were assessed by a calibration assay for MC-LR, under varied conditions where the standard analyte solutions were made up in ELISA buffer containing 0.05 % Tween 20, in PBS buffer, in tap water or filtered Thames water (Figure 3.14).

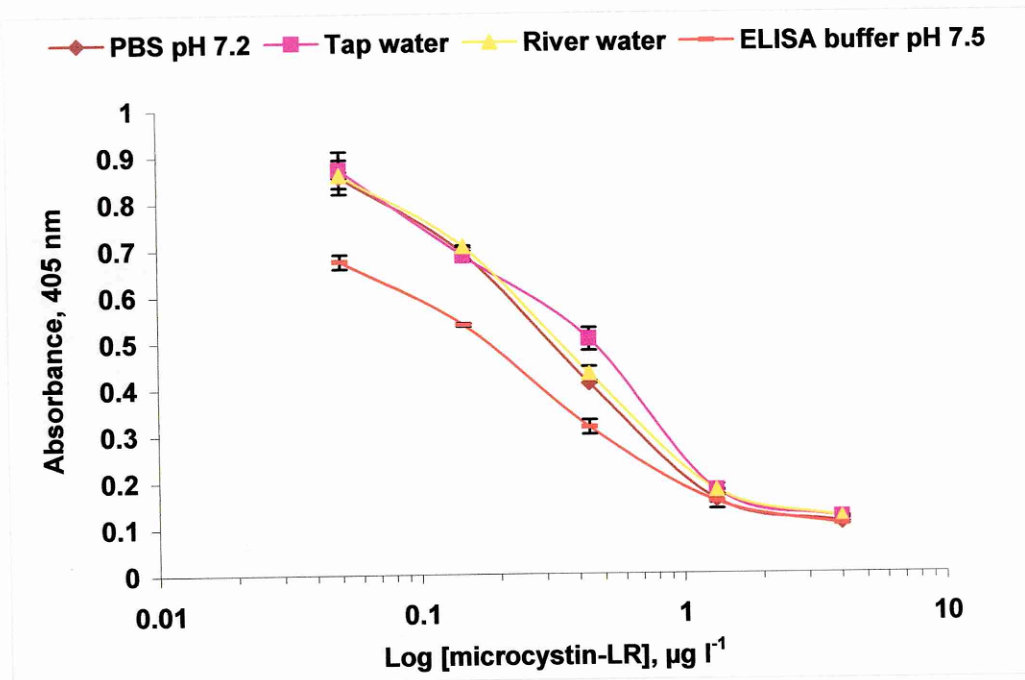


Figure 3.14: Matrix effect for analyte microcystin-LR. gelatin conjugate 1/400 coating. 0.5 % gelatin blocking. MC-LR standards in different solutions competed with SH IgG 1 /15000 for 1 hour at 37 °C. 1/20,000 2° IgG-HRP incubation for 1 hour at 37 °C. Optical density read at 405 nm after 20 minutes of ABTS substrate solution incubation. Error bars = \pm SD, $n = 3$.

The results indicated that there were no significant effects from the test matrices. Tap and river water increased binding, the curves shifted to the right, without any significant changes in graph slope. This merely shows that antibodies bind better under these conditions, probably due to the presence of calcium ions (and others salts).

A similar experiment was performed with the primary antibody diluted in ELISA buffer, PBS buffer, and river water. In this case, a minimal increase in the optical absorbance value was observed for higher antibody dilutions (Figure 3.15).

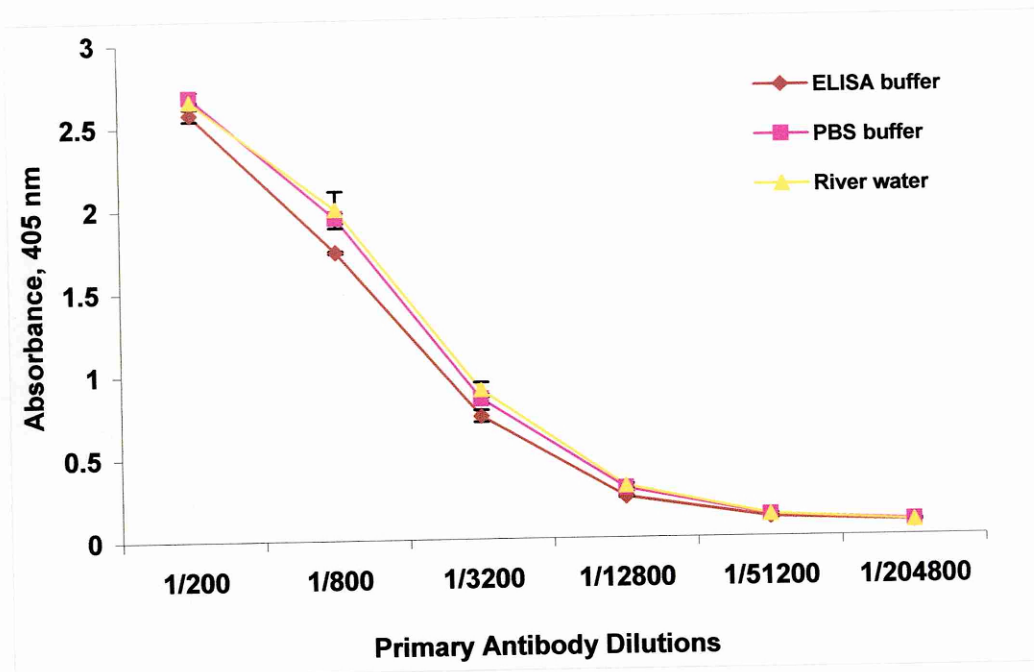


Figure 3.15: Matrix effects for primary antibody anti microcystin-LR. Gelatin conjugate 1/400 coating. 0.5 % gelatin blocking. MC-LR standards competed with different dilutions of SH IgG 1 /1500. 1/20,000 2° IgG-HRP incubation for 1 hour at 37 °C. Optical density read at 405 nm after 20 minutes of ABTS substrate solution incubation. Error bars = \pm SD, $n = 3$.

3.7 CONCLUSION

Two anti-MC-LR antibodies were screened to select an appropriate immuno-receptor for the development of a competitive immunoassay for microcystin-LR detection. The anti-MC-LR antibody raised in rabbit was evaluated using the BIAcore sensor and it was shown to be non-specific for the target analyte, showing a high cross-reactivity towards the carrier protein ovalbumin.

The sheep anti-MC-LR IgG (received by King's College London) demonstrated excellent characteristics with high MC-LR affinity, selectivity, and sensitivity when used in conjunction with the gelatin- MC-LR conjugate provided. The sensitivity enabled a detection limit of $0.022 \mu\text{g l}^{-1}$ of microcystin-LR in a competitive immunoassay to be achieved.

The conditions of the assay in terms of temperature, shaking and time of incubations were all investigated and it was concluded that a temperature of 37 °C was preferable during a pre-mixing step of the anti-MC-LR antibody with free toxin standards and a one hour incubation of the HRP labelled secondary antibody. All other steps (coating, blocking, competition) performed equally well at room temperature.

The cross-reactivity results showed a high cross-reaction of the anti-MC-LR IgG for microcystin-LR analogues. This was probably because the chemical differences between microcystins are insignificant and, hence, there is a high cross-reactivity of the anti-MC-LR antibody with other microcystins (mainly with microcystin-YR). Nodularin, despite the fact that is a pentapeptide, shares substantial structural features with microcystins. Work with this compound, similarity resulted in a substantial level of cross-reactivity to the anti-MC-LR antibody. No relevant drawbacks were observed when different matrixes were analysed for both analyte and antibody. This provided valuable information as to the suitability of the antibody for the ultimate goal of its application in an immunosensor for the detection of microcystin-LR analysis in freshwater.

CHAPTER 4: RESULTS

IMMUNOSENSOR DEVELOPMENT

4.1 INTRODUCTION

Results from the development of a microtitre plate ELISA for microcystin-LR detection, described in the previous Chapter, gave an optimal response in terms of sensitivity and specificity. The transfer of such an assay format to a membrane based ELISA (MELISA) for an immunosensor application would combine ELISA performance with the advantage of rapid, low cost and *in situ* analysis. An antibody-based format for a MELISA was investigated, aiming for higher efficiency and a reduced non-specific signal.

Fixing the membrane into intimate contact with the working electrode of a screen-printed sensor facilitated signal transduction. This was facilitated by the use of a mediator (such as hydroquinone) that acts as a cyclical redox (reduction/oxidation) electron shuttle, allowing the activity of the HRP enzyme label to be monitored amperometrically. Subsequently, the amperometric measurement of the colorimetric substrate 2,2'-azino-bis(3-ethylbenz-thiazoline-6-sulfonic acid (ABTS), in presence of H₂O₂, was explored. This was applied to the detection of microcystin-LR (MC-LR) and incorporated into a competitive flow injection assay (FIA) for preliminary investigation into colorimetric and amperometric MC-LR detection.

4.2 ELISA OPTIMISATION FOR THE DETECTION OF MICROCYSTIN-LR

The MC-LR IgG competitive ELISA, described in the previous Chapter, was transferred to a membrane bound MELISA. The membrane product chosen was UltraBind™ from Pall Gelman Sciences U.K.. The membranes are flexible, robust, porous and, due to a controlled pore structure, are consistent in term of pore size and performance across the membrane. The membranes are suitable for solid phase immuno-diagnostic tests and flow-through assays and claim low non-specific binding and background levels.

4.3 MEMBRANE SORBENT SELECTION

Two types of membrane were available: US-450, US-800, where '450' and '800' indicate pore sizes of 0.45 μm and 0.8 μm respectively. 'US' denotes an unsupported polyethersulfone membrane. Preliminary data showed that the US-800 membrane was clearly the superior for this application. The larger 0.8 μm pore size would allow better perfusion of the reagents into the inner matrix of the membrane, enabling a more efficient covalent coating/blocking of the membrane and diffusion of conjugate for binding and washing. This was also facilitated by the faster flow rate of the US-800 membrane at 3-9 secs 100 ml^{-1} at 24" Hg (from product data). The high response, fast wicking, double sided properties of the membrane (without support material) rendered the US-800 membrane suitable for amperometric detection; where a fast diffusion of the reagents to the electrode surface is essential. Having selected a suitable membrane, the optimal concentration of the coating conjugates, the blocking procedure and the concentration of primary antibody were determined.

4.3.1 Microcystin-LR-Gelatin Coating Titration

The optimised conditions adopted for the competitive ELISA (Section 2.3) needed to be reconsidered when using the membrane as a sorbent surface, compared to the polystyrene microtiter plate. The MC-LR-gelatin conjugate was applied to 6 mm membrane discs by spotting on 5 μl of the solution and leaving to incubate for 15 minutes, as recommended by the membrane manufacturers. In the protocol provided by Pall, it was also suggested to leave the membrane to air dry before proceeding further. This method of immobilisation was preferred to immersing the membranes in MC-LR-gelatin (in order to conserve the limited reagent supply), which was required in a high (undiluted) concentration.

After coating, the US-800 membranes were blocked with 5 % gelatin for 45 minutes at room temperature. The membranes were laid in microtiter plate wells where the anti-

MC-LR antibody (50 μl) was dispensed; covering the entire membrane surface. The membranes were then washed individually in PBS buffer and left to dry at room temperature. Lastly, 1/20,000 dilution of HRP labelled secondary antibody (50 μl) was added and left to incubate for 1 hour at 37 $^{\circ}\text{C}$. For the primary and secondary antibodies, the volume was sufficient to immerse the membrane with the reagents, the time of incubation were kept at 1 hour.

Following intensive washing of the membranes, the ABTS substrate solution was added (150 μl) and incubated in the dark for 20 minutes. The result from the titration profile is shown in Figure 4.1.

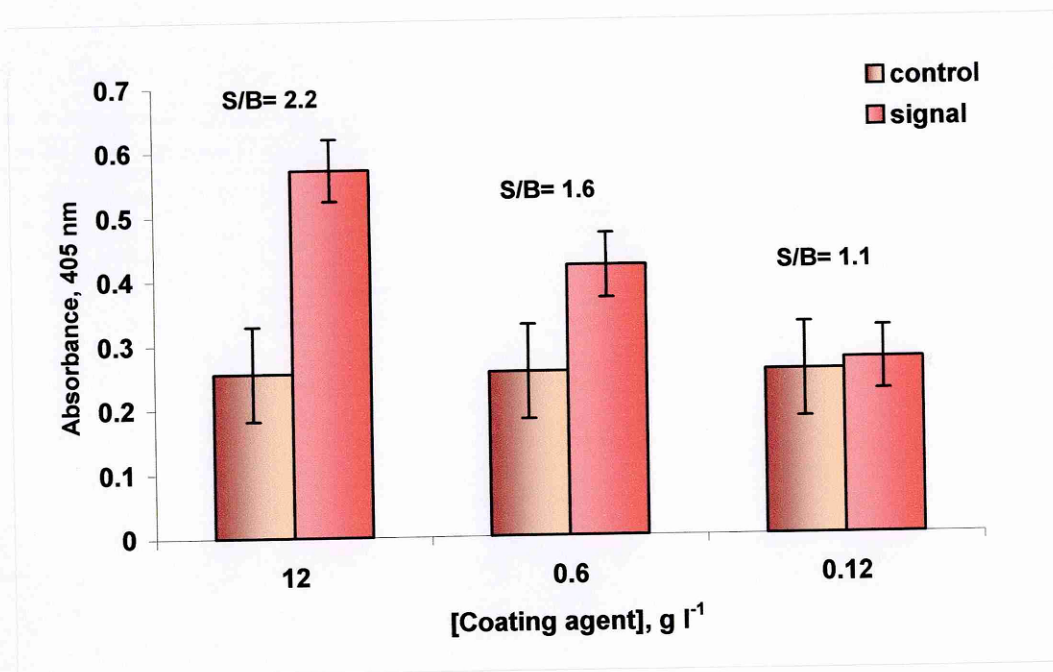


Figure 4.1: Coating antigen-conjugate titration.

Membranes coated with either MC-LR-gelatin or native gelatin in 100 mM sodium carbonate buffer. 5 % gelatin blocking. 1/1500 primary antibody. 1/20,000 secondary antibody. Optical density read at 405 nm after 20 minutes of ABTS substrate solution incubation. Error bars = \pm SD. $n = 4$. Abbreviations: S/B = signal/control.

Three coating concentrations were tested, however their suitability for further applications was compromised by the comparatively high non-specific signal. Standard deviations values were high and the % CV was 8.4, 12, and 18.2 for 12 g l^{-1} , 0.6 g l^{-1} and 0.12 g l^{-1} respectively, showing a very low coating reproducibility, though steady background levels were observed.

4.3.2 Comparing Membrane Blocker Efficiency

A variety of different blocking agents were investigated, for reducing the non-specific signal of the enzyme-linked immunoassay reaction on the membrane. After coating the membranes, either with MC-LR-gelatin conjugate (signal) or native gelatin (control), a blocking agent was deposited on the top of the membrane and left for 45 minutes at room temperature. The ELISA assay was continued by adding (in sequence) the primary anti-MC-LR antibody, the secondary antibody and the ABTS substrate for determination of HRP enzyme activity, as previously described (Figure 4.2).

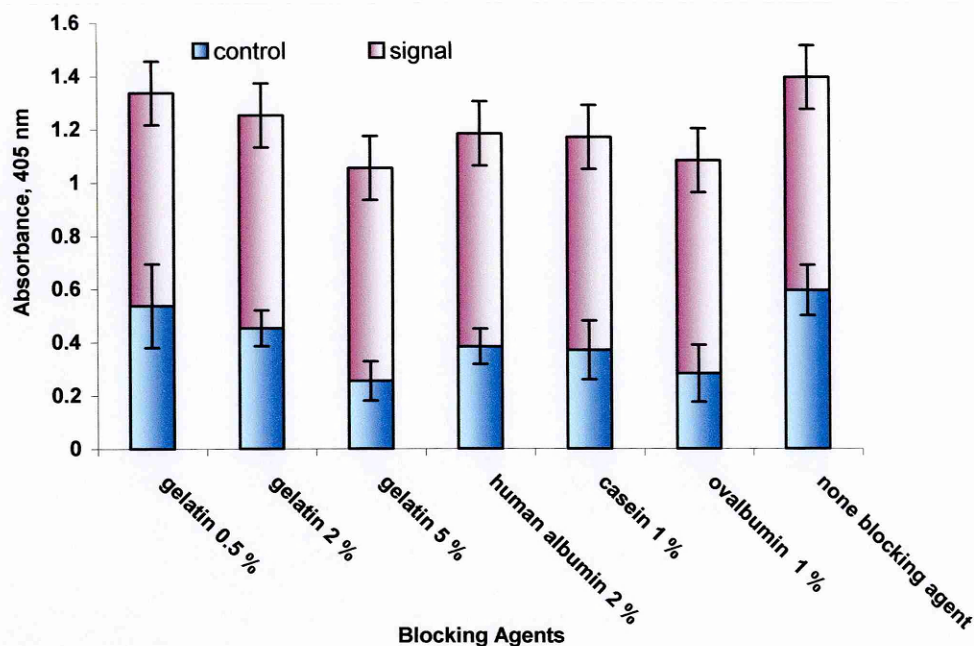


Figure 4.2: Results from the blocking agents investigation.

Either native gelatin (control) or gelatin-MC-LR conjugate (12 g l^{-1}) was immobilised on UltraBind™ membranes. Different blocking agents were applied for 45 minutes at R.T., then 1/1500 primary antibody and 1/20,000 secondary antibody. Optical density was read at 405 nm after 20 minutes of ABTS substrate solution incubation. Error bars = \pm SD. $n = 4$.

The comparison between different blocking agents on the membrane sorbent support (Figure 4.2) showed that the blocking efficiency improved when the gelatin concentration was increased from 0.5 % to 5 % (S/B from 1.6 to 2.9 respectively) and that other blocking agents did not improve performance (S/B~2). Results also showed that the blocking step was important, since its omission resulted in a significant increase in the non-specific signal (S/B= 1.4). However, in all cases, assay reproducibility was very poor with mean % CV > 20. When the time of incubation in the blocking step was increased up to 1 and half hours at room temperature, no improvement in blocking efficiency was observed.

In conjunction with a high non-specific signal, a problem related to a low specific signal was evident, the maximum optical absorbance signal was no higher than 0.6 at the highest possible conjugate coating concentration of 12 g l^{-1} . Further optimisation of the primary and secondary antibody concentrations did not lead to an increase in the signal of maximum response. Figure 4.3 illustrates the results from a MELISA competitive assay, carried out as previously described, using four different anti-MC-LR antibody concentrations and two concentrations of secondary HRP labelled antibody.

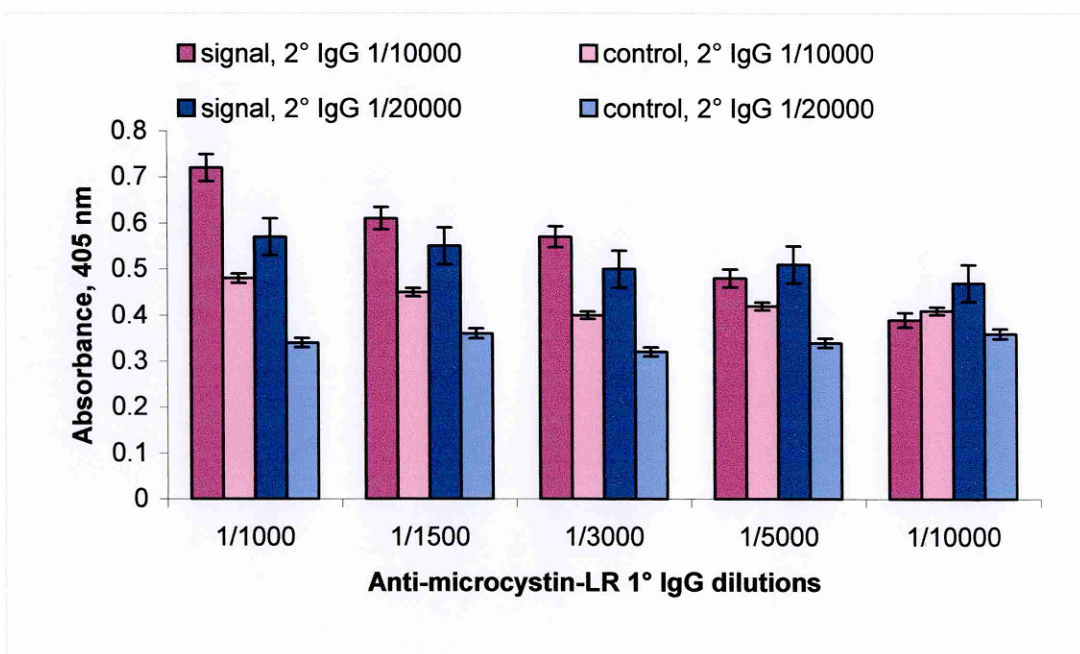


Figure 4.3: Optimisation of antibody concentrations for competitive MELISA assay. Membrane coating with either MC-LR-gelatin or control free gelatin. Serial dilutions of anti-MC-LR IgG and 1/10,000, 1/20,000 secondary HRP labelled IgG. Optical density read at 405 nm after 20 minutes of ABTS substrate solution incubation. Error bars= \pm SD. $n = 2$.

It was observed that there was no significant change in the MELISA performance when different concentrations of primary antibody were explored, whereas increasing the secondary antibody concentration to 1/10,000 dilution gave an increase in absorbance in all cases, including the control signal. Furthermore, the control membrane on which no

MC-LR conjugate was immobilised did show a signal of approximately 0.3-0.4 in each case.

It was concluded that the result was probably due to the low efficiency of the coating agent (microcystin-LR-gelatin) binding to the membrane. The carrier gelatin did not contain a high number of amino functional groups, thus it did not allow a significant number of covalent bindings with the sorbent pre-activated PES membranes.

4.4 ANTIBODY-BASED FORMAT FOR MELISA

4.4.1 Antibody Titration on Membrane

An enzyme immunoassay with anti-MC-LR antibody immobilised onto the sorbent surface was directly investigated and optimised by immobilisation onto the UltraBind™ membrane. In this case, the assay required the use of the analyte conjugated to a label enzyme. A commercial solution of the conjugate MC-LR-HRP was employed. This conjugate competed with free microcystin-LR toxin for binding to the available sites on the immobilised specific antibody.

The antibody anti-MC-LR was titrated to investigate its relative binding properties and concentration, required for membrane sorbent coating. The titration was performed following a protocol established for the ELISA kit commercially available for microcystin-LR detection (Adgen, Scotland, U.K.). Antibody dilutions over a range from 1/250 to 1/20,000 (10 µl in PBS buffer) were spotted on the top of membrane and left for 15 minutes at room temperature. The membrane discs were dried and a blocking solution (0.5 % gelatin) was added and incubated for other 30 minutes at 37 °C. Finally, the conjugate MC-LR-HRP from Adgen EnviroGard kit was added and left to react for 1 hour at 37 °C. The membranes were washed individually by immersing them several times in a PBS buffer containing 0.05 % of Tween 20. The HRP enzyme activity was determined using ABTS as a substrate (0.5 g per 1 litre of sodium acetate/citrate buffer,

pH 4.1, to which 10 μ l of 30 % hydrogen peroxidase was added). Colour formation was measured after 20 minutes incubation in the dark at 405 nm (Figure 4.4).

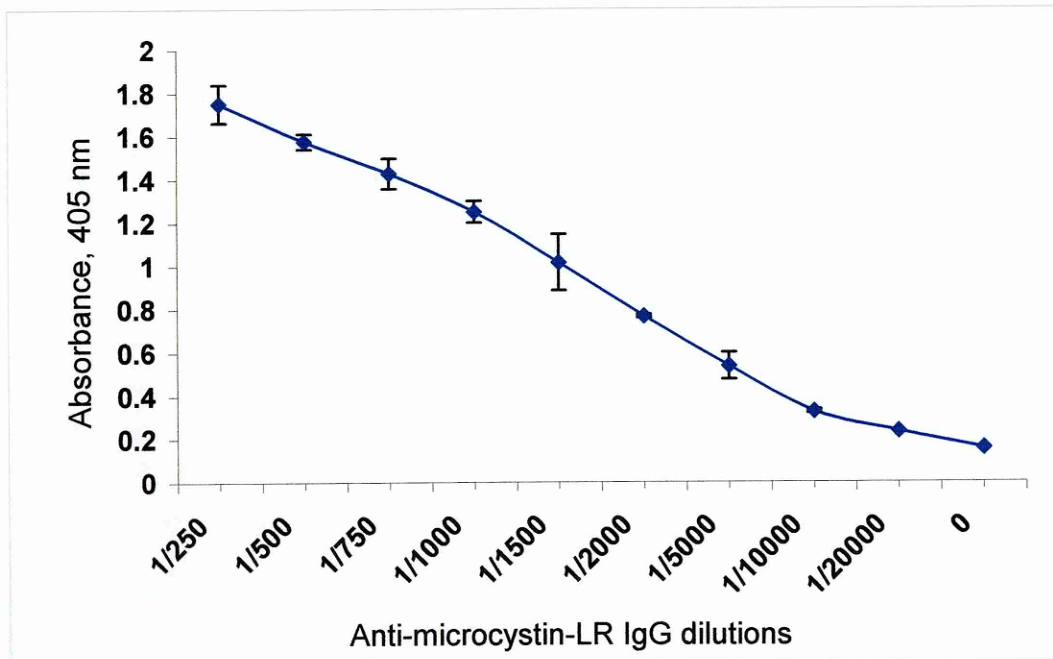


Figure 4.4: Titration of anti-microcystin-LR antibody.

Coating PES membranes with dilutions of anti-MC-LR antibody. 0.5 % gelatin blocking. MC-LR-HRP incubation for 1 hour at 37 °C. Optical density read at 405 nm after 20 minutes of ABTS substrate solution incubation. Error bars = \pm SD. $n = 3$.

The results shown in Figure 4.4 indicate that an appropriate dilution for the antibody was about 1/1000 corresponding to a concentration of $\sim 12.8 \text{ mg l}^{-1}$. This generated an absorbance (at 405 nm) of 1.4 ± 0.05 for maximum optical absorbance. This result showed the suitability of MC-LR IgG for an antibody-based MELISA and provided a firm basis for the continued development of the assay onto the membrane sorbent for the immunosensor format.

The competitive MELISA assay, based on IgG immobilised on membrane sorbent, was optimised with colorimetric detection in order to reduce the variable parameters

encountered when subsequently coupled with electrochemical detection; thus simplifying and hastening the development and optimisation process. The assay was carried out by the immobilisation of anti-MC-LR IgG at a dilution of 1/1000 and blocking, as previously described. The competition reaction was performed by adding a mixture of equal volume of the MC-LR-HRP conjugate and different MC-LR standards ranging from 0 to 10 $\mu\text{g l}^{-1}$. The mixture of analyte was kept in contact with the immobilised antibody for 1 hour at 37 °C. After final washings, the colorimetric reaction was detected by adding the ABTS substrate solution and reading the optical density at 405 nm (Figure 4.5).

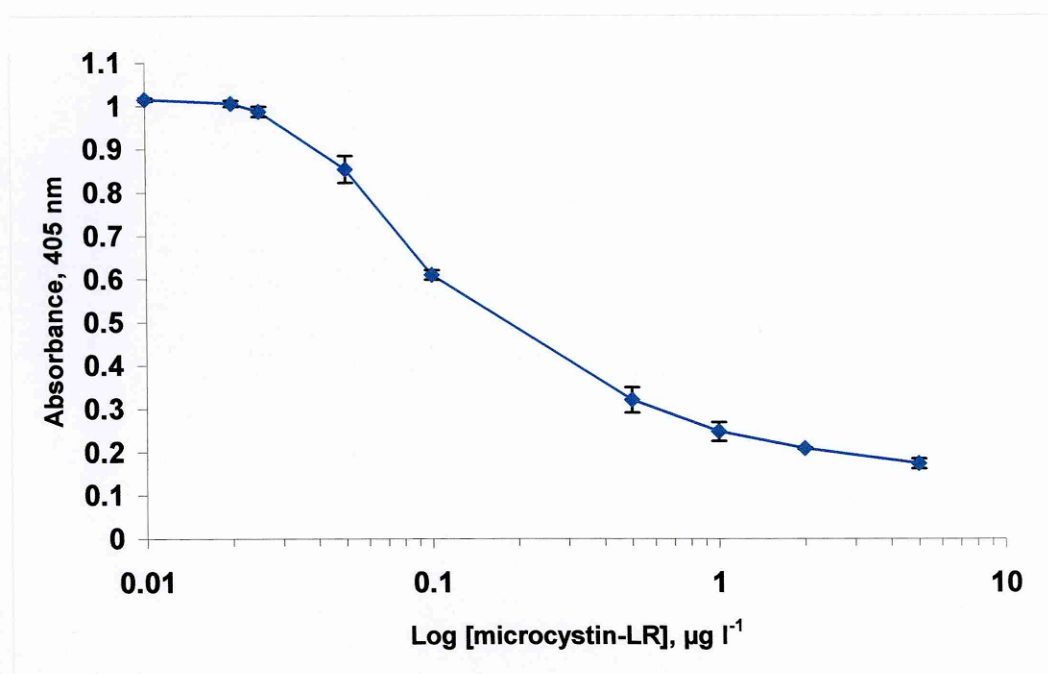


Figure 4.5: Competitive assay with IgG immobilisation on membrane.

Each membrane was coated with a 1/1000 dilution of IgG anti MC-LR and 0.5 % gelatin blocker. The MC-LR standards were then competed for 1 hour at 37 °C, with a constant concentration of the conjugate MC-LR-HRP. The optical density was read at 405 nm after 20 minutes of ABTS substrate solution incubation. Error bars= \pm SD. $n = 4$.

The steps for the immuno-reaction were reduced to two and the resulting assay was slightly faster than the previous format with coated gelatin conjugate. By reducing the steps, the problem of low reproducibility (mean assay % CV of 4.35) was overcome. The minimum amount of toxin detected ($LLD_{80} = 0.06 \mu\text{g l}^{-1}$) was still below $0.1 \mu\text{g l}^{-1}$, which is less than the freshwater concentration limit for microcystin-LR. Therefore, this EIA format was selected for implementation into an electrochemical sensor.

4.5 IMMUNOSENSOR DEVELOPMENT

4.5.1 Hydroquinone Electro-Activity

The selected mediator for this study was hydroquinone. The choice was made after literature studies and using the expertise developed in our laboratory working with this mediator. The electro-activity of hydroquinone was first investigated by cyclic voltammetry (CV), to determine the redox profile of cyclic voltammogram. The CV technique revealed redox peaks and the potentials at which hydroquinone was oxidised and reduced, quasi-reversibly. The voltammogram is shown in Figure 4.6.

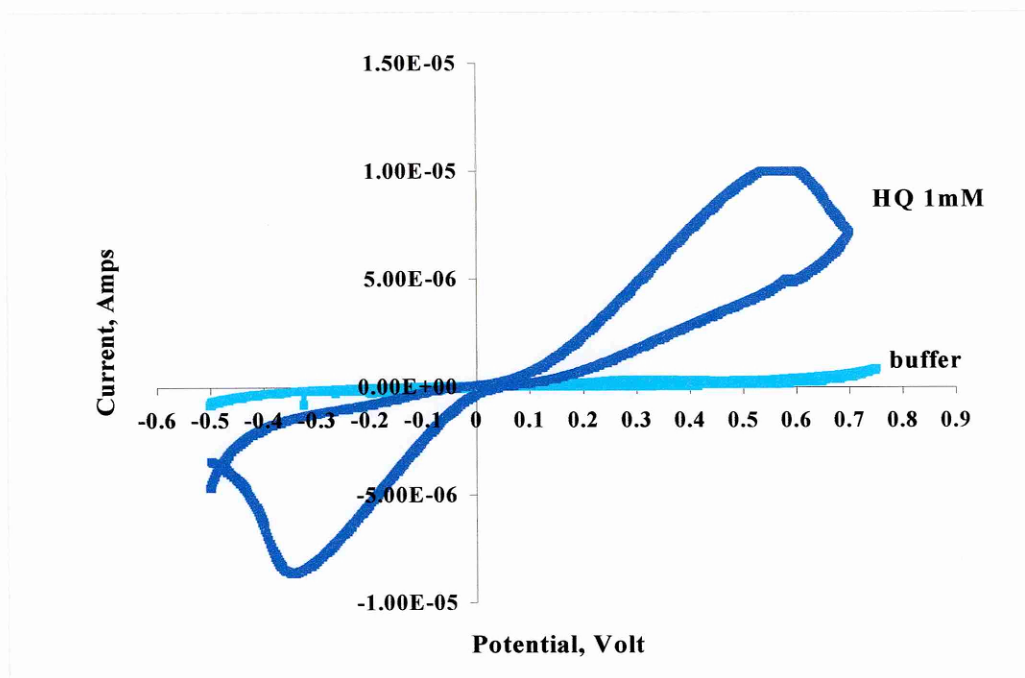


Figure 4.6: Cyclic voltammogram of hydroquinone.

Showing scan 5 of 1 mM hydroquinone in 20 mM sodium phosphate, 0.1 M KCl, pH 7.0 buffer in a 5 ml cell with a glassy carbon working electrode and screen-printed carbon counter and Ag/AgCl reference electrodes. Scan Range from -0.5 to $+0.7$ Volts, Scan Rate = $99.976 \text{ mV sec}^{-1}$.

Compared to the lack of activity in the buffer scans, two peaks could be seen distinctly with the 1 mM hydroquinone scan. The oxidation and reduction peaks were seen at $+550 \text{ mV}$ and -330 mV respectively. These observations indicated the potential at which chrono-amperometric measurements should be conducted. Above $\pm 700 \text{ mV}$ redox interferences (due to dissolved oxygen) could be observed.

4.5.2 Potential Determination

Although the redox profile of hydroquinone, given by the CV technique, indicated the range of potentials for reductive amperometric analysis with a standard glassy carbon electrode; the most appropriate value for the working potential was determined experimentally with screen printed electrodes (SPE's). Anti-MC-LR antibody or gelatin

(background) coated membranes were laid onto the screen-printed electrodes, and MC-LR-HRP conjugate solution was added on top. The membranes were subsequently analysed by chronoamperometry (CA) at different potentials (-150 mV/ -500 mV), to determine both the signal and background responses at each, as shown in Figure 4.7.

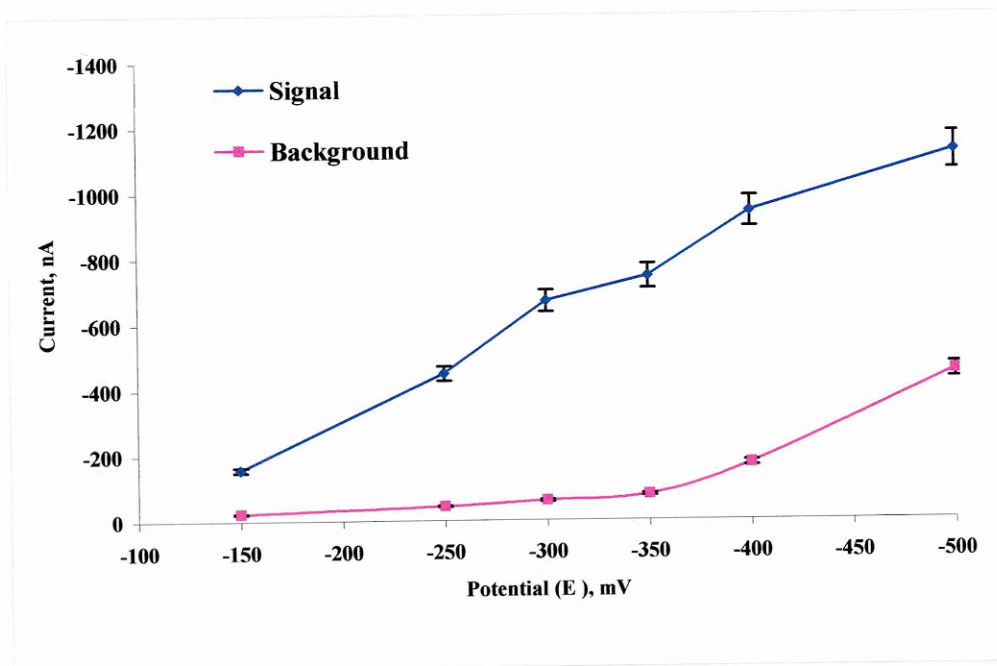


Figure 4.7: Hydroquinone HRP mediated chronoamperometry at different potentials. 1 mM hydroquinone mediated HRP current response to 0.5 mM H_2O_2 between potentials of -150 and -500 mV. Membranes coated either with 1/1000 anti-MC-LR IgG or gelatin blocker (0.5 %). MC-LR-HRP incubation for 1 hour at R.T. Error bars = \pm SD, $n = 4$.

Compared to the CV analysis using a standard mini glassy carbon electrode, the chronoamperometry (CA) data obtained using SPE's showed -300 mV to be the most suitable potential for developing the sensor. At -300 mV a significant signal (-668 nAmps) was obtained in response to HRP/ H_2O_2 , whilst the background signal from the peroxide was still acceptably low (-59 nAmps), giving a S/B ratio of 11.3. The % CV obtained at this potential was also low at 3.2 %. Above -300 mV the increasing background response from peroxide reduction was prohibitive.

4.5.3 Optimising the Hydroquinone and Peroxidase Concentrations

To optimise the signal transduction of the immuno-conjugate MC-LR-HRP, the most suitable hydroquinone and H_2O_2 concentrations were determined. The results, presented in Figure 4.8, show that a suitable concentration range for hydroquinone was between 1-10 mM. However, the strongest signal (-773 nAmps) was obtained using 1 mM hydroquinone, which generated S/B values above 14.4 and % CV of 4.9. Higher concentrations of hydroquinone resulted in a higher background response and a higher % CV.

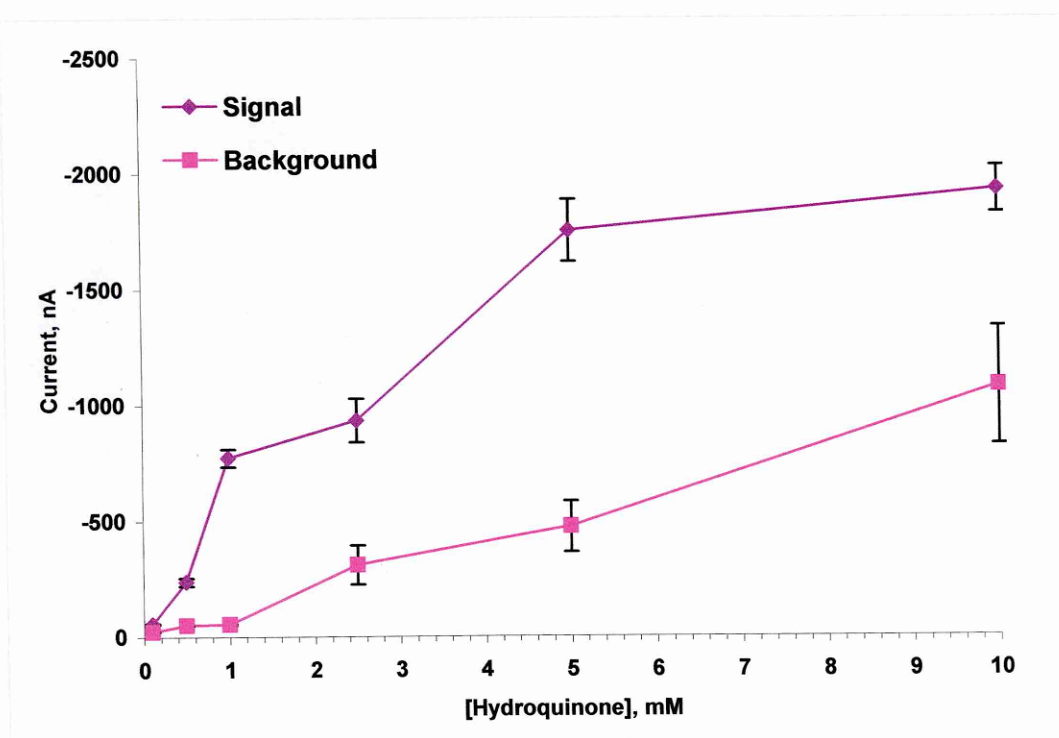


Figure 4.8: Mediated HRP Response to different hydroquinone concentrations. Between 0.1 and 10 mM hydroquinone mediated HRP current response to 0.5 mM H_2O_2 at $E = -300$ mV. Membranes coated either with 1/1000 anti-MC-LR IgG or gelatin blocker (0.5 %). MC-LR-HRP incubation for 1 hour at R.T. Error bars = \pm SD. $n = 4$.

The concentration of 0.5 mM H_2O_2 was the most suitable peroxide concentration using 1 mM hydroquinone. At that point the maximum signal response began to plateau and

the background increased. A 0.5 mM peroxide concentration resulted in a dI response of -881.5 nAmps, with a % CV < 5 and an S/B ratio of 5.1 (Figure 4.9).

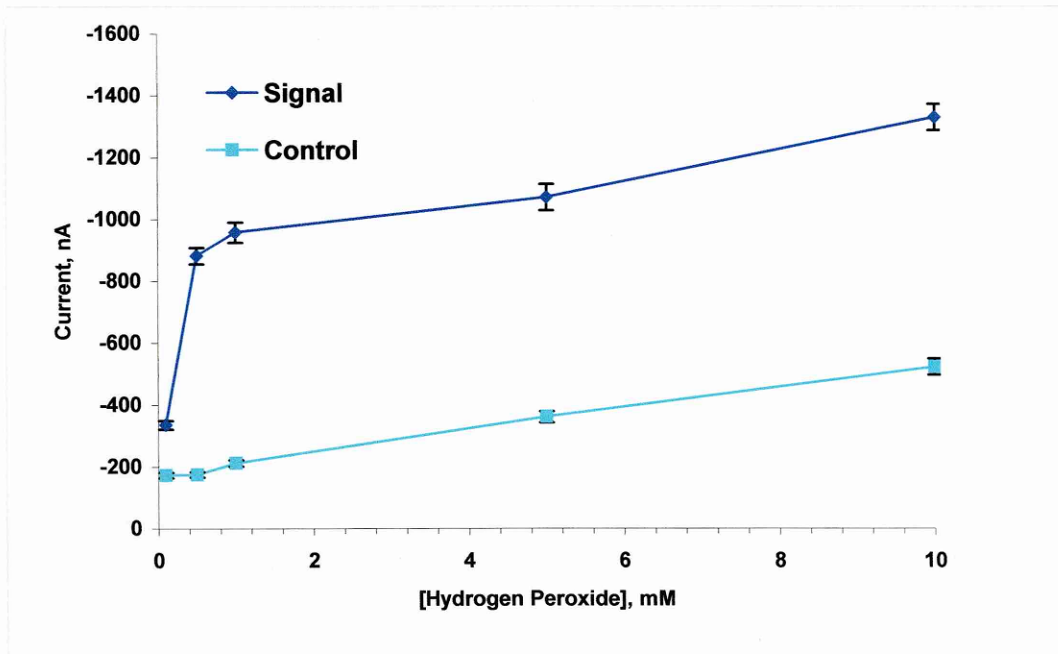


Figure 4.9: Mediated HRP Response to different peroxide concentrations. 1 mM hydroquinone mediated HRP current response to between 10 mM and 0.1 mM H_2O_2 at $E = -300$ mV. Membranes coated with either with 1/1000 anti-MC-LR IgG or gelatin blocker (0.5 %). MC-LR-HRP incubation for 1 hour at R.T. Error bars = \pm SD. $n = 4$.

4.6 COMPETITIVE MICROCYSTIN-LR IMMUNOSENSOR

4.6.1 Mediated HRP Amperometric Detection

By applying a reducing current, the catalytic activity of the HRP enzyme could be monitored by chrono-amperometry analysis mediated by hydroquinone. Figure 4.6 shows a typical time trace from a chrono-amperometric measurement using the EIA membrane, with the HRP labelled secondary antibody. With the amperometric transduction optimised, the competitive MELISA was conducted in an immunosensor

format. Each sensor membrane was coated with either 1/1000 anti-MC-LR IgG or gelatin blocker (0.5 %). A mixture of equal volumes of MC-LR concentration and MC-LR-HRP conjugate was added to the top of the membrane and left to compete for antibody binding sites, over one hour at room temperature. After gentle washing, the membrane discs were placed over the working electrode and then covered by a 15 mm² piece of polyester 250 μm² mesh. This assembly was then held in place with 30 μl of electrolytic buffer, allowing the mesh to adhere to the electrode. The HRP current response to 0.5 mM H₂O₂ was mediated with 1 mM hydroquinone at a potential of -300 mV. A high current response was indicative of a low concentration of free toxin. The range of concentrations studied was between 0 and 10 μg l⁻¹ (ppb) (Figure 4.10).

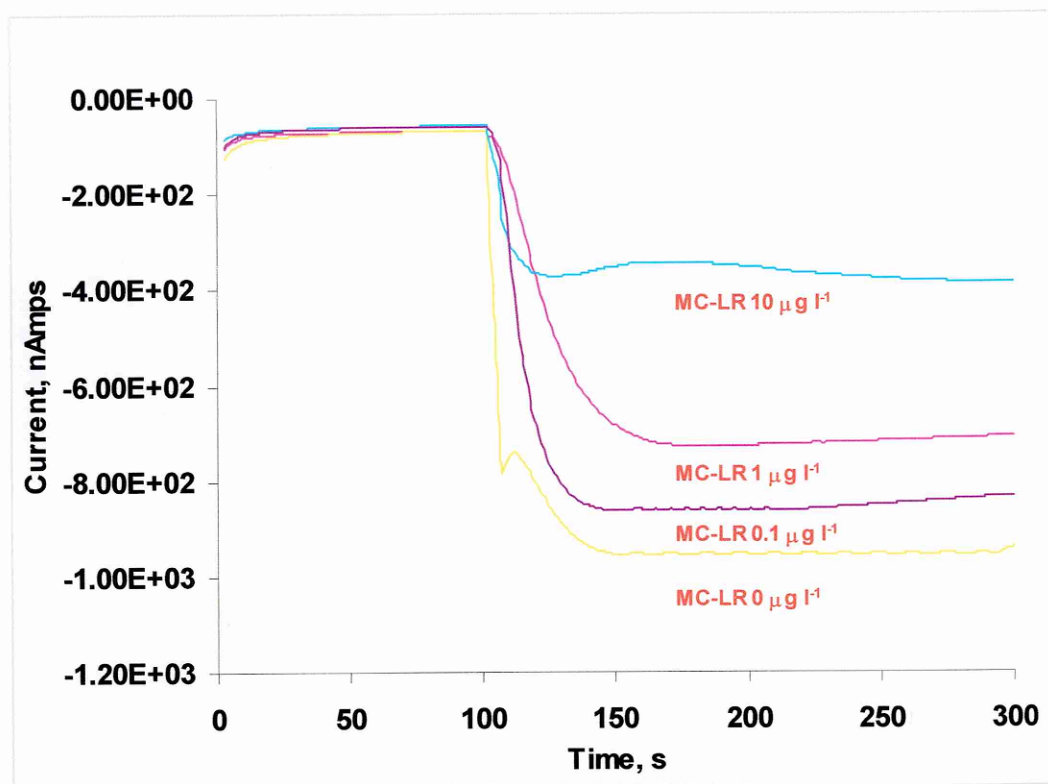


Figure 4.10: A chrono-amperometry current/time trace of microcystin-LR. 1 mM hydroquinone mediated HRP current response to 0.5 mM H_2O_2 at 100 secs at a potential of -300 mV. The coating membrane contained 1/1000 anti-MC-LR IgG. Blocking with 0.5% gelatin; 1-hour incubation with free microcystin-LR and microcystin-LR-HRP conjugate.

The initial phase (from zero to 100 seconds) allowed the electrode cell system to equilibrate to a steady current baseline (I_0). After approximately 100 seconds the hydrogen peroxide (H_2O_2) substrate was applied. The HRP activity was recorded as an increasing current response, which equilibrated to steady dynamics until substrate depletion. The value of I_0 was subtracted from the current (I_t) at the final steady state to give ΔI . This proportional current change was used for both calibration and concentration determination. The immuno-reaction on the membrane allowed the electrochemical detection of HRP conjugate activity down to a low level of detection ($\mu g l^{-1}$). Figure 4.11 shows the competitive immunosensor response to MC-LR, over a range of concentrations: 0.1 to 1000 $\mu g l^{-1}$.

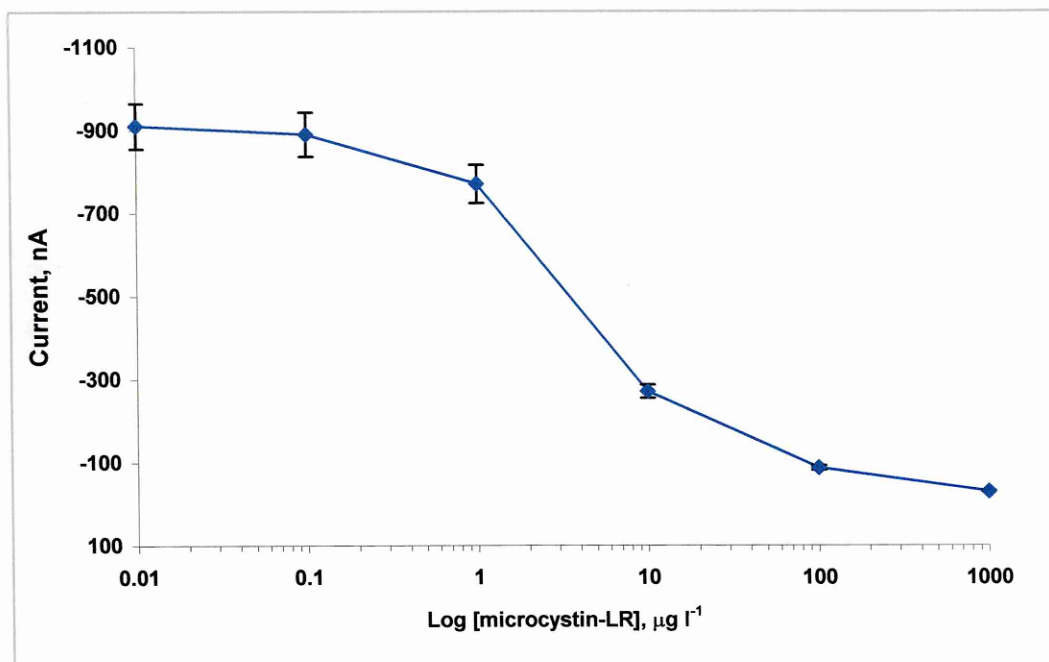


Figure 4.11: Competitive MC-LR immunosensor response.

Each membrane-based immunosensor was coated with either 1/1000 IgG or gelatin blocker (0.5 %). MC-LR standards competed with conjugate MC-LR-HRP without pre-mixing. The HRP current response to 0.5 mM H_2O_2 was mediated with 1 mM hydroquinone at $E = -300$ mV. Error bars = \pm SD, $n = 4$.

The sensitivity results showed that the hydroquinone mediated amperometric detection system gave an LLD_{80} value of $0.5 \mu\text{g l}^{-1}$, indicating a sensitivity loss of about 10 times, compared to the colourimetric MELISA. The immunosensor measurements also showed an increase in the mean assay variation compared to the MELISA % CV (Assays mean % CV = 12.2). The background current was less than -100 nAmps.

4.7 ELECTROCHEMICAL ABTS DETECTION

Rather than mediated electrochemical detection of the membrane bound assay, it was found possible to amperometrically detect and quantify the 2,2'-azino-bis(3-ethylbenzothiazoline-6-sulfonic acid (ABTS) chromogen reaction product from HRP catalysis.

4.7.1 ABTS Electro-Activity

The electro-activity of ABTS was confirmed by a cyclic voltammogram, obtained using a glassy carbon electrode in conjunction with a screen-printed counter and reference electrode. The voltammogram is shown in Figure 4.12:

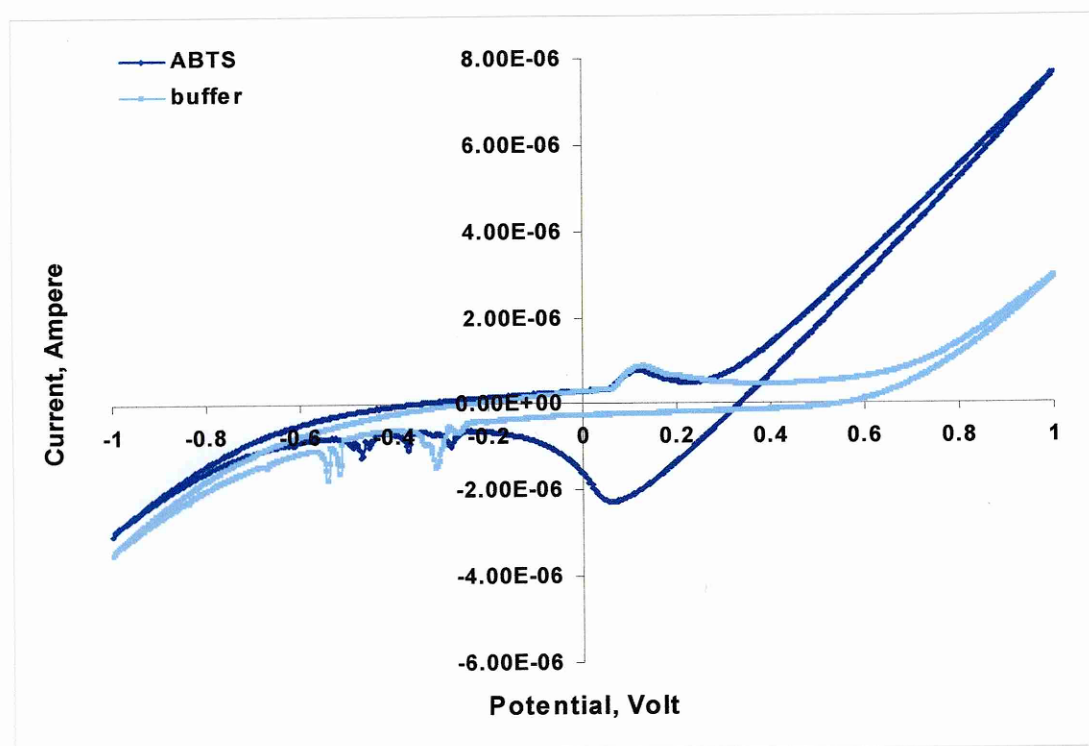


Figure 4.12: Cyclic voltammogram of ABTS.

Showing scans 5 of ABTS in a 5 ml cell with a glassy carbon working and screen-printed carbon and Ag/AgCl counter and reference electrodes. Scan range from -1 to $+1$ Volts, scan rate = 100 mV sec^{-1} .

Another smaller peak was observed for both voltammograms and it is likely to be interference from the buffer composition.

The competitive immunosensor was evaluated by using ABTS substrate detection. The ABTS substrate solution was added ($50 \mu\text{l}$) on the top of the immunosensor and the chrono-amperometry response at different concentrations of microcystin-LR was assessed. A bare membrane, on which the enzyme immunoassay was not carried out,

was also investigated to evaluate the background signal of the electrolytic. Figure 4.13 illustrates the results from these experiments.

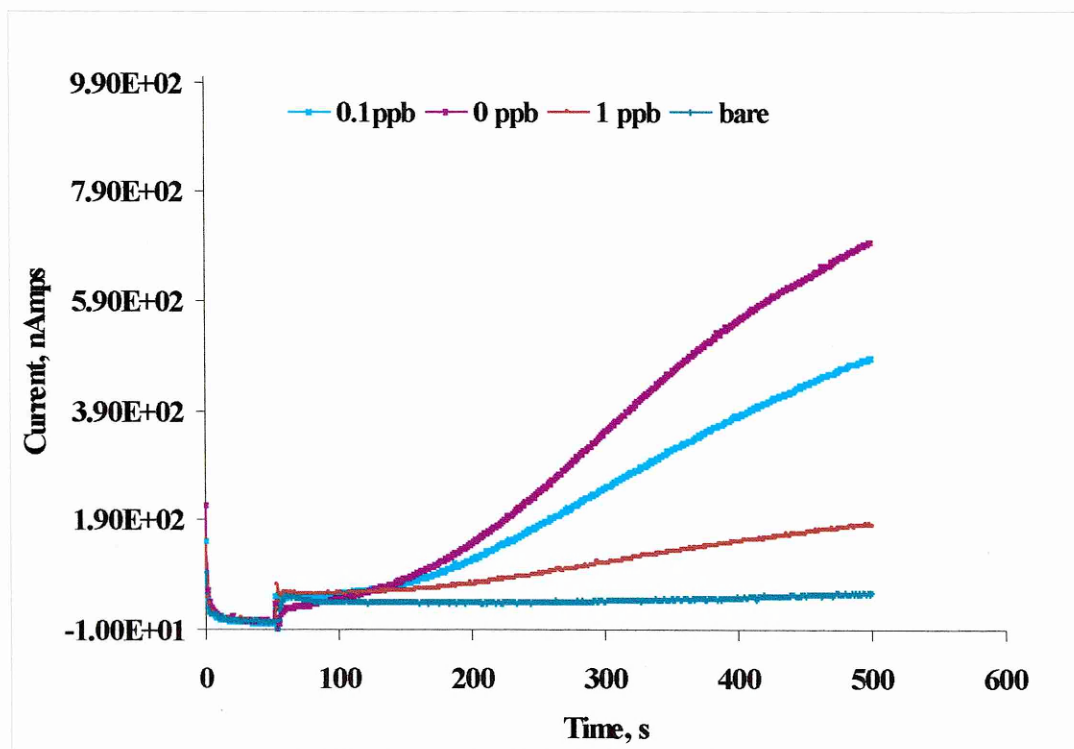


Figure 4.13: Chrono-amperometry for competitive MELISA using ABTS detection. Membrane coating with 1/1000 anti-MC-LR IgG. Blocking with 0.5 % gelatin. MC-LR standards competed without pre-mixing with conjugate gelatin-MC-LR. The HRP current was obtained with ABTS substrate solution. Bare membranes were also tested with ABTS substrate solution.

Figure 4.14 shows the calibration curve obtained from the immunosensor with ABTS substrate detection.

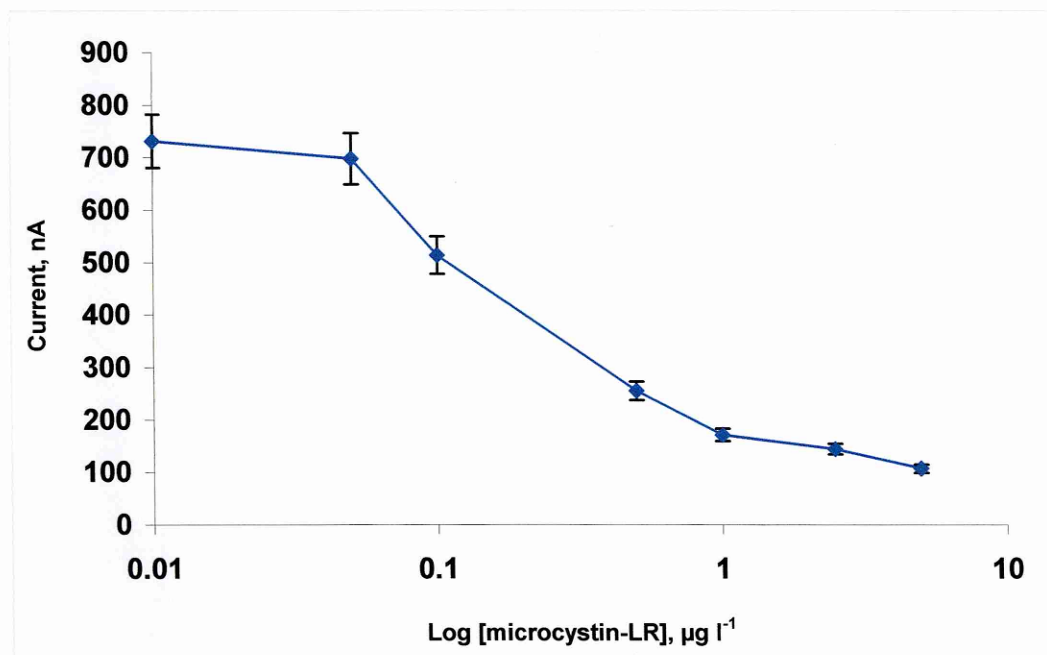


Figure 4.14: Competitive MC-LR immunosensor response.

Each immunosensor was coated with 1/1000 anti-MC-LR IgG or 0.5 % gelatin blocker. MC-LR standards competed without pre-mixing with conjugate gelatin-MC-LR. The HRP current was obtained with ABTS substrate solution. $E = +150$ mV. Error bars = \pm SD, $n = 4$.

When the ABTS substrate was used to determine the immunocomplex bound to the sensor device, a detection limit comparable to that of HQ/H₂O₂ electrochemical detection system was obtained. The lowest detection limit, calculated at 80 % of the maximum response, was 0.7 µg l⁻¹ and the mean % CV for the assay was 16. Moreover, the hydroquinone mediator displayed stability problems and a fresh solution needed to be made every hour because of its tendency to auto-oxidise. ABTS was used for a full day of experiments with no problems from stability, when kept well protected from light.

4.8 FLOW INJECTION ASSAY FOR MELISA COLORIMETRIC ASSAY

Preliminary flow injection assay (FIA) experiments were conducted and the assay was performed on-line with the immunoassay reagents sequentially pumped through a membrane held in a flow cell. Initially, the flow rate was optimised for the anti-MC-LR IgG immobilisation step. Significant differences were noticed when the speed of the flow was changed.

4.8.1 Flow Rate Optimisation

A disc of the membrane UltraBind™ was inserted into a flow cell designed by Dr J. Bolbot from Cranfield University (Silsoe, U.K.). The cell was connected to a peristaltic pump by white-black Tygon tubing, with an internal diameter of 0.57 mm. The pump was set at 2, 5, 10 revs min⁻¹ pump speed and used to pump electrolytic buffer at different flow rates of 10, 25 and 50 µl min⁻¹ through the flow cell. To examine the effect of flow rate on signal intensity, the immobilisation of anti-MC-LR IgG (diluted 1/1000) on the membrane surface was investigated. Figure 4.15 depicts the signal intensity as the flow rates were decreased from 10 to 50 µl min⁻¹.

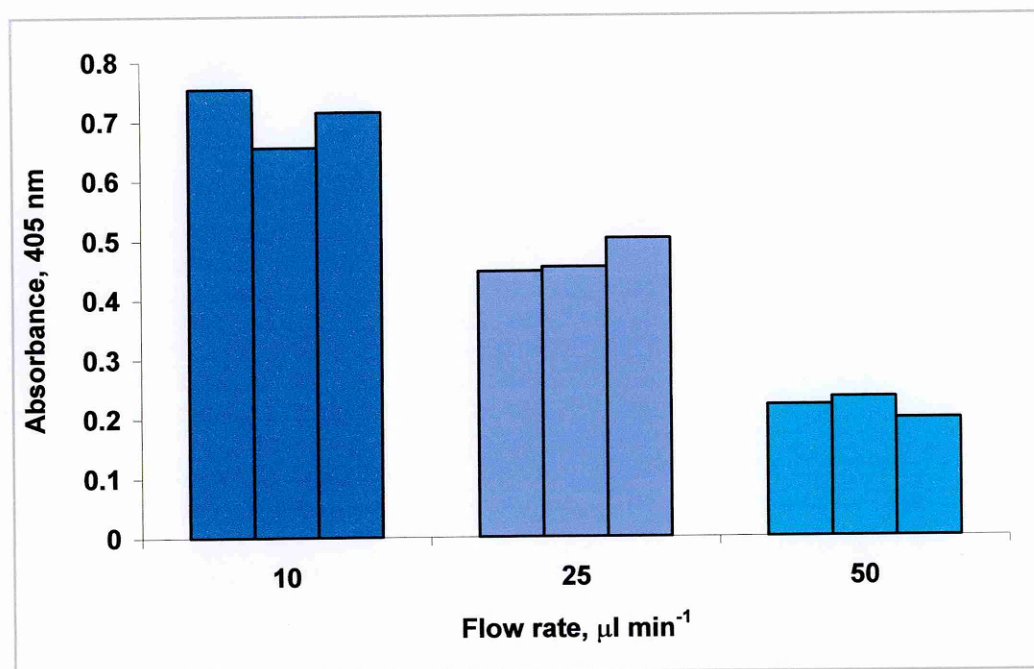


Figure 4.15: Flow rate optimisation of the MC-LR competitive assay. Membranes were coated with anti-MC-LR antibody (1/1000). Triplicate injections of conjugate MC-LR-HRP were loaded at flow rates of 10, 25, 50 $\mu\text{l min}^{-1}$.

A decrease in flow rate resulted in an increase in signal intensity. Thus, the detection threshold and signal intensity could be adjusted by changing the flow rate. A decrease in flow rate increased the signal intensity probably because of the increase in the interaction time between the injected analyte and the immobilised antibody.

The response was measured using colorimetric reaction, at the flow rate of 10 $\mu\text{l min}^{-1}$. A solution of anti-microcystin-LR antibody was immobilised by passing on-line, at the speed of 10 $\mu\text{l min}^{-1}$, using a peristaltic pump. After one minute of washing with buffer, a mixture of free toxin (200 μl , 0.01-2 $\mu\text{g l}^{-1}$) and HRP conjugate (200 μl , 1 mg l^{-1}) was run through the on-line system, at the same speed. In order to enhance the immuno-reactions, the solution was stopped for few seconds in the membrane flow-cell. The ABTS substrate solution was then passed through the flow cell and kept in contact with the membrane, at a flow rate of 10 $\mu\text{l min}^{-1}$. The coloured solution in contact with the

membrane was collected, for optical reading at 405 nm. The results of the FIA competitive immunoassay are presented in Figure 4.16.

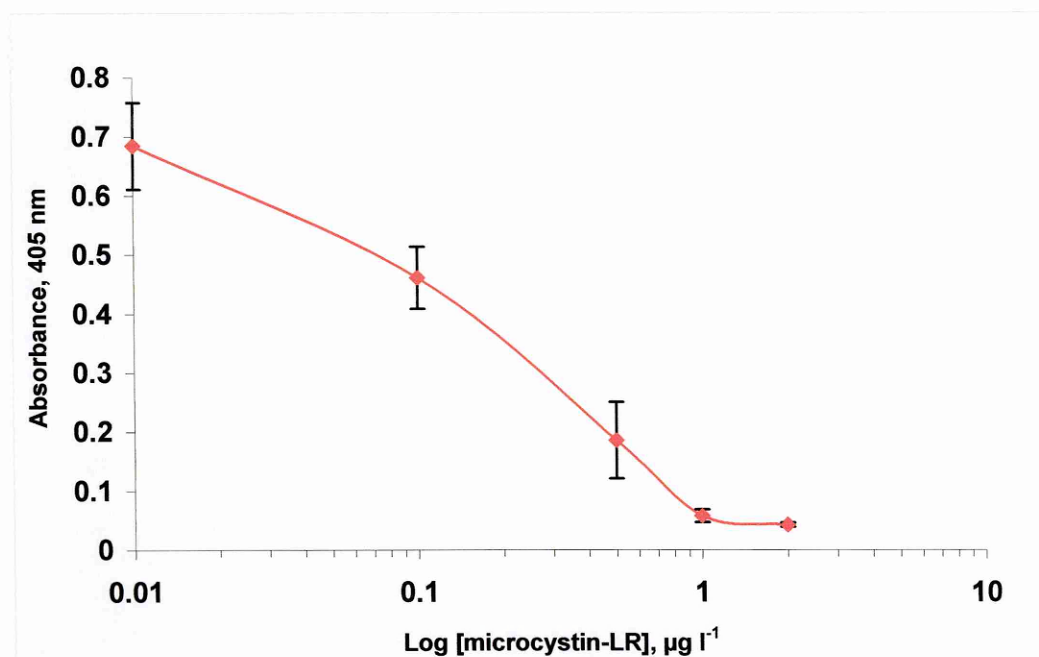


Figure 4.16: On-line competitive MELISA assay for MC-LR.

Anti-MC-LR antibody was immobilised by passing on-line at the speed of $10 \mu\text{l min}^{-1}$. Free toxin ($200 \mu\text{l}$, range $0.01\text{-}2 \text{ ng ml}^{-1}$) and HRP conjugate ($200 \mu\text{l}$, 1 mg l^{-1}) were run through the on-line system at the same speed. ABTS substrate solution ($200 \mu\text{l}$) was passed through the flow cell and kept in contact with the membrane at a flow rate of $10 \mu\text{l min}^{-1}$. The optical density was read at 405 nm.

A high sensitivity was achieved using the on-line immunoassay, since the LLD_{80} was $0.1 \mu\text{g l}^{-1}$. This is higher than the detection limit obtained with the same colorimetric competitive MELISA, made off-line. The main problem was the high value of mean % CV (16) and the high value of standard deviation, which revealed a poor reproducibility for the experiment. However, the system could be largely improved and optimised by investigating different conditions for the immunoreaction e.g. different volumes and time of flow of the immunoreagent. Lack of time did not allow any further optimisation.

4.8.2 Competitive FIA with Amperometric ABTS Detection

Some preliminary results of the on-line amperometric detection of microcystin-LR by the immunosensor approach are shown in Figure 4.17. The competitive immuno-reaction was carried out as previously described. In this case, the reaction development was determined electrochemically by passing the solutions over an electrode inserted in a flow cell and connected both to the membrane flow cell and to Autolab equipment. Only the flow of the enzyme substrate was permitted to pass through the screen-printed electrode flow-cell.

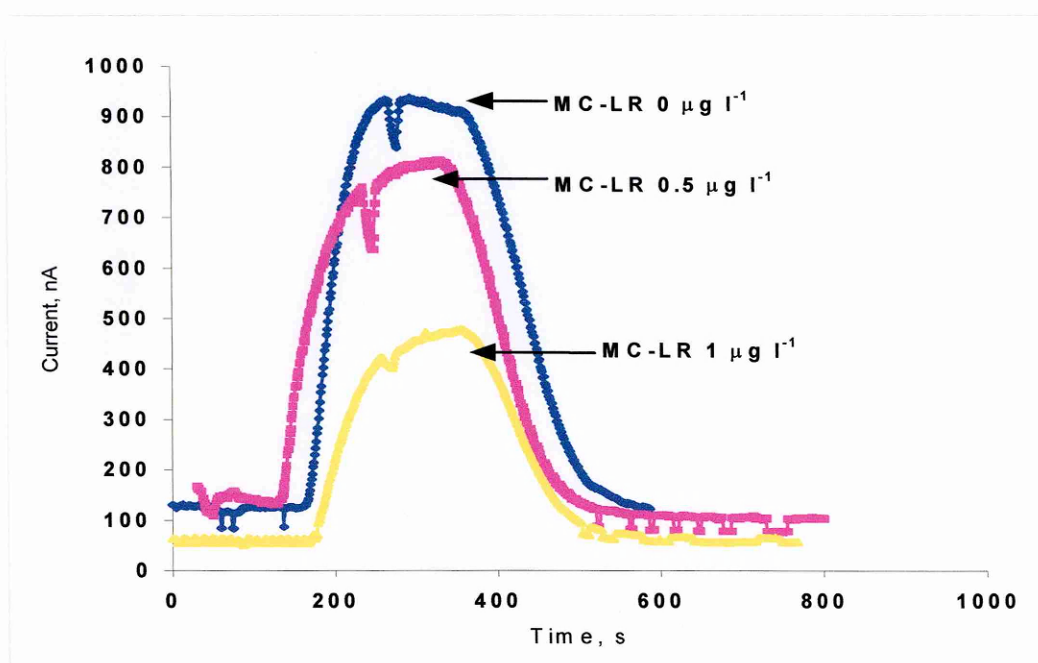


Figure 4.17: On-line detection of the competitive MELISA assay for MC-LR.

Anti-MC-LR antibody was immobilised by passing on-line flow-through at a speed of $10 \mu\text{l min}^{-1}$. A mixture of free toxin ($200 \mu\text{l}$, $0-1 \mu\text{g l}^{-1}$) and HRP conjugate ($200 \mu\text{l}$, 1mg l^{-1}) was run through the on-line system at the same speed. ABTS substrate solution ($200 \mu\text{l}$) was passed through the flow cell and kept in contact with the membrane at a flow rate of $10 \mu\text{l min}^{-1}$ for electrochemical determination at $E = +150 \text{mV}$.

4.9 CONCLUSION

The competitive ELISA assay format was transferred to a membrane based ELISA in order to investigate an immunosensor format for detecting microcystin-LR. The MELISA assay was optimised with colorimetric detection, in order to reduce the variable parameters encountered when subsequently coupled with electrochemical detection. Three coating concentrations were tested on the UltraBind™ membrane, however, their suitability for further development was quite compromised by a comparatively high non-specific signal.

In addition to high non-specific signal, a low signal, at the maximum optical absorbance of 0.6 (at the highest possible conjugate coating concentration of 12 g l⁻¹) was observed. Further optimisation of primary and secondary antibodies concentrations did not increase the signal of the maximum response. It was then concluded that the result was probably due to the low efficiency of the coating agent (microcystin-LR-gelatin) binding to the membrane. Moreover, as already observed with the assays for blocking studies, poor reproducibility was evident from the assay. This could be due to the extensive manual procedures employed throughout the assay e.g. several washes after each immuno-reaction. The need for incubation with a secondary antibody in this assay format also contributed to more intensive handling of the membranes, which may have exacerbated the problem of assay variability.

A new format for the enzyme immuno-assay (EIA) needed to be considered; with a more specific and reproducible assay transferred to the membrane based-ELISA, the system could be applied and optimised in an immunosensor format. The competitive MELISA assay, based on IgG immobilised on membrane sorbent, was carried out by the immobilisation of anti-MC-LR IgG at a dilution of 1/1000. The steps for the immuno-reaction were reduced to two resulting in a faster assay time and contributed to solving the problem of reproducibility. The LLD₈₀ value detected was 0.06 µg l⁻¹.

Therefore, this EIA approach appeared suitable for implementation into an electrochemical sensor format.

The sensitivity results showed that the hydroquinone mediated amperometric detection system gave an LLD_{80} value of $0.5 \mu\text{g l}^{-1}$, indicating a sensitivity loss of about 10 times compared to the colourimetric MELISA. The detection of microcystin-LR amperometrically using the ABTS substrate produced an LLD_{80} of $0.7 \mu\text{g l}^{-1}$. The sensitivity of on-line colorimetric detection with ABTS substrate was $0.1 \mu\text{g l}^{-1}$. A FIA system for on-line measurements was then investigated; this showed a good performance within a short time. Thus, an immunosensor incorporating the membrane-based assay has proven to be rapid, whilst providing a quantitative assessment of the antigen concentration.

CHAPTER 5: RESULTS

AFFINITY RECEPTORS BASED ON MIP FOR MICROCYSTIN-LR

5.1 INTRODUCTION

Molecular imprinting has become an established technique for preparing robust molecular recognition elements towards a wide variety of target molecules. The relative ease with which molecularly imprinted polymers (MIPs) can be prepared has led to the assessment of their use as a substitute to antibodies, for several applications such as assays and sensors (Sellergren, 2001). With this aim, a synthetic receptor specific for microcystin-LR was created and characterised. A competitive MIP assay was used for characterisation of the MIP receptor for detection of microcystin-LR. A MIP based on a computational design was compared to a MIP based on a more classical composition of monomers. Finally, the performance of such MIPs in terms of affinity, sensitivity, cross reactivity and stability were evaluated and a comparison with natural receptors as anti-microcystin-LR monoclonal and polyclonal antibodies investigated.

5.2 BULK IMPRINTING SYNTHESIS OF A MIP FOR MICROCYSTIN-LR

Two different bulk-MIP receptors for microcystin-LR were considered for assay and sensor application. The first MIP was created using methacrylic acid (MAA) as the only monomer and was thus defined as MAA-MIP. This polymer was also termed ‘classical’ in comparison with the second MIP specific for microcystin-LR, designed using a rational selection of monomers based on computer modeling (CM-MIP).

To create the MAA-MIP, the template microcystin-LR was dissolved in DMSO and added to a polymerisation mixture, containing MAA as monomer, ethylene glycol dimethylacrylate (EGDMA) as cross-linker and 1,1'-azobis (cyclohexane-carbonitrile) as radical initiator for the reaction. After thermo-polymerisation, the bulk polymer was grounded, washed, and used for characterisation studies. A methacrylic acid blank polymer was also prepared following the same procedure, but in the absence of template microcystin-LR. The molar ratio chosen between template and monomers was 1:10, since this was reported to be commonly used for the non-covalent imprinting of large molecules. The picture in Figure 5.1 (a) was obtained simply by running the Leapfrog

step of the computer-modeling program by which the interactions between the optimised configuration of the template MC-LR and the 10 MAA molecules are shown.

In the case of CM-MIP, the composition of monomers has been obtained by computational modeling study, which has been conducted using a Silicon Graphic workstation (Chianella *et al.*, 2002). Briefly, a library of monomers was generated; amongst these monomers, some of them gave better interactions with the template. The five best monomers were chosen and allowed to interact with a minimised conformation of the template. In the final step, the type of monomers and their ratio with the template was given. Such work is not included in this thesis since this polymer was used purely for comparison with MAA-polymer and the natural receptors.

The result from modeling design showed that the best composition of monomers for CM-MIP included a variety of monomers like one molecule of 2-acrylamido-2-methyl-1-propane sulfonic acid (AMPSA) and six molecules of urocanic acid ethyl ester (UAEE) for one molecule of the template microcystin-LR. The cross-linker EGDMA was added at high concentration as for the MAA-MIP as well as the initiator of the polymeric reaction 1,1'-azobis(cyclohexane-carbonitrile). A blank polymer, also synthesized using the same monomers above, (in the absence of template) has been considered in this study. The result from the computer modeling software achieved after performing all the steps required is shown in Figure 5.1 (b).

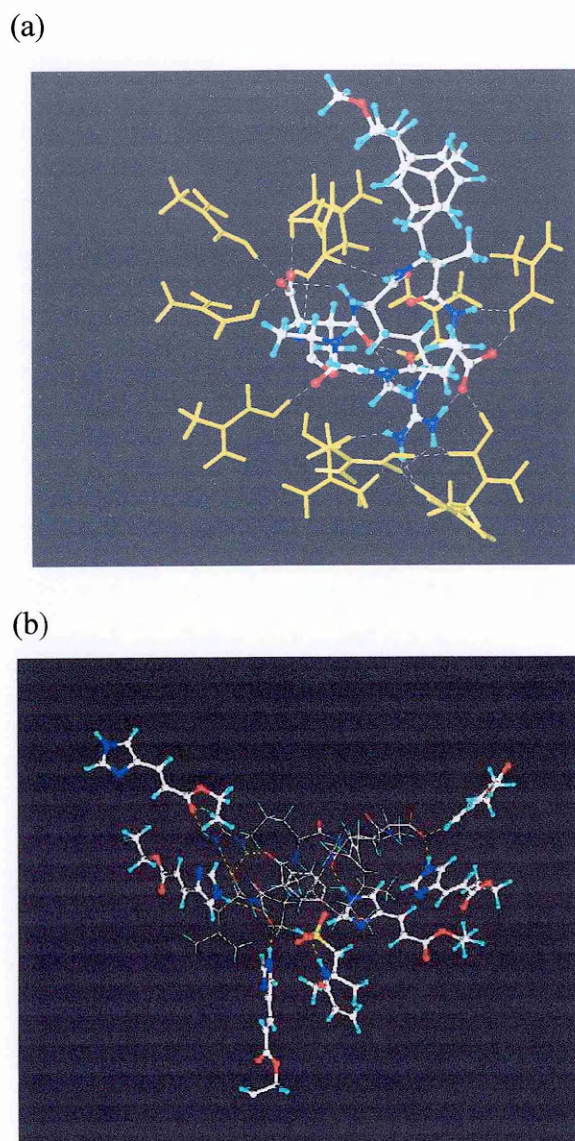


Figure 5.1: Interaction between microcystin-LR (centre of the picture) and (a)-10 MAA molecules (yellow), (b)- different monomers selected (in balls and sticks).

The full composition of each polymerisation mixture is presented in Table 5.1. In addition, the surface area and the total pore volume for the computationally designed MIP, MAA-MIP and blank polymers, calculated by BET (Brunauer-Emmett-Teller) elemental analysis using the nitrogen adsorption method are listed.

Table 5.1: Composition of monomer mixture used for MIP preparation and the physical properties of the synthesized polymers.

POLYMER	MC-LR μmol	AMPSA μmol	MAA μmol	UAEE μmol	EGDMA μmol	SURFACE AREA (m^2/g)	TOTAL PORE VOLUME (cm^3/g)
CM-MIP	1	1	-	6	1500	443.31 \pm 3.75	0.533
CM-Blank	-	1	-	6	1500	444.72 \pm 3.01	0.571
MAA- MIP	1	-	10	-	1500	414.69 \pm 2.99	0.513
MAA- Blank	-	-	10	-	1500	437.24 \pm 2.61	0.600

Abbreviations: AMPSA= 2-acrylamido-2-methyl-1-propane sulfonic acid; UAEE= urocanic acid ethyl ester; EGDMA= ethylene glycol dimethylacrylate; MC-LR= microcystin-LR; MAA= methacrylic acid; CM-MIP/ Blank= computationally designed molecularly imprinted polymer and control polymer; MAA-MIP/Blank= methacrylic acid based molecularly imprinted polymer and control polymer. \pm SD= standard deviation.

The BET analysis showed that the MIPs and blank polymers had a similar surface area and total pore volume. Thus, no differences between the polymers were observed in macroscopic terms; potential differences in performance could be accredited to the monomer composition.

5.3 COMPETITIVE ENZYME-LINKED ASSAY FOR IMPRINTED POLYMER

A MIP-based competitive enzyme-linked assay was used to characterise the MC-LR imprinted polymers. The assay was developed and optimised in another study

(Chianella, 2003) in our laboratory, to study the performance of the computationally imprinted polymer (data not shown). Similarly, this assay was applied to the MAA-MIP to determine the sensitivity and specificity versus the toxin microcystin-LR (used as a template in the synthesis procedure). A suspension of the polymer (0.5 g l^{-1}) was dispensed into a 96-well filtration microtiter plate. A commercial available labelled MC-LR-HRP conjugate was mixed with dilutions of the free toxin over a range of concentrations and incubated for one hour in the presence of the polymer. A filtration system, connected to a vacuum pump, was applied to allow the toxin and conjugate mixture to pass through the polymer particles deposited into the filtration plate. The mixture was collected directly in separated wells of a new microtiter plate. An aliquot of the filtrate solution ($10 \mu\text{l}$) was transferred to a microtiter plate and mixed with 3,3',5,5'-tetramethylbenzidine (TMB) liquid substrate ($90 \mu\text{l}$). HRP activity was measured by reading the optical density at 450 nm. Figure 5.2 shows a scheme of the enzyme linked competitive MIP assay.

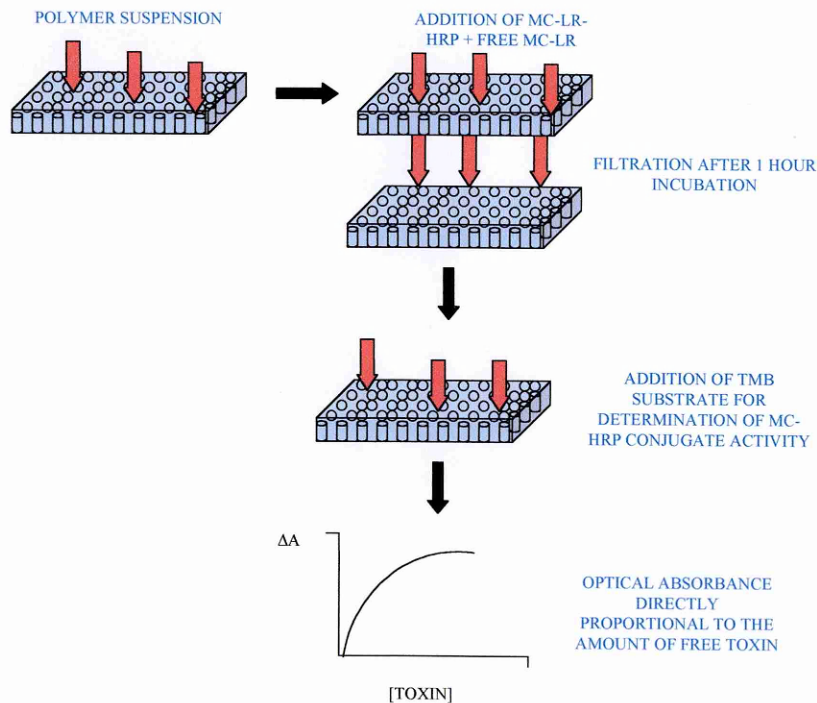


Figure 5.2: Scheme of the competitive enzyme assay.

The values of optical density were calculated as a difference of absorbance, having subtracted from each value the reading obtained when no toxin was present. This procedure avoided the risk of high non-specific signals due to excess of unbound conjugate.

5.3.1 Optimisation of Microcystin-HRP Conjugate

A range of dilutions of the conjugate MC-LR-HRP was explored, in order to optimise the concentration of the competitive enzyme-linked MIP assay. The assay test was performed as previously described, using three different dilutions of the labelled MC-LR conjugate. In Figure 5.3, the curves obtained for each of the assays are shown; the standard deviations were calculated from experiments performed in triplicate.

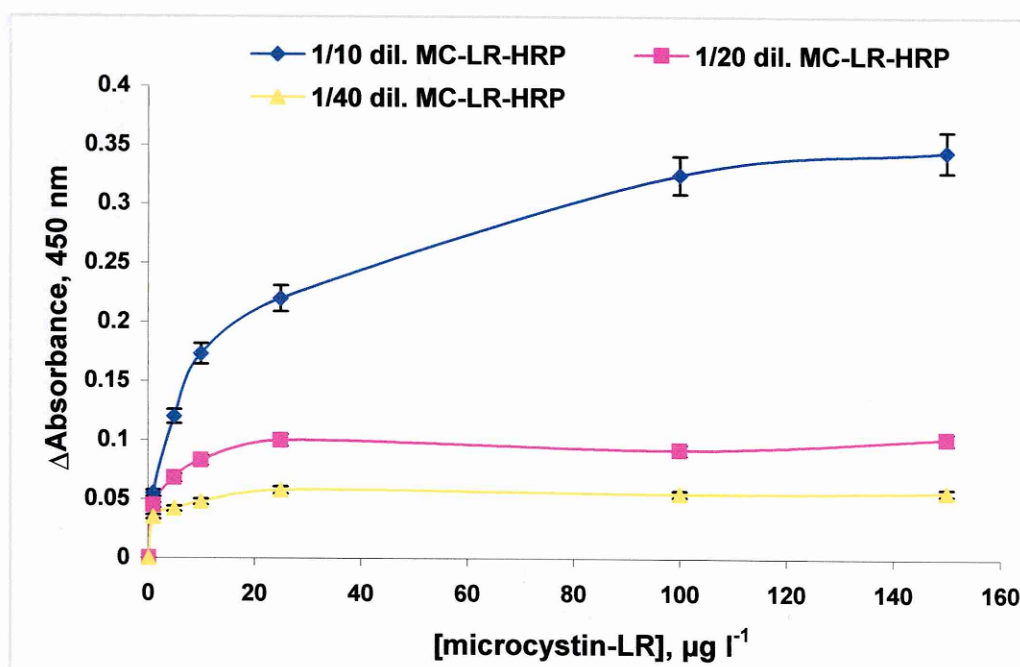


Figure 5.3: Optimisation of microcystin-HRP conjugate concentration. Enzyme-linked competitive assay responses obtained using three different conjugate dilutions. The test was performed using a polymer suspension (0.5 g l^{-1}) in 50 mM sodium phosphate buffer, pH 7.0, and using increasing microcystin-LR concentrations ($0.1\text{-}150 \text{ } \mu\text{g l}^{-1}$). Error bars = \pm SD, $n=3$.

The highest response was observed using the 1/10 microcystin-HRP conjugate dilution (which should correspond to a concentration of 0.1 mg l^{-1} , according to the commercial informations). When higher conjugate concentrations were tested, the enzyme reaction was too fast and could not be used. Therefore, such dilution was chosen and used for all the subsequent enzyme-linked competitive assay experiments.

5.3.2 Optimisation of Polymer Suspension Concentration

The enzyme-linked competitive assay was carried out using different concentrations of polymer suspension ($0.025\text{-}5 \text{ g l}^{-1}$), prepared in 50 mM sodium-phosphate buffer, pH 7.0 . The optimised concentration of microcystin-HRP conjugate was used for the experiments. Figure 5.4 shows the assay responses obtained using different polymer suspensions, the standard deviations were calculated from experiments performed in triplicate.

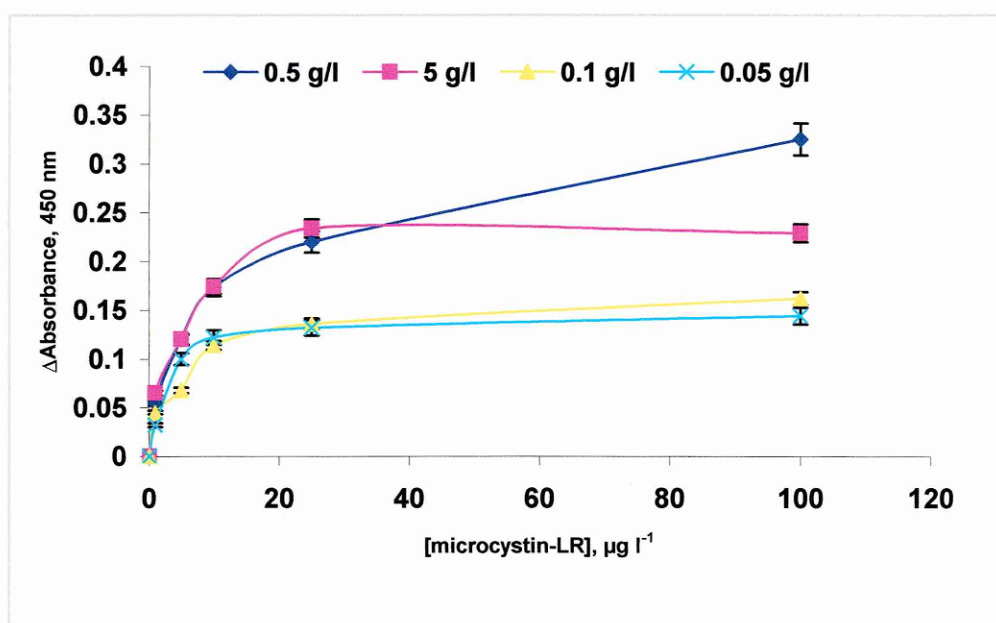


Figure 5.4: Enzyme-linked competitive assay curves obtained using four different concentrations of the polymer suspensions (5 g l^{-1} , 0.5 g l^{-1} , 0.1 g l^{-1} , 0.05 g l^{-1}). The polymer suspensions were prepared in 50 mM sodium phosphate buffer, pH 7.0 and the competitive assay carried out with 0.1 mg l^{-1} of MC-HRP conjugate with increasing microcystin-LR concentrations ($0.1\text{-}100 \mu\text{g l}^{-1}$). Error bars = $\pm \text{SD}$, $n=3$.

The use of polymer suspensions, over the concentration range analysed, did not significantly affect the assay signal, for toxin concentrations lower than $25 \mu\text{g l}^{-1}$. For higher microcystin-LR concentrations, polymer suspensions in a concentration range of $0.1\text{-}0.5 \text{ g l}^{-1}$ gave higher responses. Therefore, 0.5 g l^{-1} was chosen as the concentration of polymer suspension and used for the entire assay testing.

5.3.3 Comparing Specificity of Imprinted and Non-Imprinted Polymers

The curve in Figure 5.5 shows the specificity of the MAA-MIP, compared to a non-imprinted polymer (NIP), prepared under the same condition but in the absence of the template.

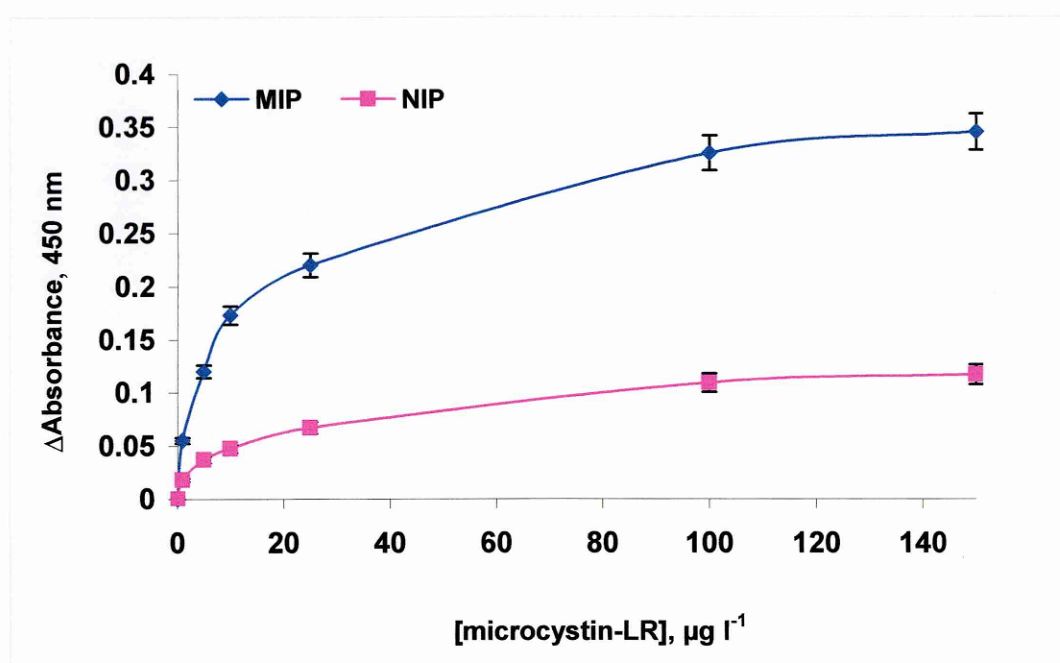


Figure 5.5: MIP-based assay for the MAA-polymer.

Competitive reaction was carried on with a suspension of either MIP or NIP in contact with HRP-MC-LR conjugate and free MC-LR dilutions ($0.01\text{-}150 \mu\text{g l}^{-1}$). The colour development in the filtrated solution was read by optical density at 450 nm after 20 minutes incubation. Error bars = \pm SD, $n=4$.

The absorbance at 450 nm increased as the concentration of MC-LR was increased. This can be explained by the competitive reaction between free MC-LR and its conjugate for the polymer binding sites. When low concentrations of MC-LR are in contact with the polymer, more conjugate is trapped by the polymer and less is left in the filtered solution, resulting in a lower signal. An increase in absorbance was observed when the MIP was incubated with higher concentrations of free toxin. For a broad range of concentrations, the ratio signal/ blank (S/B) increased considerably and a steady state response of the calibration curve for the blank polymer was observed. This demonstrated that the affinity was enhanced in the imprinted polymer, when a competition between the toxin and its conjugate was established. Unlike the MIP, the absorbance observed using the non-imprinted polymer remained below 0.1.

The LLD_{80} for the toxin MC-LR was about $1 \mu\text{g l}^{-1}$. The signal was detectable up to a concentration of $150 \mu\text{g l}^{-1}$ of toxin and since a steady state was not reached, it was concluded that the polymer binding sites were not all saturated.

5.3.4 Comparing Sensitivity and Affinity for Microcystin-LR Receptors

A limited amount of purified anti-MC-LR polyclonal antibody was supplied by Prof. Hennion, (Department of Environmental and Analytical Chemistry, Paris, France). The antibody was employed in a competitive ELISA assay, based on the commercial EnviroGard[®] kit protocol for microcystin-LR detection. The antibody was immobilised on a microtiter plate, after diluting 1:1000 at pH 7.2 from the stock concentration. The commercial conjugate MC-LR-HRP competed with free microcystin-LR in the standard samples for binding sites in the antibody coated well. The same procedure was adopted using polyclonal antibodies provided with the EnviroGard[®] microcystin-LR plate kit and monoclonal antibodies obtained with another microcystin-LR ELISA kit. In both cases, the antibodies were used as received.

The results achieved with the competitive ELISA assay, e.g. the sensitivity and the affinity of the antibodies for MC-LR, are shown in Table 5.2. These results were

compared with the performance of the artificial MIP receptors for microcystin-LR, described in the previous section. The EC_{50} values for the MIPs were calculated by determining the concentration value at the midpoint of the calibration curve. The sensitivity range was calculated by considering the LLD_{80} of toxin and the LLD_{20} value before the calibration curve reached a plateau.

Table 5.2: Values of affinity and range of sensitivity for microcystin-LR receptors.

RECEPTORS	AFFINITY (EC_{50}), $\mu\text{g l}^{-1}$ MC-LR \pm SD, n=3	SENSITIVITY RANGE, $\mu\text{g l}^{-1}$ MC-LR \pm SD, n=3
MAA-MIP	10 ± 0.06	1-120
CM-MIP	0.65 ± 0.1	0.1-100
Anti-MC-LR monoclonal antibody (Wako kit)	0.08 ± 0.07	0.025-1.6
Anti-MC-LR polyclonal antibody (EnviroGard kit)	0.30 ± 0.08	0.05-1.2
Anti-MC-LR rabbit polyclonal antibody (Prof. Hennion)	0.27 ± 0.1	0.05-0.9

Abbreviations: CM polymer= computationally designed polymer.
MAA polymer= methacrylic acid based polymer, SD= standard deviation.

The sensitivity range for polyclonal and monoclonal antibodies was much more limited than that of polymeric receptors. Regarding the minimum concentration detectable, polyclonal and monoclonal antibodies were able to detect as low as $0.05 \mu\text{g l}^{-1}$ and $0.025 \mu\text{g l}^{-1}$ of MC-LR, respectively, whereas the MAA-MIP had a limit of detection

twenty times higher than that of anti-MC-LR polyclonal antibody. Significant improvements regarding the limit of detection and affinity of the MIP were achieved using the computationally designed MIP. In this case, the limit of detection was twice that of the anti-MC-LR sheep polyclonal antibody.

5.3.5 Comparing Cross-Reactivity for Microcystin-LR Receptors

The cross-reactivity of the MAA and CM-MIP for microcystin-LR analogues such as microcystin-RR, microcystin-YR and nodularin was evaluated using the enzyme-linked competitive assay, as described in Section 5.2.1. Different concentrations of each analogue (50 μ l in 50 mM sodium-phosphate buffer, pH 7.0) were added to the 96-well filtration microplate with the polymer suspension. Table 5.3 shows the cross-reactivity of microcystin-LR antibodies and polymers tested.

Table 5.3: Cross-reactivity for MIP and antibodies with microcystin-LR analogues.

RECEPTORS	TARGET MOLECULES, % CV, \pm SD, $n=3$			
	MC-LR	MC-RR	MC-YR	NOD
MAA-MIP	100 \pm 0.5	19 \pm 0.8	30 \pm 1	36 \pm 0.5
CM-MIP	100 \pm 0.8	21 \pm 0.9	27 \pm 2	22 \pm 0.2
Anti-MC-LR monoclonal antibody (Wako kit)	100 \pm 0.2	106 \pm 0.3	44 \pm 2	18 \pm 0.2
Anti-MC-LR polyclonal antibody (EnviroGard kit)	100 \pm 0.4	54 \pm 0.5	35 \pm 0.3	68 \pm 0.8
Anti-MC-LR rabbit polyclonal antibody (Prof. Hennion)	100 \pm 0.2	92 \pm 2	122 \pm 0.8	73 \pm 1

Abbreviations: MC-LR= microcystin-LR; MC-RR= microcystin-RR; MC-YR= microcystin-YR; NOD= nodularin; % CV= percentage of cross-reactivity; SD= standard deviation.

Both imprinted polymers showed a relatively low cross-reactivity with any of the analogues; this was in contrast to polyclonal and monoclonal antibodies. The presence of the template during the polymerisation process guaranteed a certain conformation for all the monomers and cross-linker compounds. When the template was washed away, the polymer maintained many functional groups in an orientation optimal for the same molecule, used as the template. The antibodies showed high cross-reactivity for all the microcystins and nodularin, although the monoclonal antibody could discriminate between microcystin-LR and different toxins such as nodularin and microcystin-YR.

5.3.6 Comparing Stability of Microcystin-LR Receptors

Immunoassays are very powerful techniques for screening marine and freshwater toxins, due to their high sensitivity and specificity. However, natural receptors have limitations of stability and cannot be used under harsh conditions such as high temperatures, non-aqueous and extreme pH conditions (Haupt *et al.*, 1998b). Stability tests were performed by comparing the affinity of MIPs and antibodies for microcystin-LR before and after 2 hours of incubation under predefined experimental conditions.

Amongst the polyclonal antibodies anti-microcystin-LR previously investigated, only the anti-MC-LR rabbit polyclonal antibody (Prof. Hennion, Paris) was used for the stability tests, because of the high cost of such immuno-reagents. The antibody solution (1/1000 dilution) and MIP suspension (0.5 g l^{-1}) were added to 80 % dimethylformamide in sodium phosphate-buffered saline, 10 mM HCl pH 2.0, 50 mM NaOH pH 11.0, or to a solution of 10 mM CuSO_4 in PBS. In addition, 100 μl of antibody solution and polymer suspension were mixed with 100 μl of PBS and the resultant mixture maintained at temperature of 80 °C. After 2 hours of incubation under these conditions, the polymer, and antibody were reconditioned by adding sodium phosphate buffer. The remaining affinity of the receptors was evaluated using a competitive assay format, previously described for both MIPs and antibodies and expressed as a percentage of the affinity under optimum conditions. Untreated polymers

and antibodies were used as positive controls. The results of these experiments are summarised in Figures 5.6 and Figure 5.7.

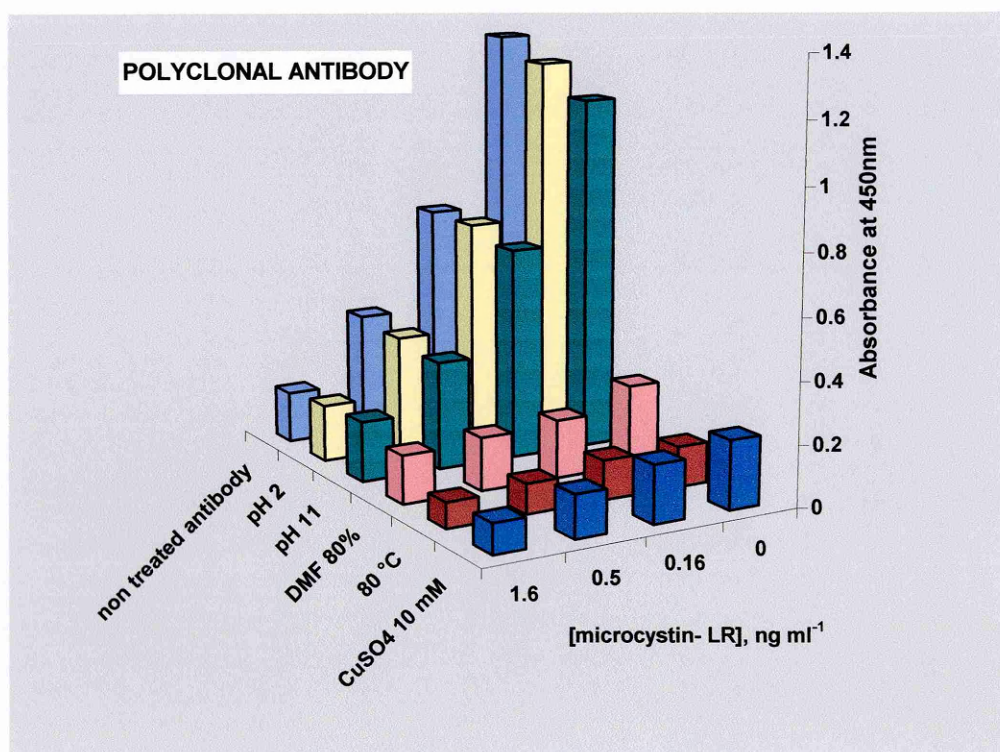


Figure 5.6: Stability test with anti-microcystin-LR polyclonal antibody.

The antibody was incubated for two hours in different conditions. After reconditioning in PBS buffer, the competitive ELISA assay was carried out and the remaining affinity of the antibody calculated. Each experiment was repeated three times, the standard deviation was 5 %.

The polyclonal antibody performed well under harsh pH conditions, maintaining functionality for at least two hours. On the other hand, a large loss in binding was observed in DMF and CuSO₄ environments, even when some residual affinity of the antibodies could still be detected after two hours treatment.

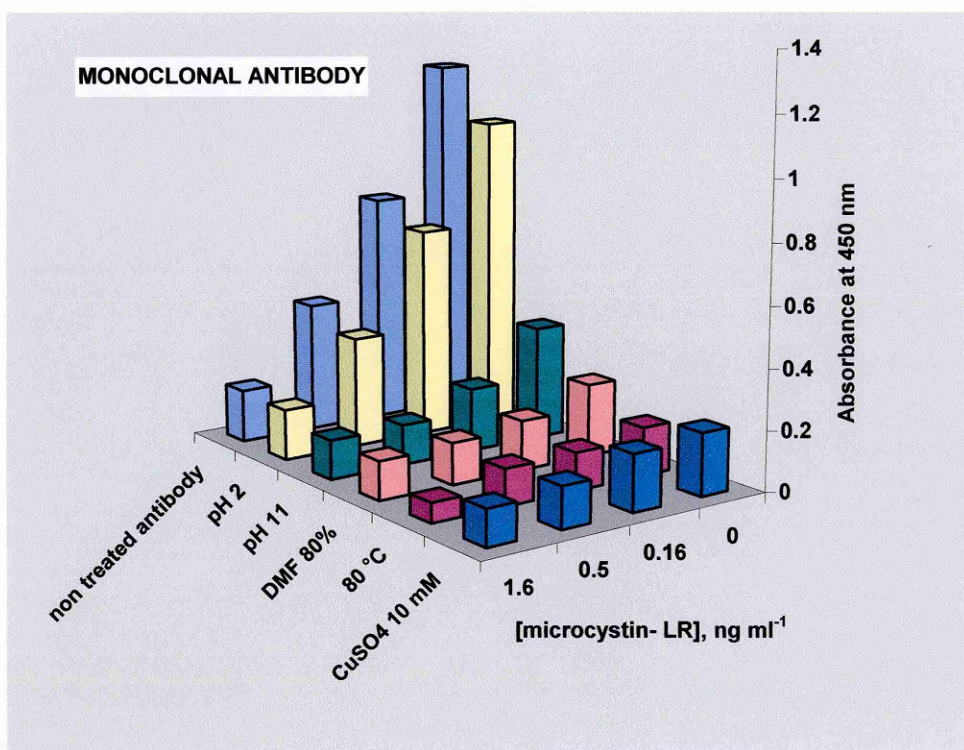


Figure 5.7: Stability test with anti-microcystin-LR monoclonal antibody.

The antibody was incubated for two hours in different conditions. After reconditioning in PBS buffer, the competitive ELISA assay was carried out and the remaining affinity of antibody calculated. Each experiment was repeated three times and the standard deviation was 5 %.

With the exception of the high pH studies, the monoclonal and polyclonal antibodies performances were similar in the tests. Antibodies, being proteins, would be expected to denature at temperatures above 42 °C. However, both antibodies were still functional when subjected to a high temperature for two hours.

The stability of the artificial imprinted receptors is shown in the two following graphics (Figure 5.8 and Figure 5.9).

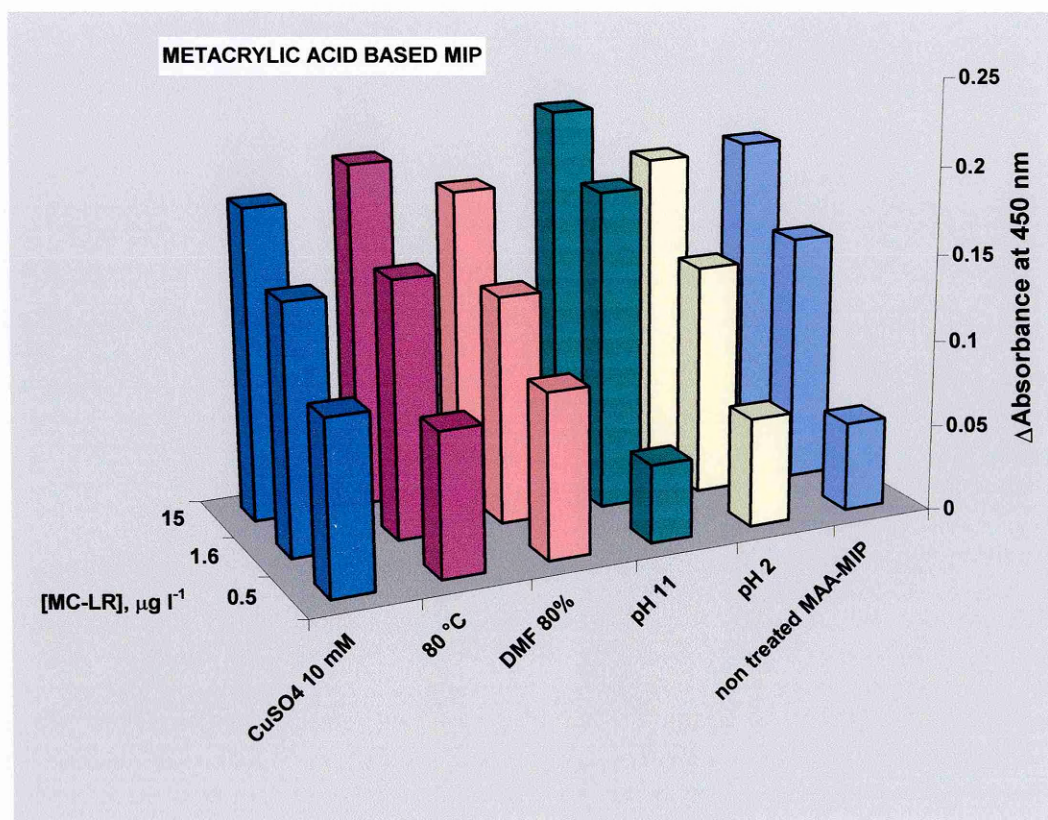


Figure 5.8: Stability test with MAA-MIP for microcystin-LR.

The polymer was incubated for two hours in different conditions. After reconditioning in PBS buffer, the competitive enzyme-linked MIP assay was carried out and the remaining affinity of the imprinted receptor calculated. Each experiment was repeated three times and the standard deviation was 7 %.

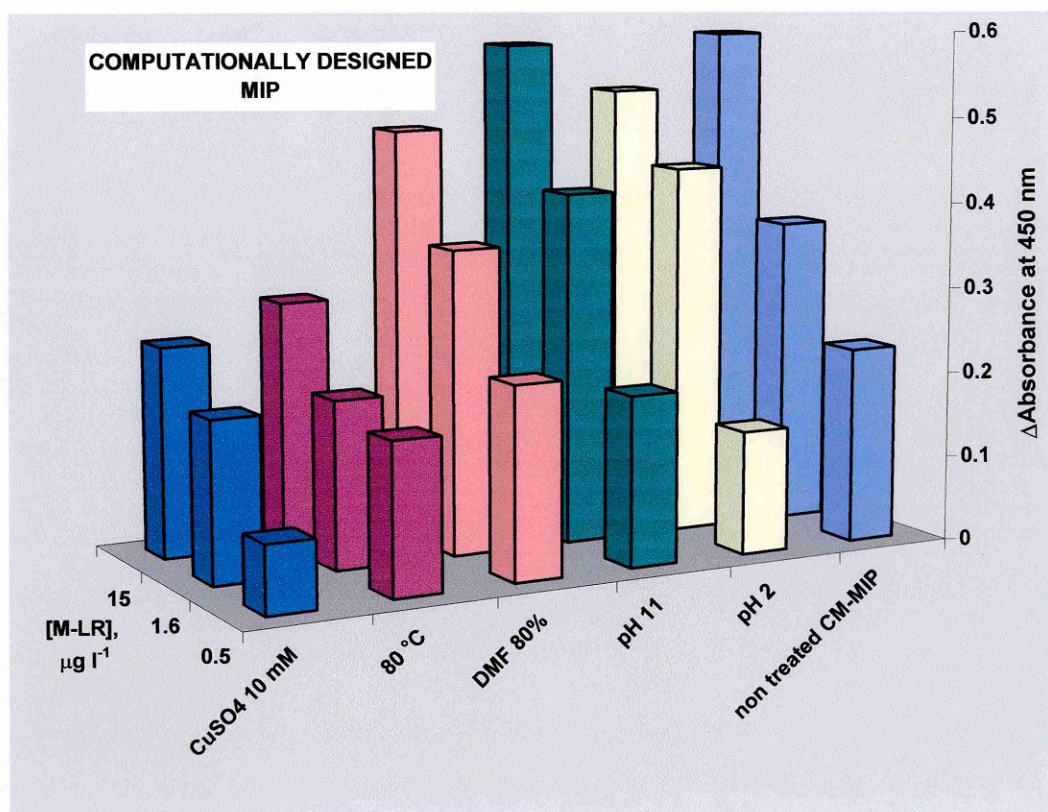


Figure 5.9: Stability test with MAA-MIP for microcystin-LR.

The polymer was incubated for two hours in different conditions. After reconditioning in PBS buffer, the competitive enzyme-linked MIP assay was carried out and the remaining affinity of the imprinted receptor calculated. Each experiment was repeated three times and the standard deviation was 7 %.

Although both the computationally designed MIP and the MAA-MIP exhibited excellent stability under acidic and basic conditions, their performance at high temperature and in presence of heavy metals was markedly different. The MAA polymer was made using only methacrylic acid as monomer, which is known for being very stable. All the results for experiments on the stability of MIPs and antibodies under harsh conditions are summarised in Table 5.4.

Table 5.4: Receptor Activity measurements carried out after different treatments ($n= 3$, \pm SD).

RECEPTORS	REMAINING ACTIVITY, %					
	Non treated	pH 2	pH 11	DMF 80 %	T = 80 °C	CuSO ₄ 10mM
MAA-MIP	100 \pm 2	99.5 \pm 3	102.4 \pm 6	102.3 \pm 1	88.8 \pm 6	98.1 \pm 3
CM-MIP	100 \pm 5	95.9 \pm 3	99.8 \pm 6	94.1 \pm 6	55.3 \pm 5	58.3 \pm 4
Anti-MC-LR monoclonal antibody (Wako kit)	100 \pm 1	88.5 \pm 3	25.6 \pm 8	19.1 \pm 1	12.6 \pm 4	16.3 \pm 1
Anti-MC-LR rabbit polyclonal antibody (Prof. Hennion)	100 \pm 1	94.8 \pm 3	87.6 \pm 5	19.9 \pm 5	9.9 \pm 2	16.8 \pm 0.1

The activity of each receptor was evaluated by competitive assay and expressed as a percentage of the initial activity of these receptors under optimum conditions. Each treatment was carried out for two hours.

5.4 CONCLUSIONS

Artificial receptors versus microcystin-LR both based on a classical approach and a new computational approach were investigated. A competitive enzyme-linked MIP assay was used for characterisation of the MAA-MIP receptor and a control blank polymer was used for comparison. The sensitivity range for the polyclonal and monoclonal antibodies was, in all cases, narrower than for the polymeric imprinted receptors. Regarding the limit of detection, polyclonal and monoclonal antibody were able to

detect as low as $0.05 \mu\text{g l}^{-1}$ and $0.025 \mu\text{g l}^{-1}$ of MC-LR, respectively, whereas the MAA-MIP had a limit of detection twenty times higher than that of anti-MC-LR polyclonal antibody ($1 \mu\text{g l}^{-1}$). For the CM-MIP, the limit of detection ($0.1 \mu\text{g l}^{-1}$) was twice that of the value of the anti-MC-LR polyclonal antibody and four times that of the anti-MC-LR monoclonal antibody. Likewise, the affinity, expressed in EC_{50} , was highly improved with the computational MIP compared to the traditional MIP (0.65 versus 10).

Both imprinted polymers showed relatively low cross-reactivity for any of the microcystin-LR analogues, in contrast to polyclonal and even monoclonal antibodies. The antibodies showed high cross-reactivity for all the microcystins and nodularin, although monoclonal antibody could discriminate between microcystin-LR and different toxins such as nodularin and microcystin-YR. The results showing high specificity for MIPs shown here are in agreement with other polymeric systems previously studied (Haupt *et al.*, 1998b).

A range of stability tests was performed for both natural and synthetic receptors. The results achieved were quite predictable, mainly concerning the loss of activity of the antibodies under all the harsh conditions considered. Nevertheless, antibodies could maintain a relatively high functionality after two hours of acidic and basic conditions. More damage was caused following incubation at very high temperature where the monoclonal and polyclonal antibodies lost more than 85 % of their activity. Similarly, in the presence of CuSO_4 (10 mM), the loss of functionality was about 80 % for both antibodies.

CHAPTER 6: RESULTS

AFFINITY RECEPTORS BASED ON MIP FOR DOMOIC ACID

6.1 INTRODUCTION

The application of MIP technology for the detection of domoic acid was investigated. The major difficulty in preparing MIPs for toxins such as domoic acid is related to the fact that they are relatively expensive, thus precluding the synthesis of a large amount of bulk polymer. Different approaches were studied with the aim of creating a specific MIP receptor for domoic acid, for applications in assay and sensor development. Based on a similar approach, already followed for microcystin-LR, a computationally designed MIP specific for domoic acid was tested by using an enzyme-linked competitive assay and with fluorescence assay based on a “gate effect” linked to the imprinted polymer. Lastly, an optical MIP sensor, obtained by grafting a MIP film onto a gold BIAcore chip, was evaluated for its sensitivity, specificity, cross-reactivity, and robustness. Likewise, monoclonal antibodies acting as natural receptors for the toxin were studied with the BIAcore system. Results from a comparison between the artificial and natural receptors (in the same format) are reported in this Chapter.

6.2 COMPUTATIONAL-BASED MIP FOR DOMOIC ACID

The computational design of a molecularly imprinted polymer specific for domoic acid was carried out. The modeling of monomer-template interactions was performed using commercial software package traditionally applied to drug design using combinatorial synthesis. A virtual library of functional monomers was created, rather than using compounds such as amino acids, which are commonly applied to drug design. The monomers included in the virtual library contained a broad variety of functionalities, capable of forming ionic bonds, hydrogen bonds, and van der Waals interactions with the template. From the Leapfrog results, the top three monomers giving the highest binding energy scores were: allylamine, acrylamide and urocanic acid. These monomers were selected and used in a simulated annealing (molecular dynamics) process in order to investigate their interactions with the template domoic acid. The interactions between template and monomers, in the minimized energy conformation, after the simulated annealing process are presented in Figure 6.1.

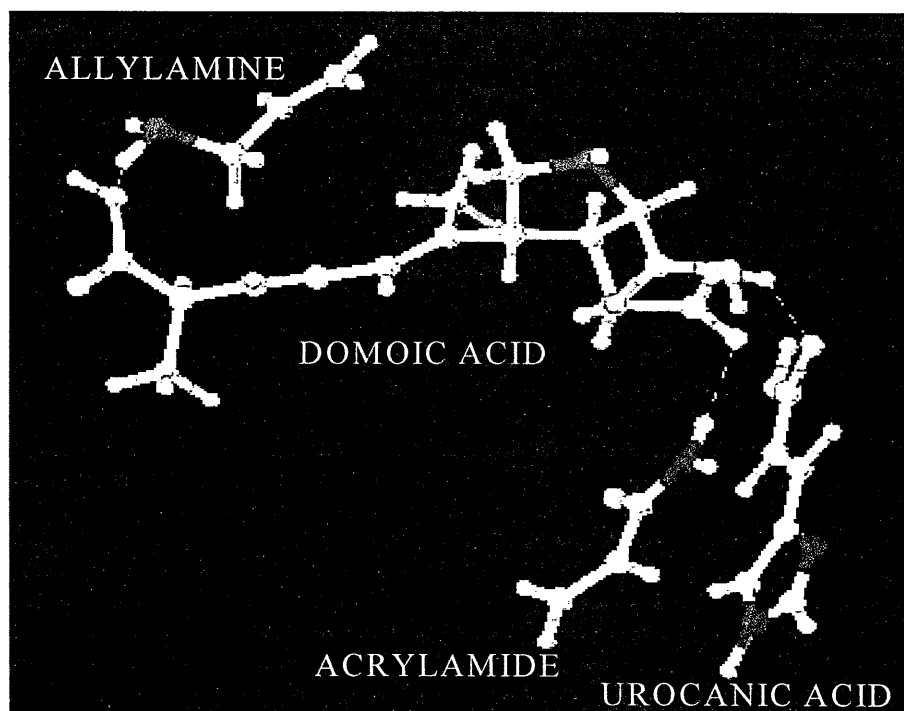


Figure 6.1: Template domoic acid and three monomers interaction as result after simulated annealing study.

The domoic acid molecule interacted with both the oxygen atoms contained within the carboxylic groups. Allylamine interacted with the oxygen of the -OH group at one extremity of the molecule through hydrogen of its primary ammine group. On the opposite side of the molecule, hydrogen of the acrylamide amino group interacted with another carboxylic oxygen of domoic acid. Lastly, the hydrogen of the -OH group on the same carboxylic function interacted with the carboxylic oxygen of the urocanic acid. Other interactions were impeded by steric hindrance. In fact, the complex seemed to take the conformation, which allowed the maximum possible distance between monomers and template. The stoichiometric ratio observed from the simulated annealing study was used in the MIP composition for domoic acid imprinting (Table 6.1). Therefore, for one mole of template, one mole of each of the monomers selected was mixed in the polymerization process.

Table 6.1: Composition of polymerisation mixture for domoic acid MIP based on computational design.

REAGENTS		Molar ratio
<i>TEMPLATE:</i>	DOMOIC ACID	1
<i>MONOMER 1:</i>	ALLYLAMINE	1
<i>MONOMER 2:</i>	ACRYLAMIDE	1
<i>MONOMER 3:</i>	UROCANIC ACID	1
<i>CROSS-LINKER:</i>	EGDMA	230
<i>INITIATOR:</i>	1,1'- azobis (cyclohexanecarbo -nitrile)	3750

Certain parameters of the modeling and screening study, e.g. dielectric constant, temperature, and type of interaction were modified in order to simulate the real polymerisation, or the re-binding conditions. On the basis of the computational modeling results, the polymer was synthesized following the same procedure used for the MC-LR classical polymer. A competitive enzyme-linked MIP- assay, similar to that conducted using the MAA-polymer for MC-LR, was performed using the MIP specific for domoic acid. Briefly, a suspension of the polymer was dispensed in a filtration microtiter plate together with solutions containing conjugate DA-HRP and different dilutions of free toxin. Following incubation, the mixture was filtered and the filtrate collected in a fresh microtiter plate. The optical density of the HRP enzyme was measured at 450 nm, after 20 minutes incubation with the TMB substrate and after stopping the reaction with 1M HCl.

The concentration of DA-HRP conjugate was optimised, providing the most favourable concentration for the competitive reaction. In Figure 6.2, different calibration curves for the competitive MIP assay, using three different concentrations of DA-HRP conjugate, are shown.

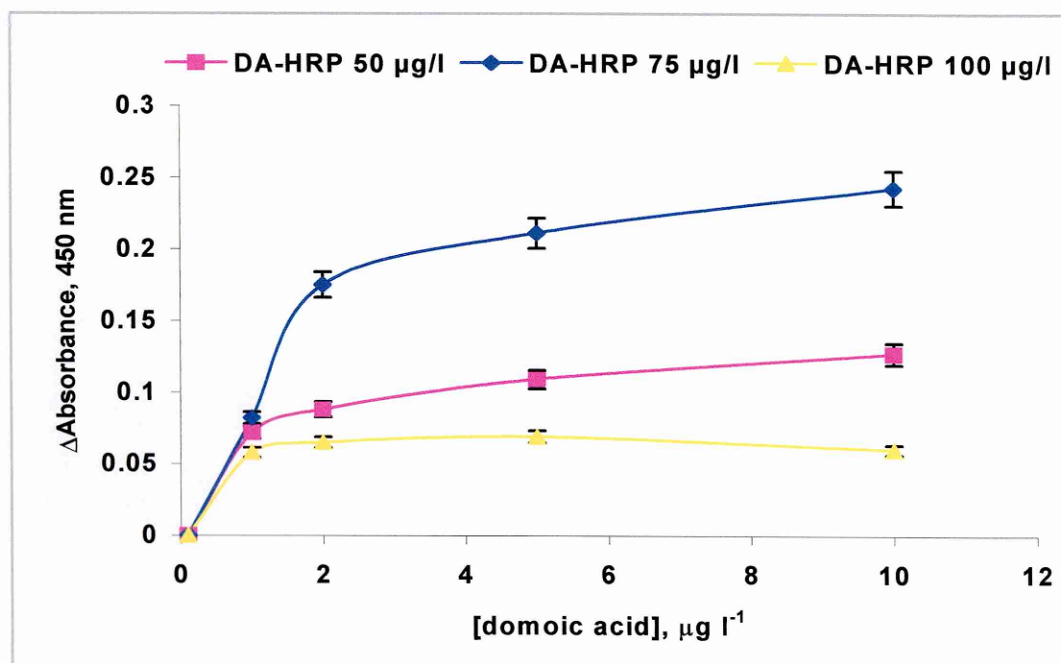


Figure 6.2: Enzyme-linked MIP assay with different concentrations of DA-HRP. A suspension of imprinted polymer was incubated for 1 hour with three DA-HRP concentrations (50, 75, 100 $\mu\text{g l}^{-1}$) and free DA dilutions (0.01-10 $\mu\text{g l}^{-1}$). The optical density was measured by adding TMB substrate and reading at 450 nm after 20 minutes. Error bars = \pm SD, $n=4$.

On the y-axis the absorbance is reported as a difference, since the value for the zero concentration of domoic acid (A_0) was subtracted. When high concentrations of the conjugate HRP-DA were used, most of the signal was due to non specific binding and thus eliminated. After subtraction of A_0 , no significant differences were observed for different concentrations of the toxin. Results from using a concentration of 0.75 mg l^{-1} revealed higher competition effects, thus this concentration was chosen for further experiments.

The MIP assays were also performed using a range of polymer concentrations, with the aim of producing optimised competitive enzyme-linked MIP assay (Figure 6.3).

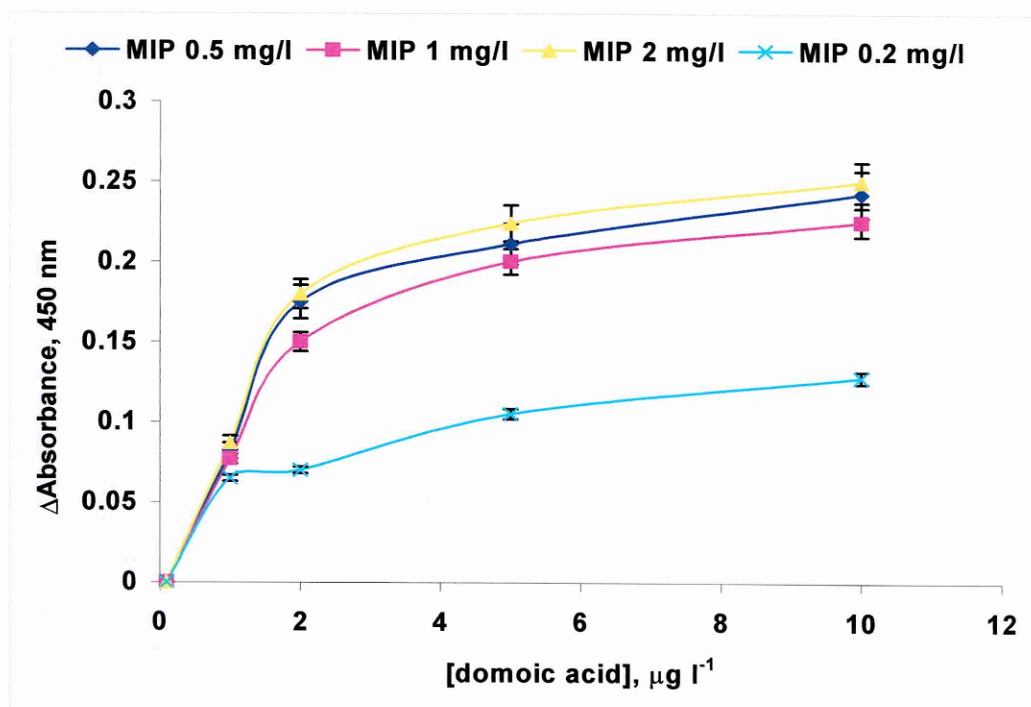


Figure 6.3: Enzyme-linked MIP assay using different concentrations of polymer. The polymer was incubated for 1 hour with DA-HRP concentrations ($75 \mu\text{g l}^{-1}$) and free DA dilutions ($0.01\text{--}10 \mu\text{g l}^{-1}$). The optical density was measured by adding the TMB substrate and reading after 20 minutes at 450 nm. Error bars = \pm SD, $n=3$.

The results were very similar for each of the three different concentrations tested, whereas lower absorbancies were observed with 0.2 mg l^{-1} of the polymer. Finally an optimised calibration curve was obtained with 0.5 mg l^{-1} and $75 \mu\text{g l}^{-1}$ of the DA-HRP conjugate, over a concentration range of between 0 and $10 \mu\text{g l}^{-1}$ free domoic acid. Another calibration curve was obtained using the same procedure with a non-imprinted polymer (NIP) as a control for the imprinted sites specificity versus the target toxin (Figure 6.4).

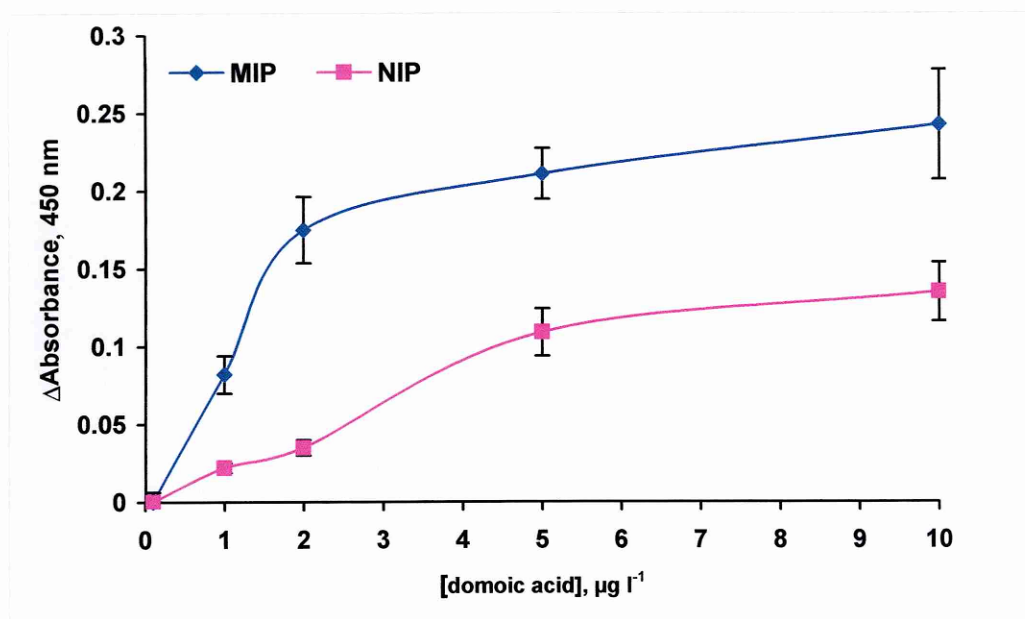


Figure 6.4: Calibration curve for domoic acid.

Suspension of either MIP or NIP was in contact with DA-HRP conjugate ($75 \mu\text{g l}^{-1}$) and DA dilutions ($0.01\text{-}10 \mu\text{g l}^{-1}$) and incubated for 1 hour. The optical density was measured by adding TMB and reading after 20 minutes at 450 nm. Error bars = \pm SD, $n=5$.

The results in Figure 6.4 showed that the LLD_{80} value of domoic acid was equal to $1.25 \mu\text{g l}^{-1}$ with a workable range of sensitivity between 1.25 and $10 \mu\text{g l}^{-1}$; the EC_{50} was calculated as $1.3 \mu\text{g l}^{-1}$. However, the significant non-specific signal, evidenced by the NIP curve, suggested that the competitive MIP assay might be not a suitable method to study this polymer. High standard deviations indicated a low reproducibility for the assay ($\% \text{CV} > 17$). The filtration step during the MIP preparation was believed to be a drawback in terms of accuracy and reproducibility for the assay. Moreover, the suspension of polymer particles used was not homogeneous and thus may have contributed to the concentration error.

6.3 MIP FLUORESCENCE ASSAY FOR DOMOIC ACID DETECTION

A second method of detection was investigated, combining a fluorescent measuring technique with the robust and selective artificial receptor system, prepared by imprinting polymerisation. The method eliminated the filtration process, used in the previous enzyme-linked competitive assay, and incorporated a stirring system into the spectrofluorophotometer instrument. This ensured a constant agitation of the polymer suspension, thus improving homogeneity.

Allylamine was one of the monomers identified in the domoic acid polymer composition, determined by the computational design. This functional monomer is able to interact with domoic acid and (with its amino groups) form a fluorescent compound by reacting with the OPA reagent, which is a mixture of o-phthalic-dialdehyde with b-mercaptoethanol. The OPA reagent gives fluorescence in the presence of primary amines (Piletsky *et al.*, 1996). A scheme of the OPA reaction with allylamine is presented in Figure 6.5.

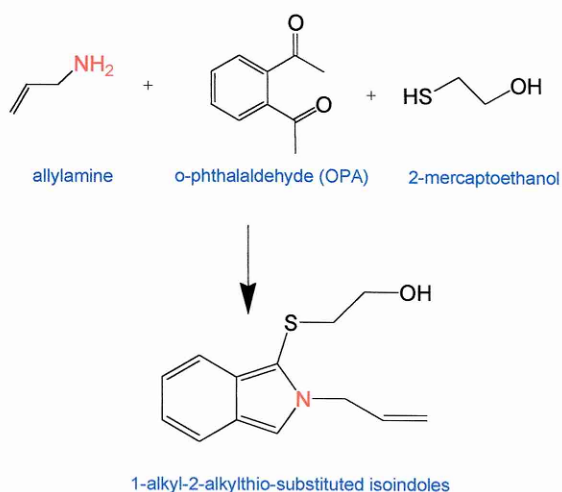


Figure 6.5: Reaction of OPA reagent with the amino group of allylamine.

Instead of a competitive reaction, the characterisation of the polymer was studied by investigating the “gate effect”. In this case, the sensor response of the imprinted polymer is related to a change in the polymer morphology and porous structure, induced by the interaction of template molecules with selective cavities of the imprinted macromolecule.

A suspension of the polymer was added to the measuring cell and mixed with domoic acid, β -mercaptoethanol and 50 nmol of *o*-phthaleic dialdehyde, as suggested by previous work (Piletsky *et al.*, 1996). The experiment was also repeated in the absence of the target analyte. The mixture was incubated for 15 minutes at room temperature, stirring constantly. The excitation wavelength was 335 nm and the emission wavelength was 450 nm. The change in fluorescence emission on reaction of the specific polymer with OPA-reagents and different concentration of domoic acid is shown in Figure 6.6.

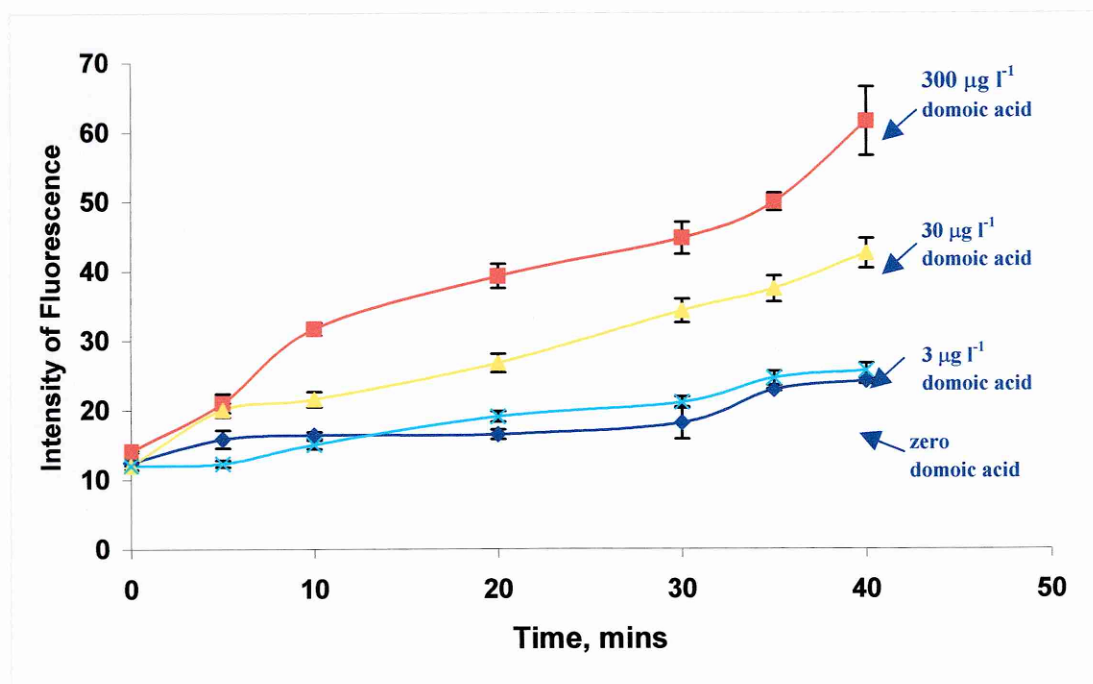


Figure 6.6: Development of fluorescence emission from the OPA-modified polymer. Polymer suspension (2.5 ml, 3 g l^{-1} in 100 mM sodium borate buffer, pH 10) was mixed with either buffer or domoic acid (50 μl) and OPA reagents, then incubated for 15 minutes at R.T. with stirring. Excitation wavelength was 335 nm and the emission wavelength was 450 nm. Error bars = \pm SD, $n=5$.

The development of fluorescence was monitored over a period of time and the results correlated with the concentration of template present in the solution. Rapid detection of domoic acid at three different concentrations was shown to be possible within 40 minutes, coupled with good reproducibility (% CV = 4.6). On the addition of domoic acid, the emission intensity significantly increased. The template-induced variation in the fluorescence intensity evidenced as a larger quantity of amino groups reacted with OPA; in the presence rather than in absence of domoic acid. In Table 6.2, the imprinting factor for this polymer is illustrated, taking into account the response of NIP as well, for each of the domoic acid concentrations.

Table 6.2: Imprinting factors for the polymer calculated in the presence and absence of domoic acid.

Domoic acid concentration ($\mu\text{g l}^{-1}$)	ΔF (MIP)	ΔF (NIP)	IF
300	61.5	19.7	3.1
30	42.5	34.2	1.2
3	25.6	27.8	0.9
0	24.1	25.3	0.95

Abbreviations: ΔF (MIP)= response for imprinted polymer; ΔF (NIP)= response for blank polymer; IF= imprinting factor; MIP= molecularly imprinted polymer; NIP= non imprinted or blank polymer

Increasing the imprinting factor by more than 3 times (in the presence of $300 \mu\text{g l}^{-1}$ of domoic acid) demonstrated that the template changed the polymer conformations and made the sites more available to the analyte molecules.

With the fluorescence assay, it was still necessary to use the bulk polymer in suspension, although the stirring system improved homogeneity during the analysis. Nevertheless, this format allowed analysis of the sample to be carried out one by one, increasing significantly the length of each experiment. Moreover, the polymer suspension was discarded after each sample monitoring, providing a cost-effective analysis.

6.4 GRAFTING TECHNIQUE FOR DOMOIC ACID POLYMER

An important aspect for any molecular imprinting project, where sensitivity and selectivity of the obtained artificial receptor plays a major role, is the analytical means that are employed to analyse and evaluate the polymer. If the target molecule is expensive, as is often the case with biomolecules such as toxins, the most convenient way can be to interface the polymer with a chemical sensor or biosensor, that is, synthesise a thin layer of polymer at the surface of a transducer. In that way, the amount of polymer needed is much smaller compared to the conventional assay. Furthermore, it can be used in theory many times e.g. highly repetitively. One of the ways to “deposit” a MIP on the surface of physical transducer is to use grafting.

Thiol chemistry allows the easy functionalisation of gold surfaces, such that further surface modifications can be performed. By immobilising a self-assembled monolayer of 2-mercaptoethylamine, followed by standard carbodiimide chemistry, it was possible to covalently bind the photo-polymerisation initiator 4,4 –azobis(cyanovaleric acid) to the surface. Photo-initiator immobilisation ensured that the formation of the MIP thin film, comprising 2-(diethylamino)ethyl methacrylate as cross-linker, occurred only at the gold surface. When the polymerisation mixture was irradiated with ultraviolet (UV) light, the photo-initiator degraded via radicals, which initiated the polymerisation reaction at the surface level.

Atomic force microscopy analysis showed the resultant grafted MP layer to be approximately 40 nm thick and deposited homogeneously, thus suitable for SPR-based analyses. A range of UV irradiation times was tested, for the polymerisation reaction. Long time UV-emission (above 30 minutes) created a thick layer of polymer, whilst exposure for a few minutes gave a polymer film of highly variable thickness (between 2 and 15 nm). Photo grafting of the MIP thin films onto treated gold surfaces were investigated by topographical studies using the atomic force microscope (AFM) and later by surface plasmon resonance (SPR).

6.4.1 Characterisation of Grafting Process by Atomic Force Microscope Imaging

A full characterisation of the grafting process was initially carried out on the gold surface of a BIAcore chip (Pioneer J1 type). The steps of the polymerisation were investigated by atomic force microscopy (AFM) imaging; the samples were scanned using the contact mode system. The “scrapping” experiment was performed with maximum additional force applied to the cantilever, such that the feed back loop would not be disturbed. Figure 6.7 (a) and (b) represent a 2 μm by 2 μm area of the gold chip following photo grafting of the MIP film.

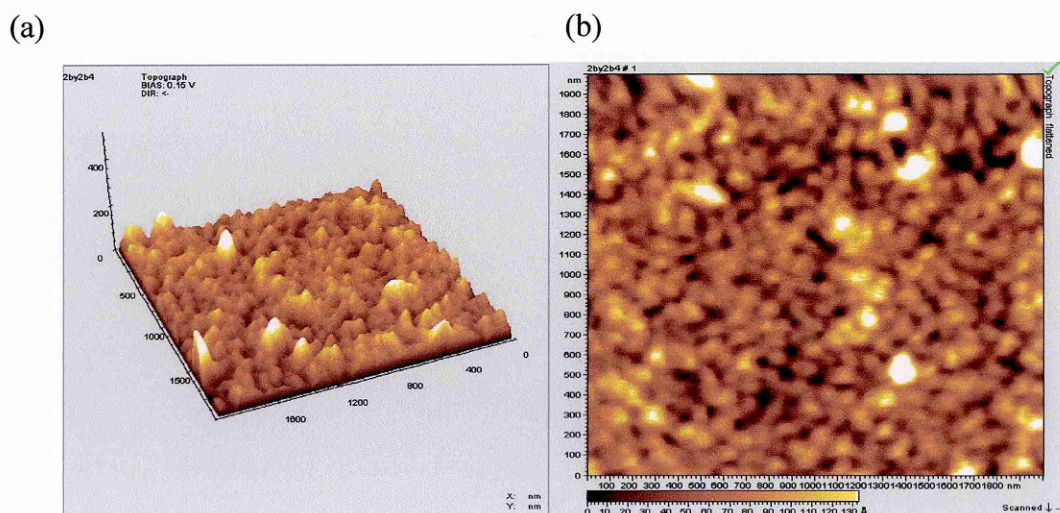


Figure 6.7: (a)- Planar topographic image. (b)- 3D topographic image of gold chip with grafted MIP.

Figure 6.7 (a) and Figure 6.7 (b) confirmed the homogeneity of the DA-MIP thin film photo-grafted onto gold; with a maximum differential height of 13 nm in thickness, within the area investigated. The polymer layer copied the gold topography very closely and showed the same features in term of homogeneity.

Once the desired MIP film was deposited onto the BIAcore chip gold surface, the thickness of the polymer film could be evaluated. The additional force was removed and the tip of the cantilever slightly lifted; it was then moved to scan a larger area (6 μm by 6 μm). Figure 6.8 presents the topographic (also called Z-image) image of the structure, where the central square represents the area shown in the previous Figure 6.7.

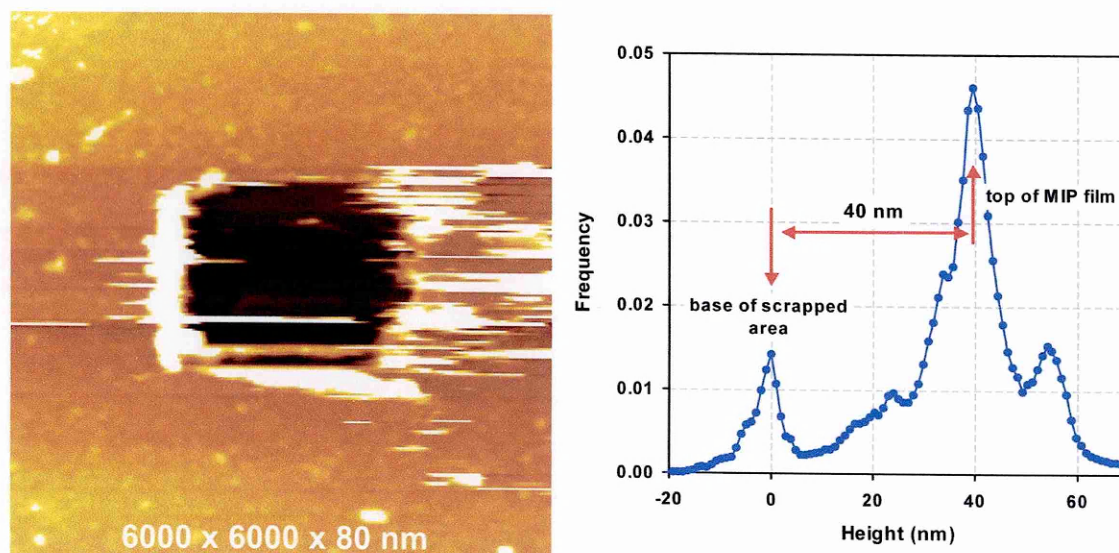


Figure 6.8: 6 μm \times 6 μm AFM image of a 2 μm \times 2 μm scrapped area on the left and a plot of pixel height vs. frequency plot of the grafted MIP on the right.

The image in Figure 6.8 shows that the texture of the scrapped area has completely changed revealing the bare gold underneath, when compared to the surrounding area covered by the polymer. It confirmed that all the MIP coating had been removed and that the thickness calculated from the topographic image is representative of the layer deposited. The white strides present on the image are due to the displacement of the

scrapped and mobile material accumulated on the side of the damaged area, created by the cantilever in contact with the surface. The graph shown in Figure 6.8 (right) depicts a MIP layer thickness, corresponding to the scrapped area, of 40 nm.

The difference between the two levels could be calculated from the Z position of the two cursors (1 and 2), representing the levels of the un-scraped and scrapped areas respectively. Figure 6.9 illustrated how the software controlling the microscope allows the calculation of thickness between the two levels (1 and 2), and how the MIP layer of 40 nm was calculated.

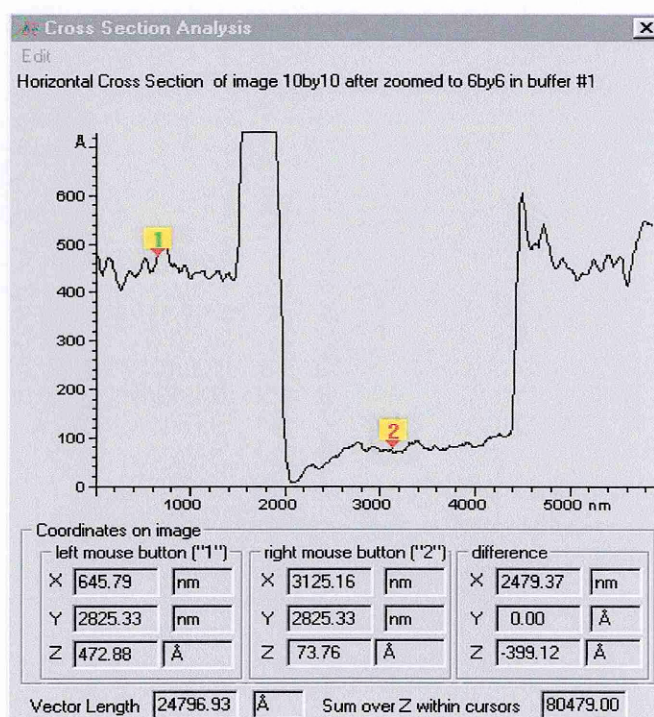


Figure 6.9: Cross section analysis of Figure 6.8.

The different thickness obtained after each step of the photo-grafting procedure for MIP thin film formation onto the gold chip are summarised in Table 6.3.

Table 6.3: Thickness of films generated during the grafting procedure.

THICKNESS MEASUREMENTS	
Cross-linked MIP polymer matrix	5-40 nm
Covalently immobilised photo-initiator layer	0.6 nm
Self-assembled aminated alkane thiol layer	0.2 nm
Gold metal substrate/transducer	>50 nm

6.4.2 Characterisation of MIP Grafting by Surface Plasmon Resonance

The BIAcore 3000™ is one of the most efficient instrument available for studying biomolecular binding events in real-time and is based on surface plasmon resonance (SPR). The molecularly imprinted polymer (specific for domoic acid) was directly synthesised and grafted on the BIAcore gold chip; which consists of a glass with a thin film of gold, deposited on one side. The chip was then inserted into the BIAcore 3000™ with the MIP/gold side in contact with the flow cells. This allowed the MIP to be used as linked receptor for the study of its specificity by recognition of the target molecule.

After obtaining an initial baseline on the sensorgram, the specificity of the sensor was evaluated by injecting 80 µl of various concentrations of a horseradish peroxidase (HRP)-DA conjugate with native HRP (used as a control), the HRP functioned as a refractive index label. Each injection was followed by regeneration.

The regeneration step was optimised by changing the volume and the flow of injection. A complete regeneration, from the interaction of the target with the MIP receptor, was obtained after injecting 10 μl 0.2 % sodium dodecyl sulphate (SDS) in 10 mM HCl at a flow rate of 5 $\mu\text{l min}^{-1}$. A faster flow rate failed to regenerate the surface completely despite using a larger volume, it was decided that a slower flow rate would increase the assay time too much. The regeneration solution did not appear to destroy the polymer receptor, since after more than 30 regeneration steps the polymer did not lose its capacity for specifically binding to the analyte (Figure 6.10).

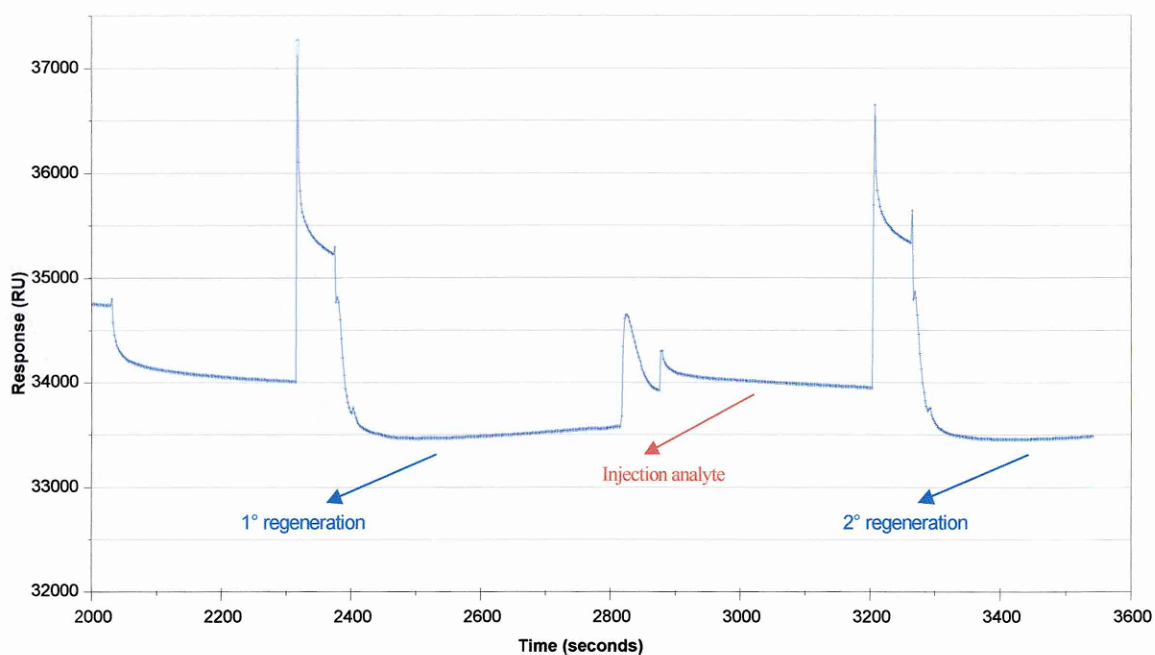


Figure 6.10: Two consecutive regeneration phases alternated by one injection of the analyte.

The solution used for regeneration differed significantly in refractive index from the running buffer, giving a bulk positive response. The response level and shape of the sensorgram during the regeneration pulse was, therefore, considered not important. The baseline level after regeneration should ideally be identical to that before the sample injection. Provided that the baseline is restored to the correct level when the response has stabilized, this did not affect the kinetic determinations. A constant flow system

running the PBS buffer containing 0.05 % Tween 20 at $30 \mu\text{l min}^{-1}$ facilitated washing away of the weak non-specific interactions.

The resultant curves for the specificity determination of the MIP are presented in Figure 6.11.

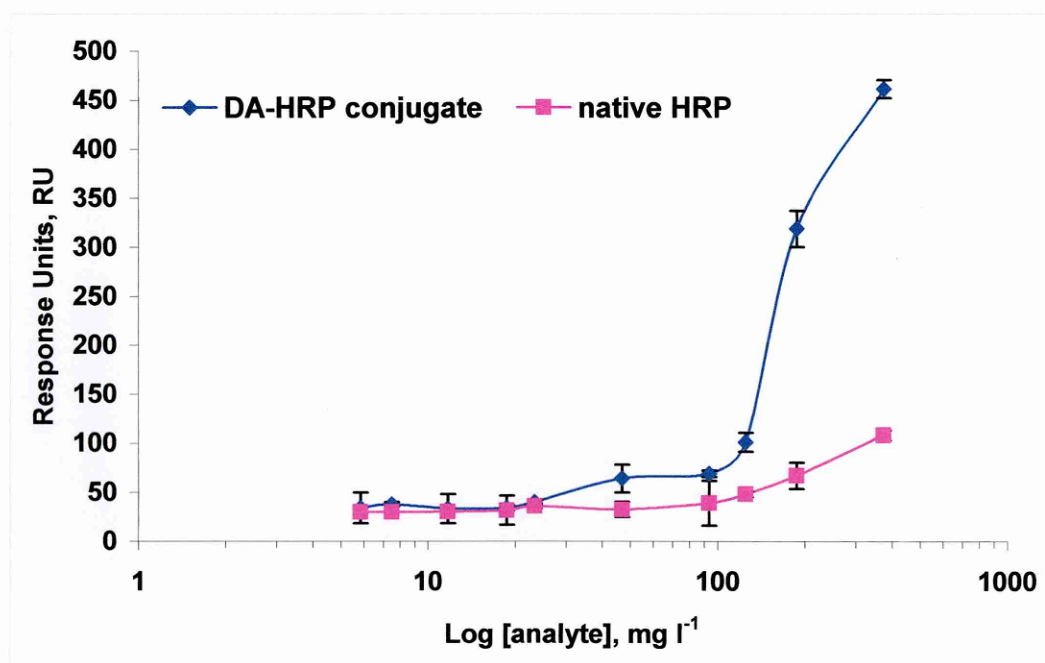


Figure 6.11: Specific binding of DA-HRP conjugate to grafted MIP compared to non-specific binding of native HRP.

Either the conjugate DA-HRP or HRP were injected in BIAcore 3000™ (80 μl) with a flow rate of $5 \mu\text{l min}^{-1}$. Error bars = \pm SD, $n=3$.

The coated MIP chip displayed a specific binding of domoic acid-HRP conjugate, shown by the increase in the response unit (RU) of the chip ($\text{RU}_{\text{max}} > 450$), whereas a much lower signal was observed for native HRP enzyme ($\text{RU}_{\text{max}} < 100$). At a concentration of 200 mg l^{-1} of conjugate, the maximum difference (signal/control) with the same concentration of free HRP was equal to 4.7. The concentration of 200 mg l^{-1} was subsequently used for the competitive reaction with the MIP optical sensor.

6.5 MIP SENSOR FOR DOMOIC ACID BASED ON THE SPR SYSTEM

Since domoic acid is a small molecule (FW= 311) for direct BIAcore analysis, a competitive reaction was performed with the MIP, using a protein refractive label of domoic acid for the detection of the toxin. The competitive reaction was carried out by injecting into the flow cell of the BIAcore 3000TM system an equal volume of conjugate DA- HRP (200 mg l⁻¹) and a broad range of domoic acid concentrations (in µg l⁻¹). A regeneration step followed each of the analyte injections; a space of approximately 5 minutes was left between injections. A sensorgram of the competitive reaction for a concentration range of 1-100 µg l⁻¹ of domoic acid is shown in Figure 6.12.

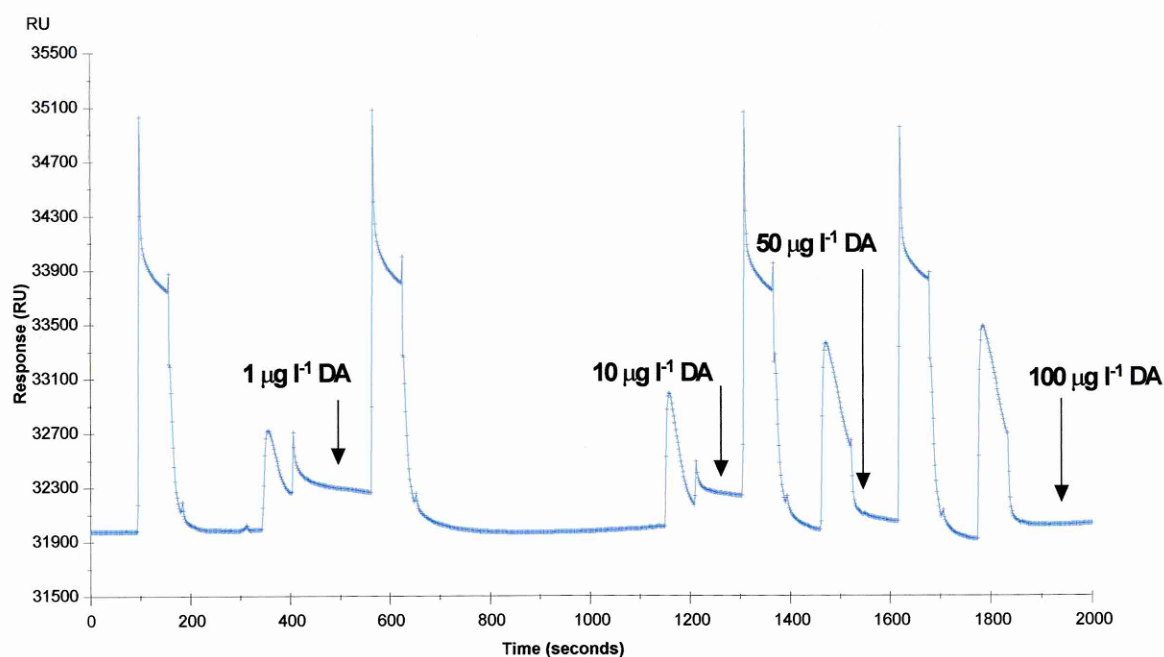


Figure 6.12: Sensorgram of a competitive MIP reaction.

A mixture (1:1) of conjugate DA-HRP (200 mg l⁻¹) and DA dilutions over a range of 1-100 µg l⁻¹ were injected into BIAcore 3000TM, in a volume of 150 µl and at a flow rate of 30 µl min⁻¹.

A calibration curve for the competitive reaction on the MIP sensor is shown in Figure 6.13.

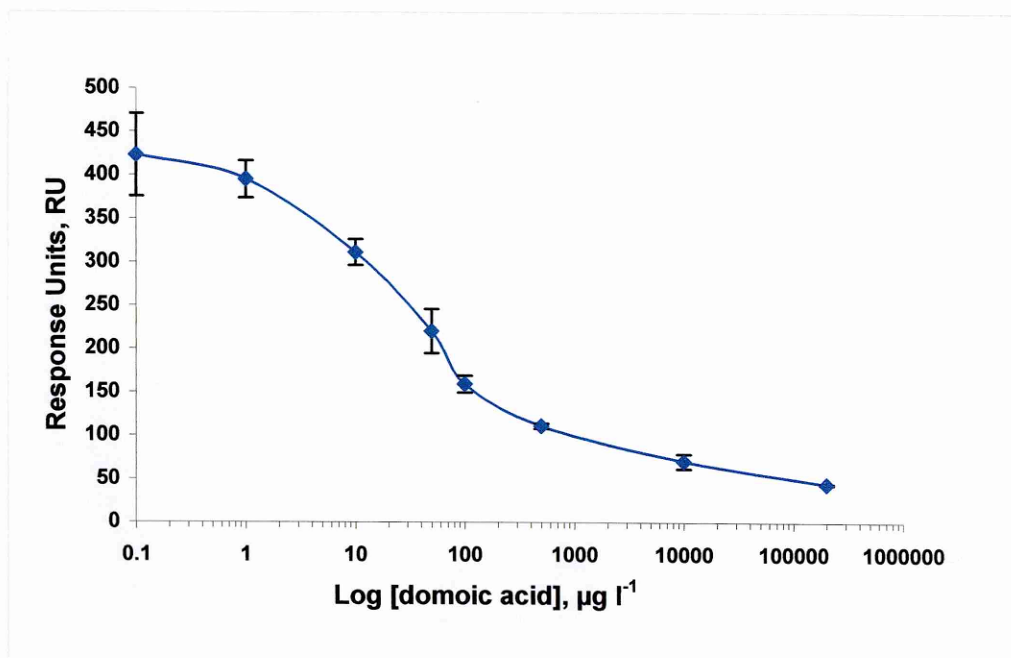


Figure 6.13: Competitive calibration curve for the domoic acid MIP sensor. A mixture (1:1) of conjugate DA-HRP (200 mg l⁻¹) and DA were injected into the BIAcore 3000TM, in a volume of 150 µl and at a flow rate of 30 µl min⁻¹. Error bars= ± SD, $n=3$.

The limit of detection calculated as an LLD₈₀ corresponding to 5 µg l⁻¹ and the EC₅₀ value was 58 µg l⁻¹. The response curve is highly reproducible, as indicated by the relatively low standard deviations and the mean % CV for the assay.

The cross reactivity (CR) of the grafted polymer for the DA analogues kainic acid (KA), glutamic acid (Glu) and aspartic acid (Asp) was also evaluated. A graph showing the different displacements of domoic acid and its analogues, from the MIP receptor, is shown in Figure 6.14.

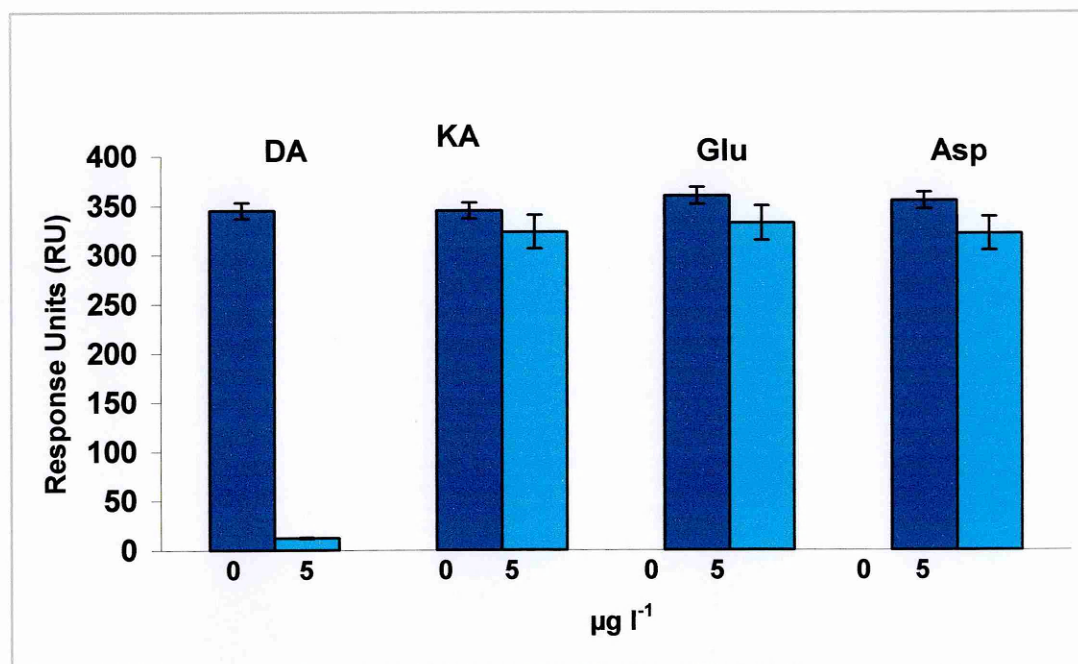


Figure 6.14: Cross-reactivity of DA analogues obtained with the MIP sensor. Injections of equal volumes (150 µl) of HRP-DA conjugate and the target analytes (0 and 5 µg l⁻¹) were made on the MIP sensor at flow rate of 30 µl min⁻¹. The response units are calculated as the difference in response between two sequential data points in the sensorgram. Errors bars= ± SD, *n*= 2.

The values of % cross-reactivity are summarised and compared to anti-domoic acid monoclonal antibody performance in Table 6.4.

6.6 IMMUNOSENSOR FOR DOMOIC ACID BASED ON SPR SYSTEM

A real-time interaction analysis using the BIAcore 3000TM was carried using an anti-domoic acid monoclonal antibody, in order to evaluate its specificity for the target toxin and to compare the performance of the natural receptor with the MIP synthetic receptor.

6.6.1 Antibody Immobilisation by the BIAcore 3000™

Antibody immobilisation was performed on a standard carboxy-dextran matrix BIAcore gold chip (CM5 type) with a covalent reaction between N-ethyl-N'-(3-dimethylaminopropyl) carbodiimide hydrochloride (EDC) and N-hydroxysuccinimide (NHS) facilitating the immobilisation, according to the protocol described by Malmqvist (Malmqvist, 1999). A sensorgram, showing different concentrations of anti-domoic acid antibody immobilisation is shown in Figure 6.15. The value of the y-axis was calculated as the difference in response units from a control channel, with immobilised non-specific antibody present.

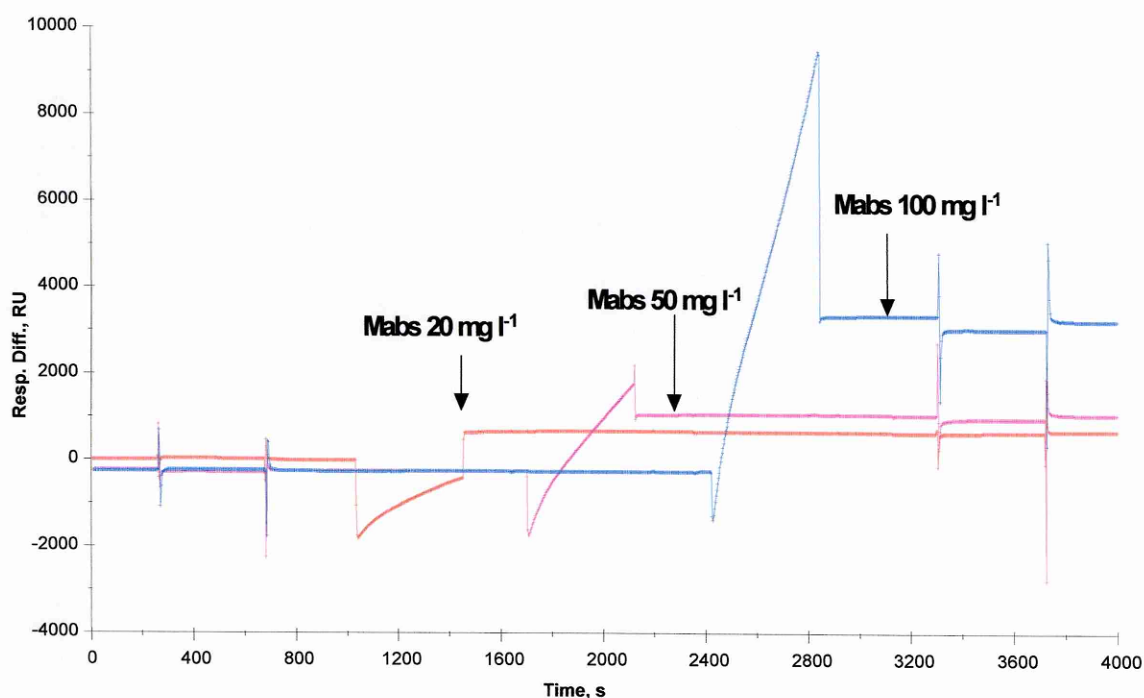


Figure 6.15: Sensorgram for the monoclonal antibody immobilisation.

Coupling reaction started with EDC-NHS activation and ended with ethanolamine blocking the residual activated sites. Anti-domoic acid antibody (20,50,100 mg l⁻¹). Abbreviations: Mabs= anti- DA monoclonal antibody.

After antibody immobilisation on the BIAcore chip surface, several injections of analyte and conjugate were tested, followed each time by a regeneration step of 10 μl 0.2 % SDS in 10 mM HCl at a flow rate of 5 $\mu\text{l min}^{-1}$. Unfortunately, the regeneration protocol lead to denaturation of the antibody and after three to five regeneration cycles the antibodies lost 80 % of their binding capacity. For this reason, immobilisation of the DA-HRP conjugate for the indirect competitive immuno-reaction was evaluated.

6.6.2 Optimisation of Conjugate HRP-DA Bound Format

To avoid the problem of regenerating the antibody bound to the sensor chip, an assay format with the bound conjugate DA-HRP was investigated. The conjugate (150 mg l^{-1}) was covalently immobilised to the dextran matrix and served as an affinity surface. Free protein ovalbumin was immobilised onto a separate channel and was used as a control surface. The anti-domoic acid antibody (6.6 $\mu\text{g ml}^{-1}$), together with different concentrations of free domoic acid, was injected in a volume of 35 μl and at a flow rate 5 $\mu\text{l min}^{-1}$. Figure 6.16 shows the sensorgram results from the competitive reaction between the immobilised DA-HRP conjugate and free analyte, binding to the antibody specific sites.

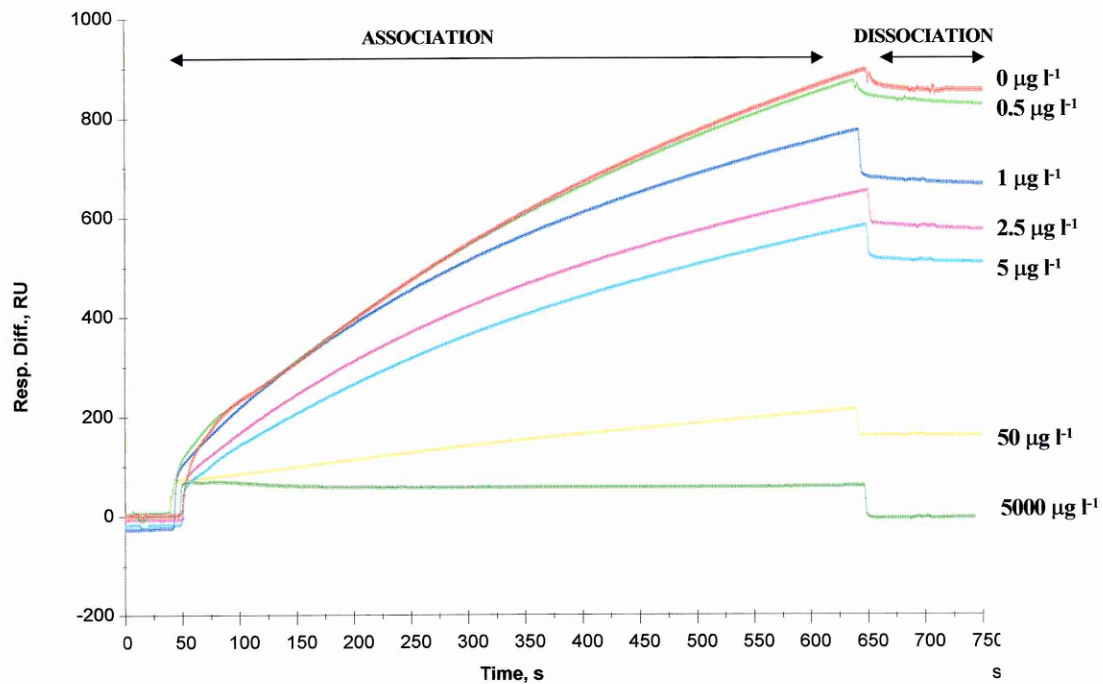


Figure 6.16: Sensorgram of the antibody-based sensor after the competitive reaction. A mixture (35 μl) of anti-domoic acid antibody ($6.6 \mu\text{g l}^{-1}$) and the target DA were added at different concentrations at a flow rate $5 \mu\text{l min}^{-1}$.

The injections were done in sequence in one single sensorgram but, to simplify the analysis, the injections were aligned to the same starting point by using the software BIAevaluation 3.2 from the BIAcore package.

From the above results, a typical sigmoidal calibration curve was obtained for anti-DA antibody over a range of concentrations between 0.5 and $5000 \mu\text{g l}^{-1}$ of domoic acid (Figure 6.17).

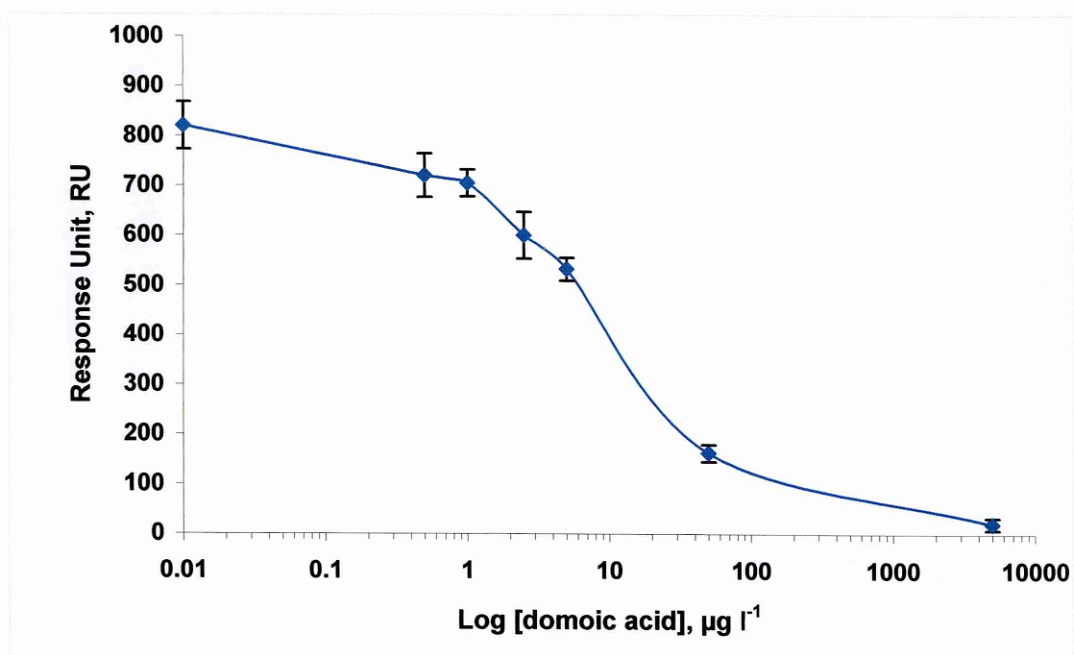


Figure 6.17: Calibration curve for anti-DA monoclonal antibody.

The curve was determined using the values of RU obtained in the sensorgram for different concentrations of domoic acid. Error bars = \pm SD, $n=2$.

From the sigmoidal curve the detection limit for the assay was determined as $LLD_{80} = 1.8 \mu\text{g l}^{-1}$ of DA and the affinity of the antibody measured as $EC_{50} = 10 \mu\text{g l}^{-1}$. The curve was reproducible, as indicated by the low standard deviations obtained and the mean % CV for the assay.

6.6.3 Cross-Reactivity for MIP and anti-Domoic Acid Antibody

The specificity of the anti-DA antibody for different compounds, which are similar in structure to domoic acid: including kainic acid (KA), aspartic acid (Asp), glutamic acid (Glu), was tested. As depicted in Figure 6.18, the monoclonal antibody could not be displaced by any of the DA analogues, used at the same concentration of $5 \mu\text{g l}^{-1}$.

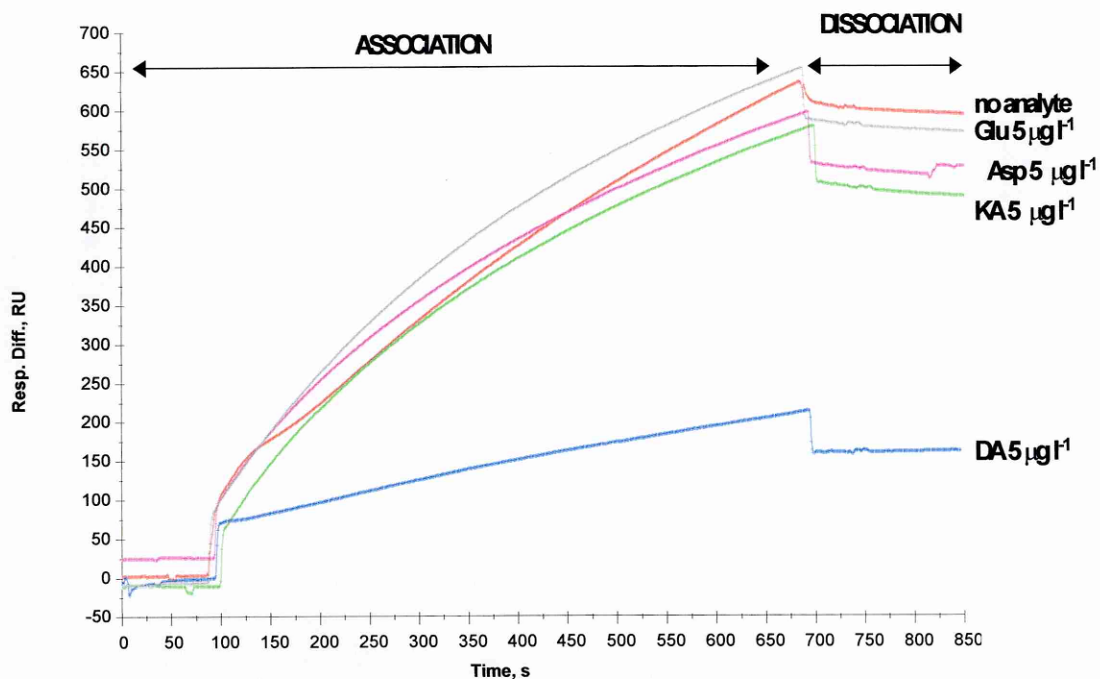


Figure 6.18: Sensorgram for cross-reactivity of domoic acid analogues. Competitive reactions were carried out on the conjugate-based sensor, adding anti-DA antibody ($6.6 \mu\text{g ml}^{-1}$) and $5 \mu\text{g l}^{-1}$ of either DA or all other analogues in different injections, separated each time by a regeneration steps. The volume injected was $35 \mu\text{l}$ at a flow rate of $5 \mu\text{l min}^{-1}$.

A summary of the two-receptor performances for DA detection is presented in Table 6.4.

Table 6.4: Comparison between MIP and monoclonal antibody specific for domoic acid.

RECEPTORS	EC ₅₀ ($\mu\text{g l}^{-1}$)	Range of detection ($\mu\text{g l}^{-1}$)	N ^o of regeneration before loss of stability	Cross reactivity (%)
MIP	48	5-3300	30 \pm 5	KA= 6.3 Glu= 8.0 Asp= 9.4
Monoclonal antibodies	9.2	0.4-60	5 \pm 1	KA= 4.1 Glu= 11.3 Asp =10.2
Abbreviations: KA= kainic acid; Glu= glutammic acid; Asp: Aspartic acid				

6.7 CONCLUSIONS

An enzyme-linked MIP competitive assay was developed using a specific MIP for domoic acid. A computational based MIP was designed specifically for the domoic acid molecule.

However, problems linked to the manual approach of the assay, together with the need to use a suspension of polymers led to the development of a fluorescence assay based on the “gate effect” event. Although the assay performance was acceptable, the equipment did not allow many tests to be conducted. A different approach, which allowed repetitive experiments over a short time, was investigated. This was based on a grafting technique that eliminated the need for bulk polymer synthesis. AFM was employed for the morphological study and the BIAcore 3000TM for studying the specificity of the grafted MIP for the target molecule. A detection limit of 5 $\mu\text{g l}^{-1}$ was achieved, though further optimisation should result in further improvements. Nevertheless, these assays demonstrated that the MIP had good potential in terms of reusability and stability, compared to the analogue antibody receptors. The physical and chemical resistance of

imprinted polymers together with the stability of their recognition properties and the low cost of preparation are all obvious advantages for imprinted polymers over natural antibodies receptors.

CHAPTER 7:

DISCUSSION

7.1 INTRODUCTION

The development of an immunosensor for microcystin-LR was carried out in stages to ensure that the final device demonstrated the desired characteristics and maximum sensitivity. A considerable portion of the experimental work was invested into developing the ELISA and determining the suitability of the antibody characteristics, since the antibody recognition component of the system was fundamental to the overall sensor performance. With this in mind, the IgG preparations were first established as a microtitre plate assay system and then transferred and developed to the required membrane format. The most suitable IgG reagent and assay was selected and progressed further to the immunosensor and amperometric transduction system. The characterisation of the immuno-reagents, assay development and investigation of the binding properties for both the polystyrene and membrane sorbents was conducted in microtitre format with colorimetric detection prior to the immunosensor development. This enabled the assay parameters to be investigated more efficiently.

Molecularly imprinted polymers (MIPs) were considered for this work as an alternative receptor, to be employed in assay and sensor applications instead of antibodies. The study focused on the characterization of different MIP compositions, based on either a new or a more 'classical' approach to the selection of monomers. Firstly, a MIP for MC-LR was investigated and a competitive enzyme-MIP assay applied to characterise the polymer. The performance of the MIP was compared to that of natural receptors, such as polyclonal and monoclonal antibodies. Secondly, a receptor based on molecular imprinting was considered for the toxin domoic acid and different approaches to producing and testing the polymer were undertaken. A bulk anti-domoic acid imprinted polymer was studied using a competitive enzyme-linked MIP assay, and then with a fluorimetric assay, based on the so-called "gate effect" phenomenon. Finally, a novel polymer film, selective for domoic acid, was developed using a grafting technique and characterised with atomic force microscope and surface plasmon resonance. These results were used for comparison with the anti-domoic acid monoclonal antibody assay findings.

7.2 EVALUATION OF ANTI-MICROCYSTIN-LR ANTIBODY

High affinity antibodies are important for most immunochemical techniques and are essential to an immunoassay's sensitivity. The BIAcore technology is an ideal system for the design and selection of immunological reagents, intended for use in an immunoassay system. With the BIAcore, a purification procedure is not always necessary and small amounts of the reactants are sufficient for full characterisation of the immuno-reagents, in a relatively short time compared to the conventional ELISA approach (Malmqvist, 1999).

For this work, it was necessary to determine the level of non-specific binding and cross-reactivity of the first batch of polyclonal anti-microcystin-LR antibody raised in rabbit (RA anti-MC-LR IgG), which were received from King's College London, to be employed in the immunosensor development.

Reinartz *et al.* (Reinartz *et al.*, 1996) reported on a study of a bi-specific multivalent antibody, using the BIAcore system. The conjugate BSA-hydroxycoumarin and BSA were immobilised on chip surfaces, at a concentration equivalent to about 10,000 RU. The bi-specific antibody samples (able to recognise both the target 7-hydroxycoumarin and alkaline phosphatase) were injected over the BSA-hydroxycoumarin and BSA coated surfaces, to determine the level of non-specific binding and cross-reactivity. It has been found that the bi-specific antibodies possessed cross-reactive binding to the BSA carrier protein. By a pre-incubation phase of the antibody samples with BSA, the cross-reactive binding of the BSA-specific antibody fraction has been successfully prevented.

A similar approach was investigated with RA anti-MC-LR antibody. Different concentrations of anti-MC-LR IgG were initially injected over a chip coated with the conjugate OVA-microcystin-LR, at an optimised concentration. This was used to determine the antibody titer and to evaluate both the concentration range and the affinity. For this experiment, the negative control was a channel onto which no ligand

was immobilised and the response from that channel was very low (<14 RU). Nevertheless, in order to describe the type and degree of specificity, it seemed to be more appropriate to use a control channel where OVA alone was coated, at the same concentration of the conjugate MC-LR-OVA. When the RA anti-MC-LR IgG (at a concentration of 50 mg l⁻¹) was injected over MC-LR-OVA and OVA coated surfaces, a high affinity to OVA was observed (300-800 RU). Pre-incubation of all the samples with OVA (1 mg ml⁻¹) was attempted, to prevent this cross-reactive binding of the OVA-specific antibody fraction to the MC-LR-OVA and OVA-coated surfaces. The pre-incubation step did not reduce specific binding but, on the contrary, it decreased the binding on both the MC-LR-OVA and OVA-coated surfaces, indicating a poor affinity for the RA IgG against the antigen microcystin-LR, and a high cross-reactivity with ovalbumin. For these reasons, no further experiments were carried out with these antibodies and they were not used for further immunoassay development.

7.3 COMPETITIVE ELISA ASSAY FOR MICROCYSTIN-LR DETECTION

The second polyclonal antibody preparation, raised in sheep against MC-LR (SH anti-MC-LR IgG), was directly screened, and selected for incorporation and development into an ELISA format. This reagent had been affinity purified specifically for MC-LR detection and provided with the appropriate antigen conjugate, designed in conjunction with the initial immunogen structure. The process of assay set-up and development was based on previous reports by Harlow and Lane (Harlow *et al.*, 1988) and Wild (Wild, 2001). These reports describe the antibody application and detail the various stages, problems encountered and suitable remedial action.

The sensitivity and specificity of the ELISA format, employing anti-MC-LR antibody, was first evaluated with the aid of checkerboard titration (Crowther, 2000). These experiments were carried out with plate-coated antigen (gelatin based). Results with anti-microcystin-LR antisera showed evidence that the antisera contained specific binding affinities with the adsorbed toxin-gelatin conjugate. The assay was optimised

using an indirect competitive format to determine the most suitable and sensitive combination of reagents for MC-LR detection. Results from control experiments, using unmodified gelatine, indicated an insignificant level of binding. The affinity of the antibody for the toxin-gelatin conjugate was high (low K_d value). With regard to competitive MC-LR detection, high affinity is important for reducing the assay detection limit (increasing sensitivity) and providing high reproducibility (Deshpande, 1996). Antibodies with a high affinity are able to bind more uniformly and rapidly, and form stronger antibody-antigen interactions (which therefore dissociate more slowly), resulting in higher complex stability and reproducibility. The initial binding event can occur within minutes, however, the strongest binding may not occur for several hours. In order to aid the mass diffusion from bulk solution to the solid phase in heterogeneous immunoassays, agitation is used to actively assist the equilibration dynamics. In addition the temperature should be elevated to physiological 37 °C, to increase the thermo-dynamics of the reaction (Deshpande, 1996). The importance of such parameters enables the speed and complexity of the assay to be reduced. Reaction incubations reduced in duration and simplified with regard to agitation and temperature may be sub-optimal in reaching binding equilibrium. The kinetics of anti-MC-LR antibody binding reaction was investigated with the aim of reducing the assay analysis time.

The results from these experiments showed that the assay response decreased with a decrease in coating duration, (by 30 % for a 15 minutes coating treatment), but increased with a reduction in blocking time (by up to 13 % with no blocking). Furthermore, the results demonstrated that an optimal coating required a minimum time of 30 minutes, even if only a small increase was observed when the time was prolonged for up to one hour. Shorter coating incubation time (15 minutes) showed the lowest signal for 1 hour blocking and highly variable results for shorter blocking, showing a % CV of 7.5 (calculated only with the value from 15 minutes coating incubation). Blocking gave almost an invariable response over a range of 15-60 minutes for 1 hour coating but showed different responses for 30 and 15 minutes coating incubation. Nevertheless, the standard deviation after 45 minutes blocking was the lowest. For all

the experiments, assays with no blocking steps were not reliable, showing a very high optical absorbance and high standard deviations. This study was important for determining the shortest time for incubation, leading to a rapid assay. Although there was a high potential for reducing the incubation time, the combination of 1 hour coating and 45 minutes blocking were selected and considered optimal for the immunoassay development during this work. With regard to the temperature and shaking parameters, it was important to maintain 37 °C during the 1-hour incubation in a water bath of the mixture of anti-MC-LR antibody and the toxin analyte. When the IgG and toxin mixture was added to the conjugate sorbent plate for the competitive reaction, it was observed that a gentle shaking was the preferred approach. The temperature was evaluated for the competitive reaction and little distinction between 37 °C and ambient temperature was discernible. The last step of the secondary antibody reaction was evaluated at room temperature and at 37° C, with or without shaking; the quiescent approach appeared to be more favourable for binding the secondary antibody to the primary specific antibody. Carrying out the assay at 37° C improved the reaction performance.

Using the indirect competitive format, the ELISA microcystin assay was able to detect 0.022 µg l⁻¹ (ppb) of microcystin-LR (with the lowest limit of detection set at the level determined at 80 % of the maximum response (LLD₈₀)), with a mean assay % CV of 3.5. The value of EC₅₀ (0.08 µg l⁻¹) showed a high affinity between antigen and antibody. This response met fully the requirements of the WHO, which has set a limit of 1 µg l⁻¹ for microcystin-LR in drinking water. Many different antibodies have been produced and used for assays and/or sensor development. The competitive ELISA demonstrated in this work had sensitivity in line with data published (Table 7.1).

Antibody specificity was also estimated by cross-reactivity measurements, i.e. to which extent an analogue compound might be recognised in the assay. The first sensitive ELISA kit described by Chu (Chu *et al.*, 1990) using polyclonal antibodies with high affinity to the microcystin-LR, has shown a high cross-reactivity with microcystin-RR and microcystin-YR variants, but less reactivity with variants microcystin-LY and microcystin-LA. An and Carmichael (An *et al.*, 1994) tested the cross-reactivity of a

laboratory-made kit using anti-microcystin-LR polyclonal antibodies with 18 microcystins and nodularin variants. They have found that the hydrophobic amino acid, 3-amino-9-methoxy-2, 6, 8-trimethyl-10-phenyl-4, 6-decadienoic acid (abbreviated Adda) was essential for these toxins to express antibody specificity.

Likewise, Nagata *et al.* (Nagata *et al.*, 1997) studied the cross-reactivity of six different monoclonal antibodies versus microcystin-LR together with many of its analogues. The six monoclonal antibodies showed a very similar pattern of competition against the panel of microcystins in the ELISA, with the exception of nodularin, thus suggesting that the epitopes recognized by the six antibodies were almost identical. The most notable feature of the reactive pattern, the less-pronounced reactivity to 6(Z)-MC-LR and 6(Z)-MC-RR, indicated the importance of the Adda structure for monoclonal antibody binding. In addition, replacement of the fourth amino acid adjacent to the Adda, arginine in MC-LR to alanine resulted in a slight decrease in reactivity. Thus, the arginine was associated with the antibody recognition, to some extent. In accordance with this idea, the antibody reacted well with nodularin, a cyclic pentapeptide toxin that also contains Adda and arginine in its ring.

The findings from this study are thus in line with the published data (Rivasseau *et al.*, 1999). The cross-reactivity of the anti-microcystin-LR antibody was estimated using microcystin-LR as the reference analyte (cross-reactivity= 100 %). Cross-reactivity was high with all the cyclic peptides considered, the values ranged from over 100 % to 50 %. High cross-reactivity was especially noted for microcystin-YR, whereas MC-LA and MC-LF revealed a minor decrease in affinity versus the anti-MC-LR IgG. Nodularin, despite the fact that is a pentapeptide, gave rise to a substantial level of cross reactivity. This suggested that such antisera could be used for rapid screening tests, to indicate the presence and the levels of these toxins, without specific reference to any particular peptide.

A summary of some of the most important receptors for microcystin-LR, their detection limits in different assays and their specificity versus the target is shown in Table 7.1.

Table 7.1: Developed of some receptors for microcystin-LR.

RECEPTORS (IMMUNOGEN/ TEMPLATE)	DETECTION LIMIT	CROSS REACTANTS	APPLICATION	YEAR OF PUBLICATION (REFERENCE)
Rabbit anti-MC-LR polyclonal antibody (MC-LR-EDA-BSA)	0.20 $\mu\text{g l}^{-1}$	MC-RR, MC-YR, NOD	Competitive ELISA	1990 (Chu <i>et al.</i> , 1990)
Rabbit anti-MC-LR polyclonal antibody (MC-LR-cBSA)	0.50 $\mu\text{g l}^{-1}$	None amongst 18 MCs and NOD	Competitive ELISA	1994 (An <i>et al.</i> , 1994)
Mouse anti-MC-LR monoclonal antibody (MC-LR-BSA)	0.02 $\mu\text{g l}^{-1}$	Major MCs derivatives	Competitive ELISA	1995 (Nagata <i>et al.</i> , 1995)
Antiserum anti MC-LR (immunogen unknow)	0.15 $\mu\text{g l}^{-1}$	MC-LA, MC-RR, MC-YR, NOD	Direct Competitive ELISA kit	1997 (EnviroGard kit)
Type 2A protein phosphatase	0.60 $\mu\text{g l}^{-1}$	MC-YR and MC-RR	Phosphatase inhibition assay	1999 (Rivasseau <i>et al.</i> , 1999)
Mouse polyclonal antisera (MC-LR/RR-PLL)	10 $\mu\text{g l}^{-1}$	MC-RR and NOD	Competitive inhibition ELISA	2000 (Baier <i>et al.</i> , 2000)
Rabbit polyclonal antisera (MC-LR-KLH)	0.50 $\mu\text{g l}^{-1}$	MC-LA, MC-LF, MC-LW, MC-D-Asp(3)-RR, MC-LY, NOD and MC-Asp(3)(Z)-Dhb(7)-HtyR	Competitive ELISA	2000 (Metcalf <i>et al.</i> , 2000)
Mouse monoclonal (MC-LR-SBTI)	0.10 $\mu\text{g l}^{-1}$	Major MCs	Time-resolved fluoroimmuno-metric assay	2001 (Mehto <i>et al.</i> , 2001)
Mouse monoclonal antibody (MC-LR-cOVA)	0.006 ng l^{-1}	All [4-arginine] MCs	Competitive ELISA	2001 (Zeck <i>et al.</i> , 2001)
MIP-based receptor	0.10 $\mu\text{g l}^{-1}$	None	MIP-base enzyme assay	2002 (Chianella <i>et al.</i> , 2002)
Sheep polyclonal antibody (MC-LR-gelatin)	0.02 $\mu\text{g l}^{-1}$	MC-YR, MC-LF, MC-LW NOD	Competitive ELISA	This work

When an immunoassay is applied to environmental analysis, the variation of the matrix may be considerable and it is always a point of concern (Zeck *et al.*, 2001). The matrix effect was studied by carrying out this work using either tap or river water samples, and comparing the standard calibration curves generated. Tap and river water appeared to increase binding throughout the calibration range studied, the graphs shifted to the right without any significant change in the graph slope. This indicated that the antibodies gave better bindings under these conditions, possibly due to the presence of calcium ions (and others salts). Similar experiments were performed with the primary antibody diluted in ELISA buffer, PBS, and river water. In this case, a minimal increase in the optical density was observed with higher antibody dilutions. This also provided valuable information as to the suitability of the antibody for the ultimate goal of using it in an immunosensor format for freshwater analysis.

Having a detection limit on ELISA format 45 times lower compared to the target concentration, it was possible to proceed further with enzyme immunoassay implementation to a sensor format. Initially, the EIA format was transferred to a membrane based ELISA (MELISA). Membrane support used for sensor device, is a commonly used strategy (Scheller *et al.*, 2001a) (Baskeyfield, 2001); the advantage being to have a homogeneous surface for the immuno-reagent immobilisation and not the surface of a working electrode such as graphite, which is not uniform and highly irreproducible.

7.4 AFFINITY MEMBRANE MELISA

The availability of commercial affinity membranes with highly uniform surface chemistries has led to an increased interest in their incorporation into immunosensor design; the advantages include improvements in the binding of reagents, homogeneity and reproducibility with consequential higher sensitivity. However, nitro-cellulose and nylon based membranes are prone to high variability and high background levels. The commercial pre-activated surface chemistry membranes were expected to offer high

homogeneity and therefore a high degree of reproducibility. Theegala (Theegala *et al.*, 2000) immobilised antibody on UltraBind™ membrane as well as Choi (Choi *et al.*, 1994) who evaluated UltraBind™ as the superior membrane product. The UltraBind™ immobilisation chemistry consists of highly reactive aldehyde groups on the membrane surface that bind to primary amines (Pemawansa *et al.*, 1990). The procedure is a fast and simple ‘spot or soak’ immobilisation that requires no pre-treatment or an additional reductant to stabilise the covalent linkages. The membranes are also highly stable and inert, especially to moisture.

The literature describes the use of affinity membranes for biocatalytic sensor development. However, they have not been used for environmental applications. No research combining commercial affinity membranes with screen-printed electrodes has been reported. Marquette (Marquette *et al.*, 1998) describes UltraBind™ 0.8 µm affinity membranes with fibre-optic transduction, utilising luminol/H₂O₂ electrochemiluminescence with flow injection analysis (FIA). The use of a 0.5 ml min⁻¹ flow rate enabled the measurement of choline, by a membrane-based ECL biosensor, in approximately 5 minutes with a detection limit of 75 pmol. Similarly, the same author (Marquette *et al.*, 2000b) immobilised cholesterol oxidase for cholesterol analysis. In comparison to Immunodynex and covalent polyamide (ABC type) membranes, UltraBind™ was reported to give a higher performance and sensitivity, with coefficients of variation lower than 8.5 %.

Another interesting application of membrane to immunosensor construction was described by Rabbany (Rabbany *et al.*, 2000). A compact membrane-based displacement immunoassay has been designed for rapid detection of explosive compounds. The system consisted of an activated porous membrane, onto which the anti-explosive antibodies were immobilised; this was inserted into micro-reactor columns, incorporated into a flow system.

During the course of this work, UltraBind™ 0.8 µm affinity membranes were applied to immunosensor analysis. Currently, no electrochemical immunosensors have been

described for microcystin-LR, or either the use of a disposable screen-printed electrode device. For this work, a 6 mm disc was chosen for the membrane dimension. This was an appropriate size to reduce limited reagent consumption, fit into microtitre wells for subsequent incubations and fit over the screen printed sensor working electrode.

Marquette *et al.* (Marquette *et al.*, 1999) investigated spot versus immersion soaking methods of immobilisation for the US-450 membrane and found that dip immersion immobilisation was more homogeneous and reproducible (7.7 % CV vs. 12 % CV). This, they suggested, was due to the hydrophobic nature of the membrane, which immersion was able to overcome by saturation into the matrix and not predominantly at the surface. This immobilization procedure was less than five minutes.

7.5 OPTIMISATION OF MEMBRANE COMPETITIVE ASSAY

The transfer of the ELISA for MC-LR to the MELISA format followed the same rationale as previously discussed. Similar problems were encountered; therefore it was necessary to optimise the assay. The most important aspect was the careful optimisation of membrane immobilisation and the blocking procedures, necessary to minimise non-specific background responses, to which membrane sorbents are prone. It was found that many of the ELISA parameters investigated were directly translatable to the membrane assay.

The effective MC-LR-gelatin conjugate reached coating saturation at 12 g l⁻¹. The antigen conjugate binding was determined as being efficient within 30 minutes coating time. Equally important as the coating efficiency was the use of a non-functional protein-blocking step to block any vacant solid phase binding sites; 5 % gelatin was found to be best blocker, although marginal response suppression was observed. Three coating concentrations were investigated, however their suitability for further development was compromised by a high non-specific signal. Coating reproducibility was very low (CV > 8), with steady background levels.

The comparison between different blocking agents on the membrane sorbent support showed that the blocking conditions improved by increasing the gelatin concentration from 0.5 % (used in the ELISA experiment) to 5 % (S/B from 1.6 to 2.9 respectively) and that other blocking agents did not give a better performance (S/B~2). However, the blocking step was necessary, since its absence did significantly increased the non-specific signal (S/B= 1.4). Nevertheless, for all cases the reproducibility was quite low with a mean % CV > 20.

Low molecular weight amine containing molecules, such as ethanolamine and glycine, were also investigated for their potential to penetrate and diffuse more readily into the porous membrane matrix, to give a higher blocking efficiency. Such low molecular weight molecules could reduce the overall membrane loading, for marginally higher diffusion over the electrodes. None at the 1 M concentration (even in combination with 5 % gelatin) were as successful as 5 % gelatin alone at reducing the non-specific binding, maintaining high signal (S/B ratio) and reproducibility.

Likewise, changes in the concentrations of the primary and secondary antibodies did not improve either the specific response or the reproducibility. It appeared that there was no relevant change in the MELISA performance since at all concentrations of primary antibody examined the absorbance maintained a similar value, whereas increasing the secondary antibody concentration to 1/10,000 gave an increase in all cases, including the control signal. Furthermore, the control membrane, on which no MC-LR conjugated was immobilised, did show a significant signal of approximately 0.3-0.4 in each case.

Rather than a high non-specific signal, the problem appeared to be related to a low specific signal, with the maximum optical absorbance signal no higher than 0.6 at the highest possible coating concentration of 12 g l⁻¹. This was probably due to the low efficiency of the coating agent microcystin-LR-gelatin. The carrier gelatin molecule does not present a high number of amino functions, thus it does not allow many covalent binding events with the sorbent pre-activated PES membranes. Moreover, as already observed during the blocking studies, a rather low reproducibility persisted in

the assay. This could be due to the extensive manual procedures employed throughout the assay e.g. several washes after each immuno-reaction. The need for incubation with a secondary antibody in this assay format also contributes to more intensive handling of the membranes, which may exacerbate the problem of assay variability.

Although the assay system developed operated fairly well, upon detailed characterisation the assay specificity and reproducibility were not considered acceptable for continued development and incorporation into the intended immunosensor device. Rather than optimising the indirect competitive assay further, or trying several alternative membranes and coating agents, the decision was taken to develop another ELISA where the antibody was immobilised directly onto the membrane. It was anticipated that this would be more suitable for membrane immobilisation in the subsequent development of the immunosensor, providing the desired capability and low non-specific signal.

7.6 ANTIBODY IMMOBILISED FORMAT FOR THE MELISA ASSAY

An enzyme immunoassay with anti-MC-LR antibody immobilised onto the sorbent surface was directly investigated and optimised, by immobilisation onto the UltraBind™ membrane. In this case, the assay required the use of the analyte conjugated to an enzyme label. To this aim, a commercial solution of the conjugate MC-LR-HRP was employed. This conjugate competed with free microcystin-LR toxin for binding sites on the immobilised specific antibody.

The titration of anti-MC-LR antibody revealed high degree of recognition and binding with the commercial MC-LR-HRP conjugate. This result demonstrated the suitability of using MC-LR IgG for MC-LR detection and provided a firm basis for the continued development to transfer the assay to a membrane sorbent, for the immunosensor format.

The MELISA was once again optimised with colorimetric detection, in order to reduce the variable parameters sometimes encountered when electrochemical detection is used, thus simplifying and hastening the development and optimisation process. Also, the minimum amount of toxin detectable was $0.06 \mu\text{g l}^{-1}$, hence the EIA format presented ideal condition for developing an electrochemical-based sensor. Moreover, this format enabled the membrane assay to be simplified, reducing the assay time to 1 hour, through the removal of the secondary labelled antibody incubation.

These reductions in the assay protocol led to a highly reproducible response with a CV of between 3-4 % to be achieved. With an asymptotic maximum of above 1.0 OD, enabling a sufficient graph slope for discriminating between individual MC-LR concentrations. The enhanced assay protocol required no mechanical agitation and only ambient temperature incubation, making this assay more suitable for rapid laboratory and decentralised 'on-site' monitoring and pre-screening applications.

Further optimisations lead to a stable immunosorbent. Three washes, after each reaction were sufficient, to remove loose and unbound antibody. The use of a saline based (PBS) washing buffer, with 0.05 % Tween 20 non-ionic detergent (PBST) to further increase the stringency, ensured that only interactions of specific affinity occurred. The conjugate buffer included 0.5 % gelatin blocking agent, helping to prevent non-specific interactions. Rather than using sodium azide as a preservative and fungicide for the antibody solutions and buffers, 0.01 % thimerosal was selected. This does not inhibit the HRP enzyme. Jenkins (Jenkins *et al.*, 1988) demonstrated that a 96 % reduction in problematic non-specific binding reactions by using 0.5 % Tween 20 and 1 % BSA in the washing and conjugate buffers.

Due to the commercial nature of the conjugate MC-LR-HRP obtained from the microcystin ELISA kit, details of the conjugation composition and method were not disclosed. Some other stabilising proteins were certainly present in the commercial conjugate solution and this led to high value for the concentration level detected by the BCA test.

HRP is an enzyme with a high turnover rate, which does not require co-factors, relatively small molecular weight (44,000 Daltons) and proven amenability to amperometric detection for immunosensor applications. The smaller molecular weight than other enzyme such as alkaline phosphatase would also aid diffusion rates particularly in the final immunosensor format. Enzyme labels have been compared by Portsmann (Portsmann *et al.*, 1985).

7.7 IMMUNOSENSOR DEVELOPMENT

The rationale for attempting to combine the fields of immunology and electrochemistry, in the design of analytical devices, is that such systems should be sensitive due to the characteristics of the electrochemical detector, whilst exhibiting the specificity inherent in the antigen-antibody interaction (Cass, 1990). Also, because electrochemistry is an interfacial (rather than a bulk solution) phenomenon, electrochemical detection can be successfully used in coloured or turbid samples that would otherwise cause interference for optical based system.

Reaction products from alkaline phosphatase (AP) and horseradish peroxidase (HRP) enzyme labels have been detected electrochemically, mostly for the development of semi-automated flow-injection analysis systems (FIA), affording faster and more reproducible sample analysis. Often the reproducibility obtained with manual immunoassay methods is determined by the technical skill of the operator. Automated FIA provides standardised reagent delivery and does not give inter-operator variation. AP catalyses substrates such as phenyl phosphate or *p*-aminophenyl phosphate, the product phenol of *p*-aminophenol can be detected electrochemically. The enzyme catalyses the hydrolysis of phosphate esters to give inorganic phosphate and a phenolic group. For the AP label, *p*-aminophenyl phosphate substrate has been determined as the optimum substrate for amperometric detection (Tang *et al.*, 1988). Electrochemical EIAs using AP have been reported by Gill (Gill *et al.*, 1990) detecting *p*-aminophenyl phosphate, Yao (Yao *et al.*, 1993) using 2,6-dichloroindophenol and Vianello (Vianello

et al., 1998) with *p*-hydroquinone. Thompson (Thompson *et al.*, 1991) compared amperometric and spectrophotometric detection methods for several AP substrates.

Many examples of familiar chromogenic substrates for HRP have also been employed for electrochemical detection. Jiao (Jiao *et al.*, 1998) reported the use of *o*-dianisidine for quantification of an ELISA for tobacco mosaic virus. Whereas Zhang (Zhang *et al.*, 1999) demonstrated the detection of ferritin in human serum by the reduction of *m*-aminophenol. Sun (Sun *et al.*, 2001) utilised the electrochemical reduction of *p*-aminophenol for the HRP label for a cucumber mosaic virus ELISA. This resulted in a 10-fold increase in sensitivity, compared to an OPD colorimetric assay. He (He *et al.*, 1997) reported the use of TMB substrate, in addition to the study and incorporation into a FIA system by Volpe (Volpe *et al.*, 1998), and the application of TMB as a mediator by Compagnone (Compagnone *et al.*, 1998). The mechanism of mediated electron transfer for horseradish peroxidase (HRP) and a hydroquinone mediator (Saurina *et al.*, 1999) is represented diagrammatically in Figure 7.1.

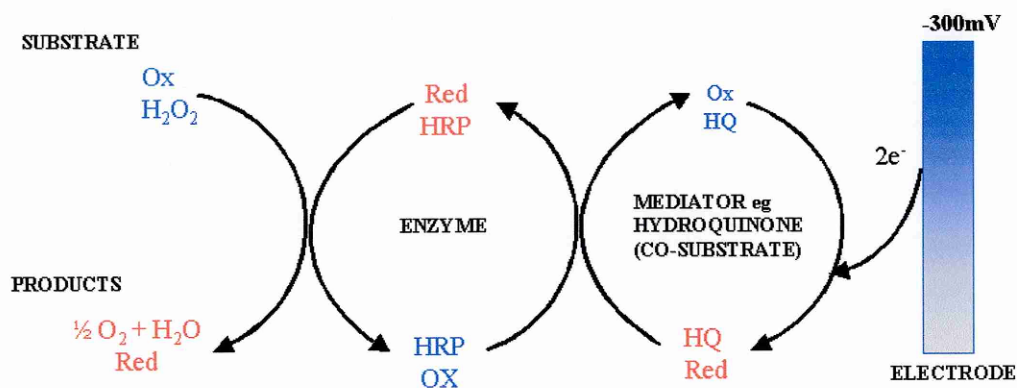


Figure 7.1: Mediated fast electron transfer for the enzyme horseradishperoxidase.

With the addition of the enzyme, the mediator is reduced at the electrode. The HRP reaction (first oxidised by H_2O_2) is actually a two step process, requiring two–electron reductions by the hydroquinone hydrogen donor (acting analogous to substrate chromogens) before HRP returns to its native reduced state (Deshpande, 1996). The

hydroquinone then generates a current by drawing equal electrons from the working electrode in turn for its own reduction from benzoquinone back to hydroquinone (Cass, 1990).

Another largely used mediator in electrochemistry is ferrocene. The application of ferrocene-modified n-type silicon electrodes to the anaerobic redox catalysis of glucose oxidase was described by Dick (Dicks *et al.*, 1993). The electrodes were modified with ferrocene either directly, by using (1,1'-ferrocenediyl) dichlorosilane, or via an underlying polypyrrole film and a glucose-sensitive electrode was made by simple adsorption of glucose oxidase from an aqueous buffered solution into the surface film.

Another alternative to hydroquinone is potassium iodide linked to an iodine redox system. Žeravík (Zeravik *et al.*, 1999) reported that using potassium iodide was three times more sensitive than hydroquinone, when compared to their previous work with the hydroquinone mechanism, discussed above (Kaláb *et al.*, 1995). A further benefit from using the potassium iodide mediator was a low reducing working potential (of between -50 to -100 mV). However, it has been reported by Volpe (Volpe *et al.*, 1998) that the colorimetric substrate TMB used electrochemically resulted in the substrate of optimum sensitivity for HRP transduction. The authors made a comparison between TMB and hydroquinone. The activity data for hydroquinone was similar to that presented in Section 4.4.2, and they reported a hydroquinone reduction potential of -250 mV versus Ag/AgCl.

Sensors and biosensors in particular are revolutionising modern analysis, generally because of their speed and simplicity. The production of electrochemical sensors can be done at a low cost production technologies developed by the electronic industries, such as thin- or thick film technologies (Bilitewski *et al.*, 1992). That is why screen-printed electrodes have found a widespread application when in combination with enzyme reactions.

Zhang (Zhang *et al.*, 2000) has recently reviewed current materials and techniques for electrochemical biosensor electrode design and construction. Screen-printing enables the controlled application of inks in several layers. The design, ink property and order that they are applied results in small, highly reproducible conductive electrodes. The techniques also afford the possibility for the controlled deposition of reagents to the electrodes, which can be applied separately or incorporated into the ink. For electrochemical biosensors, a three-electrode system is normally used, comprising a working, reference and counter (auxiliary) electrode. By applying a constant potential between the working and the reference electrode, the desired redox reaction, in which the analyte of choice is involved, gives rise to a current proportional to its concentration. The current is measured between the working and counter electrodes.

There have been repeated references to the fact that the direct electron transfer from an enzyme to an electrode is a major problem. The difficulty may be due to the location of the electroactive center deep within an enzyme's structure, or it may be due to electrode surface effects related to adsorption and orientation of the macromolecule. Several chemical approaches for effecting the electron transfer have been considered and investigated e.g., immobilising mediating molecules to facilitate electron transfer, or by covalently binding mediators to the enzyme or electrodes (Cass, 1990; Turner, 1998). Mediators are also important for circumventing the oxygen-depletion effects on oxidoreductase-based sensors, by becoming a surrogate co-substrate for oxidase.

The interface between the screen-printed electrode (SPE) (or other transducer) and the immuno-chemical recognition element has been investigated in a number of ways. The quality and integrity of the interface directly governs the sensitivity and reproducibility of the resultant sensor. For disposable SPEs, the immuno-reagent can be immobilised directly on the electrode surface. This can be achieved simply by passive adsorption of the antibody (Wang *et al.*, 1998b) or antigen, as described by Kröger (Kröger, 1998) for 2,4-D analysis in soil with carbon SPEs. Kröger (Kröger *et al.*, 1998) tried to reduce background responses and improve the reproducibility unsuccessfully by entrapment of the antigen conjugate in polymeric membranes such as cellulose acetate, polyvinyl

alcohol, and nafion. Nafion has been applied more successfully by Kaláb (Kalab *et al.*, 1997) for antibody entrapment over a gold disposable SPE, detecting of $< 0.01 \mu\text{g l}^{-1}$ 2,4-D using an acetylcholinesterase label.

Other direct immobilisation procedures involve covalent linkages to free amino groups, formed by silanisation techniques using 3-aminopropyltriethoxysilane (Kaláb *et al.*, 1995) or from self-assembled monolayers of cysteamine (Zeravik *et al.*, 1999), both upon gold SPEs. The biotin/streptavidin system has also been reported for flow-through atrazine analysis using a biotinylated carbon SPE with hydroquinone HRP mediator/substrate (Romero *et al.*, 1998). Alternatively, a sol-gel layer incorporating biomolecules has been printed directly onto a carbon SPE, as reported by Wang (Wang *et al.*, 1998a). A novel method described by Júlicher (Julicher *et al.*, 1998) enabled enzymatic *in situ* protein-antigen conjugation and immobilization on carbon SPEs, catalysed by transglutaminase.

In developing a disposable screen-printed immunosensor for 2,4-D, Kabál (Kaláb *et al.*, 1995) covalently immobilized the antigen to nylon net membrane discs placed onto a SPE within a formed microwell, utilizing the HRP label and H_2O_2 /hydroquinone mediator system. They reported a highly variable signal possibly due to the low homogeneity of the immobilized antigen and variation of contact with the electrode. Further studies with the same system in a disposable multichannel format (Skladal *et al.*, 1995) entailed adsorbing the monoclonal antibody directly onto the nitrocellulose membrane. After blocking with BSA, the rest of the immunoreaction was carried out in the microwell. Improved reproducibility ($\sim 10\%$ CV) was gained over the nylon net sensor, with $0.1 \mu\text{g l}^{-1}$ detected in under an hour. The system employed 6 mM hydroquinone and 2 mM H_2O_2 at -100 mV , compared to the 1 mM and 0.1 mM respectively at -300 mV potential used in this work.

7.8 ELECTROCHEMICAL SUBSTRATE DETECTION

The aim of the membrane immunoassay development was to incorporate the MELISA into a disposable immunosensor device, where inversely proportional competitive signal transduction could be achieved amperometrically via a mediator such as hydroquinone. A mediated system was chosen due to the reported increase in sensitivity, compared to monitoring the peroxidase substrate concentration (Saurina *et al.*, 1999) and also the low reducing potential that this application required. This helps to minimise the background response from electroactive interferences (Santandreu *et al.*, 1999). In addition to acting as a mediator, hydroquinone was also the co-substrate and hydrogen donor for the HRP enzyme. The redox equation for hydroquinone is shown in Figure 7.2. The immunosensor development required the successful intimate combination of the membrane assay with the screen-printed electrode, in addition to the optimisation of the mediated transduction system. At all stages, the emphasis was to maintain the reproducibility and sensitivity that had been achieved in the colorimetric MELISA (% CV= 4.4), thus minimising the effects upon the assay variation that the immunosensor format incurred.

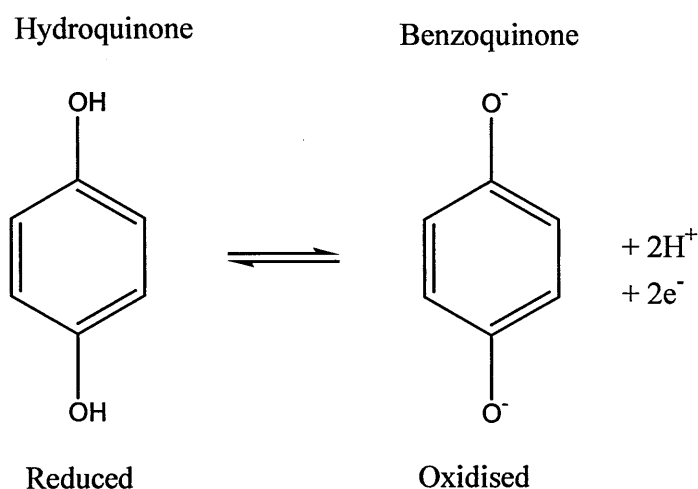


Figure 7.2: Redox reaction of hydroquinone.

The cyclic voltammogram of hydroquinone with glassy carbon working-electrode showed distinct peaks of redox activity. Although the main reduction peak was at -140 mV, when the screen-printed electrodes were tested by cyclic voltammetry and amperometrically at different potentials for HRP activity, the reduction peak was less distinct. Evaluation of the results showed that the highest response was obtained at -300 mV. The carbon working electrode dynamics and characteristics resulted in a different response with less pronounced redox detail. This was due to the more heterogeneous nature of the screen-printed carbon surface and structure, containing constituents such as polymeric binders, present in the printing inks. At potentials above -300 mV, the reduction current from the peroxidase substrate increased and reduced the specific HRP catalysed signal. Optimisation of the mediated transduction system determined an effective concentration of 1 mM hydroquinone in combination with 0.5 mM H_2O_2 to give a maximum response, with high stability/reproducibility and without causing peroxide substrate inhibition. However, Volpe (Volpe *et al.*, 1998) found that 10 mM hydroquinone was the optimum concentration with $1:1$ molar ration of H_2O_2 owing to the spontaneous reaction of the substrates.

In the competitive MELISA format, the immunosensor produced a similar response profile to the colorimetric MELISA. This demonstrated that mediated amperometric transduction was reliably representative of the bound immuno-complex, comparable in sensitivity to the colorimetric response, achieving an LLD_{80} of $0.5 \mu g l^{-1}$, in comparison to $0.06 \mu g l^{-1}$ for the MELISA. The immunosensor, therefore, gave a 10-fold lower sensitivity than the MELISA format. The optimum antibody dilution was $1/1000$, from the stock purified antisera, and a maximum response above 900 nA; the mean % CV was < 6 %. The US-800 membrane was sufficiently porous and intimately associated to enable good diffusion of the substrate and hydroquinone, between the enzyme and the electrode. The immunosensors developed by Marquette *et al.* (Marquette *et al.*, 1999) and Marquette and Blum (Marquette *et al.*, 2000a) using UltraBindTM for okaidic acid and 2,4-D respectively, had a reproducibility similar to that achieved with the microcystin-LR immunosensor.

Subsequently, the substrate hydrogen peroxide and the electron donor 2,2'-azino-bis (3-ethylbenz-thiazoline-6-sulfonic acid (ABTS) were investigated for amperometric measurements. The same substrate solution was used in this work for the colorimetric detection of HRP activity, in the microcystin-LR ELISA assay. The substrate ABTS is known to be of primary choice for chromogenic enzyme immunoassays (Portsmann, 1981; Portsmann *et al.*, 1985), however with regard to its application for electrochemical detection, there are few reports. In the presence of hydrogen peroxide, the peroxidase enzymes catalyses the dehydrogenation of ABTS, resulting in the formation of a resonance-stabilised radical cation of ABTS. The green-blue colour formed, recorded at 450 nm, is taken as a measure of the peroxidase activity (Holm, 1995). The redox chemistry of ABTS is illustrated in Figure 7.3. Two molecules of ABTS react with one of H_2O_2 giving two molecules of the radical cation.

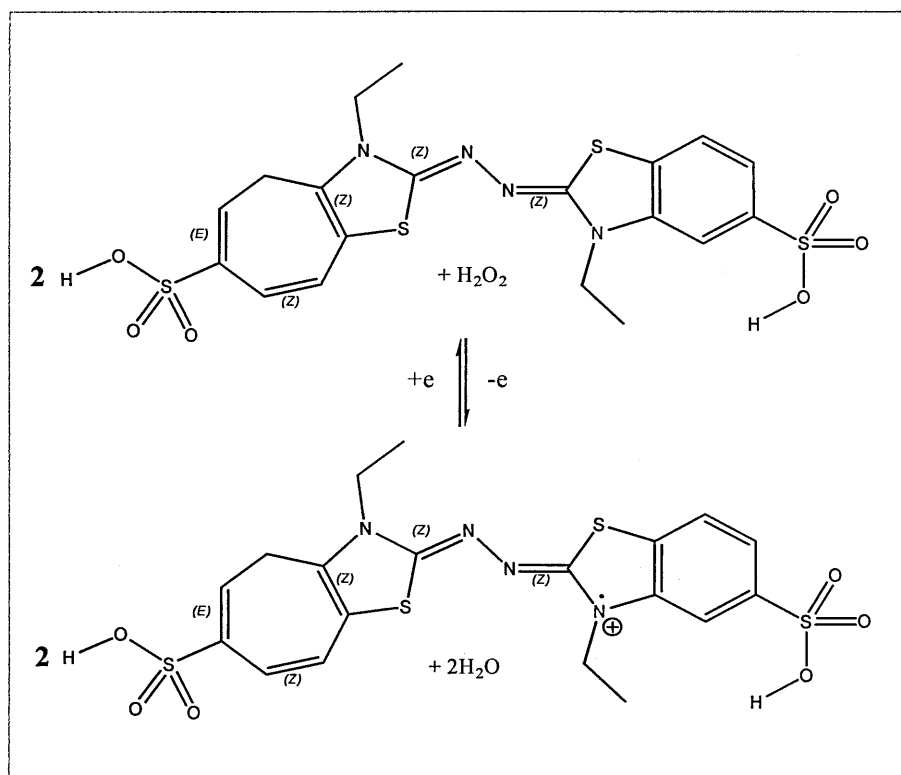


Figure 7.3: Redox reaction for ABTS.

When the ABTS substrate was used to determine the immunocomplex bound to the sensor device, a detection limit comparable to that of HQ/H₂O₂ electrochemical detection system was obtained. The lowest detection limit calculated was at 80 % of the maximum response: 0.7 µg l⁻¹ and the mean % CV for the assay was 16. Due to the non-optimised nature of the FIA colorimetric MELISA development, the degree of mean variation was high. However, further optimisation of the membrane immobilisation and binding durations/conditions, non-specific binding and fluidics/flow rates should improve this reproducibility.

Using ABTS proved convenient, since this substrate was equally used for spectrophotometric detection and thus allowed a better comparison between the immunosensor and immunoassay devices. Furthermore, the hydroquinone showed problems of stability and a fresh solution needed to be made every hour, because of its tendency to auto-oxidise and interfere with the results. ABTS was used for a full day of experiments with no problem of stability, when kept protected from the light.

The microcystin-LR MELISA was developed into a preliminary FIA assay with amperometric detection of the ABTS substrate. This was with a view to a semi-automated, faster, and more reproducible system; in contrast to the previously described disposable immunosensor. The flow-through property of the porous UltraBindTM US-800 membrane was amenable to FIA. A good sensitivity was achieved using the on-line immunoassay since the LLD₈₀ was 0.1 µg l⁻¹, which is higher than the detection limit obtained with the same colorimetric competitive MELISA made off-line. The main problem was the high value of the mean % CV (16) and the high standard deviations, which indicated a poor reproducibility for the experiment. However, the system could be largely improved and optimised by investigating different conditions for immunoreactions e.g. different volumes and time of flow of the immunoreagents, but lack of time prevented any further optimisation.

The amperometric FIA MELISA system was briefly investigated and a high correlation between the amperometric response and the microcystin-LR concentration was

observed. The potential for developing the system with a capacity of over 30 regeneration cycles and high reproducibility, may also be possible: according to Marquette (Marquette *et al.*, 1999) (Marquette *et al.*, 2000a) using antigen immobilised UltraBind™ for okaidic acid and 2,4-D immunosensor, respectively. The authors gained antibody dissociation and membrane regeneration by flowing either a 0.1 M glycine pH 2 solutions or a chaotropic solution composed of 0.1 M HCl, 0.1 M glycine and 0.1 M NaCl over it.

7.9 MOLECULAR IMPRINTING FOR MICROCYSTIN-LR

At present, the majority of reports on molecularly imprinted polymers (MIPs) describe organic polymers synthesised by radical polymerisation of the functional and cross-linking monomers, typically involving vinyl or acrylic groups and using non-covalent interactions. This can be attributed to the straightforward synthesis of these materials and to the vast choice of available monomers which can be basic (e.g. vinylpyridine) or acidic (e.g. methacrylic acid), permanently charged (e.g. *N,N,N*-trimethylamino ethylmethacrylate), available for hydrogen bonding (e.g. acrylamide) and other reactive groups. These 'simple' monomers normally have association constants with the template that are too low to form a stable complex. Thus, they have to be used in excess to shift the equilibrium towards complex formation (Haupt, 2001).

Methacrylic acid (MAA) was used for this work, as a functional monomer for imprinting the template microcystin-LR. The carboxylic group of MAA functioned as both a hydrogen bond donor and an acceptor, to form simultaneous double hydrogen bonds with the template. Such hydrogen bonding is expected to be favourable in terms of entropy, for formation of the binding sites in the imprinting process. The ratio between monomer and template was 10:1, as it is traditionally used for non-covalent imprinting for relatively large molecules (Rachkov *et al.*, 2000). The cross-linker was maintained at very high concentration, compared to the monomers, to guarantee a rigid polymer structure.

Over the last decade, thermodynamic calculations and combinatorial screening approaches have been successfully used to identify the best monomer candidates for imprinting (Takeuchi *et al.*, 1999). This approach becomes difficult with the increasing size of the monomer library, which can include thousands of polymerizable compounds. One possible solution to this problem is by the use of molecular modeling software and searching algorithms traditionally applied to drug design, recently adopted for the design of affinity polymers (Piletsky *et al.*, 2001).

An imprinted polymer designed using a computer modeling software (CM-MIP), and subsequently synthesised, for the target microcystin-LR was used for comparison study versus a classic imprinted polymer, obtained with MAA monomers (MAA-MIP). An elemental analysis (BET analysis) was performed to ensure that both CM-MIP and MAA-MIP had a similar surface area and total pore volume. This confirmed that the physical characteristics were not the cause of the different behaviour from the two imprinted polymers for microcystin-LR. Therefore, their performance could be attributed exclusively to the composition of monomers selected for polymerisation and thus their capacity for interacting with the template.

Since MIPs share with antibodies one of their most important features, the ability to bind a target molecule selectively, they could conceivably be employed in an immunoassay-type binding assay in place of antibodies. This was first demonstrated by Mosbach's group who developed a molecularly imprinted sorbent assay (MIA) based on competitive radio-ligand binding protocols. This work, not only showed a very good correlation with antibody-based enzyme immunoassays, but also demonstrated a cross-reactivity profile very similar to those reported for natural receptors (Vlatakis *et al.*, 1993). Imprinted polymer based assays are most conveniently performed using radiolabels, because the labelled analyte has the same structure as the original template. However, this involves the handling of radioactive materials and produces radioactive waste.

More recently alternative assay formats, that avoid the use of radio-labels, have been reported. A competitive fluorescence immunoassay has been proposed that uses a fluorescence probe for detection. The assay was specific for the herbicide 2,4-dichlorophenoxyacetic acid. Although the probe, a coumarin derivative, was unrelated to the analyte, it had some structural similarity with it. The specificity and sensitivity of the assay were on a par with a radio-ligand displacement assay, using the same molecularly imprinted polymer and radiolabelled 2,4- dichlorophenoxyacetic acid (Haupt *et al.*, 1998a).

MIP-based ELISA type assays have been developed in which the analyte was labelled with an enzyme such as peroxidase. Since enzyme labels are rather bulky compared with the small analyte, particular approaches have to be used to permit the analyte-enzyme conjugate to access the binding sites in the MIP. For a competitive reaction, the polymer suspension was incubated in the presence of a mixture of a conjugate HRP-MC-LR in a defined concentration and over a range of free microcystin-LR concentrations. By adopting a filtration system, the mixture free/ HRP conjugate toxins was passed through the polymer and filtrated into a clean microtiter plate. From the filtrate solution, it was possible to measure the activity of the HRP enzyme still in solution, which was directly proportional to the free toxin concentration. This is explained by assuming that for a higher concentration of the toxin, a higher number of the polymer binding sites is occupied. Consequently, a larger amount of HRP-MC-LR conjugate was passed in the filtrated solution and measured by optical absorbance. The optimisation of this competitive enzyme assay protocol for microcystin-LR allowed the characterisation of the MAA-MIP receptor. The limit of detection obtained for the toxin microcystin-LR was approximately $1 \mu\text{g l}^{-1}$, thus it was comparable to the sensitivity value reported for natural receptors employed in other assays.

A number of publications cover the problems found when using receptors for molecular recognition systems. Nevertheless, not many research groups have reported on tests for evaluating the different performance criteria for natural and artificial receptors, for the same target molecule. To this aim, the performance of polyclonal and monoclonal as

well as two different MIP artificial receptors was studied. The sensitivity range of polyclonal and monoclonal antibodies was, in all cases, narrower than for the polymeric imprinted receptors. This might indicate that the antibodies have a smaller distribution of binding sites, when compared to polymers. Regarding the limit of detection, polyclonal and monoclonal antibody were able to detect as low as $0.05 \mu\text{g l}^{-1}$ and $0.025 \mu\text{g l}^{-1}$ of MC-LR, respectively, whereas the MAA-MIP had limit of detection twenty times higher than that of the anti-MC-LR polyclonal antibody ($1 \mu\text{g l}^{-1}$). Significant improvements regarding the limit of detection and the affinity for MIPs has been achieved using a computationally designed MIP. In this case, the limit of detection ($0.1 \mu\text{g l}^{-1}$) was twice the value of the anti-MC-LR polyclonal antibody and four times that of anti-MC-LR monoclonal antibody. Likewise, the affinity, expressed in EC_{50} , was significantly improved with the computational MIP, compared to the traditional MIP (3.2 versus 0.65). It was believed that the computationally designed polymer gave a stronger interaction, to form more stable template-functional monomers adducts for the polymerisation, which lead to an enhancement of the imprinting effect and a better affinity for the target molecule. It has been reported that polymers designed using a computational approach, very often, have affinity and specificity, which match those of natural receptors (Piletsky *et al.*, 2001).

Both of the imprinted polymers, developed during this work, showed relatively low cross-reactivity for any of the microcystin-LR analogues; in contrast to the polyclonal and monoclonal antibodies used. The antibodies showed high cross-reactivity with all the microcystins and nodularin, although the monoclonal antibody could discriminate between MC-LR and different toxins, such as nodularin and microcystin-YR. Depending of the final application of those receptors, negligible cross-reaction can be considered either an advantage or a disadvantage. The capacity for recognising large numbers of microcystin toxins could be very useful for the *in situ* monitoring of toxins in water samples. However, they would be unsuitable for the identification of one specific component of the same family. The result of the high specificity of MIPs, shown here are in agreement with other polymeric systems previously studied (Haupt *et al.*, 1998b). Hence MIPs are finding large applications for many demanding separation

processes, e.g. purification of enantiomers. More and more the characteristics of MIPs will be applied to assays or sensors for the detection of specific targets.

A range of stability tests was performed with both the natural and synthetic receptors. The results achieved were quite predictable, mainly concerning the loss of activity of the antibodies under the harsh conditions considered. Nevertheless, it was illuminating to see how the antibodies could maintain a relatively good functionality, after two hours of either acidic or basic conditions. More damaging was incubation at very high temperatures where the monoclonal and polyclonal antibodies lost more than 85 % of their activity, and in the presence of CuSO_4 (10 mM) where the loss was about 80 % for both antibodies.

Although the computationally designed MIP and MAA-MIP both showed an excellent stability in acidic and basic conditions, their performance at high temperature and in the presence of heavy metals was markedly different. Unlike MAA-MIP, the affinity for the computationally designed MIP decreased by almost 50 % after two hours of heating in water at 80 °C and after exposure to heavy metals. The increased sensitivity towards high temperatures could be explained by the ability of the acid monomer 2-acrylamido-2-methyl-1-propane sulfonic acid (AMPSA) to catalyse the hydrolysis of the polymer through its groups SO_3^- . The results from an elemental analysis of the polymer before and after treatment confirmed that a possible hydrolysis has occurred. In fact, a significant decline in sulphur content (by up to 50 %) was observed following treatment in boiling water. The 'classic' MAA polymer was made using only methacrylic acid as the monomer, which is known for being very stable. Thus, the activity of this polymer was almost constant following treatment.

The high sensitivity of the computationally designed MIP towards heavy metals might be explained by the ability of the imidazole ring of urocanic acid ethyl ester (UAEE) to form a strong complex with transition metals. One conclusion from this stability study was that further progress towards a more successful mimicking of natural receptors could improve some characteristics (such as affinity and specificity), but would likely

decrease other features such as polymer stability. This study evidenced how the increasing complication of the polymer structure can lead to a decrease in its stability.

Although the high specificity and stability of MIPs makes them promising alternatives to the enzymes, antibodies, and natural receptors used in sensor technology (Piletsky *et al.*, 1998), there are still limitations associated with the development of MIP sensors. For example, the absence of a general procedure for MIP preparation, the difficulty in transforming the binding event into a detectable signal and also the problems found in their performance in aqueous solution.

7.10 MOLECULAR IMPRINTING FOR DOMOIC ACID

The MIP for domoic acid was initially studied with a similar approach to that described for microcystin-LR in the previous section. In fact, this work showed the attempt of using the computational approach in the synthesis of an imprinted polymer specific for domoic acid, similarly as it has been previously done for microcystin-LR. In particular, the process included the selection by computer modeling of monomers able to form strong complexes with the template (Subrahmanyam *et al.*, 2001). The modeling of monomer-template interaction was performed using commercial software traditionally applied to drug design using combinatorial synthesis. A virtual library of functional monomers was created rather than using e.g. amino acids. The monomers included in the virtual library contained a broad variety of functionalities, capable of forming ionic bonds, hydrogen bonds, and van der Waals interactions with the template. From the Leapfrog results, the top three monomers interacting with the template were: allylamine, acrylamide and urocanic acid.

The presence of solvent and cross-linker influenced the binding between monomers and template. This effect was briefly evaluated by comparing the total energy (E_T) of the monomers-template complex, obtained by computer modeling, without and with the cross-linker (EGDMA) and the solvent (DMSO). The calculated total energy (E_T) of the

monomers-template complex was comparable to that in the presence of saturated quantities of cross-linker molecules, showing small disruption of the complex. The modeling result indicates that the complexation between the selected monomer and template is strong even in polar environment, which is important for successful imprinting of a water-soluble template such as domoic acid.

The computationally designed MIP was then tested for its affinity for the target toxin by using enzyme-linked competitive assay with a conjugate of the toxin to the enzyme HRP, supplied by Prof. Hock (Munich, Germany). The concentration of the conjugate was optimized for the use of a MIP as the affinity receptor. In the case of domoic acid, the lowest detection limit was approximately $1 \mu\text{g l}^{-1}$, over a working range of sensitivity between 1 and $10 \mu\text{g l}^{-1}$: the EC_{50} was calculated as $1.3 \mu\text{g l}^{-1}$.

Assay formats using an enzymatic reaction with MIP is of great potential for experiments conducted for microcystin-LR, however the size of the conjugate compared to the original template did not guarantee a high specificity, during the detection process, especially for targets of a small size. The non-specific signal observed with the non-imprinted polymer (NIP) showed that the use of an enzyme competitive assay for the bulk polymer was not a suitable method for studying this polymer. Steric hindrance may be responsible for the non-specific signal i.e. the conjugate was trapped in the polymers sites by weak interactions leading to a loss of specificity. Moreover, high standard deviations ($\% \text{CV} > 17$) were observed, possibly because of the difficulty in optimising the filtration step during the MIP assay procedure; this step was believed to affect the accuracy and reproducibility of the assay. Finally, the suspension of polymer particles used did not allow complete homogeneity and thus may have caused a concentration error.

Since the MIP-enzyme competitive assay for domoic acid did not give satisfactory results, a second method of detection was investigated combining a highly sensitive fluorescent measuring technique with the robust and selective artificial receptor system, prepared by imprint polymerisation. This method eliminated the filtration process, used

in the previous enzyme assay, and incorporated a stirring system into the spectrofluorophotometer instrument to ensure a constant agitation of the polymer suspension, thus improving homogeneity.

The sensor response for the imprinted polymers was related to a “gate effect”, which consists of a change in the polymer morphology and porous structure induced by the interaction of template molecules with selective cavities. The nature of the observed sensor response may be explained by assuming that the interactions between the template molecules with polymeric domains (containing the selective cavities), results in a conformational re-organisation of the polymeric structure (Figure 7.4), affecting the diffusion of organic molecules (Piletsky *et al.*, 1996; Yoshimi *et al.*, 2001).

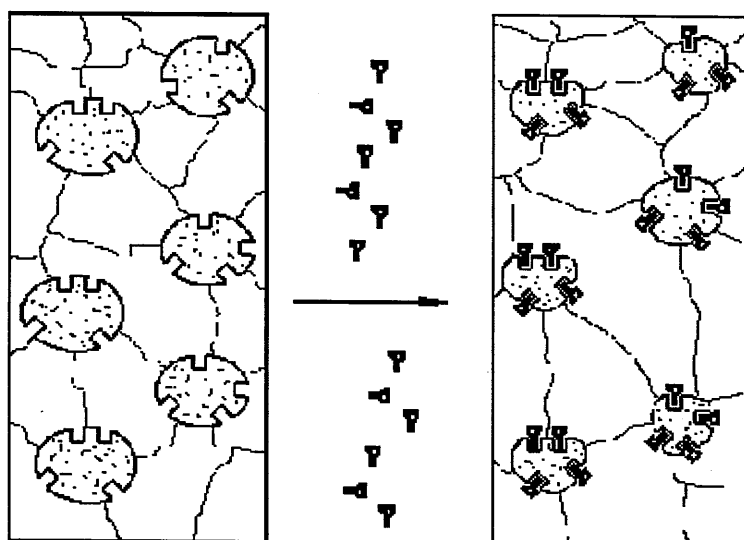


Figure 7.4: Possible changes in the MIP network structure.

The result of its interaction with the template: template binding- in this case causing shrinking in MIP receptor domains – induces opening of “gates” for transport of molecules and ions through the MIP membrane (Piletsky *et al.*, 1996).

The “gate effect” based fluorescence assay for DA amino acid detection brought to a substantial improvement in the reproducibility of the measurement, compared to the previous enzyme-MIP assay. A fluorescent signal was produced in the absence of the

template by the blank polymer but with a minimum response. However, the sensitivity was not high, the detection of domoic acid at a minimum concentration of 0.3 mg l^{-1} was shown to be possible. Upon addition of domoic acid, the emission intensity significantly increased. This template-induced variation in the fluorescence intensity evidenced as a larger quantity of amino groups reacted with OPA, in the presence rather than in absence of domoic acid. With the fluorescence assay, it was necessary to use the bulk polymer in suspension; although the stirring system improved homogeneity during the analysis. This format allowed the analysis of the sample sequentially, thus increasing the time of the experiments.

A more accurate quantification of domoic acid concentration should require a better retention signal and differential measurements set-up, which is impossible with the suspension-based assay. Another possible solution could be the use of optical fibres with fluorescence sensors with interfacial substrate signals generated by optrodes with immobilised MIP and blank polymers. Such a sophisticated assay would still be expensive and destructive because after each sample, the polymer suspension must be discarded. For all of these reasons a different approach, based on MIP grafting, was investigated.

7.11 GRAFTED IMPRINTED POLYMER FOR DOMOIC ACID

An important aspect for any molecular imprinting project, where sensitivity and selectivity of the obtained artificial receptor play a major role, is the analytical means that are employed to analyse and evaluate the polymer. If the target molecule is expensive, as is often the case with biomolecules such as toxins, the most convenient way is to interface the polymer with a chemical sensor or biosensor. For example by synthesising a thin layer of polymer on the surface of a transducer. Using this approach, the amount of polymer needed is much smaller than that in a conventional bulk-polymerisation method. The technique of grafting polymerisation has been used in

recent studies for the preparation of thin films of molecularly imprinting polymers, for different applications.

Schweitz (Schweitz, 2002) reported on a preparation protocol for a MIP film coatings used for capillary columns. The MIP coatings were synthesised *in situ* under conditions that allowed a wide variability in the MIP composition. By immobilizing a photolabile radical initiator on the capillary surface, prior to the introduction of the pre-polymerisation mixture, the polymerization reaction can be confined to the vicinity of the capillary surface, resulting in a covalently attached MIP coating. The use of different solvents (porogens) during the polymerization reaction facilitated control of the MIP coating, in term of morphology and appearance. The MIP coatings synthesised using solvents such as toluene, dichloromethane, and acetonitrile, all provided enantiomer separation of the amino alcohol propanolol when the S enantiomer was used as a template for the MIP.

Similarly, silica particles containing surface-bound free radical initiators have been used as a support for the grafting of thin films of MIPs. The technique offered a means of fine-tuning the layer thickness for improved kinetic properties or enhanced capacity in chromatographic or sensor application. Thus, polymers grafted as thin films (ca. 0.8 nm as average film thickness) on silica with 10 nm average pore diameter showed the highest column efficiency for enantiomer separation (Sulitzky *et al.*, 2002). In another report, films of TiO₂ were imprinted with chloroaromatic acids such as 2,4-D and used as recognition layers for sensors based on ion-sensitive field-effect transistors (Lahav *et al.*, 2001). The functionalized devices that include the imprinted interfaces displayed an impressive selectivity for the detection of substrates and a detection limit in the micromolar range.

The technique of grafting polymerisation has been used for the preparation of thin films of molecularly imprinting polymers on the surface of hydrophobised gold (Panasyuk-Delaney *et al.*, 2001; Sulitzky *et al.*, 2002). Gold surfaces have the distinguishing property of an exceptional affinity for sulfur groups. Thus, the self –assembly of RSH or

RSSR groups by chemisorption at gold surfaces has become an increasingly important approach to creating well-controlled, intricately designed sensing layers. Thiols have been used in the preparation of many self-assembled monolayer studies. These monolayers were extremely durable and provided a supporting membrane for the covalent attachment of molecules away from the sensing surface. One of the essential features of self-assembled monolayers (SAMs), for sensing applications, is the presence of a terminal group, X (Au-S-X), which can be used either for tuning the hydrophilicity or permselectivity of the layer or for covalently binding biomolecules (Cunningham, 1998).

The grafting procedure is also useful for solving two other problems associated with the development of SPR-based sensors. One of such problem is related to the difficulties found with integrating MIPs (especially conventional rigid cross-linked polymers) with a transducer. Grafting combines polymer formation with immobilisation and, as a result, no additional immobilisation step is required. Another problem is linked to the specific requirements for SPR detection mechanism, which is sensitive to processes taking place in close proximity to the gold surface (~100 nm). The photo-grafting procedure, in principle, is ideally suited for this task since it provides the possibility to control the deposition rate by controlling the time and intensity of UV exposure. For this work, photo grafting was used for the design of the SPR sensor for domoic acid. The first part of the work included the characterisation of the formed coatings and optimisation of the grafting procedure. This approach required small amounts of polymer, which made the sensor fabrication feasible even for expensive target molecules such as toxins.

A bare gold Biacore SPR surface was functionalised with a self-assembled monolayer (SAMs) for the synthesis of a MIP film. This is the first time such an approach has been reported. The SAM consisted of 2-mercaptoethylamine; subsequent carbodiimide chemistry was performed to covalently attach the photoinitiator, 4,4'-azobis(cyanovaleric acid). Photoinitiator immobilisation ensured that the formation of the MIP thin film, comprising 2-(diethylamino) ethyl methacrylate as functional monomer and ethylene glycol dimethacrylate as cross-linker, occurred only at the gold

surface. Atomic force microscopy (AFM) analysis showed the resultant grafted MIP layer to be approximately 40 nm thick and deposited homogeneously, thus suitable for SPR-based analyses. Additional evidence for the quality and homogeneity of the grafted polymer films was obtained from AFM images. The atomic force microscope is a powerful high resolution imaging tool, which allows the study of micro- and nano-structures and to characterise material surfaces and interfaces. In contrast to other methods, specimens prepared for the AFM remain in a plastic state, which enables a direct observation of the dynamic molecular response to be made, creating a unique opportunity for studying the structure-function relationships of proteins and their functionally relevant assemblies.

A polymer-coated fiber optic probe has been described for the hydrolysis product of the chemical warfare nerve agent soman and sarin. A luminescent europium complex ligated by divinylmethyl benzoate (ligating monomer) and by the analyte pinacoyl methylphosphonate was co-polymerised with styrene, after which the analyte molecule was removed by washing. Re-binding of the analyte was quantified from the laser-excited luminescence spectra. Although it was not clear whether imprinting had contributed to the selectivity of the sensor, the detection principle appeared attractive as very low detection limits could be obtained (7 ppt in this particular case) (Jenkins *et al.*, 1999). In a following work, the same author (Jenkins *et al.*, 2001) described the direct imprinting of non-hydrolysed organo-phosphates including pesticides and insecticides. The detection limits for these developed MIP sensors were less than 10 parts per trillion (ppt) with long linear dynamic ranges (ppt to ppm) and response times of less than 15 minutes.

A surface plasmon resonance (SPR) sensor using a molecularly imprinted polymer – coated sensor chip for the detection of sialic acid was developed by Kugimiya (Kugimiya *et al.*, 2001). The thinly coated polymer was prepared by co-polymerizing *N,N,N*-trimethylsminoethylmethacrylate, 2-hydroxyethylmethacrilate and ethylene-glycol dimethacrylate in the presence of *p*-vinylbenzeneboronic acid ester with sialic acid. The sensor showed a selective response to ganglioside, of which sialic acid is

located at the non-reducing end; a linear range from 0.1 to 1.0 mg of ganglioside was observed. The molecularly imprinted polymer-coated SPR chips can be less expensive than natural biomaterial-coated SPR chips. For example, the sialic acid imprinted polymer could be produced at a cost 200 times lower than sialic acid selective lectin (E-selectin). Although the proposed sensor was not very sensitive, it may be developed as an important device for clinical diagnosis in the future.

Since domoic acid is small molecule (FW= 311), which does not significantly change the refractive index, a conjugate of domoic acid and HRP was used for the analysis of the MIP film specificity. The MIP grafted onto the BIAcore chip displayed a specific binding of HRP-domoic acid conjugate, shown by an increase in the sensor response (response units) of the chip ($RU_{max} \geq 450$). The MIP sensor generated a much lower signal for the free HRP enzyme ($RU_{max} < 100$). The maximum difference in sensor response for HRP-DA and free HRP was obtained for a 200 mg l^{-1} concentration of conjugate/HRP ($S/B = 4.7$). This concentration was used for the following experiments where a competitive reaction between the free toxin and its conjugate was performed. From the response curve, a limit of detection of $2 \text{ } \mu\text{g l}^{-1}$ was determined over a range of concentrations between 2 and $3300 \text{ } \mu\text{g l}^{-1}$. The result was encouraging in terms of good sensitivity, since a value comparable to that of the natural receptors was achieved. Regarding the regeneration procedures of the MIP receptors grafted onto the chip gold surface, the response and activity of the ligand after the regeneration pulse was confirmed and the analyte binding capacity of the surface was unchanged after the regeneration process. An ideal regeneration would remove all the analyte from the sensor surface following injection, leaving the surface in a state identical to that before the injection. The MIP-film chip was shown to be robust, since regeneration was carried out about 40 times with negligible changes in response.

The same approach was carried with the monoclonal antibody raised against domoic acid. Both natural and artificial receptors showed a high affinity for the target toxin, since the value of EC_{50} was calculated as 10 and $58 \text{ } \mu\text{g l}^{-1}$, respectively. In term of sensitivity, the MIP had approximately three times a higher detection limit (LLD_{80})

compared to that of monoclonal antibody ($5 \mu\text{g l}^{-1}$ versus $1.8 \mu\text{g l}^{-1}$ of domoic acid respectively). The calibration curve for the MIP sensor showed a maximum value of approximately 400 RU, which was half of the maximum RU value observed for the antibody. Furthermore, the detection range in the case of MIP was significantly broad ($3300 \mu\text{g l}^{-1}$). This was due to the varied distribution of the polymer binding sites, which presented a different affinity for the target molecule, as already demonstrated by Mosbach (Mosbach *et al.*, 1996).

When directly immobilised on the gold surface, the antibodies lost much of their activity after a few regeneration cycles. Despite MIPs, the natural receptors are not robust enough to stand extreme situations and environments e.g. seawater. When the indirect format was adopted with the conjugate immobilised on the chip and the antibody injected, the sensitivity of antibody was in the pg range. Using this approach, regeneration could be carried out more easily since the immobilised protein was more robust. Some of the main recognition systems published are presented in Table 7.3.

Table 7.2: Summary of the principal receptors systems specific for domoic acid.

RECEPTORS	DETECTION LIMIT	CROSS-REACTIVITY	APPLICATION	YEAR OF PUBLICATION (REFERENCE)
Rabbit polyclonal antisera	40 $\mu\text{g l}^{-1}$	None reported	ELISA/RIA	1991 (Newsome <i>et al.</i> , 1991))
Polyclonal antiserum (DA-OVA/ DA-KHL)	0.25 mg l^{-1} (in serum)	Not significant with KA, Asp, Glu, Sax	Competitive ELISA	1994 (Smith <i>et al.</i> , 1994)
Cloned Glutamate Receptor	not reported	100 folds better affinity than Glu, 3 folds better than KA	Microplate receptor competition assay	1996 (Van Dolah <i>et al.</i> , 1997)
Sheep polyclonal antibody	0.01 $\mu\text{g l}^{-1}$ 38 ng/g mussel tissue	Not reported	Indirect competitive ELISA	1998 (Garthwaite <i>et al.</i> , 1998)
Polyclona antibody (DA-BSA)	1.4 $\mu\text{g l}^{-1}$ 0.02 mg g^{-1}	Not significant with KA, Asp, Glu	Competitive ELISA	1999 (Branaa <i>et al.</i> , 1999)
Monoclonal antibody (DA-BSA/DA-OVA/DA-HGG)	0.15 $\mu\text{g l}^{-1}$	Not significant with KA, Asp, Glu and most of isomers;	Indirect competitive EIA	1999 (Kawatsu <i>et al.</i> , 1999)
Monoclonal antibody	4 $\mu\text{g l}^{-1}$ 0.004 $\mu\text{g DA g}^{-1}$ mussel tissue	None with KA, Asp, Glu, geranic acid and 2-methyl-3-butenoic acid	Competitive ELISA	2002 (Kania <i>et al.</i> , 2002)
MIP-based receptor	5 $\mu\text{g l}^{-1}$	25% KA, 14%Glu, 12% Asp	Assay/Sensor	This work

Abbreviations: KA= kainic acid; Asp= aspartic acid; Glu=glutammic acid; Sax= saxitoxin; DA-BSA= domoic acid – bovines serum albumin; DA-OVA= domoic acid- ovalbumin; DA-HGG= domoic acid-human gamma globulin

CHAPTER 8:

CONCLUSIONS AND FURTHER WORK

The work described in this thesis has detailed the development of affinity sensors specific for two of the most common toxins found in water: the marine toxin domoic acid from algae and the freshwater toxin microcystin-LR from cyanobacteria.

The first part of the work aimed to select the most sensitive receptor as the recognition system for the target toxins. This included investigating sensing elements such as natural receptors (antibodies) and artificial receptors (based on molecular imprinted polymer). Antibodies against microcystin-LR were then used for the recognition system in the development of a disposable amperometric screen-printed immunosensor for microcystin-LR detection in water. The process included antibody selection and characterisation, which enabled a membrane-based enzyme immunoassay to be developed and incorporated into the immunosensor design as the immunosorbent solid phase.

An anti-MC-LR antibody raised in rabbit was initially evaluated using the BIAcore sensor and it was found to be non-specific for the target analyte, showing a high cross-reactivity towards the carrier protein ovalbumin, compared to the toxin. A second anti-MC-LR IgG, raised in sheep, demonstrated excellent characteristics with high MC-LR affinity, selectivity, and sensitivity when used in conjunction with the gelatin- MC-LR conjugate provided. The sensitivity enabled a detection limit of $0.022 \mu\text{g l}^{-1}$ of microcystin-LR, in a competitive ELISA format. The EC_{50} value ($0.08 \mu\text{g l}^{-1}$) indicated a high affinity between the antigen and antibody, from the competitive binding results. Antibody specificity was also evaluated and a high cross-reactivity for the anti-MC-LR antibody with other microcystins (mainly with microcystin-YR) was observed, as predicted from previous published results.

The parameters of the immunoassay in term of temperature, shaking and time of incubations were all investigated. It was concluded that a temperature of $37 \text{ }^\circ\text{C}$ was preferred during a pre-mixing step of the anti-MC-LR antibody with free toxin standards, and a one-hour incubation of the HRP labelled secondary antibody. All other steps (coating, blocking, competition) performed equally well at room temperature. The

total length of the competitive ELISA was approximately 2 hours and 15 minutes, considering also some time for three wash steps. Different matrixes were also analysed for both analyte and antibody but no relevant drawbacks were observed in the immunoassay response. This provided valuable information as to the suitability of the antibody for the ultimate goal: its application in an immunosensor for the detection of microcystins analysis in freshwater.

The competitive ELISA assay format was then transferred to a membrane-based ELISA with the aim of developing an immunosensor for the detection of microcystin-LR. Three coating concentrations were initially tested on the UltraBind™ membranes, but their suitability for further application was compromised by the comparatively high non-specific binding signal. The coating reproducibility was low (% CV > 8), although a steady background level was observed. Moreover, the assay reproducibility using different blocking agents was low with mean % CV > 20. Further optimisation with the primary and secondary antibody concentrations did not increase the signal of the maximum response. Although the membrane assay system developed functioned well, after detailed characterisation the assay specificity and reproducibility were not acceptable for continued development and incorporation into the intended immunosensor device. Rather than optimising the indirect competitive assay further, or trying several other alternative membranes and coating agents, the decision was taken to develop another ELISA where the antibody was immobilised directly onto the membrane.

A new format for the enzyme immuno-assay (EIA) needed to be considered, with a more specific and reproducible assay transferred to a membrane based ELISA; the system could finally be applied and optimised as an immunosensor format. The competitive MELISA assay, based on IgG immobilised on a membrane sorbent, was carried out by immobilisation of anti-MC-LR IgG 1/1000. The steps for the all immuno-reactions were reduced to two and the assay more rapid than the previous format adopted. Furthermore, by reducing one step, the problem of reproducibility was significantly reduced. The minimum amount of toxin detected was $0.06 \mu\text{g l}^{-1}$.

Therefore, this EIA format appeared more suitable for implementation in an electrochemical sensor.

The sensitivity results from the anti-MC-LR immunosensor showed that hydroquinone mediated amperometric detection system gave an LLD_{80} value of $0.5 \mu\text{g l}^{-1}$, indicating a sensitivity loss of about 5 times compared to the colorimetric MELISA. The immunosensor measurements showed a slight increase in mean assay variation, compared to the MELISA % CV (5.8 versus 4.35). The background current was less than -100 nAmps .

Although the immunosensor was successful at detecting microcystin-LR, further assay development and optimisation could still be undertaken to improve the performance and sensitivity. The sensor stability and response, particularly with regard to sample matrices of varying and greater organic content, needs to be investigated, in addition to the sensor inter/ intra assay and operator reproducibility. Characterisation results from the immunosensor response for cross-reactivity to individual compounds and various mixtures of compounds in different concentrations would be required. The immunosensor demonstrated a good correlation with the HPLC results and would therefore provide a valuable tool for decentralised monitoring and sample screening applications. It would be interesting to determine the sensor performance when applied to real complex matrices, such as river and seawater.

Other future developments would be:

- To reduce the electrode dimensions
- To increase the reproducibility of the immunosensor device construction
- To increase the number of analytes detectable simultaneously i.e. to develop a multi-analyte array.

Increased sensitivity can be investigated by incorporating the mediator into the screen-printed working electrode or by employing an alternative substrate such as TMB.

The development of an electrochemical on-line immunosensor, based on detecting ABTS via colour development, was briefly investigated. The detection system proved to be sensitive ($LLD_{80} = 0.7 \mu\text{g l}^{-1}$) and, hence, a more detailed investigation was carried out. The initial results from the on-line sensor system were encouraging; continued optimisation of the system, as an alternative automated and continuous analytical system to the disposable immunosensor, was carried out. Although the sensor-immobilised antibodies could be successfully used to detect the target toxin, synthetic binding molecules were shown to be equally specific but more robust than the natural elements.

The molecularly imprinted polymer technique was considered for producing an artificial 'antibody-like' receptor for microcystin-LR. The MIP receptors for microcystin-LR were synthesised and a competitive MIP assay used for characterisation of the MAA-MIP receptor. Attention was mainly focused on a comparison study between two examples of natural receptors (polyclonal and monoclonal antibodies against microcystin-LR) and two different artificial receptors based on MIPs; both specific for the same toxin. The results obtained suggested broad application of MIPs for the future of artificial microcystin-LR recognition systems. Although more optimisation will be necessary to confirm these results, it can be concluded that MIPs can have comparable sensitivity and specificity to polyclonal antibodies. Furthermore their activity (unlike monoclonal and polyclonal antibodies) is less influenced by harsh conditions such as extreme pHs, the presence of salts and high temperatures. The cross-reactivity was negligible for the MIP receptors, making them possibly suitable and this make them very interesting for the identification of other toxins (e.g. toxins from microcystins family), for which standards are not yet available in the market (that thus cannot be identified by immunoassay or HPLC systems). This lack of cross-reactivity gives the MIP receptors an advantageous characteristic, since natural bio-molecules, even monoclonal antibody, can suffer from this type of interference.

The characterisation of specific receptors, based on MIPs, and their application in assay or sensor devices was another objective of this study, in particular for domoic acid. The

MIP for domoic acid was synthesised using a novel approach based on computational modeling. From previous studies, the computational selection of monomers (type and composition) for polymer synthesis was considered to be possible. An enzyme-based competitive assay using colorimetric detection was optimised using a computational-designed imprinted polymer, specific for domoic acid. The detection limit achieved with this detection system was approximately $1 \mu\text{g l}^{-1}$ over a working range of between 1 and $10 \mu\text{g l}^{-1}$. The EC_{50} was calculated as $1.3 \mu\text{g l}^{-1}$, indicating high affinity for the MIP receptors to domoic acid.

A maximum signal of 0.24 optical density, with a high non-specific signal was obtained using a non-imprinted polymer. Moreover, low reproducibility was a feature of this approach with a value of $\% \text{CV} > 17$; probably linked to the manual techniques required for the assay, and the need to use a suspension of polymers. An attempt to improve the transduction of the signal for the MIP was undertaken by investigating a fluorescence assay based on the “gate effect.” Although the reproducibility of the assay improved ($\% \text{CV} < 10$), the assay sensitivity was lower than the colorimetric enzyme assay. A more extensive optimisation program would have been necessary to improve this. Unfortunately, the assay equipment did not allow many tests to be conducted at once, resulting in an expensive (because the polymer suspension could not be re-use) and time-consuming method.

A different approach, which allowed repetitive experiments over a short time period was investigated; based on grafting a MIP film onto a gold chip surface, thus eliminating the need for bulk polymer synthesis. This aimed to generate a more reliable system of detection and less use of the toxin for characterisation. The AFM was employed for a morphological study, and the BIAcore for studying the specificity of the grafted MIP for the target molecule. A detection limit of $2 \mu\text{g l}^{-1}$ was achieved with the MIP SPR sensor, further optimisation should lead to further improvements. Nevertheless, these assays demonstrated that the MIP had good potential in terms of reusability and stability, compared to the analogues antibody receptors. The physical and chemical resistance of imprinted polymers together, with their stability and the low

cost of preparation are all obvious advantages that imprinted polymers have over natural antibody receptors.

The unique capability of the SPR biosensor to obtaining kinetic data provides a quantitative approach to studying the biochemical effects of the toxins, in addition to the structural features of the toxin-bound receptor complexes. There are only a few reports on the use of SPR biosensors based on MIP technology, for studying the effects of toxins. This is partially because most natural toxins are low molecular weight molecules, with extremely high association rates and affinity to their target proteins. The work described here demonstrates the potential application of an SPR biosensor using MIP technology for environmental toxicological research.

PUBLICATIONS

Results from this thesis have been published and presented as follows:

Lotierzo, M., Tothill, I.E., Chen, B. and Turner, A.P.F (1999). Evaluation of cyanobacterial toxins-antibodies interaction for affinity sensor development (ALGAETOX). *Fourth Workshop on Biosensors and Biological Techniques in Environmental Analysis*, Menorca, Spain, 1-3 December 1999.

Lotierzo, M., Piletsky, S.A., Tothill, I.E., Chen, B. and Turner, A.P.F. (2000). Comparison between natural antibodies and artificial receptors used in affinity sensor development. P-194, pp 442, *The Sixth World Congress on BIOSENSORS*, San Diego, USA, 24-26 May 2000.

Lotierzo, M., Chianella, I., Tothill, I.E., Chen, B. Piletsky, S.A. and Turner, A.P.F. (2000). Algal toxins receptors for affinity sensors development. *BIOSET Workshop on Biosensors for Environmental Monitoring: Monitoring in Real Environments*. Cascais, Portugal, 11-13 September 2000.

Chianella, I. **Lotierzo, M.** Piletsky, S.A., Tothill, I.E., Chen, B. and Turner, A.P.F. (2000). Development of a receptor based on molecularly imprinted polymer for algal toxins. *MIP2000 1st International Workshop on Molecular Imprinting*. 3-5 July 2000.

Chianella I., **Lotierzo, M.**, Piletsky, S.A, Tothill I.E., Chen B, Karim, K. and Turner A.P.F. (2001). Rational design of the polymer specific for microcystin-LR using computational approach. *Analytical Chemistry*, 74, 1288-1293.

Lotierzo, M., Tothill, I.E, Abuknesha, R. and Turner, A.P.F. (2001). Development of an immunosensor for detection of microcystin-LR toxin. *EURESCO Conference on Molecular Bioenergetics of Cyanobacteria*, Strasbourg, France, 25-30 May 2001.

Henry, O.Y.F., **Lotierzo, M.**, Piletsky, S.A., Cullen, D.C., Tothill, I.E. and Yoshimi, Y. (2002). Photografted molecular imprinted polymer thin films for SPR analysis with recognition properties towards the marine toxin domoic acid. *MIP2002 2st International Workshop on Molecular Imprinting*. 16-19 September 2002.

Lotierzo, M., Piletsky, S.A, Henry, O.Y.F., Tothill I.E., and Turner A.P.F. (2002). Surface plasmon resonance sensor for domoic acid based on grafted imprinted polymer. *Analytical Chemistry (submitted)*.

REFERENCES

- Alvarez-Icaza, M. & Bilitewski, U. (1993).** "Mass-production of biosensors." *Analytical Chemistry* **65**(11): A525-A533.
- An, J.S. & Carmichael, W.W. (1994).** "Use of a colorimetric protein phosphatase inhibition assay and enzyme-linked-immunosorbent-assay for the study of microcystins and nodularins." *Toxicon* **32**(12): 1495-1507.
- Andersson, H.S., Karlsson, J.G., Piletsky, S.A., Koch-Schmidt, A.C., Mosbach, K. & Nicholls, I.A. (1999).** "Study of the nature of recognition in molecularly imprinted polymers, ii [1] - influence of monomer-template ratio and sample load on retention and selectivity." *Journal of Chromatography A* **848**(1-2): 39-49.
- Ash, C., Mackintosh, C., Mackintosh, R. & Fricker, C.R. (1995).** "Use of a protein phosphatase inhibition test for the detection of cyanobacterial toxins in water." *Water Science and Technology* **31** (5-6): 51-53.
- Baier, W., Loleit, M., Fischer, B., Jung, G., Neumann, U., Weiss, M., Weckesser, J., Hoffmann, P., Bessler, W.G. & Mittenbuhler, K. (2000).** "Generation of antibodies directed against the low-immunogenic peptide-toxins microcystin-LR/RR and nodularin." *International Journal of Immunopharmacology* **22**(5): 339-353.
- Baskeyfield, D.E.H. (2001).** Development of a disposable amperometric immunosensor for isoproturon herbicide detection in water and soil extracts. PhD thesis, *Cranfield University at Silsoe - Supervisor: I.E. Tothill, N. Magan & A. Walker.*
- Bilitewski, U., Chemnitius, G.C., Ruger, P. & Schmid, R.D. (1992).** "Miniaturized disposable biosensors." *Sensors and Actuators B-Chemical* **7**(1-3): 351-355.
- Böhm, H.J. (1992).** "The computer program Ludi: A new method for the de-novo design of enzyme inhibitors." *Journal of Computer-Aided Molecular Design* **6**(1): 61-78.
- Branaa, P., Naar, J., Chinain, M. & Pauillac, S. (1999).** "Preparation and characterization of domoic acid-protein conjugates using small amount of toxin in a reversed micellar medium: Application in a competitive enzyme-linked immunosorbent assay." *Bioconjugate Chemistry* **10**(6): 1137-1142.
- Carmichael, W.W. (1992).** "Cyanobacteria secondary metabolites - the cyanotoxins." *Journal of Applied Bacteriology* **72**(6): 445-459.

- Carmichael, W.W. (1997).** "The cyanotoxins." *Advances in Botanical Research* **27**: 212-256.
- Cass, A.E.G. (1990).** Biosensors - a practical approach. Oxford, *IRL Press at Oxford University Press*.
- Chianella, I. (2003).** Development of affinity sensors for microcystin-lr based on computationally designed molecularly imprinted polymer. PhD thesis, *Cranfield University at Silsoe - Supervisor: I.E. Tothill, S. Piletsky & B. Chen*.
- Chianella, I., Lotierzo, M., Piletsky, S., Tothill, I., Chen, B., Karim, K. & Turner, A.P.F. (2002).** "Rational design of a polymer specific for microcystin-lr using a computational approach." *Analytical Chemistry* **74**: 1288-1293.
- Choi, M.J., Gorovits, B.M., Choi, J., Song, E.Y., Nam, K.S. & Park, J. (1994).** "A visual membrane immunoassay for the detection of methamphetamine using an enzyme-labeled tracer derived from methamphetamine and amphetamine." *Biological & Pharmaceutical Bulletin* **17**(7): 875-880.
- Christie, I.M., Treloar, P.H. & Vadgama, P. (1992).** "Plasticized poly(vinyl chloride) as a permselective barrier membrane for high-selectivity amperometric sensors and biosensors." *Analytica Chimica Acta* **269**(1): 65-73.
- Chu, F.S., Huang, X. & Wei, R.D. (1990).** "Enzyme-linked-immunosorbent-assay for microcystins in blue- green-algal blooms." *Journal of the Association of Official Analytical Chemists* **73**(3): 451-456.
- Clark, L.C. & Lyons, C. (1962).** "Electrode systems for continuous monitoring in cardiovascular surgery." *Annals of the New York Academy of Sciences* **102**: 29-45.
- Clark, R.F., Williams, S.R., Nordt, S.P. & Manoguerra, A.S. (1999).** "A review of selected seafood poisonings." *Undersea & Hyperbaric Medicine* **26**(3): 175-184.
- Codd, G.A., Brooks, W.P., Priestley, I.M., Poon, G.K., Bell, S.G. & Fawell, J.K. (1989).** "Production, detection, and quantification of cyanobacterial toxins." *Toxicity Assessment* **4**(4): 499-511.
- Codd, G.A., Metcalf, J.S. & Beattie, K.A. (1999).** "Retention of *Microcystis aeruginosa* and microcystin by salad lettuce (*lactuca sativa*) after spray irrigation with water containing cyanobacteria." *Toxicon* **37**(8): 1181-1185.
- Codd, G.A., Skulberg, O.M. & Carmichael, W.W. (1984).** "Toxic cyanobacteria in european waters." *British Phycological Journal* **19**(2): 191-191.

- Compagnone, D., Schweicher, P., Kauffman, J.M. & Guilbault, G.G. (1998).** "Sub-micromolar detection of hydrogen peroxide at a peroxidase/tetramethylbenzidine solid carbon paste electrode." *Analytical Letters* 31(7): 1107-1120.
- Cortese, R., Monaci, P., Luzzago, A., Santini, C., Bartoli, F., Cortese, I., Fortugno, P., Galfre, G., Nicosia, A. & Felici, F. (1996).** "Selection of biologically active peptides by phage display of random peptide libraries." *Current Opinion in Biotechnology* 7(6): 616-621.
- Crowther, J.R. (2000).** The ELISA guidebook: Theory and practice. New Jersey, USA, *Humana Press*.
- Cunningham, A.J. (1998).** Introduction to bioanalytical sensors. New York, *John Wiley & Sons*.
- Deshpande, S.S. (1996).** Enzyme immunoassays: From concept to product development. London, *Chapman and Hall Publishers*.
- Dicks, J.M., Cardosi, M.F., Turner, A.P.F. & Karube, I. (1993).** "The application of ferrocene-modified n-type silicon in glucose biosensors." *Electroanalysis* 5(1): 1-9.
- Falconer, I.R. (1999).** "An overview of problems caused by toxic blue-green algae (cyanobacteria) in drinking and recreational water." *Environmental Toxicology* 14(1): 5-12.
- Furey, A., Lehane, M., Gillman, M., Fernandez-Puente, P. & James, K.J. (2001).** "Determination of domoic acid in shellfish by liquid chromatography with electrospray ionization and multiple tandem mass spectrometry." *Journal of Chromatography A* 938(1-2): 167-174.
- Garthwaite, I., Ross, K., M., Miles, C., O., Hansen, R., P., Foster, D., Wilkins, A., L. & Towers, N., R. (1998).** "Polyclonal antibodies to domoic acid, and their use in immunoassays for domoic acid in sea water and shellfish." *Natural Toxins* 6(3-4): 93-104.
- Ghindilis, A.L., Atanasov, P., Wilkins, M. & Wilkins, E. (1998).** "Immunosensors: Electrochemical sensing and other engineering approaches." *Biosensors & Bioelectronics* 13(1): 113-131.
- Ghindilis, A.L., Krishnan, R., Atanasov, P. & Wilkins, E. (1997).** "Flow-through amperometric immunosensor: Fast 'sandwich' scheme immunoassay." *Biosensors & Bioelectronics* 12(5): 415-423.

- Gill, E.P., Tang, H.T., Halsall, H.B., Heineman, W.R. & Misiego, A.S. (1990).** "Competitive heterogeneous enzyme immunoassay for theophylline by flow-injection analysis with electrochemical detection of *p*-aminophenol." *Clinical Chemistry* **36**(4): 662-665.
- Goldberg, J., Huang, H.B., Kwon, Y.G., Greengard, P., Nairn, A.C. & Kuriyan, J. (1995).** "3-dimensional structure of the catalytic subunit of protein serine/threonine phosphatase-1." *Nature* **376**(6543): 745-753.
- Gorton, L., Csöregi, E., Domínguez, E., Emnéus, J., Jönsson-Pettersson, G., Markovarga, G. & Persson, B. (1991).** "Selective detection in flow-analysis based on the combination of immobilized enzymes and chemically modified electrodes." *Analytica Chimica Acta* **250**(1): 203-248.
- Gosling, J.P. (2000).** Immunoassay: A practical approach. Oxford, *Oxford University Press*.
- Hallegraeff, G.M. (1993).** "A review of harmful algal blooms and their apparent global increase." *Phycologia* **32**(2): 79-99.
- Harlow, E. & Lane, D. (1988).** Antibodies: A laboratory manual. New York, *Cold Spring Harbour Laboratory Press*.
- Haupt, K. (2001).** "Molecularly imprinted polymers in analytical chemistry." *Analyst* **126**(6): 747-756.
- Haupt, K. & Fradet, A. (2001).** "Molecularly imprinted polymers: Concept and applications." *Actualite Chimique* (4): 23-32.
- Haupt, K., Mayes, A.G. & Mosbach, K. (1998a).** "Herbicide assay using an imprinted polymer based system analogous to competitive fluoroimmunoassays." *Analytical Chemistry* **70**(18): 3936-3939.
- Haupt, K. & Mosbach, K. (1998b).** "Plastic antibodies: Developments and applications." *Trends in Biotechnology* **16**(11): 468-475.
- Haupt, K., Noworyta, K. & Kutner, W. (1999).** "Imprinted polymer-based enantioselective acoustic sensor using a quartz crystal microbalance." *Analytical Communications* **36**(11-12): 391-393.
- He, Y.N., Chen, H.Y., Zheng, J.J., Zhang, G.Y. & Chen, Z.L. (1997).** "Differential pulse voltammetric enzyme-linked immunoassay for the determination of helicobacter pylori specific immunoglobulin g (IgG) antibody." *Talanta* **44**(5): 823-830.

-
- Hiemenz, P.C. & Rajagopalan, R. (1997).** Principles of colloid and surface chemistry. New York, *Marcel Dekker Inc.*
- Hock, B. (1997).** "Antibodies for immunosensors - A review." *Analytica Chimica Acta* 347(1-2): 177-186.
- Holm, K.A. (1995).** "Automated-determination of microbial peroxidase-activity in fermentation samples using hydrogen-peroxide as the substrate and 2,2'-azino-bis(3-ethylbenzothiazoline-6-sulfonate) as the electron-donor in a flow-injection system." *Analyst* 120(8): 2101-2105.
- Horacek, J. & Skládal, P. (1997).** "Improved direct piezoelectric biosensors operating in liquid solution for the competitive label-free immunoassay of 2,4-dichlorophenoxyacetic acid." *Analytica Chimica Acta* 347 (1-2): 43-50.
- Issert, V., Grenier, P. & BellonMaurel, V. (1997).** "Emerging analytical rapid methods for pesticide residues monitoring in foods: Immunoassays and biosensors." *Sciences Des Aliments* 17(2): 131-143.
- Iverson, F., Truelove, J., Nera, E., Tryphonas, L., Campbell, J. & Lok, E. (1989).** "Domoic acid poisoning and mussel-associated intoxication - preliminary investigations into the response of mice and rats to toxic mussel extract." *Food and Chemical Toxicology* 27(6): 377-.
- James, K.J., Gillman, M., Lehane, M. & Gago-Martinez, A. (2000).** "New fluorimetric method of liquid chromatography for the determination of the neurotoxin domoic acid in seafood and marine phytoplankton." *Journal of Chromatography A* 871(1-2): 1-6.
- Jenkins, A.L., Uy, O.M. & Murray, G.M. (1999).** "Polymer-based lanthanide luminescent sensor for detection of the hydrolysis product of the nerve agent soman in water." *Analytical Chemistry* 71(2): 373-378.
- Jenkins, A.L., Yin, R. & Jensen, J.L. (2001).** "Molecularly imprinted polymer sensors for pesticide and insecticide detection in water." *Analyst* 126(6): 798-802.
- Jenkins, S.H., Heineman, W.R. & Halsall, H.B. (1988).** "Extending the detection limit of solid-phase electrochemical enzyme-immunoassay to the attomole level." *Analytical Biochemistry* 168(2): 292-299.
- Jiao, K., Zhang, S.S., Wei, L., Liu, C.F., Zhang, C.L., Zhang, Z.F., Liu, J.Y. & Wei, P. (1998).** "Detection of tmv with oda-H₂O₂-HRP voltammetric enzyme-linked immunoassay system." *Talanta* 47(5): 1129-1137.

-
- Julicher, P., Haalck, L., Meusel, M., Cammann, K. & Spener, F. (1998).** "In situ antigen immobilisation for stable organic-phase immunoelectrodes." *Analytical Chemistry* **70**(16): 3362-3367.
- Kalab, T. & Skladal, P. (1997).** "Disposable multichannel immunosensors for 2,4-dichlorophenoxyacetic acid using acetylcholinesterase as an enzyme label." *Electroanalysis* **9**(4): 293-297.
- Kaláb, T. & Skládál, P. (1995).** "A disposable amperometric immunosensor for 2,4-dichlorophenoxyacetic acid." *Analytica Chimica Acta* **304**: 361-368.
- Kania, M. & Hock, B. (2002).** "Development of monoclonal antibodies to domoic acid for the detection of domoic acid in blue mussel (*mytilus edulis*) tissue by elisa." *Analytical Letters* **35**(5): 855-868
- Kawatsu, K., Hamano, Y. & Noguchi, T. (1999).** "Production and characterization of a monoclonal antibody against domoic acid and its application to enzyme immunoassay." *Toxicon* **37**(11): 1579-1589.
- Köhler, G. & Milstein, C. (1975).** "Continuous cultures of fused cells secreting antibody of predefined specificity." *Nature* **256**: 495-497.
- Kriz, D. & Mosbach, K. (1995).** "Competitive amperometric morphine sensor-based on an agarose immobilized molecularly imprinted polymer." *Analytica Chimica Acta* **300**(1-3): 71-75.
- Kröger, S. (1998).** A disposable electrochemical affinity sensor for 2,4-D in soil extracts. PhD thesis, *Cranfield University*.
- Kröger, S., Setford, S.J. & Turner, A.P.F. (1998).** "Immunosensor for 2,4-dichlorophenoxyacetic acid in aqueous organic solvent soil extracts." *Analytical Chemistry* **70**(23): 5047-5053.
- Kröger, S. & Turner, A.P.F. (1997).** "Solvent-resistant carbon electrodes screen printed onto plastic for use in biosensors." *Analytica Chimica Acta* **347**(1-2): 9-18.
- Kröger, S., Turner, A.P.F., Mosbach, K. & Haupt, K. (1999).** "Imprinted polymer based sensor system for herbicides using differential-pulse voltammetry on screen printed electrodes." *Analytical Chemistry* **71**(17): 3698-3702.
- Kugimiya, A. & Takeuchi, T. (2001).** "Surface plasmon resonance sensor using molecularly imprinted polymer for detection of sialic acid." *Biosensors & Bioelectronics* **16**(9-12): 1059-1062.

- Lahav, M., Kharitonov, A.B., Katz, O., Kunitake, T. & Willner, I. (2001).** "Tailored chemosensors for chloroaromatic acids using molecular imprinted tio₂ thin films on ion-sensitive field-effect transistors." *Analytical Chemistry* **73**(3): 720-723.
- Lehn, J.-M. (1995).** Supramolecular chemistry. Weinheim, *Wiley-VCH, Weinheim*.
- Mallat, E., Barceló, D., Barzen, C., Gauglitz, G. & Abuknesha, R. (2001a).** "Immunosensors for pesticide determination in natural waters." *Trac-Trends in Analytical Chemistry* **20**(3): 124-132.
- Mallat, E., Barzen, C., Abuknesha, R., Gauglitz, G. & Barceló, D. (2001b).** "Part per trillion level determination of isoproturon in certified and estuarine water samples with a direct optical immunosensor." *Analytica Chimica Acta* **426**(2): 209-216.
- Malmqvist, M. (1999).** "Biacore: An affinity biosensor system for characterization of biomolecular interactions." *Biochemical Society Transactions* **27**(2): 335-340.
- Malmqvist, M. & Karlsson, R. (1997).** "Biomolecular interaction analysis: Affinity biosensor technologies for functional analysis of proteins." *Current Opinion in Chemical Biology* **1**(3): 378-383.
- Marco, M.P. & Barceló, D. (1996).** "Environmental applications of analytical biosensors." *Measurement Science & Technology* **7**(11): 1547-1562.
- Marco, M.P., Gee, S. & Hammock, B.D. (1995).** "Immunochemical techniques for environmental-analysis .1. Immunosensors." *Trac-Trends in Analytical Chemistry* **14**(7): 341-350.
- Marquette, C.A. & Blum, L.J. (1998).** "Electrochemiluminescence of luminol for 2,4-d optical immunosensing in a flow injection analysis system." *Sensors and Actuators B-Chemical* **51**(1-3): 100-106.
- Marquette, C.A. & Blum, L.J. (2000a).** "Regenerable immunobiosensor for the chemiluminescent flow injection analysis of the herbicide 2,4-d." *Talanta* **51**(2): 395-401.
- Marquette, C.A., Coulet, P.R. & Blum, L.J. (1999).** "Semi-automated membrane based chemiluminescent immunosensor for flow injection analysis of okadaic acid in mussels." *Analytica Chimica Acta* **398**(2-3): 173-182.
- Marquette, C.A., Ravaud, S. & Blum, L.J. (2000b).** "Luminol electrochemiluminescence based biosensor for total cholesterol determination in natural samples." *Analytical Letters* **33**(9): 1779-1796.

-
- Mehto, P., Ankelo, M., Hinkkanen, A., Mikhailov, A., Eriksson, J.E., Spoof, L. & Meriluoto, J. (2001).** "A time-resolved fluoroimmunoassay for the detection of microcystins, cyanobacterial peptide hepatotoxins." *Toxicon* **39**(6): 831-836.
- Meriluoto, J. (1997).** "Chromatography of microcystins." *Analytica Chimica Acta* **352**(1-3): 277-298.
- Metcalf, J.S., Bell, S.G. & Codd, G.A. (2000).** "Production of novel polyclonal antibodies against the cyanobacterial toxin microcystin-Lr and their application for the detection and quantification of microcystins and nodularin." *Water Research* **34**(10): 2761-2769.
- Mos, L. (2001).** "Domoic acid: A fascinating marine toxin." *Environmental Toxicology and Pharmacology* **9**: 79-85.
- Mosbach, K. (1994).** "Molecular imprinting." *Trends in Biochemical Sciences* **19**(1): 9-14.
- Mosbach, K. & Ramstrom, O. (1996).** "The emerging technique of molecular imprinting and its future impact on biotechnology." *Bio-Technology* **14**(2): 163-170.
- Nagata, R., Yokoyama, K., Clark, S.A. & Karube, I. (1995a).** "A glucose sensor fabricated by the screen printing technique." *Biosensors & Bioelectronics* **10**(3-4): 261-267.
- Nagata, S., Tsutsumi, T., Hasegawa, A., Watanabe, M.F. & Ueno, Y. (1995b).** "Determination of microcystin in environmental water by highly sensitive immunoassay." *Japanese Journal of Toxicology and Environmental Health* **41**(1): P10-P10.
- Nagata, S., Tsutsumi, T., Hasegawa, A., Yoshida, F., Ueno, Y. & Watanabe, M.F. (1997).** "Enzyme immunoassay for direct determination of microcystins in environmental water." *Journal of Aoac International* **80**(2): 408-417.
- Newman, J.D., White, S.F., Tothill, I.E. & Turner, A.P.F. (1995).** "Catalytic materials, membranes, and fabrication technologies suitable for the construction of amperometric biosensors." *Analytical Chemistry* **67**(24): 4594-4599.
- Newsome, H., Truelove, J., Hierlihy, L. & Collins, P. (1991).** "Determination of domoic acid in serum and urine by immunochemical analysis." *Bull. Environ. Contam. Toxicol.* **47**: 329-334.
- Nishiwakimatsushima, R., Ohta, T., Nishiwaki, S., Suganuma, M., Kohyama, K., Ishikawa, T., Carmichael, W.W. & Fujiki, H. (1992).** "Liver-tumor promotion by

the cyanobacterial cyclic peptide toxin microcystin-lr." *Journal of Cancer Research and Clinical Oncology* 118(6): 420-424.

Ohta, T., Sueoka, E., Iida, N., Komori, A., Sugama, M., Nishiwaki, R., Tatematsu, M., Kim, S.J., Carmichael, W.W. & Fujiki, H. (1994). "Nodularin, a potent inhibitor of protein phosphatase-1 and phosphatase-2a, is a new environmental carcinogen in male f344 rat-liver." *Cancer Research* 54(24): 6402-6406.

Osada, M., Marks, L.J. & Stewart, J.E. (1995). "Determination of domoic acid by 2 different versions of a competitive enzyme-linked-immunosorbent-assay (ELISA)." *Bulletin of Environmental Contamination and Toxicology* 54(6): 797-804.

Panasyuk-Delaney, T., Mirsky, V.M., Ulbricht, M. & Wolfbeis, O.S. (2001). "Impedometric herbicide chemosensors based on molecularly imprinted polymers." *Analytica Chimica Acta* 435(1): 157-162.

Pemawansa, K.P.W., Heisler, M.D., Blackwell, S.L., Cymes, L., Mahalak, K.L. & Kraus, M.A. (1990). "An advanced affinity membrane for covalent binding of amino ligands." *Biotechniques* 9(3): 352.

Perez, N., Whitcombe, M.J. & Vulfson, E.N. (2000). "Molecularly imprinted nanoparticles prepared by core-shell emulsion polymerization." *Journal of Applied Polymer Science* 77(8): 1851-1859.

Piletsky, S.A., Karim, K., Piletska, E.V., Day, C.J., Freebairn, K.W., Legge, C. & Turner, A.P.F. (2001). "Recognition of ephedrine enantiomers by molecularly imprinted polymers designed using a computational approach." *Analyst* 126(10): 1826-1830.

Piletsky, S.A., Matuschewski, H., Schedler, U., Wilpert, A., Piletska, E.V., Thiele, T.A. & Ulbricht, M. (2000a). "Surface functionalization of porous polypropylene membranes with molecularly imprinted polymers by photograft copolymerization in water." *Macromolecules* 33(8): 3092-3098.

Piletsky, S.A., Piletska, E.V., Chen, B.N., Karim, K., Weston, D., Barrett, G., Lowe, P. & Turner, A.P.F. (2000b). "Chemical grafting of molecularly imprinted homopolymers to the surface of microplates. Application of artificial adrenergic receptor in enzyme-linked assay for beta-agonists determination." *Analytical Chemistry* 72(18): 4381-4385.

Piletsky, S.A., Piletskaya, E.V., Panasyuk, T.L., El'skaya, A.V., Levi, R., Karube, I. & Wulff, G. (1998). "Imprinted membranes for sensor technology: Opposite

- behavior of covalently and noncovalently imprinted membranes." *Macromolecules* **31**(7): 2137-2140.
- Piletsky, S.A., Piletskaya, K., Piletskaya, E.V., Yano, K., Kugimiya, A., Elgersma, A.V., Levi, R., Kahlow, U., Takeuchi, T., Karube, I., Panasyuk, T.I. & Elskaya, A.V. (1996).** "A biomimetic receptor system for sialic acid based on molecular imprinting." *Analytical Letters* **29**(2): 157-170.
- Piletsky, S.A., Terpetschnig, E., Andersson, H.S., Nicholls, I.A. & Wolfbeis, O.S. (1999).** "Application of non-specific fluorescent dyes for monitoring enantio-selective ligand binding to molecularly imprinted polymers." *Fresenius Journal of Analytical Chemistry* **364**(6): 512-516.
- Portsmann, B.T. (1981).** "Comparison of chromogens for the determination of horseradish peroxidase as a marker in enzyme immunoassay." *Journal of Clinical Chemistry and Clinical Biochemistry* **19**: 435-439.
- Portsmann, B.T., Portsmann, T., Nugel, E. & Evers, U. (1985).** "Which of the commonly used marker enzymes gives the best results in colourimetric and fluorimetric enzyme immunoassays: Horseradsh peroxidase, alkalyne phosphatase, β -galactosidase ?" *Journal of Immunological Methods* **79**: 27-37.
- Puchades, R., Maquieira, A. & Atienza, J. (1992).** "A comprehensive overview on the application of flow injection techniques in immunoanalysis." *Critical Reviews in Analytical Chemistry* **23**(4): 301-321.
- Quilliam, M.A. (1999).** "Phycotoxins." *Journal of Aoac International* **82**(3): 773-781.
- Rabbany, S.Y., Lane, W.J., Marganski, W.A., Kusterbeck, A.W. & Ligler, F.S. (2000).** "Trace detection of explosives using a membrane-based displacement immunoassay." *Journal of Immunological Methods* **246**(1-2): 69-77.
- Rachkov, A. & Minoura, N. (2000).** "Recognition of oxytocin and oxytocin-related peptides in aqueous media using a molecularly imprinted polymer synthesized by the epitope approach." *Journal of Chromatography A* **889**(1-2): 111-118.
- Ramstrom, O. & Ansell, R.J. (1998).** "Molecular imprinting technology: Challenges and prospects for the future." *Chirality* **10**(3): 195-209.
- Reinartz, H.W., Quinn, J.G., Zänker, K. & O' Kennedy, R. (1996).** "Bispecific multivalent antibody studied by real-time interaction analysis for the development of an antigen-inhibition enzyme-linked immunosorbent assay." *Analyst* **121**: 767-771.

- Rinehart, K.L., Namikoshi, M. & Choi, B.W. (1994).** "Structure and biosynthesis of toxins from blue-green-algae (cyanobacteria)." *Journal of Applied Phycology* 6(2): 159-176.
- Rivasseau, C., Hennion, M.C. & Sandra, P. (1996).** "Determination of microcystins in cyanobacterial samples using microliquid chromatography." *Journal of Microcolumn Separations* 8(8): 541-551.
- Rivasseau, C., Racaud, P., Deguin, A. & Hennion, M.C. (1999).** "Development of a bioanalytical phosphatase inhibition test for the monitoring of microcystins in environmental water samples." *Analytica Chimica Acta* 394(2-3): 243-257.
- Roitt, I.M. (1994).** Essential immunology. Oxford, *Oxford Blackwell Scientific Publications*.
- Romero, J.M.F., Stiene, M., Kast, R., de Castro, M.D.L. & Bilitewski, U. (1998).** "Application of screen-printed electrodes as transducers in affinity flow-through sensor systems." *Biosensors & Bioelectronics* 13(10): 1107-1115.
- Runnegar, M.T.C., Jackson, A.R.B. & Falconer, I.R. (1988).** "Toxicity to mice and sheep of a bloom of the cyanobacterium (blue green-alga) *Anabaena circinalis*." *Toxicon* 26(6): 599-602.
- Ryan, O., Smyth, M.R. & O' Fagain, C. (1994).** Horseradish peroxidase: The analyst's friend. London, *Portland Press*.
- Saito, S., Nakano, Y., Kushida, K., Shirai, M., Harada, K. & Nakano, M. (1994).** "Cross-reactivity and neutralizing ability of monoclonal antibodies against microcystins." *Microbiology and Immunology* 38(5): 389-392.
- Santandreu, M., Alegret, S. & Fabregas, E. (1999).** "Determination of beta-hcg using amperometric immunosensors based on a conducting immunocomposite." *Analytica Chimica Acta* 396(2-3): 181-188.
- Saurina, J., Hernandez-Cassou, S., Alegret, S. & Fabregas, E. (1999).** "Amperometric determination of lysine using a lysine oxidase biosensor based on rigid-conducting composites." *Biosensors & Bioelectronics* 14(2): 211-220.
- Scheller, F.W., Bauer, C.G., Makower, A., Wollenberger, U., Warsinke, A. & Bier, F.F. (2001a).** "Coupling of immunoassays with enzymatic recycling electrodes." *Analytical Letters* 34(8): 1233-1245.
- Scheller, F.W., Wollenberger, U., Warsinke, A. & Lisdat, F. (2001b).** "Research and development in biosensors." *Current Opinion in Biotechnology* 12(1): 35-40.

- Schweitz, L. (2002). "Molecularly imprinted polymer coatings for open-tubular capillary electrochromatography prepared by surface initiation." *Analytical Chemistry* (in press).
- Sellergren, B. (1997a). "Important considerations in the "design" of receptor sites using noncovalent imprinting." *Abstracts of Papers of the American Chemical Society* 213: 97-IEC.
- Sellergren, B. (1997b). "Noncovalent molecular imprinting: Antibody-like molecular recognition in polymeric network materials." *Trac-Trends in Analytical Chemistry* 16(6): 310-320.
- Sellergren, B. (2001). Man-made mimics of antibodies and their applications in analytical chemistry. Amsterdam, *Elsevier Publishers*.
- Sergeyeva, T.A., Piletsky, S.A., Brovko, A.A., Slinchenko, E.A., Sergeeva, L.M., Panasyuk, T.L. & El'skaya, A.V. (1999). "Conductimetric sensor for atrazine detection based on molecularly imprinted polymer membranes." *Analyst* 124(3): 331-334.
- Skladal, P. & Kalab, T. (1995). "A multichannel immunochemical sensor for determination of 2,4- dichlorophenoxyacetic acid." *Analytica Chimica Acta* 316(1): 73-78.
- Smith, D.S. & Kitts, D.D. (1994). "A competitive enzyme-linked immunoassay for domoic acid determination in human body fluids." *Food and Chemical Toxicology* 32(12): 1147-1154.
- Subrahmanyam, S., Piletsky, S.A., Piletska, E.V., Chen, B.N., Karim, K. & Turner, A.P.F. (2001). "'bite-and-switch' approach using computationally designed molecularly imprinted polymers for sensing of creatinine." *Biosensors & Bioelectronics* 16(9-12): 631-637.
- Sulitzky, C., Ruckert, B., Hall, A.J., Lanza, F., Unger, K. & Sellergren, B. (2002). "Grafting of molecularly imprinted polymer films on silica supports containing surface-bound free radical initiators." *Macromolecules* 35(1): 79-91.
- Sun, W., Jiao, K., Zhang, S.S., Zhang, C.L. & Zhang, Z.F. (2001). "Electrochemical detection for horseradish peroxidase-based enzyme immunoassay using p-aminophenol as substrate and its application in detection of plant virus." *Analytica Chimica Acta* 434(1): 43-50.

- Surugiu, I., Danielsson, B., Ye, L., Mosbach, K. & Haupt, K. (2001a).** "Chemiluminescence imaging elisa using an imprinted polymer as the recognition element instead of an antibody." *Analytical Chemistry* **73**(3): 487-491.
- Surugiu, I., Svitel, J., Ye, L., Haupt, K. & Danielsson, B. (2001b).** "Development of a flow injection capillary chemiluminescent elisa using an imprinted polymer instead of the antibody." *Analytical Chemistry* **73**(17): 4388-4392.
- Takeuchi, T., Fukuma, D. & Matsui, J. (1999).** "Combinatorial molecular imprinting: An approach to synthetic polymer receptors." *Analytical Chemistry* **71**(2): 285-290.
- Tang, H.T., Lunte, C.E., Halsall, H.B. & Heineman, W.R. (1988).** "P-aminophenyl phosphate - an improved substrate for electrochemical enzyme-immunoassay." *Analytica Chimica Acta* **214**(1-2): 187-195.
- Theegala, C.S. & Suleiman, A.A. (2000).** "Quantification of antibody immobilization using peroxidase enzyme-substrate reaction." *Microchemical Journal* **65**(2): 105-111.
- Thévenot, D.R., Toth, K., Durst, R.A. & Wilson, G.S. (2001).** "Electrochemical biosensors: Recommended definitions and classification." *Analytical Letters* **34**(5): 635-659.
- Thompson, R.Q., Barone, G.C., Halsall, H.B. & Heineman, W.R. (1991).** "Comparison of methods for following alkaline-phosphatase catalysis - spectrophotometric versus amperometric detection." *Analytical Biochemistry* **192**(1): 90-95.
- Thornton, A.J. & Brown, D.E. (1991).** "Fermentation glucose assay using the exactech blood-glucose biosensor." *Biotechnology Techniques* **5**(5): 363-366.
- Tothill, I. & Turner, A.P.F. (2003).** Biosensors. New York, *Elsevier Science Ltd*.
- Tothill, I.E. (2001).** "Biosensors developments and potential applications in the agricultural diagnosis sector." *Computers and Electronics in Agriculture* **30**(1-3): 205-218.
- Tothill, I.E. & Turner, A.P.F. (1996).** "Developments in bioassay methods for toxicity testing in water treatment." *Trac-Trends in Analytical Chemistry* **15**(5): 178-188.
- Turner, A.P.F. (1987).** Biosensors, fundamentals and applications. Oxford, *Oxford University Press*.

- Turner, A.P.F. (1998).** "Array of hope for biosensors in europe." *Nature Biotechnology* 16(9): 824-824.
- Ueno, Y., Makita, Y., Nagata, S., Tsutsumi, T., Yoshida, F., Tamura, S., Sekijima, M., Tashiro, F., Harada, T. & Yoshida, T. (1999).** "No chronic oral toxicity of a low dose of microcystin-LR, a cyanobacterial hepatotoxin, in female balb/c mice." *Environmental Toxicology* 14(1): 45-55.
- Van Dolah, F.M., Leighfield, T.A., Haynes, B.L., Hampson, D.R. & Ramsdell, J.S. (1997).** "A microplate receptor assay for the amnesic shellfish poisoning toxin, domoic acid, utilizing a cloned glutamate receptor." *Analytical Biochemistry* 245: 102-105.
- Vianello, F., Signor, L., Pizzariello, A., Di Paolo, M.L., Scarpa, M., Hock, B., Giersch, T. & Rigo, A. (1998).** "Continuous flow immunosensor for atrazine detection." *Biosensors & Bioelectronics* 13(1): 45-53.
- Vlatakis, G., Andersson, L.I., Muller, R. & Mosbach, K. (1993).** "Drug assay using antibody mimics made by molecular imprinting." *Nature* 361(6413): 645-647.
- Volpe, G., Compagnone, D., Draisci, R. & Palleschi, G. (1998).** "3,3',5,5'-tetramethylbenzidine as electrochemical substrate for horseradish peroxidase based enzyme immunoassays. A comparative study." *Analyst* 123(6): 1303-1307.
- Wang, J., Pamidi, P.V.A. & Rogers, K.R. (1998a).** "Sol-gel-derived thick-film amperometric immunosensors." *Analytical Chemistry* 70(6): 1171-1175.
- Wang, J., Tian, B.M. & Rogers, K.R. (1998b).** "Thick film electrochemical immunosensor based on stripping potentiometric detection of a metal ion label." *Analytical Chemistry* 70(9): 1682-1685.
- Ward, C.J., Beattie, K.A., Lee, E.Y.C. & Codd, G.A. (1997).** "Colorimetric protein phosphatase inhibition assay of laboratory strains and natural blooms of cyanobacteria: Comparisons with high-performance liquid chromatographic analysis for microcystins." *Fems Microbiology Letters* 153(2): 465-473.
- Wild, D. (2001).** The immunoassay handbbook. London, *Nature Publishing group*.
- Wilson, R. & Turner, A.P.F. (1992).** "Glucose-oxidase - an ideal enzyme." *Biosensors & Bioelectronics* 7(3): 165-185.
- Wulff, G. (1995).** "Molecular imprinting in cross-linked materials with the aid of molecular templates - a way towards artificial antibodies." *Angewandte Chemie-International Edition in English* 34(17): 1812-1832.

-
- Yang, M.S., Lam, P.K.S., Huang, M.H. & Wong, B.S.F. (1999).** "Effects of microcystins on phosphorylase-a binding to phosphatase-2a: Kinetic analysis by surface plasmon resonance biosensor." *Biochimica Et Biophysica Acta-General Subjects* **1427**(1): 62-73.
- Yao, H.O., Jenkins, S.H., Pesce, A.J., Halsall, H.B. & Heineman, W.R. (1993).** "Electrochemical homogeneous enzyme-immunoassay of theophylline in hemolyzed, icteric, and lipemic samples." *Clinical Chemistry* **39**(7): 1432-1434.
- Ye, L. & Mosbach, K. (2001).** "Molecularly imprinted microspheres as antibody binding mimics." *Reactive & Functional Polymers* **48**(1-3): 149-157.
- Yoshimi, Y., Ohdaira, R., Iiyama, C. & Sakai, K. (2001).** "'gate effect" of thin layer of molecularly-imprinted poly (methacrylic acid-co-ethyleneglycol dimethacrylate)." *Sensors and Actuators B-Chemical* **73**(1): 49-53.
- Zeck, A., Eikenberg, A., Weller, M.G. & Niessner, R. (2001).** "Highly sensitive immunoassay based on a monoclonal antibody specific for [4-arginine]microcystins." *Analytica Chimica Acta* **441**(1): 1-13.
- Zeravik, J. & Skladal, P. (1999).** "Screen-printed amperometric immunosensor for repeated use in the flow-through mode." *Electroanalysis* **11**(12): 851-856.
- Zhang, S., Wright, G. & Yang, Y. (2000).** "Materials and techniques for electrochemical biosensor design and construction." *Biosensors & Bioelectronics* **15**(5-6): 273-282.
- Zhang, S.S., Jiao, K., Chen, H.Y. & Wang, M.X. (1999).** "Detection of ferritin in human serum with a map-h₂o₂-hrp voltammetric enzyme-linked immunoassay system." *Talanta* **50**(1): 95-101.

APPENDIX

I: MASS SPECTROSCOPY FOR CONJUGATE ANALYSIS

The conjugate microcystin-LR-HRP was purchased as a part of an ELISA kit for detection of microcystin-LR. Being the conjugate microcystin-LR-HRP part of a commercial kit, its real composition and concentration were unknown. A MALDI-TOFF analysis of this conjugate was carried on in order to obtain more information on the conjugate and other components present in the solution. This analysis was conducted by M-Scan Ltd. (Ascot, Berkshire, U.K.) upon pure lyophilised samples dissolved in 0.1 % aqueous trifluoroacetic acid (TFA), using a sinapinic acid matrix and a Voyager STR Biospectrometry Research Station laser-desorption mass spectrometer coupled with delayed extraction.

The particular advantage of MALDI mass spectrometry is its ability to produce large mass ions and determine accurately their mass, with high sensitivity and minimal fragmentations (Wilson and Walker, 1994). The spectra for HRP-microcystin-LR and HRP are shown in Figure I.1 and I.2 with their interpretations as follows.

Microcystin-LR-HRP: The spectrum obtained from the sample indicates an average protonated mass for the major component of this sample of m/z 45,666. The signal at *ca.* m/z 88,102 is consistent with the major component in the dimer form. A further signal was observed at m/z 67,031 (**Figure I.3**)

HRP enzyme: A major signal was present which indicates an average protonated mass for this sample of m/z 43,106. The signal at *ca.* m/z 85,594 is consistent with the major component in the dimer form (**Figure I.4**).

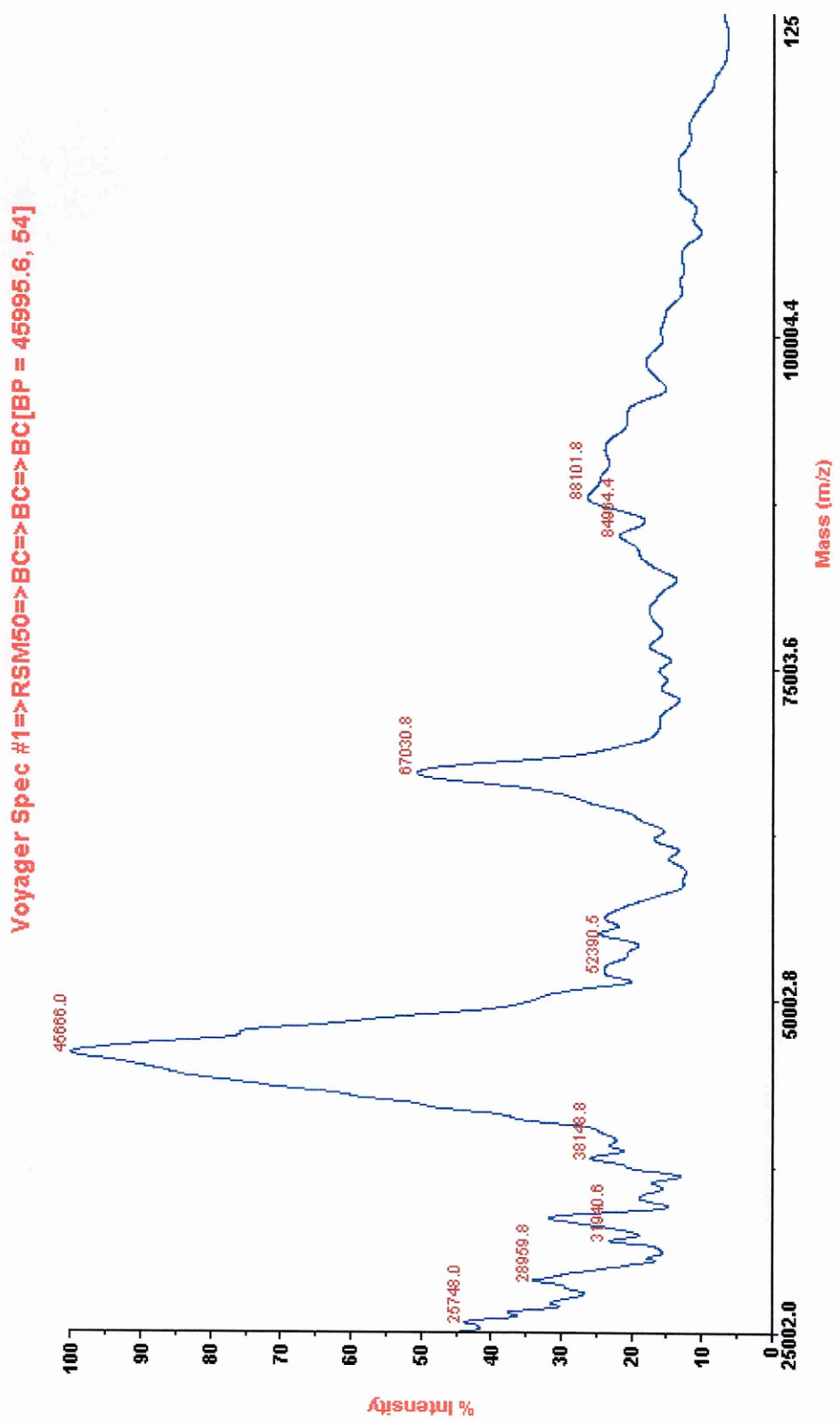


Figure I.1: MALDI Mass Spectrometry Spectra for MC-LR-HRP Conjugate.

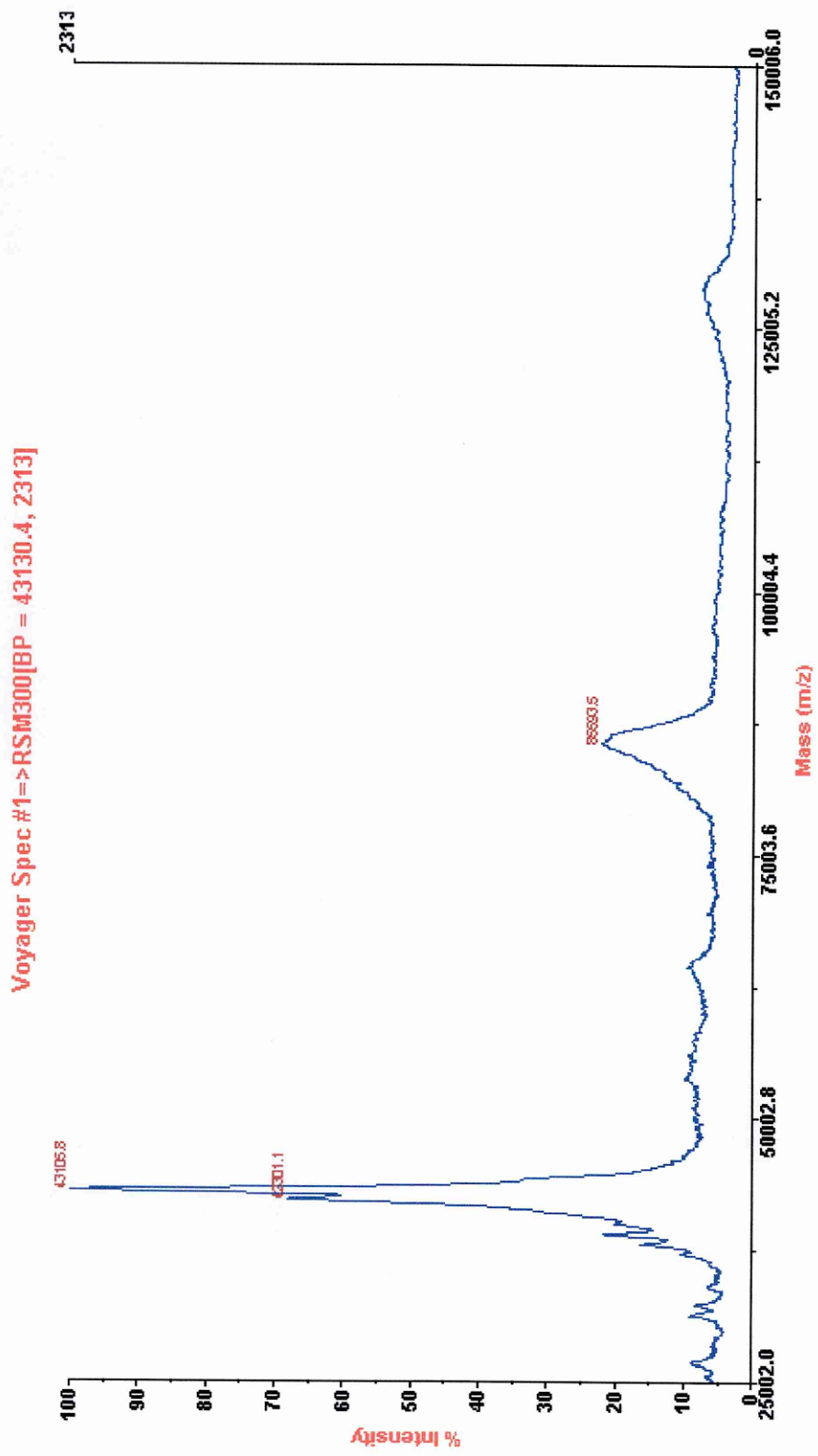


Figure I.2: MALDI Mass Spectrometry Spectra for HRP enzyme.

II: COMPUTATIONAL MODELING PROGRAM

The program was applied in Dream Mode (Figure II.1 A) for 80,000 iterations performed in three different runs (20,000, 20,000 and 40,000). Figure II.1 B shows the Leapfrog Input Data windows after the selection of database.

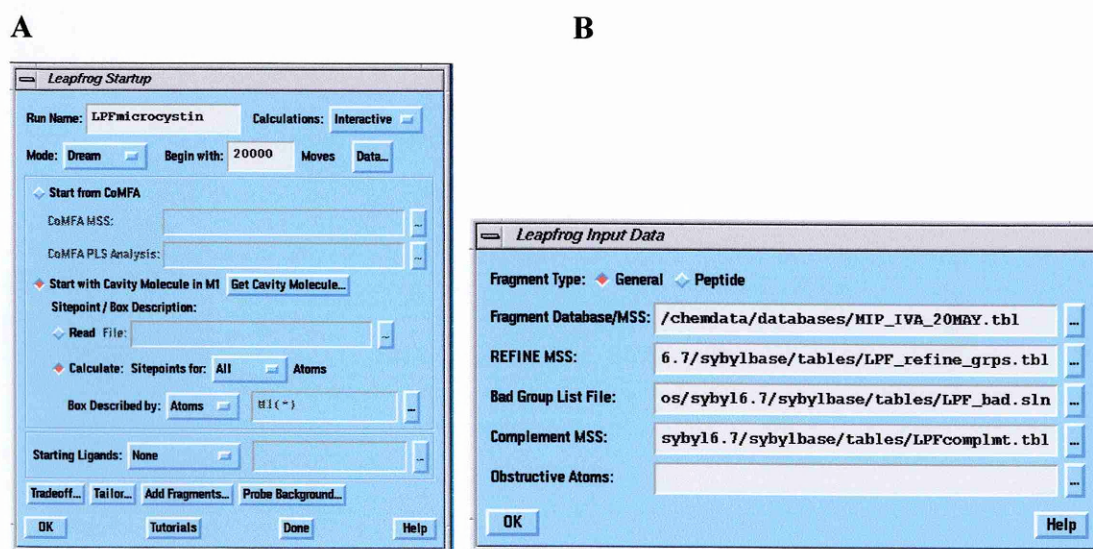


Figure II.1: SYBYL windows for Leapfrog algorithm.

The main Leapfrog window (Leapfrog Startup) is shown in A; Leapfrog Input Data window with database selected for running the program is reported in B.

Clicking the 'Taylor' button on Leapfrog Startup, the window shown in Figure II.2 A appears. This window reports the categories containing all the parameters used for Leapfrog applications. In this work, most of the categories were left as default with the exception of Energy Startup and Relative Move Frequencies. The only change made in Leapfrog Energy Startup window was the inclusion of H-Bonding energy that was not active in default conditions. Each of the Move Frequencies is shown in Figure II.2 B. The values chosen for the move frequencies were selected according to the features of the monomers and on the basis of previous works performed using Leapfrog.

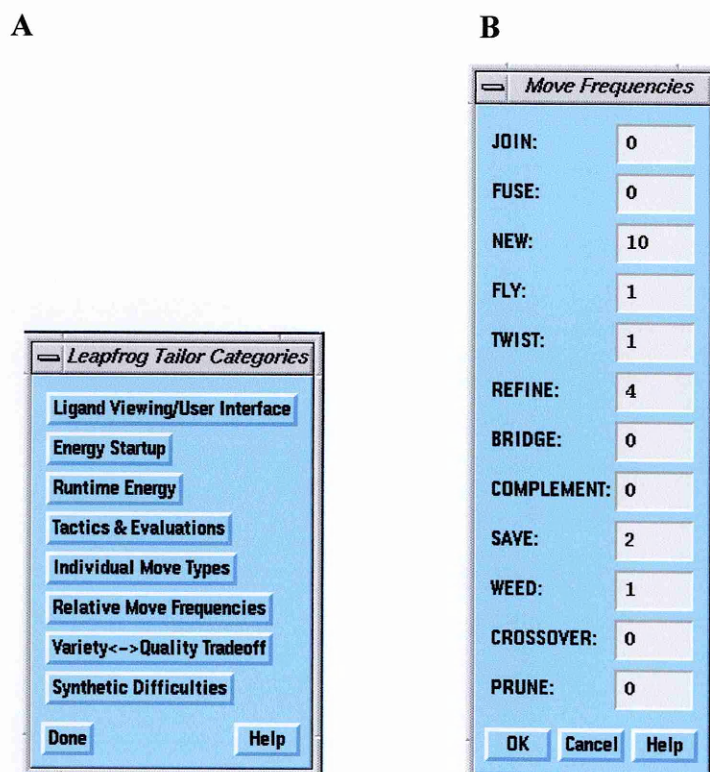


Figure II.2: SYBYL windows for Leapfrog algorithm.

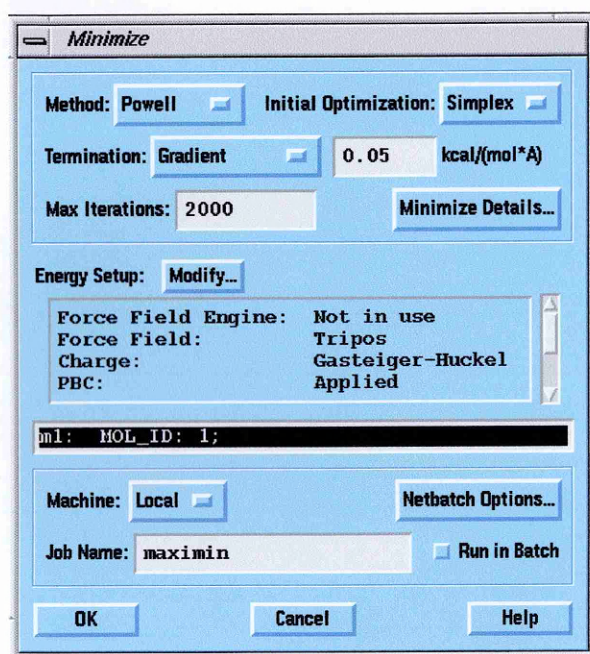
The window reporting the Leapfrog Tailor Categories is reported in **A**; and the window Move Frequencies is shown in **B**.

After the three Leapfrog runs (20,000, 20,000 and 40,000 iterations), the results from each run were examined evaluating the empirical binding score. The monomers giving the highest binding score represent the best candidates for the polymer preparation.

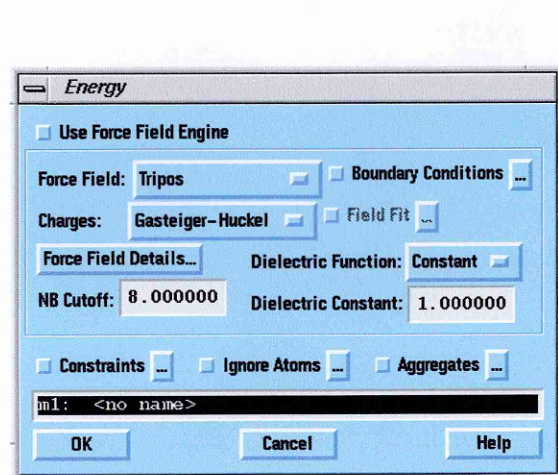
The third step of computer modeling describes a process for the optimisation of the monomers composition. In order to simulate the pre-arrangement of functional monomers with the template in the monomer mixture prior to polymerisation, multiple copies of the best four monomers (according to Leapfrog results) were placed around domoic acid, using solvation experiments, creating a solvated box. The box was then charged with the Gasteiger-Hückel method and its energy was minimised using the Powell option, termination Gradient, default parameters for dielectric constant and function and convergence at 0.05 Kcal/mol in 2000 steps (Figure II.3A, B and C). The energy minimisation of the solvated box was performed

applying boundary conditions in order to keep the monomers reasonably close to the toxin. In the fourth step, a simulated annealing process was applied to optimise the arrangement of functional monomers around the template. Annealing conditions were fixed as 1000K-300K sweeping in 32,000 consequent steps. Equilibrium length was determined in 2000 femtoseconds (fs). The energy minimisation, performed among each of the molecular dynamics steps, was carried out with the conditions reported in Figure II.3A, B and C.

A



B



C

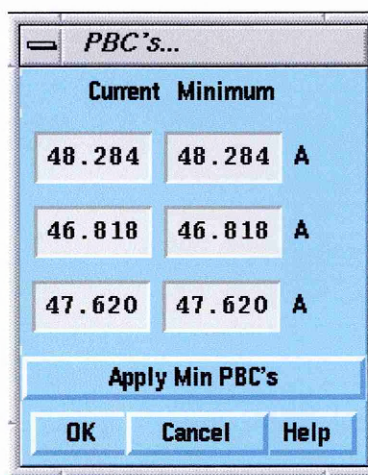


Figure II.3: SYBYL windows for energy minimisation of the solvated box.

The main window is reported in **A**; the windows showing charges and active boundary conditions (PBC) are reported in **B** and **C**. Boundary conditions were applied both during energy minimisation and molecular dynamics.

At the end of the program, the number and the position of the functional monomers were examined. The type and quantity of the monomers participating in the complex with the template (first shell layer), or monomers which interacted with the first shell layer of monomers (second shell layer), stabilising complex indicated the type and ratio of the template and monomers in an optimised MIP composition.